THE MECHANISM OF SUPER-RATE BURNING OF CATALYZED DOUBLE BASE PROPELLANTS

N. Kubota, et al

Princeton University

Prepared for:

Office of Naval Research

March 1973

PRINCETON UNIVERSITY

DEPARTMENT OF AEROSPACE AND MECHANICAL SCIENCES

UNCLASSIFIED
Security Classification

DOCUMENT CONTROL DATA - R & D
(Security classification of title, body of abstract and indexing annotation must be entered when the overall report is classified)

1. ORIGINATING ACTIVITY (Corporate author)
Princeton University
Department of Aerospace & Mechanical Sciences
Princeton, New Jersey 08540

2a. REPORT SECURITY CLASSIFICATION
UNCLASSIFIED

2b. GROUP

3. REPORT TITLE
THE MECHANISM OF SUPER-RATE BURNING OF CATALYZED DOUBLE BASE PROPELLANTS

4. DESCRIPTIVE NOTES (Type of report and inclusive dates)
Scientific Interim

5. AUTHOR(S) (First name, middle initial, last name)
N. Kubota, T. J. Ohlemiller, L. H. Caveny and M. Summerfield

6. REPORT DATE
March 1973

7a. TOTAL NO. OF PAGES
xvii + 204

7b. NO. OF REFS
111

8a. CONTRACT OR GRANT NO.
N00014-67-A-0151-0023

b. PROJECT NO.

c.

d.

9a. ORIGINATOR'S REPORT NUMBER(S)
AMS Report No. 1087

9b. OTHER REPORT NO(S) (Any other numbers that may be assigned this report)

10. DISTRIBUTION STATEMENT
1. Distribution of this document is unlimited.

11. SUPPLEMENTARY NOTES
Tech,. Other

12. SPONSORING MILITARY ACTIVITY
Power Branch
Office of Naval Research
Dept. of the Navy, Washington,D.C.

13. ABSTRACT

This study is directed at understanding how organic lead salts (at the 1% level) alter the burning mechanisms of double base propellants to produce large (up to 300%) burning rate increases (super-rate burning) and domains of reduced burning rate pressure and temperature sensitivity (plateau burning). Investigations were carried out with nitrocellulose and trimethylolethane trinitrate (TMETN) double base propellants with systematic variations in additives (including lead powder, lead oxide, lead salicylate, copper powder, copper salicylate, finely divided carbon, and oxamide), particle size, and degree of dispersion. Diagnostic experiments (from 0.1 to 100 atm) examined burning rate behavior, gas-phase structure, burning-surface structure, temperature profiles in the reaction zones, and global effects. The micro-thermocouple experiments revealed that 1% lead salts have less than a 10% effect on surface temperature and surface heat release but produce significant increases (70 to 100%) in the fizz zone temperature gradients. Lead salts decompose and directly affect the surface reaction layer ($\sim$ 20μ thick at 20 atm). The lead salts' decomposition products react with the nitrate esters to produce an increased amount of solid carbon. The portion of decomposed organic molecules which appears at the surface in the form of carbon rather than readily oxidizable aldehydes reduce the effective fuel to oxidizer ratio (aldehyde to NO_2) and, thus, shifts the equivalence ratio toward the stoichiometric value; this accelerates the reaction rates in fizz zone and produces super rate burning.

DD FORM 1 NOV 65 1473

UNCLASSIFIED
Security Classification

UNCLASSIFIED

Security Classification

14 KEY WORDS	LINK A		LINK B		LINK C	
	ROLE	WT	ROLE	WT	ROLE	WT
Solid Propellant Combustion						
Burning rate model						
Double base propellants						
Nitrocellulose						
Nitrate esters						
Trimethylolethane trinitrate						
Lead salts						
Lead salicylate						
Super rate burning						
Burning rate catalysts						
Plateau burning						
Flame structure studies						
Thermocouple measurements						
Ultra violet radiation						
Processing double base propellants						

UNCLASSIFIED

Security Classification

THE MECHANISM OF SUPER-RATE BURNING OF CATALYZED DOUBLE BASE PROPELLANTS

Aerospace and Mechanical Sciences Report
No. 1087

by

N. Kubota, T. J. Ohlemiller,
L. H. Caveny and M. Summerfield

Performed under Office of Naval Research
Contract N00014-67-A-0151-0023
Requisition NR 092-516/8-8-72(473)
MARCH 1973

Transmitted by:

Martin Summerfield
Principal Investigator

1. Approved for public release; distribution unlimited.
2. Reproduction in whole or in part is permitted for any purpose of the United States Government.
3. Requests for additional copies should be made to the National Technical Information Service, U.S. Department of Commerce, Springfield, Va. 22151

MARCH 1973

Guggenheim Laboratories
Department of Aerospace and Mechanical Sciences
PRINCETON UNIVERSITY
Princeton, New Jersey

ACKNOWLEDGEMENTS

This research was carried out under Contract N00014-67-A-0151-0023 from the Power Branch, Office of Naval Research. Dr. R. Roberts, Head, Po : Branch, was the Technical Supervisor and Mr. J. R. Patton, also of the Power Branch, was the Project Monitor.

The authors thank Dr. C. Boyars, Visiting Senior Research Scientist and Dr. I. W. May, of the Ballistics Research Laboratories, for their valuable discussions and comments and for their constructive review of this research. Also, the authors thank Professor W. A. Sirignano for his review and comments concerning the gas phase reactions.

The experimental work was accomplished with the capable support of the Technician Staff. In particular, Mr. C. R. Felsheim was responsible for the specialized processing of the propellants used in this study, Mr. E. R. Crosby participated in the photographic work, and Mr. J. H. Semler assisted in the experiments using the delicate micro-thermocouples.

This report was typed by Mrs. Anne Chase. Her patient and skillful handling of this task is very much appreciated.

This report is also the Ph.D. Thesis of Naminosuke Kubota and carries number 1087-T in the records of the Department of Aerospace and Mechanical Sciences.

ABSTRACT

This study is directed at understanding how organic lead salts used as catalysts alter the burning mechanisms of double base propellants (i.e., two nitrate esters inter-diffused) to produce burning rate increases (known as super-rate burning) and domains of reduced burning rate pressure sensitivity (known as plateau burning). Simultaneously, these same lead salts greatly reduce the temperature sensitivity of burning rate in the super-rate range. These effects are of great practical interest since they provide design flexibility and yield performance which is largely constant over a prescribed range of operating pressures and initial temperatures.

The experimental investigations were carried out with particulate nitrocellulose (PNC) and trimethylolethane trinitrate (TMETN) double base propellants instead of with the more hazardous-to-formulate nitrocellulose (NC) and nitroglycerin (NG) propellants which are more widely used. Experiments confirmed that the burning characteristics of NC/NG and PNC/TMETN propellants are very similar. Thirty-two propellants with systematic variations in additives (including metallic lead powder, lead oxide, lead salicylate, metallic copper powder, copper salicylate, finely divided carbon, ammonium polyphosphate, oxamide, and ammonium perchlorate), particle size, and degree of dispersion were specially formulated for this study. The lead salts produced burning rate increases up to 300%.

The combustion wave is seen to consist of four identifiable zones: (1) the surface reaction layer; (2) the fizz zone, characterized by the first steep temperature gradient in the gas phase; (3) the dark zone, in which the temperature is almost constant; and, finally, (4) the luminous flame zone, which includes the final combustion processes. This study reveals that the burning-rate of double base propellants is governed by the chemical reactions that occur in a very thin surface reaction layer ($\sim$ 100μ at 1 atm, $\sim$ 20μ at 20 atm) and fizz zone ($\sim$ 200μ at 1 atm, 100μ at 20 atm).

Diagnostic experiments were carried out to determine the burning rate behavior of the specially formulated propellants over a pressure-range from 0.1 atm to 100 atm. The gas phase structure, burning-surface structure, temperature profiles in the reaction zones, and global effects were examined using high speed photography, micro-thermocouples (bead size 4μ), burning rate measurements, and burning extinction by rapid depressurization.

The micro-thermocouple experiments revealed that the addition of lead salts has only very small effects on the

surface temperature (T_s) and the heat release at the surface (Q_s). For example, at 20 atm, the addition of a mixture of 1% lead salts and 1% copper salts increases T_s from 345°C to 375°C, representing less than 10% increase in ($T_s - T_0$), and produces no detectable change in Q_s (90 cal/g). However, these same additives significantly increase the temperature gradients in the fizz zone, e.g., between 10 and 20 atm, increases of 70% to 100% over the noncatalyzed propellant were measured.

The dark zone reaction mechanisms were studied by means of high speed photography. During super-rate burning of a catalyzed propellant, the luminous flame is displaced further from the burning surface than the luminous flame of noncatalyzed propellants. For example, at 20 atm, the luminous flame is positioned 0.25 cm above the burning surface for a noncatalyzed propellant, and 1.1 cm for a catalyzed propellant. From such observations it was concluded that the heat feedback from reactions beyond the fizz zone to the burning surface does not affect significantly the burning rate.

Burning surface observations using high speed photography and extinguished propellant samples revealed that, when lead salts are added to the propellants, large amounts of solid carbon are formed on the surface at low pressures where super-rate burning occurs. The quantity of carbon decreases with increased pressure, and the super-rate burning diminishes at the same time.

As a result of this study, we summarize the important changes attributed to the lead salts as follows. Lead salts directly affect the surface reaction layer ($\sim$ 20μ thick at 20 atm), where the lead salts decompose ultimately into finely-divided metallic lead or lead oxide particles. The decomposition products of the lead salts react with the nitrate esters in the surface reaction layer, altering their decomposition mechanism so as to produce an increased amount of solid carbon on the surface. Although these reactions are not known in detail, the shift in mechanism surprisingly does not significantly alter the net exothermicity. The presence of lead salts accelerates the fizz zone reactions and thereby increases the heat feedback to the surface; this produces super-rate burning.

We conclude that these actions of the lead salts to produce increased carbon at the propellant surface and the acceleration of the fizz zone reactions are directly coupled as follows. The portion of decomposed organic molecules which appears at the surface in the form of carbon rather than readily oxidizable aldehydes could reduce the effective fuel: oxidizer (aldehyde: NO_2) ratio. This increased NO_2 proportion constitutes a shift in equivalence ratio toward

the stoichiometric value. Such a shift for NO_2/aldehyde mixtures results in a greatly accelerated reaction rate. This is the proposed mechanism of fizz zone reaction rate acceleration.

The degree of super rate decreases as the burning rate increases (producing the plateau effect), since the time available for the initial catalytic action in the surface reaction layer decreases. This decrease in available time is a consequence of the higher burning rate and the decreased thermal wave thickness. Thus, since the fraction of the reactants affected by the lead compounds (and excess concentration of NO_2) decreases, the reaction rate in the fizz zone approaches the normal reaction pathway, and then super-rate burning diminishes.

The burning rate model resulting from this study differs from the two previously published models. Our experimental evidence does not support Camp's theory (1958) of photo-sensitized subsurface reactions. Powling, et al (1971) hypothesized that carbon, formed when lead compounds are added, catalyzes the NO reduction in the gas phase; evidence in this study supports the conclusion that lead compounds act instead to increase the proportion of NO_2 in the fizz zone.

While the research reported herein leads to a reasonable explanation of super-rate burning, no firm explanation was found for the termination of super-rate effects at the pressure where plateaus are measured, nor is there any experimentally-supported explanation in the literature. This is still an unfinished task and a very important one.

TABLE OF CONTENTS

	Page
Acknowledgements	ii
Abstract	iii
Table of Contents	vi
List of Tables	ix
List of Figures	x
SECTION I. INTRODUCTION	1
SECTION II. PREVIOUS STUDIES OF BURNING MECHANISM OF DOUBLE BASE PROPELLANTS	3
A. Summary of Double Base Propellant Burning Behavior	4
(1) Thermal Decomposition Processes of Nitric Esters and Nitric Ester-Based Propellants	4
(2) Gas Phase Reactions of NO_2 and NO	8
(3) Physical Picture of Double Base Propellant Burning Processes	10
B. Theoretical Burning Rate Models of Double Base Propellants Proposed by Previous Investigators	10
C. The Nature of Super-Rate, Plateau and Mesa Burning	13
(1) Burning Rate Behavior of Catalyzed Double Base Propellants	14
(2) Burning Rate Behavior of Catalyzed Liquid Nitrate Esters	15
(3) The Effect of Lead Compounds on Gas Phase Reactions	16
D. Plateau Propellant Combustion Models Proposed by Other Workers	17
E. Anticipation of Conclusions: New Model Proposed in This Study	20
SECTION III. EXPERIMENTAL RESULTS ON BURNING RATE BEHAVIOR	22
A. Experimental Results of this Investigation and Comparison with the Results of Previous Investigators	22
(1) The Comparison of NC/NG and PNC/TMETN Burning Behavior	23
(2) The Effect of PNC Content	23
(3) The Effect of Carbon Content	23
(4) The Effect of the Catalyst Particle Size	24
(5) The Effect of Catalyst Mixing	24
(6) Catalyst Type	25
B. Experimental Results on Burning Rate Behavior at Low Pressures and on Minimum Burning Pressure	27
C. Summary of Experimental Observations of Overall Burning Rate Behavior	29

Table of Contents (continued)

SECTION IV. THE STRUCTURE OF THE GAS PHASE ZONE 30
A. General Discussion of the Gas Phase Reaction Zone 30
B. Observations of the Gas Phase Zone of Catalyzed Propellants by Previous Investigators 31
C. Investigation of Overall Reaction Order and Catalyst Activity in Dark Zone 34
(1) Physical and Chemical Background for the Estimation of the Overall Reaction Order in the Dark Zone. 34
(2) Definition of the Catalyst Activity in the Dark Zone 37
D. Experimental Results of Studies in the Dark Zone Structure 38
(1) Measurement of Dark Zone Length with Film Sensitive to Visible Light 38
(2) Measurement of Dark Zone Length with Film Sensitive to Infrared Radiation 39
(3) General Observations of Dark Zone Structure 39
E. Discussion of Results: Relation to Earlier Experimental Results 40
F. Possible Reaction Mechanisms in the Dark Zone 43
G. Reaction Mechanism in Fizz Zone 45
H. Summary of Preceding Section 47

SECTION V. STUDIES ON THE CONDENSED PHASE REACTION ZONE AND THE REACTION AT THE BURNING SURFACE 48
A. Review of Findings of Previous Investigators 48
B. Experimental Results of This Investigation 50
(1) Burning Surface Structures 50
(2) Burning Surface Observations on Propellant Samples After Rapid Depressurization Extinguishment 51

SECTION VI. TEMPERATURE PROFILES OF CATALYZED AND NONCATALYZED PROPELLANT BURNING 53
A. Findings of Previous Investigators 53
B. Experimental Results of This Investigation 55
C. Discussion of Experimental Results 58

SECTION VII. DISCUSSION OF SUPER-RATE COMBUSTION MODELS PRESENTED BY OTHER WORKERS AND THE MODEL PROPOSED IN THIS STUDY 61
A. Discussion of Super-Rate Combustion Models in Light of Available Experimental Evidence 61
B. Super-Rate Burning Model Proposed in This Study 64
(1) Catalyst Behavior in Condensed Phase and at the Burning Surface 65
(2) Catalyst Behavior in Gas Phase 65

Table of Contents (continued)

C. General Equations for Double Base Propellant Burning 68
D. Normal and Super-Rate Burning Model Representing Stoichiometric Shift 72
(1) Burning Rate Model for Noncatalyzed Propellant 73
(2) Burning Rate Model for Catalyzed Propellant 74
E. Discussion of the Models for Noncatalyzed and for Catalyzed Burning 76
F. Summary of the Discussion of Combustion Models 78

SECTION VIII. SUMMARY OF OBSERVATIONS AND CONCLUSIONS 79
A. Major Experimental Observations of this Study and Their Implications 79
B. Supporting Observations 80
(1) Observations of this Study 80
(2) Observations from Other Investigators 81

SECTION IX. CONCLUSIONS OF THIS STUDY 82

LIST OF SYMBOLS 84

LIST OF ABBREVIATIONS 87

LISTING OF PHYSICAL CONSTANTS AND PARAMETERS FOR BURNING RATE MODEL CALCULATION 89

REFERENCES 90
TABLES 101
FIGURES 107

APPENDIX A - SPECIFICATIONS OF ALL PROPELLANT FORMULATIONS USED IN THIS INVESTIGATION A1

APPENDIX B - SUMMARY OF OHLEMILLER AND SUMMERFIELD'S PLATEAU MODELLING WORK BASED ON THE CAMP UV RADIATION HYPOTHESIS B1

APPENDIX C - EXPERIMENTAL PROCEDURE AND MEASUREMENTS C1

APPENDIX D - PROCESSING PROCEDURE OF PNC/TMETN PROPELLANTS INCLUDING CHEMICAL PROPERTIES AND SOURCES OF INGREDIENTS D1

LIST OF TABLES

Table No.	Title	Page
1	Overall Reaction Order n in Dark Zone Determined from Burning Rate Index m and Dark Zone Index d	101
2	Reaction Steps That Have Been Proposed in Double Base Propellant Burning	102
3	Summary of Combustion Models in Terms of Processes Considered in the Several Flame Zones	104
4	Experimental Evidence in Support of Proposed Theoretical Mechanisms	105
A-1	Specifications of All PNC/TMETN Propellant Formulations Used for This Study	A2
A-2	Specifications of All NC/NG Propellant Formulations Used for This Study	A3

LIST OF FIGURES

Figure	Caption	Page
1	Definition of super rate, plateau and mesa-burning	107
2	Plateau propellant burning rate and temperature sensitivity of widely used propellant	108
3	Combustion zones and processes of double base propellant	109
3A	Reaction scheme of combustion processes of double base propellants	109
4	Effect of various lead compounds added to basic propellant on the lowest pressure index and pressure range of plateau burning (based on results of Preckel (ref. 45))	110
5	Comparison of burning rates of NC/NG and PNC/TMETN propellants showing that the pressure indices are about the same	111
6	Comparison of plateau burning rate of NC/NG and PNC/TMETN propellants showing that the super rate characteristics are comparable when TMETN replaces NG	112
7	Increase in burning rate corresponding to increase in PNC	113
8	Carbon powder addition increasing burning rate of PNC/TMETN propellants	114
9	Pressure dependence and carbon powder concentration effects on NC/NG propellant burning rate	115
10	Addition of carbon powder to plateau propellants diminishing super rate	116
11	Effect of catalyst particle size on burning rate showing that smaller granulations are more effective	117
12	Effect of additive dispersion on burning rate showing that improved dispersion increases catalyst effectiveness	118
13	Effect of elemental lead and ccpper powder on burning rate showing that lead is more effective than copper	119
14	Increasing PbO percentage is most effective at lower pressures	120
15	Additive effect of PbSa and CuSa on burning rate higher pressures (showing synergistic effect that extends plateau range to lower pressures)	121
15A	Effect of catalyst content on burning rate showing that adding catalyst beyond a certain level decreases super rate	122
16	Increase in burning rate with increasing AP content	123

Figure	Caption	Page
17	Combined effect of PbSa and Pb2-EH on burning rate	124
18	Comparison of catalyst components shows that organic part of lead salt (used alone) has no effect on burning rate	125
19	Effect of additives on burning rate and on deflagration limit pressure in N_2	126
20	Effect of additives to PNC propellants on pressure of deflagration limit in N_2	127
21	Microphotograph of residue of propellant burning showing crystalline particles and carbonaceous particles	128
22	Photograph of solid carbon on the burning surface of propellant modified by a phosphorus containing compound	128
23	Effect of catalyst on dark zone length showing increased length with finer granulation of PbSa and CuSa	129
24	Effect of burning rate on dark zone length showing lengthening of dark zone with higher burning rates	130
25	Comparison of dark zone lengths of catalyzed and noncatalyzed propellants showing distended luminous flame with increased burning rate	131
26	Effect of pressure on the two "dark zone" lengths observed in the presence of PbSa and CuSa	132
27	Effect of pressure on the two "dark Zone" lengths observed in the presence of PbSa and CuSa	133
28	Comparison of PbSa and CuSa effects on flame structure; PbSa alone cause a faint weak-luminosity zone while CuSa does not; CuSa, however, generates large carbonaceous particles which disrupt the normally planar high luminosity flame zone	134
29	Effect of catalyst on flame structure and burning rate (p = 27 atm) showing that CuSa produces a rough carbonaceous layer on surface; the further addition of PbSa eliminates this effect but introduces a considerable weak luminosity zone	135
30	Pressure vs burning rate and dark zone length showing the existence of weakly luminous zone by the addition of PbSa	136
31	Pressure vs burning rate and dark zone length	137

Figure	Caption	Page
32	Infra-red photographs of noncatalyzed and catalyzed propellant flames showing that catalyst addition increases infra-red emission in dark zone	138
33	Effect of catalyst on flame structure showing ejected particles from burning surface of catalyzed propellant (photographed using IR film)	139
34	Variation of dark zone length with pressure of plateau, mesa propellant showing rapidly decreasing dark zone length with increasing pressure in mesa region	140
35	Temperature profiles in gas phase (including beginning of luminous flame	141
36	Catalyst "activity" in dark zone and relative increase in burning rate as functions of pressure; the parameter is catalyst particle size	142
37	Catalyst "activity" in dark zone and relative increases in burning rate as functions of pressure; the parameter is catalyst type	143
38	Photomicrograph of burning surface structure showing carbonaceous fragments and a spherical particle (probably K_2O) leaving the surface	144
39	Photomicrograph of surface during burning showing the appearance of brightly emitting spots on carbonaceous filaments when PbSa is added (this is not observed with the basic propellant)	145
40	Photomicrographs of extinguished (by rapid depressurization) burning surface of noncatalyzed and catalyzed propellant samples showing decreasing amount of and size of carbon particles on the surface with increasing pressure	145
41	Burning surface temperature of double base propellants vs pressure as measured by previous investigators	146
42	General features of a typical temperature profile in catalyzed and noncatalyzed propellants combustion	147
43	Oscillogram of temperature profile showing voltage fluctuations near point where surface arrives at thermocouple	147

Figure	Caption	Page
44	Measured temperature vs distance in condensed phase and gas phase showing increasing temperature gradients and dark zone temperatures with increasing pressure, noncatalyzed propellant	148
45	Measured temperature vs distance in condensed phase and gas phase showing increasing temperature gradients and dark zone temperatures with increasing pressure; catalyzed propellant	149
46	Comparison of temperature profiles in fizz zone between noncatalyzed and catalyzed propellants	150
47	Temperature gradient of the gas phase on burning surface vs pressure showing higher rate of heat feedback from gas phase to condensed phase when propellant is catalyzed	151
48	Temperature gradient of the gas phase on burning surface vs burning rate showing rapidly decreased heat feedback from gas phase to condensed phase at low pressures	152
49	Measured temperature vs distance in condensed phase and gas phase showing how flammability retarding additives reduce temperature gradients and fizz zone temperatures	153
50	Surface temperature determined by temperature inflection method (propellant 1056 at 8 atm)	154
51	Dependence of burning surface temperature on pressure and comparison of burning surface temperature of catalyzed and noncatalyzed propellant	155
52	Relationship between the surface heat release and the burning rate showing no detectable difference of Q_s between noncatalyzed and catalyzed propellants	156
53	Zones emphasized by previous investigators	157
54	Proposed reaction pathways for super-rate burning	158
55	Calculated burning rate and temperature sensitivity vs pressure of noncatalyzed and catalyzed propellant	159
56	Calculated mass fraction of propellant passing through reaction path 2 and nondimensionalized heat release rate parameter for path 1 and path 2	160

Figure	Caption	Page
57	Calculated burning rate, burning surface temperature, and dark zone temperature vs pressure for noncatalyzed and catalyzed propellants	161
58	Postulated plateau burning rate model	162
B-1	Proposed reaction pathways for platonized propellants	B11
B-2	Calculated burning rates for catalyzed and noncatalyzed propellants (for this case, catalysis is assumed to accelerate the surface zone reactions and double their exothermicity)	B12
B-3	Calculated typical burning rates for catalyzed and noncatalyzed propellants (for this case, catalysis is assumed to decrease the gas phase activation energy only; no thermal effects are assumed)	B13
C-1	Close-up of strand holder prior to test. (1 - 100 atm strand burner)	C10
C-2	Exploded view of strand burner for measuring burning rates in 1 - 100 atm range	C10
C-3	Instrumentation for measuring burning rates and temperature profiles in 1 - 100 atm range	C11
C-4	Insensitivity of burning rate of double base propellant on N_2 purge gas rate	C12
C-5	Apparatus for measuring burning rates and temperature profiles at subatmospheric pressures	C13
C-6	Close-up of strand burner for measuring burning rates at subatmospheric pressures	C13
C-7	Strand burner for gas phase observations	C14
C-8	Photograph of assembled strand burner for gas phase observations	C14
C-9	Photograph of assembled strand burner for burning surface observations	C15
C-10	Close-up of strand burner for burning surface observations	C15
C-11	Photograph of assembled strand burner used for extinction of propellant burning by rapid depressurization	C16
C-12	Schematic drawing of the strand burner for extinction of propellant burning by rapid depressurization	C16
D-1	Processing of plastisol nitrocellulose propellant	D9
D-2	Theoretical equilibrium composition products as a function of pressure	D10

SECTION I

INTRODUCTION

The ultimate aim of research on the combustion characteristics of double base propellants is to acquire sufficient understanding of the governing factors so that propellants can be modified and improved more efficiently and so that the combustion properties encountered during applications can be anticipated. The combustion characteristics of practical interest include ignition following exposure to a variety of stimuli, susceptibility to combustion instability, and dependence of burning rate on pressure and initial temperature. An understanding of the basic steady state combustion mechanism is a necessary prerequisite for models describing the above mentioned items. In addition to the applied aspect of this research, equally important scientific objectives exist. These include understanding the chemical steps in the high temperature decomposition processes, the site and mechanism of catalyst action, and developing techniques for probing very thin flame zones.

Double base propellants consist of two types of nitrate ester physically mixed (and extensively inter-diffused by high temperature curing). Each nitrate ester has both fuel and oxidizer within the same molecule but one ester may be under-oxidized and the other over-oxidized. The main ingredients of a conventional double base propellant are nitrocellulose and nitroglycerin (or a similar ingredient such as metriol trinitrate).

Many simple double base propellants obey a relationship known as Vieille's Law, in which the burning rate is proportional to the pressure raised to a power, n, known as the burning-rate exponent. This exponent is often constant over a wide range of pressures, however, the presence of small quantitites of various lead compounds* (in some double base propellants) results in a greatly increased burning rate exponent at low pressures, as manifested in an increased burning rate in this range. This increased burning is known as "super-rate burning" and is followed by a "plateau-burning" region, in which the burning rate is nearly independent of pressure, and a "mesa-burning" region in which the burning rate actually decreases with increasing pressure. The regions are illustrated on a typical pressure/burning-rate curve in Fig. 1. It is observed that propellants catalyzed with lead compounds, or platonized propellants as they are commonly referred to, have greatly reduced temperature sen-

*Such compounds are not catalysts in the pure chemical sense since they are permanently altered by the combustion wave; since they do accelerate the burning rate, they are commonly called catalysts in the looser sense of a rate accelerator.

sitivities of burning rate in the plateau and mesa-burning regimes (a fact which makes them useful in widely varying temperature environments). Figure 2 shows the burning rate behavior of a widely used propellant having very low temperature sensitivity in the plateau and mesa-burning regimes.

These burning-rate characteristics of double base propellants are governed by the chemical reactions that occur in a very thin ($\sim$ 100μ) surface layer and gas phase zone. As shown in Fig. 3, the combustion regime can be divided into four zones, namely, the subsurface-reaction zone; the fizz zone, characterized by the first steep temperature gradient; the dark zone, in which the temperature is almost constant; and, finally, the luminous flame zone, which includes the final combustion processes.

The processes occurring during the combustion of platonized double base propellants are so complex that up to now an empirical approach has been the only feasible method of modifying and optimizing propellant performance. Such an approach is particularly restrictive whenever the burning rate is strongly dependent on the physical and chemical properties of the catalyst that produce super rate, plateaus, and mesas. In recent decades, several models have been offered that partially account for the combustion trends; however, the validity of these partial explanations has not been established because of the lack of detailed knowledge of the combustion mechanism.

This study is concerned primarily with the super-rate burning mechanism of platonized double base propellants, and, secondarily, attention is given to the phenomena that lead to plateau and mesa burning. The object of the investigation was to determine the zone (or zones) affected by the catalyst. A systematic study has been carried out to determine the effect on burning rate behavior of a variety of catalysts over a pressure-range from 0.1 atm to 100 atm. Also examined were the gas phase structure, the burning-surface structure, and the temperature profile in the reaction zone. A combustion model which accounts for the super-rate burning is discussed in terms of the experimental results of this and previous studies.

SECTION II

PREVIOUS STUDIES OF BURNING MECHANISM OF DOUBLE BASE PROPELLANTS

The related experimental and theoretical studies of the combustion mechanism of double base propellants were studied prior to this investigation so that full advantage could be taken of previous findings. The previous work can be divided into the following categories:

1. The decomposition processes of simple nitrate esters, such as methylnitrate, ethylnitrate, etc.

2. The decomposition processes of nitrocellulose and of double base propellants.

3. The gas-phase reactions involving NO_2 and NO.

4. The theoretical models of the burning-rate/pressure relationships of double base propellants.

5. The nature of super-rate, plateau and mesa burning.

6. The theoretical models predicting the plateau-burning characteristic of platonized double base propellants.

Whenever appropriate, references are made to findings that will influence the explanations of super-rate, plateau, and mesa behavior. Also, several interesting contradictions and differences between investigators are pointed out.

Since the discovery of double base propellants, also referred to as smokeless powder, numerous investigators have attempted to improve and control its burning characteristics. In the early twentieth century, it was established that the burning rates of many double base propellants obey a relationship known as Vieille's Law, in which the burning rate is proportional to the pressure raised to a power m, known as the burning-rate exponent.

During the Second World War, the accidental discovery was made that the use of lead compounds as lubricants in the propellant extrusion process resulted in a greatly increased burning-rate exponent at low pressures, as manifested in an increased burning rate in this range. Investigation of this phenomenon brought to light the fact that the presence of small quantities of a variety of lead compounds creates similar increases in burning rate at low pressures. Further exploration of this super-rate burning phenomenon lead to the discovery of the "plateau-burning" region and the "mesa-burning" region.

It was soon realized that platonized propellants, with their reduced temperature sensitivity in the plateau and mesa-burning range, could be used effectively to minimize the sensitivity of the performance of a rocket to the temperature of the environment. Much work has been devoted to understanding the mechanism of plateau and mesa-burning, with a view to optimizing the performance characteristics of rocket motors.

A. Summary of Double Base Propellant Burning Behavior

Considerable experimental work was conducted in the field of double base propellant burning between 1941 and 1946 (most of that work was reported in the early 1950's). During that time, many important burning characteristics of double base propellant burning processes were found and several theoretical burning rate models were presented.

(1) Thermal Decomposition Processes of Nitric Esters and Nitric Ester-Based Propellants

Generally, the primary ingredients in double base propellants are nitrate esters. Typical nitrate esters are nitrocellulose (NC) and nitroglycerin (NG) which are mixed homogeneously with stabilizers and burning rate modifiers. NC and NG have oxygen available in the form of $O\text{-}NO_2$ which attached to the organic moiety (e.g., cellulose) from which they are derived. In the burning process, some oxidizer from the nitrate group, released by thermal decomposition, reacts with the other molecular decomposition products to produce heat. In examining the details of this process, one seeks to understand how they translate into the global characteristics of double base propellants such as the pressure dependency of the burning rate and how it is effected by catalysts added to propellants.

Extensive experimental work has been performed in an effort to determine the decomposition processes of double base propellants. However, the details of the processes remain largely unknown, mainly because of the complexity of the chemical structure of double base propellants. Therefore, it is necessary to study the reaction processes of more simple nitrate esters which approximate the reaction process of double base propellants.

The simplest nitrate ester is methylnitrate which has a chemical structure of CH_3ONO_2; many investigators have studied its decomposition process. Adams[1] proposed the decomposition process as:

$$CH_3ONO_2 \rightarrow CH_3O\cdot + NO_2 \qquad \Delta H \sim 35 \text{ Kcal/mole}$$

$$\downarrow$$

$$CH_2O + 1/2\ H_2 + NO_2 \qquad \Delta H \sim 8 \text{ Kcal/mole}$$

$$\downarrow$$

$$CO,\ H_2O,\ NO,\ H_2,\ N_2,\ N_2O,\ CH_2O,\ CO_2$$

The first two reaction schemes are endothermic, however, the overall reaction is exothermic and the final flame temperature is 1800°K. The observed pressure dependence of the burning rate follows a second order rate law; the overall activation energy is consistent with the oxidation reaction by NO_2 which is the slowest step and is the proposed rate controlling step. However, the above reaction scheme is invalid for other nitrate esters even if it should have any validity for methyl nitrate as described in this subsection.

Powling[2] and others have studied the decomposition process of liquid ethylnitrate, ($C_2H_5ONO_2$), at atmospheric pressure. They measured the variation of chemical composition with distance through the flame by gas sampling techniques and found that no nitrogen dioxide was observed in the products even near the decomposing surface. Similar results were obtained by Hicks.[3] On the other hand, Adams and Bawn[4] suggest from their experimental results (1) that the primary step in the decomposition of gaseous ethylnitrate is again the breaking of the $C_2H_5O\text{-}NO_2$ bond, (2) that the measured activation energy corresponds to the $O\text{-}NO_2$ bond strength, and (3) that consequently, the decomposition rate obeys a first order law.

Levy[5,6] proposed a decomposition mechanism of ethylnitrate. The ethoxy radical produced by the breaking of the $O\text{-}NO_2$ bond decomposes to an aldehyde and some radicals. The reactions of the aldehyde with radicals and nitrogen dioxide require little or no energy of activation and proceed, therefore, more rapidly than the decomposition of the nitrate ester. All these mechanisms are consistent with the Powling results if the nitrogen dioxide is removed so rapidly by reactions with radicals that its concentration is too small to be observed experimentally.[1]

The proposed decomposition process of ethylene glycol dinitrate is:[1]

$$\begin{matrix} CH_2ONO_2 \\ | \\ CH_2ONO_2 \end{matrix} \rightarrow \begin{matrix} CH_2O\cdot \\ | \\ CH_2ONO_2 \end{matrix} + NO_2 \qquad \Delta H \sim 35 \text{ Kcal/mole}$$

$$\begin{matrix} CH_2O\cdot \\ | \\ CH_2ONO_2 \end{matrix} \rightarrow 2CH_2O + NO_2 \qquad \Delta H \sim -27 \text{ Kcal/mole}$$

The breaking of one O-NO_2 bond gives a free radical which decomposes to formaldehyde and nitrogen dioxide. Powling and Smith[7] studied the decomposition process of butane -2, 3-diol dinitrate at atmospheric pressure by infrared spectroscopic methods. The results of the spatial variation of composition measurements show that the concentration of nitrogen dioxide and acetaldehyde decreases rapidly above the decomposing surface and the concentration of nitric oxide increases until the location where the nitrogen dioxide completely disappears (about 2mm from the surface). A steep temperature gradient is observed above the decomposing surface until nitrogen dioxide disappears and the concentration of nitric oxide becomes constant. It is concluded that NO_2 reduction to NO by the oxidation of acetaldehyde just above the surface controls the rate of decomposition of the dinitrate. Powling notes further evidence for this in the fact that the flame speeds for the combustion of such dinitrates are identical with those of mixtures of nitrogen dioxide and the appropriate aldehyde. Powling also observed a similar decomposition process in the measurement of butane-1, 4-diol dinitrate which decomposes to nitrogen dioxide and formaldehyde and ethylene. The steep temperature increase and the rapid concentration decrease of nitrogen dioxide and formaldehyde are observed within 1 mm from the decomposing surface. It is proposed[8] that the dinitrate decomposes to produce equal amounts of aldehyde and nitrogen dioxide as

$$\begin{matrix} R \text{ —— } CHONO_2 \\ | \\ R \text{ —— } CHONO_2 \end{matrix} \rightarrow 2RCHO + 2NO_2$$

NO_2 is then converted to NO by the oxidation reaction with RCHO.

As is evident from the discussion, most kinds of nitrate esters appear to decompose to NO_2 and C-H-O species with the breaking of the O-NO_2 bond as the initial stage. A strong heat release occurs in the gas phase near the decomposing surface due to NO_2 reduction to NO with the accompanying oxidation of C-H-O species to H_2O, CO, and CO_2. NO reduction to N_2 in similar circumstances is a strongly exothermic reaction, however, the rate of reaction is slow and the reaction is not observed in the decomposition of some nitrate ester systems. Even when the reaction occurs, the heat release does not contribute to the heat feedback to the surface because the reaction occurs at a distance far from the surface.

The nature of the decomposition process in various nitrate esters is summarized by Adams and Wiseman,[1] Huggett[9] and Adams.[8] They show that the decomposition process can

be divided basically into three stages for simple nitrate esters as follows:

Stage 1. $RONO_2 \rightarrow NO_2$ + organic molecules (mainly aldehydes)

Stage 2. NO_2 + organic products of stage 1

$\rightarrow$ NO + H_2, CO, CO_2, H_2O at low pressure

Stage 3. NO + H_2, CO etc. $\rightarrow$ N_2 + CO_2, H_2O, etc. at high pressure

Stage 2 occurs at high or low pressure.

Whether nitrogen dioxide is the initial decomposition product of nitrocellulose and of double base propellants is of great interest in the effort to understand the physical and chemical picture of the combustion process of double base propellants. Various kinds of experimental methods to find NO_2 have been used by many investigators. Crawford, Huggett and McBrady[10] collected the gaseous products from low-pressure combustion of a double base propellant. Large amounts of NO were found but no NO_2 was seen. Heller and Gordon[11] also did not observe NO_2 in the gaseous products given off by a burning double base propellant for a wide range of pressure using a gas sampling technique. Powling and others[12] used a gas sampling probe to analyze the combustion products. No nitrogen dioxide was found even when the gas was sampled near the burning surface. However, during the burning of a nitrocellulose strand, a small amount of NO_2 was found near the burning surface of the strand and was not found at 10 mm above the burning surface. Dickson, et al[13] investigated the combustion products of a double base propellant with a rapid-scanning infrared spectrometer at 100 to 150 psig. NO_2 was never observed.*

Robertson and Napper[14] found that the decomposition process of double base propellants was autocatalytic, NO_2 being evolved first and then reacting to increase the rate of nitrogen dioxide evolution. The first step of the decomposition is also discussed by Wilfong and others[15] as being the breaking of the RO-NO_2 bond, followed by production of complex organic gases. Rideal and Robertson[16] found 10 percent NO_2 in the gases which were evolved from heated nitrocellulose at 160°C under low pressure. Recently May,[17] and White and Morgan[18] found NO_2 from the decomposi-

*The failure to observe NO_2 only indicates that sampling and measurement techniques of those investigators were such as to allow the reduction of NO_2 to NO to take place.

tion products of a double base propellant by "electron spin resonance" technique at subatmospheric pressures. Gelernter, et al[19] and Shafizadeh, et al[20] reported the existence of NO_2 in the initial products of the slow thermal decomposition of nitrocellulose.

However, Dauerman, Salser and Tajima,[21,22,23] using a mass spectrometer, reported a basically different process in the initial decomposition of double base propellant from the results observed by other investigators. They reached the conclusion that nitrogen dioxide is not the initial product of decomposition of double base propellants: the initial product appeared to be nitrogen trioxide*. They propose that the first step of the decomposition is the breaking of the $R\text{-}ONO_2$ bond producing NO_3, followed by the decomposition to NO_2 or NO. So far many gas sampling, infrared analytical and mass spectrometer techniques have been applied to the first stage decomposition products, but no other experimental results similar to those of Dauerman, Salser and Tajima have been reported.

(2) Gas Phase Reactions of NO_2 and NO

Since the previous discussion indicates that NO_2 and then NO are the principal oxidizers produced in a double base propellant flame, we will examine the gas phase reactions of these materials more closely.

It is important to understand the reaction mechanism of aldehydes with nitrogen dioxide since these are the major decomposition products of nitrate esters in the first stage of combustion. Pollard and Wyatt[24,25,26] studied the combustion process of formaldehyde and nitrogen dioxide mixtures at subatmospheric pressures. They found that the reaction occurs very rapidly at temperatures above 160°C, and that the NO_2 is reduced almost quantitatively to nitric oxide, and the aldehyde is oxidized to carbon monoxide, dioxide and water. The order of reaction was one with respect to both the reactants. The same result is reported by McDowell and Thomas.[27] The proposed reaction steps are

$$CH_2O + NO_2 \rightarrow CH_2O_2 + NO$$

$$CH_2O_2 \rightarrow CO + H_2O$$

$$CH_2O_2 + NO_2 \rightarrow CO_2 + H_2O + NO$$

*Dauerman, et al, never observed NO_3 directly. The conclusion was based on the fact that the NO_2/NO ratio found by mass spectrometry exceeded that from NO_2 alone. However there are other possible sources for the excess NO_2.

They found the flame velocity is independent of pressure and the maximum velocity is 140 cm/sec for a mixture containing 43.2% HCHO (mol %). The velocity depends significantly upon the mixture ratio, for example, it drops about half this value for a mixture containing 60% HCHO. Powling and Smith[7] measured the flame velocity of acetaldehyde and nitrogen dioxide mixtures. The velocity is very sensitive to the ratio of CH_3CHO/NO_2, as Pollard and Wyatt observed for the flame of HCHO and NO_2. The velocity is about 10 cm/sec at 37% CH_3CHO and decreases to 4 cm/sec at 60% CH_3CHO.

The combustion of H_2, CO and hydrocarbons with NO is important in the dark zone and flame zone of double base propellants. It is well known that nitric oxide behaves in a complex way in a combustion process, in that at certain concentrations it catalyzes a reaction to promote the process, while it may inhibit the reaction at different concentrations. Sawyer and Glassman[28] attempted to establish a measurable reaction between H_2 and NO in a flow reacter at one atmosphere. Over a wide range of mixture ratios, they found that the reaction did not occur readily below temperatures of nitric oxide dissociation, except in the presence of some radicals. Cummings[29] measured the burning velocity of a mixture of NO and H_2 with a burner flame over a wide pressure range, and found it to be independent of pressure (about 56 cm/sec) between 1 and 40 atm. However, Strauss and Edse[30] found that, with a mixture ratio of 0.5, the burning velocity increased from 56 cm/sec at 5.1 atm to 81 cm/sec at 52 atm.

The mixtures of CO and NO are also difficult to ignite and only mixtures rich in NO could be ignited at 1450°C. Extensive experimental study of reaction mechanism involving NO_2 and NO was done by Sawyer.[31] He found that the hydrogen/nitrogen dioxide reaction is about 3 times as fast as the reaction of hydrogen with a 2:1 mixture of nitric oxide to oxygen, and no reaction is obtained between hydrogen and nitric oxide.

In summary, the gas phase reactions between the aldehydes and NO_2 occur easily with strong exothermicity. The rate of reaction is largely dependent on the NO_2/aldehydes mixture ratio, and is increased with increased NO_2 concentration for aldehyde rich mixtures. On the other hand, no appreciable gas phase reactions involving NO are likely to occur at less than 1000°C. The reactions discussed above are important in understanding the gas phase reaction mechanism of double base propellants as described in Section IV.

(3) Physical Picture of Double Base Propellant Burning Processes

The thermal decomposition processes of nitric ester-based propellants can be summarized as follows:

Stage 1. Nitrogen dioxide and aldehydes are produced in the thermal degradation process. This reaction process occurs endothermically in the solid phase and/or at the burning surface.

Stage 2. The nitrogen dioxide exothermically oxidizes the aldehydes and other C-H-O species producing nitric oxide. This reaction process occurs very rapidly in the early stages of the gas phase reaction zone and probably occurs in the solid phase and/or at the burning surface.

Stage 3. The oxidation reactions of organic molecules produced at stage 3 by the nitric oxide to produce nitrogen, carbon dioxide, carbon monoxide, water, etc. These reactions occur very slowly in the gas phase, exothermically, only when the temperature is high enough.

The above reaction stages are about the same as the reaction stages of simple liquid nitrate esters summarized by Adams.[1] Huggett[9] presented a scheme of the reaction processes of a double base propellant as shown in Figs. 3 and 3A, which was based on the experimental observations of Crawford, Huggett and McBrady,[10] and Klein and others.[32] Each reaction stage is separately named; the zone of stage 1 is the "subsurface reaction zone", or "foam zone"; the zone of stage 2 is the "fizz zone"; the zone between stage 2 and stage 3 is the "preparation zone", or more commonly the "dark zone"; the zone after stage 3 is the "flame zone".

The main object of this investigation is to find out the location and mode of action within this multi-stage combustion wave of such burning rate modifiers as lead and copper salts.

B. Theoretical Burning Rate Models of Double Base Propellants Proposed by Previous Investigators

Combustion models for double base propellants have been developed by a number of investigators. An early study was that made by Boys and Corner,[33] and Corner.[34,35] The physical basis of their treatment is that a single stage gas-phase reaction is rate controlling and the reaction front will, therefore, automatically adjust its position relative to the surface so that combustibles are supplied at the proper rate via thermal decomposition at the surface.

Rice and Ginell[36] and Parr and Crawford[37] extended the gas phase reaction mechanism to spatially divided successive reaction zones. The method applied by Rice and Ginell assumes the reaction zone to be divided into three parts. The first zone just above the burning surface is called the fizz zone, the second zone is called the preparation zone and the final third reaction zone is called the flame zone. In the fizz zone a second order reaction occurs, but they simply assumed the heat release occurs instantaneously in a plane at the end of the zone. In the preparation zone following the fizz zone no heat is evolved; it is simply the preparation stage for further reactions. In the flame zone a second order reaction is assumed and heat is released again, in a plane at the end of the zone. Heat conduction back toward the burning surface occurs throughout the gas reaction zone. The basic assumption in their theoretical model is that the activation energies of both gas phase reactions are sufficiently low that these reactions do not depend strongly on temperature. They assumed that the required time, τ, to traverse the distance of each separate zone (at the end of which heat is produced) is independent of temperature and only a function of pressure. τ is defined as

$$\tau = 1/kp^{n-1}$$

where p = pressure, n = order of reaction and k = reaction rate constant. Generally, k is expressed as $k = Z \exp(-E/RT)$, where Z = collision frequency, R = gas constant, E = activation energy and T = temperature. They assumed k is constant.

Parr and Crawford applied a different mathematical treatment to the same physical model. They used the same type of successive integration of the combined energy and reaction rate equations (as Boys and Corner's) in the spatially divided zones without introducing planar heat release zones. They considered the "foam zone" as an additional zone between the fizz zone and the burning surface. The foam zone is assumed to be a liquid-and-gas mixed bubbling layer covering the burning surface.

The essential difference of the Parr and Crawford model from Rice and Ginell model is that Parr and Crawford assumed a first order reaction with respect to pressure at the interface of the gas and solid phase; however, Rice and Ginell assumed an Arrhenius type, zeroth order reaction with respect to pressure, at the burning surface. These theories can be made to reasonably fit experimental data for normal propellant compositions by proper selection of the parameter values, for example, activation energy, pre-exponential factor, and heat of reaction, in each of the separate zones.

Adams[1] proposed a different reaction scheme from that of both Rice and Ginell and Parr and Crawford. He assumed that an exothermic zeroth order reaction occurs at the burning surface to produce a gaseous product which is then converted to an intermediate product by a first order reaction. The intermediate product is converted to a final combustion product. All the reaction processes are considered to be exothermic. Adams included the diffusion equations for the reacting species together with the conservation of mass and energy equations. The solution of this model, with the assumption of unit Lewis number for each species, gives an explicit expression for mass burning rate. However, the equation does not contain an explicit dependency on pressure, therefore, the derived burning rate equation is not complete. The burning surface temperature in the equation must be expressed by some other relation in terms of pressure, but Adams does not give any such relation.

Wilfong, Penner and Daniels[15] proposed a surface decomposition theory which assumed that the rate determining step was the first order decomposition reaction at the burning surface. They considered that the rate of decomposition was proportional to the number of nitrate ester groups and the rate of breaking of $O\text{-}NO_2$ bonds. The calculated burning rate, with an assumed activation energy and frequency factor, requires a burning surface temperature of about 1000°C to give the measured burning rate. However, this temperature is very high compared with experimentally observed values, as described in Section VI. In their hypothetical model the effect of pressure on the burning rate does not appear and the heat generated in the gas phase plays no explicit role in determining the burning surface temperature.

Huggett[9] and Geckler[38] have presented reviews of the theoretically derived burning rate equations described above. Spalding[39] discussed the burning rate equations qualitatively from a theoretical viewpoint and introduced some important results; (1) When the surface decomposition is highly exothermic, the gaseous flame tends to be blown away at low pressures. In this region also the pressure exponent will be zero. (2) As the surface temperature rises, the burning rate in the gas phase decreases at fixed pressure. (3) Decomposition via a foam reaction as Parr and Crawford described can be handled in much the same way as decomposition by a surface reaction as Rice and Ginell used in their model.

The burning rate equations discussed above are useful in comparing with experimental data for deducing the rate controlling steps of the combustion processes of double base propellants. Furthermore, the location of lead compound action can be indicated from the burning rate equations when

quantitative experimental data are applied to the equations. The burning rate equations of the super-rate burning are discussed in Section VII-B.

C. The Nature of Super-Rate, Plateau and Mesa Burning

The super-rate, plateau and mesa-burning characteristics of platonized double base propellants have been defined in Section I. The first published reference to the latter was from the Allegheny Ballistics Laboratory (ABL) in 1948.[40,41,42] Since then, extensive work has been carried out, largely with metal compounds, in developing super-rate, plateau and mesa-burning propellants for practical use. For a time it appeared that the addition of a wide variety of metal compounds increased the burning rate. However, the increases in burning rate so obtained were insignificant compared with the increases obtained when lead compounds were added to propellants. Furthermore, it was recognized that metal compounds other than lead compounds did not give plateau and mesa burning in the pressure range of rocket combustion. Thereafter, the search for metal compounds giving plateau burning was focused largely on lead compounds; it was soon discovered that most lead compounds in adequate amounts give plateau type burning.[43,44]

The pressure index is commonly used to evaluate the effectiveness of catalysts in producing plateau and mesa burning. The pressure index is approximately zero for plateau burning and is negative for mesa burning as shown in Fig. 2. The pressure index and the domain of super-rate, plateau and mesa burning are greatly dependent upon the physical and chemical properties of lead compounds, properties such as quantity, particle size, and chemical structure. Figure 4 shows the relationship between pressure and the minimum measured pressure index for various kinds of lead compounds, based on the results of Preckel.[45] The definition of pressure index used in the figure is approximate but the general effects of lead compounds on combustion in the given pressure range are readily observed. Several kinds of lead compounds such as $PbBr_2$, PbI_2, and $PbCl_2$, do not yield a reduced pressure exponent. Preckel[45,46,47,48] studied the effects of various kinds of lead salts and found that aliphatic lead salts give plateau burning at low pressures with low burning rate, while aromatic lead salts give plateau burning at high pressures with high burning rates.

Camp[49,50] carried out extensive studies of the relationship between additives and temperature sensitivity of the burning rate vs pressure curves. Typical results of these studies are shown in Fig. 2. With super-rate and plateau burning, the temperature sensitivity decreases as pressure is increased; moreover, the lowest temperature sensitivity always appears at the upper end of the plateau burning region,

i.e., in the mesa burning region. At pressures above that of mesa-burning, greatly increased temperature sensitivity is observed. Camp made a further observation that, between certain initial propellant temperatures, there is negative temperature sensitivity in the mesa burning region of some propellants. No negative temperature sensitivity has been reported in the super-rate and plateau-type regions. Preckel[51] reported that the temperature sensitivity of typical catalyzed propellants in the rocket pressure range is about 0.1%/F compared with at least 1%/F for noncatalyzed propellants, hence their great usefulness in widely varying temperature environments.

(1) Burning Rate Behavior of Catalyzed Double Base Propellants

Preckel[51,52] found that higher lead salt concentrations move the region of plateau burning to lower pressures and consequently lower burning rates, and that the reverse shifting of the plateau occurs when carbon powder is added to plateau-burning propellants. However, he found that above 0.5% carbon, the plateau-slope increases with increasing carbon content, at a less-than-proportional rate and the relative increase of plateau pressure falls off. Above 1% carbon the plateau disappears. Small-particle carbon powder apparently result in higher burning rates but with particles greater than 0.1μ in size, little or no rate increase is observed. Preckel observed a similar effect on plateau burning when hydrated alumina or acetylene black were added to plateau propellants. However, titanium oxide, magnesium oxide and levigated alumina are not effective in this regard. This experimental result indicates that solid carbon is not the only catalyst to enhance super-rate burning; there are others such as copper salicylate as described in Section II-A-(6). Examinations of Preckel's data reveal that the effectiveness of solid carbon in enhancing super-rate burning increases as the specific area of the carbon particles is increased. The solid carbon particle sizes used by Preckel are much smaller (0.01 ∿ 1.0μ) than that of other additives.

Camp and others[53] and Preckel[52] obtained an important experimental result, i.e., the effectiveness of lead compounds in producing super-rate burning decreases as the propellant's heat of explosion increases. This implies that propellants with lower content of NG or lower nitrated NC are more strongly influenced by lead compounds.

Powling and others[12] examined the effects of metal oxides on burning rate, and found that the burning rates of the propellants containing Fe_2O_3, Co_2O_3, CuO, ZnO, SnO_2 and Al_2O_3 increased linearly with pressure, i.e., no plateau and mesa-burning was observed. PbO was the only metal oxide to

produce super-rate, plateau and mesa burning. The increased burning rate at low pressure with PbO was much higher than that with other metal oxides. The burning rate of the basic propellant was reduced by the addition of MgO and NiO over the entire pressure range in which the tests were conducted. Finally, it is reported that metallic nickel powder decreases the burning rate at low pressures and causes a slight increase at high pressures.[54]

(2) Burning Rate Behavior of Catalyzed Liquid Nitrate Esters

In an attempt to understand the combustion mechanism of catalyzed double base propellant, several investigators conducted experiments to measure the burning rate of strands of liquid nitrate-esters. The various measurement techniques were very similar to that in a conventional solid propellant strand-burner. The liquid esters were kept in a tube shaped container, and the liquid surface regression speeds were measured by optical methods or by the fuse-wire method used in solid-propellant strand burners. The only important difference between the solid and the liquid strand burning-rate measurements is that the liquid strand-burning speed is very much dependent on the diameter of the container.

Steinberger and Carder[55,56] measured the burning rate of liquid strands comprised of 63% nitroglycerin and 37% diethyleneglycol. When 5% of lead aspirate was added to the basic liquid strand, they observed an increased burning rate between 600 and 2000 psi. This effect is qualitatively the same as in the case of a double base propellant. The burning rate of the liquid strand was increased by 70 percent at 1000 psi, by the addition of the lead aspirate.

Powling and others[12] measured the burning rate of ethyl nitrate, butane-2,3-diol dinitrate, glycol dinitrate and a glycol dinitrate/triacetin mixture. They used lead acetylsalicylate as a catalyst: it is slightly soluble in the liquid nitric esters. They concluded from their experimental results that catalysis by the lead salt occurs in all cases, but that the effect is never pronounced. However, the mixture of glycol dinitrate and 3 percent of lead acetylsalicylate yielded a substantially higher burning rate, 47 percent higher than that of the basic glycol dinitrate at 500 psig. They also observed very slight negative catalysis with certain mixtures.

Extensive burning rate measurements on liquid propellants have been carried out at the Naval Ordnance Test Station, China Lake, California. Whittaker and others[57] observed mesa burning between 1600 and 1800 psi with a liquid system without lead compounds. The liquid system consisted of 2-nitropropane (33% by weight) - 95% nitric acid (67%).

Adams and Lloyd[58] observed mesa burning with a liquid system consisting of glycol dinitrate, triacetin, NC and lead acetylsalicylate.

From the above discussion, it is concluded that it is possible to produce super-rate, plateau and mesa-burning with liquid nitric esters, however, the effect is not as pronounced or as common as it is in the case of leaded double base propellants. In fact, it is reported that gelling the liquid nitric esters produces greater super-rate burning effects than one gets with these same materials in their normal fluid state.[12,58]

(3) The Effect of Lead Compounds on Gas Phase Reactions

It has been shown by many investigators that gas phase reactions of nitrate esters are affected by the addition of lead compounds. Adams, Parker and Wolfhard[59] studied the gaseous combustion zone of ethylnitrate. The temperature of the flame was about 1200°K at atmospheric pressure, and the gaseous products were 28.9% NO, 3.7% N_2, 2.5% N_2O, 7.0% H_2, 30% CO, 2.5% CO_2, and 25.4% CH_4. The addition of 0.1 ~ 1.0% by weight of lead tetramethyl to the ethyl nitrate reduced the flame temperature to 800 ~ 900°K; moreover, the burning rate was reduced by a factor of 3. The combustion products were 47.5% NO, <0.1% N_2, 1.4% N_2O, 4% H_2, 21.7% CO, 6.7% CO_2, and 17.9% CH_4. It was observed that the reduction-reaction involving NO is inhibited by the addition of lead tetramethyl; however, it is difficult to conclude from this that the lead tetramethyl is active in the inhibition of the reduction reaction at stage 3 of the flame [see Section II, A,(3)]. It is possible that the formation of NO is affected by lead tetramethyl early in the decomposition stage, i.e., at stage 1 or the gas phase reaction involving NO_2 at stage 2 with reduced temperature at this stage. The above authors examined the effect of alkyl radicals on the flame speed by using different kinds of metal alkyls. They concluded that the flame speed is not affected by alkyl radicals and that the inhibiting effect is due to the high degree of dispersion of the lead oxide formed during oxidation.

Ellis, Smythe, and Treharne[60] studied the effect of lead oxide on the thermal decomposition of ethyl nitrate vapor. They proposed that the presence of a small amount of PbO-particle surface could retard the burning rate due to the destruction of radicals. However, the presence of copper surface accelerates the thermal decomposition of ethyl nitrate, and the rate of the decomposition process is controlled by a reaction step involving the NO_2 molecule. Chamberlain, Hoare and Walsh[61] studied the inhibiting effect of lead oxide on hydrocarbon oxidation in a vessel coated with a thin film of PbO. They suggested the importance of the process of aldehyde-oxidation by the PbO. Bardwell[62] obtained a similar

result: he found that lead oxide acts as a powerful inhibitor in suppressing cool flames and low-temperature ignitions.

Hoare and others[63] proposed the following reaction scheme of formaldehyde on the surface of the lead oxide:

$$CH_2O + PbO \rightarrow CO_2 + H_2 + Pb$$

The re-oxidation of lead at 330°C was expected to occur rapidly; the surface of the lead oxide then would remain unchanged in the presence of oxygen. They concluded that, as a consequence, general hydrocarbon combustion in which formaldehyde is a degenerate branching intermediate is inhibited in the presence of PbO by the rapid removal of formaldehyde.

It is well known that a small amount of lead tetraethyl is effective as an antiknock agent in gasoline engines. This effect is due to the inhibition of the gas-phase reaction by the lead or lead oxide, which are derived from the lead tetraethyl.[64,65]

In summary, it may be said that the inhibiting action of lead compounds on hydrocarbon combustion occurs largely in the gaseous phase of the combustion zone.

D. Plateau Propellant Combustion Models Proposed by Other Workers

Exte[illegible]xperimental work has been done in the field of catalyz[illegible]ouble base propellant burning, and several qualitative combustion models have been presented to explain the super-rate, plateau and mesa-burning phenomena. These models can be divided into two classes, namely, "condensed phase models" and "gas phase models". The classification is based on the assumed region of catalyst-activity in accelerating or decelerating the burning rate.

A condensed-phase model has been proposed by Camp and co-workers.[66,67] They propose that the absorption of radiant energy below the burning surface of a catalyzed propellant plays a dominant role in the production of super-rate burning. They argue that photochemically induced, subsurface reactions are largely responsible for promoting the normal burning rate. They observed that their hypothesis requires the following to be true:

1. The super-rate burning should increase when the radiation intensity of the flame is increased.

2. The super-rate burning should be a maximum when the absorption of radiant energy is a maximum in the surface sub-layer.

3. Super-rate burning should not occur if the propellant is rendered opaque.

The above authors observed a significant increase in the burning rate upon the addition of 0.05% of fine aluminum powder (a strong radiator) to a plateau-type propellant. However, upon the addition of 5% of the powder, the super-rate of the propellant was reduced to half its original value. The addition of 20 and 30% of the metal produced almost complete suppression of the mesa characteristic, while the corresponding noncatalyzed propellant burning rate was increased to 10 to 15% above normal by the addition of the same amount of the metal. Similar behavior was observed upon the addition of carbon black: at very low concentrations (about 0.05 to 0.10%), there is an enhancement of super-rate burning, but above 0.5%, burning the mesa burning disappears. This enhancement of super-rate burning by carbon black is also reported by Preckel.[51] Camp and co-workers concluded that the experimental results justify their hypothesis: for, when the aluminum or carbon-black powder concentration is low the addition of these materials increases the radiation energy of the flame and the energy induces photochemical reaction in the surface sub-layer. This increases the burning rate as specified in item 1 relating to their hypothesis. Furthermore, when the concentration is high, the radiation energy of the flame is increased, but, if at the same time, the additive renders the propellant opaque, the radiation energy can no longer penetrate sufficiently in the condensed phase and enhancement of the burning does not occur; instead, there is a decrease in the burning rate owing to the decreased penetration of the radiant energy, as specified in item 3. Camp and co-workers also measured the burning rate of a plateau type propellant containing 1.5 $\sim$ 2.5% of an ultraviolet-light absorber such as 2, 2', 4, 4' - tetrahydroxybenzophenone or Uvinul 490. They observed significant increases in super-rate burning, and the super-rate domain was found to shift to the higher pressure side. However, the super-rate was diminished by the addition of over 5% of the ultraviolet-light absorber. They correlated the percentage of the super-rate with the transmissivity of the propellant material and conclude that ultraviolet-light is important in initiating a photochemical reaction in the condensed phase, the effective wavelength for reaction-initiation lying between 300 and 400 mμ.

In order to explain the mesa-burning phenomenon, Camp and co-workers proposed that agglomerated globules of lead metal on the burning surface shield the surface from radiant-energy transfer. They suggested that the accumulation of lead metal on the surface increases in the pressure range in which the slope of the burning-rate/pressure curve is zero or negative.

A gas phase model has been proposed by Powling and others.[12] This combustion model is based on observation of the behavior of the solid carbon generated on the burning surface of catalyzed propellants. They studied the burning surface by means of motion pictures and observed large amounts of carbon on the burning surface of catalyzed propellant during super-rate and plateau burning. Furthermore, the amount of carbon was observed to decrease at mesa-burning pressures, while no carbon was found above this range. As an aid in the interpretation of the observed results, they introduced two experimental considerations: (1) that nitric-oxide reduction during the oxidation of charcoal is catalytically accelerated by fine lead powder deposited on the charcoal as observed by Watts,[68] (2) reactions involving NO_2 are less likely to be prominent in the catalyzed step than those involving NO, and the catalytic action of lead salts occurs at, or very close to, the burning surface. On this basis, it is possible to construct the following reaction scheme;

1. Super-rate burning occurs when nitric oxide is reduced by certain exothermic reactions catalyzed by lead and by carbon generated at the surface.

2. Mesa burning occurs when the carbon is eliminated by catalyzed oxidation with nitric oxide.

3. At pressures above the mesa-burning range, the carbon is completely eliminated; consequently, the burning rate is lower than that of noncatalyzed propellants in this range.

Steinberger[69] proposed a gas phase model somewhat different from that proposed by Powling and others. He conducted several experiments to determine the region of activity of the lead compounds. Several organic lead salts were pyrolyzed in a furnace, and the decomposition products, "pyrolysates", were incorporated into double base propellants. The pyrolysates were found to be better catalysts than the salts from which they were derived. Therefore, it was concluded that the decomposition products, rather than the original salts, are the active agents in providing super-rate burning. The final products of the pyrolysates obtained at temperatures from 350°C are metallic lead and lead oxide. This led him to conclude further that the metallic lead or the lead oxide plays the important role in the production of super-rate burning, and that the organic parts of the lead salts contribute in so far as they produce finely-divided metallic lead or lead oxide. Steinberger suggested the following mechanisms for the subsequent vapor-phase reactions involving lead:

$$NO_2 + Pb \rightarrow NO + PbO$$

$$PbO + H_2CO \rightarrow Pb + H_2 + CO_2$$

or

$$NO + Pb \rightarrow PbO + 1/2\ N_2$$

$$PbO + CO \rightarrow Pb + CO_2$$

The above reaction steps are known to occur readily.[70] The effect of such catalysis is expected to be felt close to the burning surface as an increase in the heat feedback from the gas phase to the condensed phase. However, Steinberger did not discuss how the super-rate reaction steps are retarded to produce plateau and mesa burning. A reaction process similar to the above has been proposed by Preckel.[52]

Sinha and Patwardhan[71] suggested a gas phase reaction model in which the super-rate behavior is caused by the reaction between nitric oxide and free radicals produced by the lead. They proposed the following reaction scheme: the lead salts decompose to metallic lead in the condensed phase and lead alkyls. The lead alkyls decompose to metallic lead and free radicals in the fizz zone which react with nitric oxide to produce heat. Consequently, the heat transfer from the gas phase to the condensed phase is increased and super-rate burning occurs. As the pressure increases, the free radicals are removed from the fizz zone owing to the increased collision frequency and hence the heat produced by the reaction between the free radicals and nitric oxide is reduced. This results in a decrease in the super-rate behavior until eventually, the effect of the free radicals becomes negligible and the burning rate reverts to that of a normal, noncatalyzed propellant.

In summary, it can be said that the various plateau-burning models presented by previous investigators are based on different reaction schemes, each predicting the particular trends of interest to each investigator. Unfortunately, none of the models unify all of the important findings or predict the overall burning-rate/pressure relationship of catalyzed double base propellants.

E. Anticipation of Conclusions: New Model Proposed in This Study

In the four sections to follow (Sections III to VI, inclusive) we will proceed step-by-step through the various items of experimental evidence that have some bearing on the question of mechanism of double base burning and super-rate burning. It will be shown that, while some of the evidence may be taken to support either the Camp model or the Powling

model, much of the evidence tends to contradict both of them. This situation prompted the author of this study to adopt a new model, one that seems to accommodate most of the important evidence available.

The new model has the following essential features; first of all, it abandons the hypothesis (central to the Camp model) that UV radiation feedback and photo-induced reactions in the condensed phase are the basis of the observed super-rate; it abandons also the hypothesis that carbon produced by decomposition at the surface (central to the Powling model) is directly involved in the acceleration of reactions in the combustion wave. The new model rests on the hypothesis that super-rate is the result (1) of acceleration of exothermic reactions in the thin fizz zone, leading to enhanced conductive feedback of energy to the unreacted solid, and (2) that this acceleration in the fizz zone is the result of a shift in the stoichiometry of the reactions as a result of carbon formation enhancement by the catalyst. No clear-cut hypothesis is offered in this study for the sharp termination of super-rate effects that is observed in the burning rate curves of plateau propellants in the plateau region. None of the super-rate mechanisms previously advanced in the literature has within itself the required sharp cut-off mechanism, nor has the one advanced in this study. The search for a plausible mechanism for super-rate cut-off is still an unfinished task.

In the following sections, as we proceed through the various items of evidence on the mechanism of burning, the reader's attention will be drawn to the question of whether the particular experimental fact supports or does not support one or more of the three models. When we reach Section VII, the entire series of facts will be reviewed, and it will be shown that the evidence seems to favor the new model proposed in this study.

SECTION III

EXPERIMENTAL RESULTS ON BURNING RATE BEHAVIOR

The purpose of studying burning rate behavior is to obtain information concerning the behavior of catalysts during super-rate, plateau and mesa burning. In particular, in this section we will be concerned with burning rate vs pressure and how the details of this type of curve are affected by the physical and chemical nature of catalysts.

All the experimental work in this report was carried out with particulate nitrocellulose (PNC) and trimethylolethane trinitrate (TMETN) double base propellant instead of with the usual nitrocellulose (NC) and nitroglycerin (NG) propellant. However, several types of experiments were performed to compare the burning characteristics of NC/NG propellant and PNC/TMETN propellant.

The chemical structure and physical properties of TMETN are similar to those of NG. PNC and NC are created from the same material, but PNC is kept wet with at least 30% heptane. The properties are described in detail in Appendix D. The theoretical combustion products and the adiabatic flame temperature are shown in Fig. D-2 in Appendix D. The processing techniques for PNC/TMETN propellant are in use at the Naval Ordnance Station,[72] Indian Head, Maryland and a similar manufacturing technique has been developed in our laboratory. The main advantage of PNC/TMETN propellant over NC/NG propellant is that it is possible to blend the propellant ingredients in conventional solid propellant mixers such as used in the manufacture of composite propellants. Furthermore, the manufacturing process is simpler and safer since NG is not involved.

The chemical compositions and the specifications of all the propellants used in this investigation, i.e., propellant composition, particle size of catalyst and the method of catalyst distribution in the propellant, are listed in Tables A-1 and A-2 of Appendix A. The propellant manufacturing process is described in Appendix D, and the burning rate measurement technique and operating procedures are described in Appendix C-(1).

A. Experimental Results of this Investigation and Comparison with the Results of Previous Investigators.

The effects on burning rate of different types of catalysts, catalyst particle size, catalyst distribution, and nitrate ester have been studied.

(1) The Comparison of NC/NG and PNC/TMETN Burning Behavior

Figure 5 shows the noncatalyzed burning rate/pressure relationship of NC/NG and PNC/TMETN propellants. The burning rate of NC/NG propellant is higher than that of PNC/TMETN propellant. However, the pressure index is about the same, i.e., 0.7, over the pressure range between one and one hundred atmospheres. It is well known that decreasing the propellant energy lowers the burning rate. Thus, the PNC/TMETN system, having a lower energy than the NC/NG system, fits this trend.

Figure 6 shows a comparison of the burning rates of catalyzed NC/NG and PNC/TMETN propellants. Lead salicylate (1.2%) and lead 2-ethylhexoate (1.2%) were used as catalysts. The amount of NC was simply replaced by the same amount of PNC, and NG and diethylphthalate were replaced by TMETN and triethylene glycol dinitrate in order to produce roughly similar combustion products. The burning rate curves show approximately similar characteristics; at low pressures no super-rate burning occurs, while around 5 atmospheres the maximum super-rate burning occurs, and again relatively high super-rate burning takes place at about 40 atm. Above one hundred atmospheres super-rate burning is no longer evidenced and burning rates of both catalyzed propellants are almost the same as for the noncatalyzed material. In Fig. 6, the burning rate curve of the corresponding noncatalyzed NC/NG propellant is not available. The burning rate-pressure relationships of NC/NG and PNC/TMETN are not quite the same owing to small differences in chemical structure and in the energy levels of the propellants. However, the burning characteristics of NC/NG and PNC/TMETN propellant are observed to be generally similar. Therefore, the results of the burning mechanism study of PNC/TMETN type propellants should be directly applicable to NC/NG type propellants. Other evidence of similarities in combustion characteristics will be described in this section.

(2) The effect of PNC content in noncatalyzed propellants is shown in Fig. 7. An increased content of PNC gives higher burning rates over the pressure range between 1 atm and 100 atm. The pressure index of the propellant with a higher content of PNC is about the same as that of the standard propellant above 17 atmospheres; however, at lower pressures the high PNC propellant is subject to a higher burning rate and lower pressure index than the low PNC propellant.

(3) The effect of carbon content on burning rate was examined for noncatalyzed and catalyzed propellants. The experimental results are shown in Figs. 8 and 9. For PNC/TMETN type propellant, increasing the carbon content results

in an increase in burning rate at pressures over 20 atmospheres, and the burning rate is almost independent of carbon content between 10 and 20 atmospheres. Below 10 atmospheres, 0.1% carbon increases the burning rate slightly and 0.2% carbon decreases the rate. For NC/NG type propellant, the effect of carbon content is negligible at high pressures, however 1.0% and 0.3% carbon contents decrease the burning rate at low pressures, probably because the carbon absorbs the heat from the exothermic reaction in the fizz zone or at the burning surface. However, small amounts of carbon may accelerate the burning when used in conjunction with a catalyst as shown in Fig. 10; a propellant containing 0.1 percent carbon has its burning rate accelerated at low pressures. The burning rate of catalyzed propellant is clearly affected by carbon powder. A propellant containing 0.1% carbon shows considerable super-rate burning but the addition of another 0.1% carbon decreases the super-rate as shown in Fig. 10. These results do not agree with the results of Preckel,[51] which show a burning rate increase up to 1% of carbon and a shift of the plateau region to the higher pressure side.

(4) The effect of the catalyst particle size on burning rate was studied for two cases. The particle sizes of PbSa and CuSa (lead and copper salicylate) were measured with a microscope. The particles are not spherical but rather have a flake shape; therefore the definition of particle size is somewhat arbitrary. However, relative size can be defined in terms of the average size of the flakes. Small particle-size catalysts were obtained by grinding under heptane in a ballmill for 24 hours. In this way an average particle size of 3μ was obtained from the original particle size of 10μ (the particle sizes were measured under a microscope). Burning rates are shown in Fig. 11; clearly, the small particle-size catalyst gives higher super-rate burning than the larger particle size. It is observed that at pressures below 10 atmospheres the super-rate decreases more rapidly for the small particle-size catalyst. However, the general super-rate trends with respect to pressure are not affected by catalyst particle size.

(5) The effect of catalyst mixing (in the propellant prior to curing) on burning rate is shown in Fig. 12. When the catalyst powder is mixed directly with the mixture of PNC and TMETN, the mixing may not be homogeneous because of the high viscosity of the mixture. However, when the catalyst powder is first mixed and dispersed in liquid heptane and then added to the mixture of PNC and TMETN, fairly homogeneous mixing can be obtained. The graph shows the expected result that the homogeneous propellant has a higher super-rate than the non-homogeneous compound.

(6) Catalyst type has been found to effect significantly super-rate, plateau and mesa burning. The burning rate behavior of a propellant was studied with different purely metallic additives, namely Pb powder, Cu powder, and a powdered mixture of Pb and Cu. Figure 13 shows that Pb (0.98%, No. 1068) powder is more effective than Cu (0.98%, No. 1075) powder in increasing the burning rate, and that the mixture of Pb (0.98%) and Cu (0.98%), (No. 1076), produces almost the same effect as Pb alone in this regard. These metallic-powder catalysts do not give plateau-type burning; like other metallic-powder catalysts they simply increase the burning rate over the entire pressure range.

The burning rate was also measured with PbO (0.98%, No. 1081) as a catalyst. An increased content of PbO (3.92%, No. 1082) increases the burning rate at low pressures but decreases the rate at high pressures. Furthermore, it decreases the pressure index as shown in Fig. 14. Despite its super-rate effect, the PbO catalyst (5μ particle size) does not produce plateau or mesa-burning characteristics. This behavior disagrees with the results of Preckel[45] and Powling and others,[12] who obtained mesa-type burning with PbO (in an NC/NG system). The overall burning rate behavior of the propellant with PbO was found to differ from that with the purely metallic catalysts which were not effective in increasing burning rate at low pressures.

The effects of aromatic lead and copper salts on burning rate behavior have also been studied. Figure 15 shows the burning rate behavior of propellants with PbSa, CuSa and PbSa + CuSa as catalysts. PbSa (0.98%, No. 1045) increases the burning rate in the range 1 atm to 70 atm and produces plateau and mesa burning above 70 atm. CuSa (0.98%, No. 1044) increases the burning rate below 30 atm and decreases the burning rate above 60 atm. When PbSa (0.98%) and CuSa (0.98%), (No. 1047), are mixed together, enhanced super-rate burning is observed from 7 atm to 60 atm, and the plateau and mesa-type burning behavior is observed above 70 atm. From these observations, the effect on burning rate of coupling between the PbSa and CuSa catalysts can be deduced. At pressures below 7 atm the catalytic effect on the burning rate is provided by either (or both) the PbSa or the CuSa. Additional PbSa or CuSa does not affect the burning rate; apparently the rate accelerating effect is saturated. However, at pressures above 7 atm, the catalytic effect of PbSa is enhanced by CuSa and an increase in super-rate burning is observed. At pressures above 70 atm, the super-rate burning is reduced slightly by CuSa because of some rate inhibiting effect of CuSa. This same inhibiting effect is observed when only CuSa is added to the propellant. The above points will be examined further in Section V in the light of the results of micro-photographic observation of the burning surface.

An additional 0.98% of PbSa and 0.98% of CuSa, (No. 1051), does not increase the super-rate burning significantly over the entire super-rate burning pressure range as shown in Fig. 15A.

Ammonium perchlorate was added to the basic PNC propellant to illustrate the extent that a strong oxidizer can dominate the burning rate controlling processes. A double base propellant with a solid oxidizer added is commonly referred to as a composite modified double base propellant (CMDB). As seen from Fig. 16, the burning rate of basic double base propellant increases as much as 300% when the AP percentage is increased to 20%. Gas phase observation by means of high speed photographs[73,74] reveal that the flame zone is unlike double base propellant flames and more like the flames of ammonium perchlorate composite propellants. The dark zone which is observed for basic PNC double base propellant is eliminated by the addition of AP, and the luminous flame is much closer than the corresponding double base flames. It is apparent that the burning rate is controlled by the heat feedback from the diffusion type flame between AP decomposition products and fizz zone products of the double base propellants.

It should be mentioned that while the coupling effect of a lead salt catalyst with a copper salt (with the same organic moiety) is as described above, the coupling effect with another lead salt (having a different organic moiety) can be much more complicated. This is indicated in Fig. 17. The catalytic effect on burning rate of Pb2-EH (lead 2-ethylhexoate) is shown in Fig. 17. It is observed that Pb2-EH (1.2%, No. 1046) by itself produces super-rate burning in the low-pressure range and that this effect is almost negligible at pressures above 100 atm. When Pb2-EH (1.20%) mixed with PbSa (1.20%), is added to the propellant, (No. 1039), enhanced super-rate burning is observed in the pressure domains around 5 atm and between 24 atm and 60 atm, while a suppressing effect on super-rate is observed between 8 atm and 23 atm. The burning rate of the propellant catalyzed with PbSa + Pb2-EH in this latter pressure range is less than that of the propellant catalyzed with either of the two Pb-salts alone. Furthermore, a negative effect on burning rate is observed over 60 atm, as well, when Pb2-EH is added to the propellant containing PbSa.

To determine what catalytic effect, if any, the organic part of metallic salt has on burning rate, Sa (salicylic acid) was added to the basic propellant (No. 1026). Figure 18 shows that the burning rate of the propellant containing Sa only (0.98%, No. 1066) is the same as that of the non-catalyzed propellant. When lead metal powder (0.98%) is added together with salicylic acid (0.98%) to the basic propellant yielding No. 1071, the burning rate is increased

relative to that of the propellant containing only Sa. However, at pressures below 70 atm the burning rate of the propellant containing Pb and Sa was lower than that of the propellant containing only Pb. These results show that salicylic acid alone does not contribute directly to the increased burning rate observed with the PbSa catalyst; in fact, the salicylic acid tends to decrease the catalytic effectiveness of metallic lead powder at pressures below 70 atm.

B. Experimental Results on Burning Rate Behavior at Low Pressures and on Minimum Burning Pressure

Generally, a gas phase reaction is a function of pressure: the higher the pressure, the faster the chemical reaction. Therefore, at low pressures the rate of energy transfer from the gas phase to the condensed phase during propellant burning is expected to decrease, and the propellant burning is sustained largely by the condensed phase reactions just beneath the surface. Therefore, the burning rate behavior at subatmospheric pressures can provide information concerning the activity of the catalysts in the condensed phase.

The chemical compositions of all the propellants used in this investigation are listed in Tables A-1 and A-2 of Appendix A. The burning rate measurement-technique and instrumentation are described in Appendix C-(2).

Figure 19 shows the results of the experiment to determine the effect of several catalysts on burning rate at low pressures. This set of curves shows the change in burning characteristics at about 1.5 atmospheres for several kinds of propellants. It is observed in all cases that the pressure index is suddenly lowered from 0.7 to 0.2 below the pressure of 1.5 atm. However, the curves show that the burning rates are different with different catalysts. The behavior of the noncatalyzed propellants is such that the burning rate becomes nearly independent of pressure below approximately 1.5 atmospheres and the burning is extinguished below 0.35 atmospheres. A similar trend is observed for the burning of a propellant with 1% PbSa as a catalyst. However, the minimum burning pressure of the propellant with CuSa 1% is clearly different from that of the other propellants, as shown in Fig. 20.

The minimum burning pressure of the propellant containing 1% PbSa and 1% CuSa is about the same as that of the propellant containing 1% CuSa. It is interesting to compare the activity of CuSa and PbSa as burning-rate catalysts. The burned surface of extinguished samples of a propellant with CuSa or PbSa as the catalyst was observed under a microscope. It was found that the surfaces of both propellants

were covered with large amounts of carbonaceous particles. However, a difference was noted in that some crystalline white and translucent particles on the carbonaceous particles were observed for propellant containing 1% CuSa as shown in Fig. 21. The translucent particles were found to be similar to those which occur during the slow decomposition (at 180°C) of CuSa. However, such particles were not seen on the carbonaceous residue of the propellant containing PbSa. Also the slow decomposition (up to 220°C) of PbSa does not reveal such particles. It is possible, from these observations, that the minimum burning pressure is lowered by the action of finely divided metallic Cu powder, which is formed by the decomposition of CuSa and is distributed over the carbonaceous particles. These decomposed products seemed to be similar to products called "pyrolysates" by Steinberger.[69] It is known that NO is reduced to N_2 by carbon at low pressures. Watts[68] found that carbon treated with metallic Cu powder is more effective in reducing NO concentrations than is untreated carbon; the reaction was first order as regards NO concentration. This behavior lends support to the hypothesis put forward above, i.e., that the minimum burning pressure is lowered by the effect of Cu powder dotted on carbon residue, the Cu powder resulting from the decomposition of the propellant. In fact, the temperature profile measurements show a higher gas phase temperature which occurs when CuSa is added to the propellant. This is described in Section VI.

The minimum burning pressure of the propellant containing 1% metallic copper powder was lowered only slightly. This can be explained by the fact that the particle size of metallic copper powders ($\sim$ 6μ) is much larger than that of the copper powders generated by decomposition of CuSa, and that the effective catalytic surface area is therefore insufficient to promote burning. It is considered that when CuSa is decomposed in the subsurface zone or at the burning surface, Cu is dispersed on a molecular level at the first decomposition stage. Watts[68] also found that carbon treated with metallic lead powders was effective in reducing nitric oxide in an exothermic reaction, but not as effective as carbon treated with copper. It should be noted that the minimum burning pressure is not lowered by the addition of PbSa, for the reason that Pb is not generated from PbSa during burning at subatmospheric pressures, when the temperature field is too low to decompose the PbSa. This appears to be the case from observations under a microscope of a carbonaceous residue, which do not indicate any crystalline particles generated by the decomposition of PbSa.

Another observation is that the burning rate is decreased by the addition of ammonium polyphosphate, $(NH_4)_2(PO_3H)_m$, and oxamide, $(CONH_2)_2$. When ammonium poly-

phosphate (3.0%, No. 1089) is added to the basic propellant (No. 1026), the burning limit pressure of the latter is lowered. Observation of the burning surface shows that large amounts of carbon are generated at the surface by the addition of ammonium polyphosphate, as shown in Fig. 22, and that the burning surface is consequently protected from heat loss to the surroundings (it should be noted, however, that Powling and others[12] observed no carbon on the burning surface when 1.3% $(NH_4)_2HPO_4$ was added to a propellant). The validity of the conclusion regarding blocking of heat loss was examined by changing the orientation of the burning propellant-strand. When the propellant strand was kept horizontal and one end was ignited, the burning was easily extinguished after it had become steady, this tendency being caused by the falling of the carbonaceous residue from the burning surface. It is concluded that the carbon residue is important for the continuation of steady burning and for lowering the minimum burning pressure.

C. Summary of Experimental Observations of Overall Burning Rate Behavior

It was shown that lead compounds, other metallic compounds, metal powders and carbon powder increase the burning rate of double base propellants. However, lead compounds should be distinguished phenomenologically from other catalysts because lead compounds are the only catalysts producing super-rate,plateau and mesa burning; this super-rate, plateau and mesa burning is very sensitive to the quantity, particle size, distribution in the propellant and the addition of other catalysts as discussed in this section.

Copper salicylate, CuSa, is effective in producing a higher super-rate burning when it is added to a low super-rate propellant, while CuSa alone is not effective for producing super-rate burning. The dominant domain of action of CuSa in the reaction process appears to be different from that of PbSa. On the basis of the results here and the results of the burning surface observations described in Section V it appears that CuSa acts mainly in the early stage (subsurface) and PbSa acts mainly in the latter stages (above the surface); the action of CuSa enhances the action of PbSa. Figure 15 shows the enhancement of super-rate burning by CuSa; the peculiar effects of CuSa are kept even when CuSa is added to a super-rate burning propellant containing PbSa.

SECTION IV

THE STRUCTURE OF THE GAS PHASE ZONE

The transfer of energy from the gas phase to the burning surface by conductive heat feedback is the main driving force for maintaining continuous burning of double base propellants at rocket operating pressures. The heat generated at the burning surface is approximately independent of burning pressure as described in Section VI, whereas heat feedback from the gas phase increases with pressure and therefore becomes the dominant source at high pressures. The conducted heat from the gas phase to the surface promotes two processes: heat up of the propellant from the initial propellant temperature to the surface temperature and production of gaseous products at the burning surface (this gasification may also produce heat promoting both processes). Thus, the reaction processes in the gas phase are an important factor in determining the burning rate behavior of the propellants. This section compares the gas phase reaction structures of catalyzed and noncatalyzed propellants as an aid in understanding of catalyzed propellant burning mechanisms.

A. General Discussion of the Gas Phase Reaction Zone

It is well known that when a strand of double base propellant burns at pressures below about 7 atm, the flame is non-luminous; thus burning without a luminous flame is called "fizz burning". As pressure increases, a luminous flame appears at some distance from the burning surface; this burning with a luminous flame is called "flame burning". Further increases in pressure cause the luminous flame to approach the surface more closely. The phenomenon was first observed by Crawford and others.[10] They measured the distance between the burning surface and the luminous flame position (i.e., the length of the dark zone), for pressures between 20 and 70 atm and found that the distance is inversely proportional to the cube of the pressure. This observation will be discussed later in this section.

The temperature profile in the gas phase has been measured by several workers by means of fine thermocouples embedded in propellant samples (e.g., 32,75). Similar measurements were made in this investigation and the results are described in Section VI. It has been established that a very steep temperature gradient exists just above the burning surface, i.e., in the fizz zone. Approximately 200 microns above the surface, the temperature gradient becomes less steep, i.e., in the dark zone, and the gradient rapidly increases again as the luminous flame zone develops, i.e., in the flame zone. However, no second steep temperature gradient is observed in the case of fizz burning because of the absence of the luminous flame. The temperature pro-

file through a double base propellant combustion wave is schematically shown in Fig. 3.

Davis[108] studied the reaction mechanism of the dark zone and luminous flame zone of double base propellants by means of a fast-scanning infrared spectrometer. He found little change in the infrared emission spectra as the distance from the burning surface increases. From his data he concludes that the concentrations of the predominant species causing the emission, namely H_2O and CO_2, do not change appreciably beyond the fizz zone. The conclusions of Davis are not consistent with the data of Maltsev[103] which showed increases as large as 50% in the H_2O and CO_2 infrared emission levels within the fizz and flame zones.

B. Observations of the Gas Phase Zone of Catalyzed Propellants by Previous Investigators

Various kinds of experimental techniques have been used to study the gas-phase reaction mechanism of double base propellants, i.e, techniques such as the measurements of heat of explosion, gas composition analyses, and the measurements of temperature profiles through the combustion zones.

Heats of explosion of catalyzed and noncatalyzed propellants were measured by several investigators[76,77,78,51]. Lenchitz and Haywood[76] measured heat of explosion at various pressures with great precision. They found in the super-rate region (p = 10 atm) that the heat of explosion (~530 cal/g at low pressure) of propellant modified with lead stearate is 40 cal/g higher (about 8% higher) than that of non-modified propellant, whereas the burning rate of the modified propellant is approximately twice that of the non-modified propellant. However, as the degree of super-rate decreases (above 35 atm) with increasing pressure, the difference in the heat of explosion between the modified and the non-modified propellants decreases. Above the mesa region, the heats of explosion of both the modified and the non-modified propellants are constant above 40 atm. Above 40 atm, the heat of explosion of the modified propellant is approximately 70 cal/g less than that of the non-modified and the burning rate of the modified is less than that of the non-modified. Also, above the mesa region, Lenchitz found that the heat of explosion of the modified propellant was approximately the same as a reference propellant in which lead stearate was replaced entirely by relatively inert materials (the materials were not disclosed) which were used in the basic formulation.

Crawford, Huggett and McBrady[78] measured the heats of explosion of a catalyzed propellant containing nickel metal powder and a corresponding noncatalyzed propellant. They

observed that the heat of explosion of the catalyzed propellant increased rapidly with increasing pressure and that complete combustion was virtually achieved at 350 psi. The measured maximum value was 1200 cal/g. However, the heat of explosion of the noncatalyzed propellant was approximately 650 cal/g at 350 psi and achieved the maximum value, 1200 cal/g above 700 psi.

Maltsev and Summerfield[79] studied the emission spectra of catalyzed and noncatalyzed double base propellant as an aid in determining the site and mode of action of platonizing catalysts. They found a substantial change in the emission spectrum of the gaseous flame for propellants catalyzed by CuSa; the extensive band system of CuH* appeared, increasing the near ultraviolet to blue intensity of the flame. The burning rate of the propellant containing 1% CuSa was increased 50 percent over noncatalyzed propellant at the same pressure. This increased radiation energy due to the addition of CuSa could possibly increase the burning rate by promoting photosensitized reactions in the subsurface zone, as proposed in Camp's super-rate burning model. However, when PbSa was added as a catalyst, no appreciable change of the emission spectrum in the composition of the products were observed, except Pb lines.

The gas phase of a cellulose acetate and nitroglycerin gel with and without lead acetyl salicylate, was probed by Powling and others.[12] They found that a greater reduction of NO (to N_2) occurred at any given distance from the decomposing surface when the propellant was catalyzed by the lead compound. They concluded the greater reduction of NO occurred as the result of the catalysis by solid carbon, which was formed on the decomposing surface. However, such increased reduction of NO was not observed when a lead compound was added to nitrocellulose even though the burning rate doubled. When lead stearate was added to a double base propellant, it increased NO reduction approximately 2 percent by volume compared with a nonleaded propellant. This observation was made at the burning surface, whereas a small reduction of NO concentration was observed at a distance of 1 cm from the burning surface in the dark zone. They found a similar effect of pressure on the decreasing NO concentration as in the case of liquid nitrate esters.

Lenchitz and Haywood[76] measured the ratio of carbon dioxide to carbon monoxide for catalyzed and noncatalyzed propellant combustion products using the "Orsat" method. When super-rate burning occurs the ratio in the catalyzed products is almost twice that in noncatalyzed products, but, as the super-rate decreases with increased pressure the ratio reaches the same value for both cases. With further increase in pressure, the ratio of carbon dioxide and carbon monoxide for the catalyzed propellant products becomes lower than

that for the noncatalyzed propellant products. These results are consistent with the above measurements in heats of explosion. Together they suggest that the overall oxidation process is enhanced in the super-rate region and somewhat suppressed in the mesa-burning region. However, their experimental results do not show what stage of the flame zone is affected by the catalyst so as to greatly accelerate the burning rate.

Dauerman and Tajima[21,22,23] examined the thermal decomposition process of noncatalyzed and catalyzed double base propellants at low pressures using a mass spectrometer to sample the gases emerging from the propellant surface during radiative heating. The process consisted of three stages which can be identified from the records of mass peak intensity vs time. In the first stage, the chemical activity of noncatalyzed and catalyzed propellants is approximately equal and the principal products are $CH_3CO\cdot$ and NO_3. In the second stage, the rates of evolution of $CH_3CO\cdot$ and NO_3 increase and a higher rate of redox reactions is evidenced by the appearance of the reduced oxides of nitrogen such as NO and NO_2 for catalyzed propellant. In this reaction stage the products are H_2O, CO, CO_2, HCOOH, H_2CO, and CH_3CHO. In the third stage, the higher chemical activity of the catalyzed propellant is very obvious and the mass fraction ratio of C-H-O species to NO_3 and NO_2, which is indicative of the rate of oxidation, shows clearly the difference between catalyzed and noncatalyzed propellants. Dauerman and Tajima conclude from the experimental results described above that the process accelerated by the addition of catalysts is the oxidation process of C-H-O species by NO_3 and possibly NO_2. The first degradation step of double base propellants (formation of NO_3 rather than NO_2) is viewed differently from the observations of previous investigators as described in Section II and no similar observations have been reported. However, their results are significant for understanding the process of catalytic action. Their findings greatly weaken the model proposed by Powling and others[12] that the process of catalytic action is the reduction of nitric oxide by a carbon/lead complex.

In summary, the decomposition at the burning surface and the reaction processes in the gas phase of double base propellants are found to be similar to the processes of decomposition of simple nitrate esters as described in Section II-A. When super-rate burning catalysts are added to a basic double base propellant, the first stage of the decomposition process is altered (as reported by Dauerman and Tajima[23]), the reaction following a different pathway. The gas phase reaction is also affected by the addition of the above catalysts, and the heat of explosion increases in the

super-rate burning region, as reported by Lenchitz and Haywood.[76] However, these experimental results do not indicate which reaction stages are accelerated to produce super-rate burning.

Since a number of different reactions are referred to in the respective reaction zones, the role of the latter reactions in producing the observed trends in burning rate is not fully understood. As an aid to an understanding of the fundamental reaction steps of double base propellant burning, a list of possible reactions occurring in the combustion zones is presented in Table 2.

The following subsections describe the effect of the burning rate catalysts in the dark zone and in the fizz zone.

C. Investigation of Overall Reaction Order and Catalyst Activity in Dark Zone

The final combustion products of propellants catalyzed by lead compounds are the same, although different proportions have been reported in comparing noncatalyzed and catalyzed propellant in the super-rate pressure region; furthermore, the heat of explosion of catalyzed propellants is affected by the lead compounds and the burning pressure as described previously. However these experimental results do not necessarily mean that the key site of action of lead compounds is in the gas phase; it is possible that these changes in the final combustion products and the heat of explosion are effected by more important changes in the reaction processes at the burning surface, i.e., the subsurface or the very early stages of the gas phase flame zone.

Now, it is important to study the reaction processes of the dark zone to find out the possible action of catalysts in this part of the gas phase. As an indication of the action of catalysts, the overall chemical reaction order and a "catalyst activity" in the dark zone are evaluated based on the following physical and chemical discussion. If some fundamental differences in the overall reaction order and the "catalyst activity" between catalyzed and noncatalyzed propellant are found, they indicate some catalytic action in the dark zone.

(1) Physical and Chemical Background for the Estimation of the Overall Reaction Order in the Dark Zone.

For the analysis of the reaction order in the dark zone, we proceed as follows. The basic assumptions for the gas flow through the dark zone are:

1. one-dimensional burning
2. steady burning at constant pressure
3. negligible radiation absorption
4. constant physical properties in the gas
5. constant molecular weights of all gaseous species.

With reference to the list of symbols at the end of the text, the energy and mass-balance equations are given as

$$\lambda_g \frac{d^2T}{dx^2} - \rho_g u_g c_g \frac{dT}{dx} + \mathcal{R} Q_g = 0 \qquad \text{(IV-1)}$$

$$\rho_g D_i \frac{d^2\varepsilon_i}{dx^2} - \rho_g u_g \frac{d\varepsilon_i}{dx} - \mathcal{R}_i = 0 \qquad \text{(IV-2)}$$

In the dark zone, the temperature distribution is approximately linear and temperature gradient is relatively small as described in Section VI. Therefore, heat conduction, the first term in Eq. (IV-1) is neglected. Similarly, the rate of mass diffusion, the first term in Eq. (IV-2), is assumed to be small compared with the rate of mass convection, the second term in Eq. (IV-2). Thus, the above equations reduce to

$$- \rho_g u_g c_g \frac{dT}{dx} + \mathcal{R} Q_g = 0 \qquad \text{(IV-1a)}$$

$$- \rho_g u_g \frac{d\varepsilon_i}{dx} - \mathcal{R}_i = 0 \qquad \text{(IV-2a)}$$

The following sample calculation is given to illustrate the validity of neglecting the first term in Eq. (IV-1). According to the experimental data obtained by Klein, et al[32] at a pressure of 42 atm, $dT/dx \simeq 1380°C/cm$ and $d^2T/dx^2 \simeq -11300°C/cm^2$ in the dark zone between 0.06 cm and 0.17 cm above the burning surface. Therefore, the first term in Eq. (IV-1) becomes $\lambda_g d^2T/dx^2 \simeq 0.0002 \times (-11300) = -2.26$ cal/cm^{3}sec. Similarly, the second term in Eq. (IV-1) becomes $\rho_g u_g c_g dT/dx = \rho_p r c_g dT/dx \simeq 1.54 \times 0.7 \times 0.35 \times 1380 = 520$ cal/cm^3-sec. By means of these data, the second term in Eq. (IV-1) is found to be approximately 230 times larger than the first term in Eq. (IV-1). Consequently, the term $\lambda_g d^2T/dx^2$ can be neglected in relation to the term $\rho_g u_g c_g dT/dx$. Similar experimental results are presented by Heller and Gordon[11] and also are obtained in this study as described in Section VI.

The chemical reaction process in the dark zone is actually a complex sequence of reactions as studied by Sotter.[80] However, it can be represented as a single step reaction whose apparent reaction order we will determine. The mathematical complexity which would arise from considering a whole series of reactions is not justified by our present limited knowledge of the nature of the detailed flame reactions.

The rate equation for an nth order reaction is (ignoring the temperature dependence of ρ_g):

$$\mathcal{R} = \rho_g \frac{d\varepsilon}{dt} = \rho_g u_g \frac{d\varepsilon}{dx} = -Z_g e^{-E_g/RT_g} \varepsilon^n \rho_g^n \qquad \text{(IV-3)}$$

Equations (IV-1a), (IV-2a) and (IV-3) are combined, then

$$\frac{dT}{dx} = \frac{1}{c_g u_g} Q_g \varepsilon^n Z_g e^{-E_g/RT_g} \rho_g^{n-1} \qquad \text{(IV-4)}$$

The mass flow continuity relation between the gas phase and solid phase is

$$u_g = r\rho_p/\rho_g \qquad \text{(IV-5)}$$

Combining Eqs. (IV-4) and (IV-5) and the perfect gas law gives

$$\frac{dT}{dx} = \frac{1}{c_g \rho_p r} Q_g \varepsilon^n Z_g e^{-E_g/RT_g} (RT_g)^{-n} p^n \qquad \text{(IV-6)}$$

Generally the relation between burning rate and pressure is expressed by Vieille's law,

$$r = ap^m \qquad \text{(IV-7)}$$

where m is the pressure index. For many propellants m and a are constants over a relatively large pressure range, e.g., 10 to 50 atm. Equations (IV-6) and (IV-7) combine to give

$$\frac{dT}{dx} = \frac{1}{c_g \rho_p a} Q_g \varepsilon^n Z_g e^{-E_g/RT_g} (RT_g)^{-n} p^{n-m} \qquad \text{(IV-8)}$$

The temperature gradient, dT/dx, in the dark zone is approximately equal to $\Delta T_g/L_d$, where ΔT_g is the temperature change across the dark zone. Then, solving for L_d, one gets

$$L_d = \frac{ac_g \rho_p (RT_g)^n \cdot \Delta T_g}{Q_g \varepsilon^n Z_g \exp(-E_g/RT_g)} p^{m-n} \qquad \text{(IV-9)}$$

$$\sim p^{m-n} = p^{d} \qquad \text{(IV-10)}$$

Now the dark zone length is related to the effective overall order of the chemical reactions in the dark zone and the burning pressure*. Therefore it is possible to determine the overall order of the reactions, n, by measurements of the pressure index, m, and the variation of the dark zone length with pressure. The dark zone index d is defined as $d = m - n$.

(2) Definition of the Catalyst Activity in the Dark Zone

The mass continuity equations, Eq. (IV-5), Eq. (IV-3) for noncatalyzed and catalyzed propellant burning give

$$\frac{\rho_{g,n} u_{g,n}}{\rho_{g,c} u_{g,c}} = \frac{\rho_{p,n} r_n}{\rho_{p,c} r_c} \qquad \text{(IV-11)}$$

The density of the catalyzed propellant is approximately the same as that of the noncatalyzed propellant. The gas density in the dark zone of the catalyzed propellant is approximately the same as that of the noncatalyzed propellant since the average molecular weights (based on compositions of Ref. 12) and temperatures (see Section VI) are not significantly different in both cases at the same pressure. Thus, the mass continuity relation simplifies to

$$\frac{u_{g,n}}{u_{g,c}} = \frac{r_n}{r_c} \qquad \text{(IV-12)}$$

The overall reaction time of the gas, τ_d, for producing a luminous flame at the end of the dark zone after the gas is ejected from the burning surface is given by $\tau_d = L_d/u_g$. (The thickness of the fizz zone ($\sim$ 0.2 mm) is negligibly small compared with the thickness of the dark zone which is about 5 mm at 20 atm.) If the gas phase reactions in the dark zone are accelerated by the addition of a catalyst to a propellant, τ_d should decrease. Thus, the ratio of the reaction times $(\tau_{d,n} - \tau_{d,c})/\tau_{d,n}$ of the catalyzed to noncatalyzed propellants, defined as "catalyst activity" η_d, is a good index of the action of a burning rate catalyst in the dark zone,

$$\eta_d = 1 - \frac{\tau_{d,c}}{\tau_{d,n}} = 1 - \frac{r_n L_{d,c}}{r_c L_{d,n}} \frac{T_{g,n}}{T_{g,c}} \simeq 1 - \frac{r_n L_{d,c}}{r_c L_{d,n}} \qquad \text{(IV-13)}$$

---

*When the luminous flame appears above 15 atm, T_g is approximately 1300°C and ΔT_g is about 200°C.

The parameter η_d has the important advantage of normalizing the effects of pressure and burning rate. The catalyst activity is experimentally obtained by measurements of the burning rate and the dark-zone length. When the dark zone is greatly accelerated by the addition of catalyst, η_d approaches unity, and when inhibition occurs η_d is negative.

D. Experimental Results of Studies of the Dark Zone Structure

The dark zone lengths for various kinds of propellants were measured by means of high speed 16 mm photographs. The measurement technique and equipment are described in Appendix C and the chemical compositions of all the propellants used in this experiment are listed in Appendix A.

(1) Measurement of Dark Zone Length with Film Sensitive to Visible Light.

Figure 23 is a graph of log L_d vs log p for catalyzed and noncatalyzed propellants. The dark-zone index d of the noncatalyzed propellant is -1.69, while that of the catalyzed propellant varies between -1.96 and -2.27 between 14 atm and 50 atm. The relation between the dark zone length and the burning rate is shown in Fig. 24. A somewhat surprising result is that the higher burning-rate propellant has the longer dark-zone length. It appears that when the burning-rate is increased by means of catalysts, the luminous flame zone, where the greatest heat release occurs in the burning process, is displaced a greater distance from the burning surface than during noncatalyzed combustion.

When the propellant is catalyzed with PbSa and CuSa, a new, weakly visible flame appears just before the main luminous flame, as shown in Fig. 25. Consequently, there are now two dark zone lengths. The first is the distance from the surface to the beginning of the weak luminous flame and the second is the distance from the surface to the usual fully luminous flame. Figures 26 and 27 show a comparison between the first and second dark zone lengths. The measurement of these lengths with high-speed photographs is difficult because of the diffuseness of the boundary as shown in Figs. 25 and 28; however, the measured dark zone index d of the first dark zone is found to be approximately the same as that of the second dark zone. When the propellant is catalyzed with PbSa only, a very faint weak luminosity zone appears as shown in Fig. 29, but no similar zone is observed with CuSa as the catalyst. Therefore, it appears that the PbSa produces the weakly luminous zone when both PbSa and CuSa are used as catalysts. Upon the addition of CuSa, the normally planar boundary between the dark zone and the luminous flame zone is disturbed by projected carbonaceous material generated on the burning surface as shown in Fig.29.

As discussed above, the weakly luminous zone appears when PbSa is added to a basic propellant. However, at less than 15 atm the height of the zone above the burning surface is difficult to measure because the image on the photographs is weak (see Fig. 30). When CuSa is added to a basic propellant, the measurement of dark zone lengths is not clearly defined; the averaged height measurements are shown in Fig. 31.

(2) Measurement of Dark Zone Length with Film Sensitive to Infrared Radiation

Figure 32 shows the flames of noncatalyzed and catalyzed propellants at various burning pressures in the photographic infrared (up to about 0.90 microns). The dark zone of the noncatalyzed propellant is clearly distinguishable in the infrared region and is approximately of the same length as the dark zone measured with the film sensitive to visible light. However, the dark zone of the propellant catalyzed with PbSa and CuSa cannot be distinguished as clearly in this case as with the film sensitive to visible light. At pressures below 30 atm, the luminosity of the catalyzed propellant flame is stronger than that of the noncatalyzed propellant flame in both the infrared and visible ranges, but at pressures above this value, the difference is not noticeable. This observation is related to the experimental results obtained by Lenchitz and Haywood.[76] They measured an increased heat of explosion in the super-rate burning region; as the super-rate burning diminished, no differences in the heat of explosion between the catalyzed and noncatalyzed propellants are measured. Many streaks are seen in the gas phase above the burning surface of the catalyzed propellant in the film sensitive to infrared, as shown in Fig. 33, while this appears as a dark zone on the film sensitive to visible light. The steaks are clearly solid particles which are thought to be carbonaceous in character. The dark zone of the catalyzed propellant appears luminous in the infrared photographs owing to thermal radiation from the very fine particles ejected from the burning surface.

(3) General Observations of Dark Zone Structure

The gas phase zones of the catalyzed and noncatalyzed propellants are observed by means of a high speed motion picture, at a speed of 63 frames per second. The noncatalyzed propellant (No. 1026) has a few relatively small particles coming off its burning surface at low pressures ($\sim$ 8 atm); as the pressure is increased to about 30 atm, the particles are no longer observed and a clear boundary appears between the dark zone and the flame zone. The catalyzed propellant (No. 1031) has relatively large-sized particles coming off its burning surface at low pressures ($\sim$ 8 atm), and as the pressure is increased to about 30 atm, the size of the particles decreases while the number of particles increases.

The propellant catalyzed with PbSa (No. 1045) shows a gas phase structure similar to that of the propellant catalyzed with PbSa and CuSa (No. 1031), but the observed particle size of the PbSa propellant is much smaller at low pressures. The behavior of the propellant catalyzed with CuSa (No.1044) is quite different from that of the others. At low pressures ($\sim$ 8 atm), a very large solid layer is observed to come off the surface and break up into relatively large particles in the gas phase. While at higher pressures ($\sim$ 30 atm), this large solid layer is not observed. However, relatively large particles appear, in sizes much larger than those observed with the PbSa propellant (No. 1044) and the PbSa + CuSa propellant (No. 1031); the flame zone takes on a "ragged" appearance, this apparently being due to the large particles ejected from the burning surface. As a consequence, the boundary between the dark zone and the flame zone is disturbed and the length of the dark zone becomes a function of time and of position along the burning surface.

The results of the dark-zone length measurements in the mesa-burning region are shown in Fig. 34. The burning rate is observed to decrease with increasing pressure above 75 atmospheres, and the length of the dark zone decreases rapidly with increasing pressure.

E. Discussion of Results: Relation to Earlier Experimental Results

The dark zone length is known to be dependent upon the propellant composition and pressure. In early discussions of burning rate behavior by other investigators, it was put forward that the final luminous flame assists the propellant burning, and that the higher the pressure, the higher the burning rate, as the luminous flame comes closer to the burning surface. It is felt that this effect is probably only valid at very high pressures, i.e., over 200 atmospheres; even there, however, there exists no experimental check of this idea.

The results of this investigation show that the luminous flame occurs at a greater distance from the burning surface when the burning rate is increased with catalysts; therefore, heat conduction from this zone is not responsible for super-rate burning.

By an optical method, Maltsev[81] measured the temperature distributions (starting somewhat above the surface) of the same catalyzed and noncatalyzed propellants that were used in this investigation. His results show that the maximum temperature occurs at approximately the same distance from the surface as the luminous flame studied in this investigation. This is shown in Fig. 35. The absolute values of the

temperatures obtained in Maltsev's measurements differ from the flame temperature trends observed during this study, probably owing to difficulties in measuring the emissivity of the flame. Nevertheless, the trends of his temperature profiles may be accepted, and the position of the luminous flame front measured in this study coincides with the position of the steep temperature increase in the gas phase.

The "activity" of the catalyst on the gas phase reactions in the dark zone, η_d, (defined in Eq. (IV-13) is shown in Fig. 36. When maximum super-rate burning occurs, η_d is approximately 0.5 at a pressure of 16 atm while in the region of super-rate burning above this pressure, η_d is approximately 0.3. It should be kept in mind that this increase of η_d, together with a corresponding increase in burning rate, occur despite the fact that the flame zone of the catalyzed propellant is displaced further from the burning surface than in the noncatalyzed case. When propellants are catalyzed with PbSa or CuSa, η_d is in the range 0.5 $\sim$ 0.1 as shown in Fig. 37. It is seen from the figure that the catalyst activity in the dark zone is not significant for the propellant catalyzed with CuSa. (Note that the addition of CuSa to a basic propellant affects significantly the burning surface structure and produces carbonaceous particles as described in Section V.)

Crawford, Huggett and McBrady[54] measured the burning rates and dark zone lengths of noncatalyzed propellant and of propellants catalyzed with metallic nickel powder. They found that the catalyzed propellant burns with a brilliant flame close to the propellant surface, and that at any given pressure the dark zone is only about 1/13 as long as that of the noncatalyzed propellant. However, they found the burning rates of the nickel catalyzed and noncatalyzed propellants to be nearly the same between 200 and 800 psi. The catalyst activity η_d computable from their data is approximately 0.92 which is quite different from the value for plateau-type catalysts, which is in the range 0.5 $\sim$ 0.1. This result indicates an essential difference between the catalytic mechanism of this metallic-powder catalyst and that of plateau-type catalysts. It is important to note that the catalysts which yield super-rate burning act in the condensed phase and/or in the gas phase very close to the burning surface, while catalysts like nickel metal powder which do not increase the burning rate act only well out into the gas phase, i.e., not close to the burning surface.

The dependency of dark-zone length on pressure was first discussed by Crawford.[10] He obtained a relationship, based on his experimental results, in which the dark-zone length is inversely proportional to the cube of the pressure. However, when he increased the size of his propellant sample from 2.7 mm to 9.5 mm in diameter, he observed the dark-zone

length to be inversely proportional to the square of the pressure.* Heath and Hirst[82] found the length to be inversely proportional to 1.6th power of the pressure; moreover, they found that the exponent depends upon the nature of the propellant. The results obtained in this investigation are shown in Table 1, which gives the pressure exponent, m, and the dark zone index, d. It is found, as mentioned by Heath and Hirst, that the dark zone is dependent upon the burning rate characteristics.

An estimation procedure for the order of the overall reaction in the dark zone was deduced in Section IV-C. The calculated results are tabulated in Table 1, together with the available data of previous investigators. It is observed that the pressure index, m, for the burning rate, varies between 0.28 to 0.80, and the dark zone index, $d = m - n$, varies between -1.69 to -2.27, these parameters being dependent upon the propellant composition and the pressure range. It is observed that the propellant with the lower pressure exponent has a more negative dark zone index, i.e., the pressure-dependence of the dark zone is larger. As is clearly observed in Fig. 34, the dark zone length decreases rapidly with increased pressure in the mesa-burning region. Note, however, the calculated overall order of reaction, n, is approximately 2.5 for all propellants irrespective of whether or not the propellant is catalyzed. The results indicate that the overall reaction rate behavior in the dark zone of the catalyzed propellant is probably fundamentally the same as that in the dark zone of the noncatalyzed propellant.

It is important also to note in attempting to understand the mesa-burning mechanism, that the flame zone does not distend as the burning rate decreases, but in fact, moves closer to the burning surface. This again indicates that the conductive energy transfer from the luminous flame to the burning surface is not important, and that there must instead be some inhibiting reaction near or at the burning surface, i.e., in the fizz zone which produces the mesa. Such an

---

*An explanation of this observation is as follows: when the diameter of a propellant-sample is small compared with the length of the dark zone, the luminous flame front is not one-dimensional but conical in shape owing to mixing between the reaction gas and the surrounding atmosphere. Thus, the average dark zone length appears longer than in the one-dimensional case. As the diameter of the propellant sample is increased the diffusion of the surrounding gases into the reaction zone becomes less significant, and the flame front gradually assumes a one-dimensional shape. In this study, it was found that the dark-zone length becomes independent of the diameter of the sample when the latter exceeds 5 mm.

observation is striking, as the luminous flame would be expected to be displaced some distance further from the surface in order that the energy transfer to the condensed phase be decreased during mesa burning.

F. Possible Reaction Mechanisms in the Dark Zone

The order of the chemical reaction in the dark zone can be evaluated from measurements of the length of the dark zone and of the burning rate, as shown above. Generally, in calculating the flame speed of a premixed gas, the net reaction is assumed to be second order in the gas phase. However, it is well known that oxidation reactions involving nitric oxide are usually termolecular, for example (82, 84, 85):

$$2NO + Cl_2 \longrightarrow 2NOCl$$

$$2NO + Br_2 \longrightarrow 2NOBr$$

$$2NO + O_2 \longrightarrow 2NO_2$$

The experimental results of Hinshelwood and Green[86] tend to support the following reaction mechanism between NO and H_2

$$2NO + H_2 \longrightarrow N_2 + H_2O_2 \qquad \text{(slow)}$$

$$H_2O_2 + H_2 \longrightarrow 2H_2O \qquad \text{(fast)}$$

The measured order of the overall reaction varies between 2.60 and 2.89. However, Pannetier and Souchav[87] suggested that the above slow reaction could not be expected to occur owing to the improbable nature of a termolecular process. They proposed

$$2NO \rightleftharpoons N_2O_2 \qquad \text{(fast)}$$

$$N_2O_2 + H_2 \longrightarrow N_2 + H_2O_2 \qquad \text{(slow)}$$

$$H_2O_2 + H_2 \longrightarrow 2H_2O \qquad \text{(fast)}$$

In the above group of reactions, the slow reaction involving N_2O_2 is the rate controlling step. The reaction involving NO is fast enough to maintain equilibrium with the N_2O_2. Consequently, it can be seen that the rate of production of N_2 and H_2O is third order with respect to NO and H_2. The overall sum of these reaction steps is in fact third order, while the elementary reactions are all bimolecular, i.e., second order.

According to the results of numerous gas-composition analyses[88,12] of double base propellants, only trace amounts of nitric oxide ($\sim$ 0.1%) are found in the final combustion

products at high pressures, as almost all the NO is consumed in the final luminous flame. However, at low pressures, relatively large amounts of NO (∿ 30%) are found.[88,12] The results of gas sampling show the existence of NO (∿ 20%) in the dark zone even at high pressures. The main oxidation reactions producing heat in the dark zone involve nitric oxide, therefore these reactions probably control the dark zone length.

The probable set of chemical reactions in the dark zone were analyzed theoretically by Sotter.[80] He included sixteen reversible and four irreversible chemical reactions involving twelve chemical species. In his analysis the most important reactions were found to be (similar results were obtained by Davis[108])

$$H + H_2O \rightleftharpoons H_2 + OH$$

$$CO + OH \rightleftharpoons CO_2 + H$$

$$2NO + H_2 \longrightarrow 2HNO$$

$$2HNO + H_2 \longrightarrow 2H_2O + N_2 \quad \text{(fast)}$$

The last chemical equation, involving nitric oxide, is termolecular. Therefore, the overall order of the reaction is expected to exceed that of the second order reaction generally assumed in the premixed gas burning model.

It is well known that the high exothermicity accompanying the reduction of NO to N_2 is responsible for the appearance of the luminous flame in the combustion of a double base propellant, and that the flame disappears when there is insufficient heat produced in this way, i.e., during fizz burning. As discussed in Section II-A-(2), the reduction of NO does not occur until the temperature is of the order of 1000°C. However, attainment of this temperature in the reaction zone does not guarantee the appearance of a luminous flame, for there is another factor to be taken into account, namely, the stabilization of the flame above the reaction zone. If the luminous flame spreading speed is lower than the efflux velocity of the product gases (at the edge of dark zone), blow off of the luminous flame occurs and no luminous flame is observed. (The efflux speed of the product gases is proportional to burning rate, which is essentially independent of this luminous flame.) According to laminar flame-speed theory, this flame speed S_L is proportional to $p^{n/2-1}$, where n is the order of the reaction. On the other hand, the efflux velocity u_g of the product gases in the dark zone is proportional to p^{m-1}, where m is the burning-rate pressure-index. Now the overall order of the reaction (n) is approximately 2.5, as shown in the previous subsection, while the burning-rate pressure index is of the order of 0.7

in the low-pressure region where fizz-burning occurs. Therefore, it follows that the flame speed should increase as $p^{0.25}$, where as the efflux velocity in the dark zone should decrease as $p^{-0.3}$. At a certain critical pressure, one would expect the laminar flame speed to exceed the efflux velocity of the product gases, and thereafter become stabilized above the surface of the propellant. This rather simple analysis provides a qualitative explanation of the observed transition from non-luminous fizz-burning to luminous flame-burning in the combustion of a double base propellant.

The mechanism of sustaining the luminous flame the same distance above the burning surface cannot be explained by the above discussion. It is well known that the reaction involving NO only occurs at certain critical temperatures as described in Section II-A-(2). Therefore, for the appearance of luminous flame, it may require the formation of a critical concentration of some autocatalytic intermediate or the attainment of a critical temperature which brings about a sudden increase in reaction. Equation (IV-8) itself cannot predict the position of the standing luminous flame above the burning surface. The details of the chemical reaction mechanism in the dark zone must be known to predict it.

G. Reaction Mechanism in Fizz Zone

At the outset, it is intuitive that the initial reactions occurring in the gas phase just above the burning surface (i.e., the fizz zone) should significantly affect the burning-rate behavior of a double base propellant.

As described in this section, the main heat feedback from the gas phase to the condensed phase is dependent on the relatively steep temperature gradient in the fizz zone. Therefore, it is important to study the reaction mechanism in the fizz zone to understand the super-rate burning phenomenon.

The general reaction process in the gas phase of a double base propellant has been described in Section III. A feasible reaction scheme in the fizz zone just above the burning surface, based on the experimental results of this investigation and of previous investigators, is discussed in this section in an attempt to understand basic differences between noncatalyzed and catalyzed propellant burning.

Klein and others[32] found that there is steep temperature gradient at the burning surface and that the gradient is relatively mild at distances greater than 200μ from the burning surface. This steep temperature gradient is important in the description of the burning rate and in the understanding of the overall reaction process. The experimental results of this investigation, as described in Section VI, show that

when the propellant is catalyzed, this temperature gradient is increased in the super-rate pressure range, and that it increases with increasing pressure. This increased gradient with catalysis is also observed at atmospheric pressures, where the burning rate is approximately 50% above that of the noncatalyzed propellant. It is clear that effect of the catalyst is to promote the burning rate by accelerating the gas phase reaction rate in this narrow gas phase zone, i.e., the fizz zone. On the other hand, as described in Section IV, the accelerating effect on the gas phase reactions in the dark zone is not as pronounced, as the dark zone is longer than in the noncatalyzed case. (It should be noted, however, that the dark zone reaction is accelerated significantly by the addition of pure metallic powder catalysts such as Ni without increasing the burning rate.) In light of the above observation, the action of those catalysts producing super-rate burning should be differentiated from that of pure metallic powder catalysts such as Ni.

In the past, a number of gas composition analyses of the combustion products in the dark zone were carried out, together with gas sampling analyses in the fizz zone.[88,12,11] However, there are no reliable analyses in the fizz zone owing to its thinness and the fact that the propellant surface does not progress in a perfectly flat manner.

Schuyler[89] discussed possible chemical reaction schemes in the fizz zone. He introduced 37 reversible chemical reaction steps which were induced by the reaction of aldehyde and nitrogen dioxide. However, he did not reach any firm conclusions.

Powling and others[12] sampled the gas near the burning surface of nitrocellulose and found no difference in nitric oxide concentration between noncatalyzed and catalyzed material; neither did they find a difference between the nitric oxide concentration near the surface and the nitric oxide concentration at one centimeter from the burning surface. This was in spite of a doubling in the burning rate and an increase in the temperature near the surface from 600°C to 750°C with the addition of a catalyst. They found traces of nitrogen dioxide near the burning surface, i.e., 0.3% with the noncatalyzed and 0.04% with the catalyzed propellant. On the basis of their findings on simpler nitrate esters (and in spite of the above evidence to the contrary), they proposed that the accelerated burning with the addition of a catalyst is due to the heat generated by the reduction of nitric oxide through some catalytic effect of solid carbon created at the surface. Despite the more favorable evidence from simpler nitrate esters, since the concentration of nitric oxide of catalyzed NC is about the same as that of noncatalyzed NC near the burning surface, the above mechanism does not seem

valid for propellants.* It is conceivable that their gas sampling actually captured gases above the thin fizz zone instead of within this zone. The additional heat from a catalyzed propellant may then be a result of catalysis in the fizz zone before occurrence of the oxidation reactions involving nitric oxide. The fact that Powling and co-workers found nitrogen dioxide near the burning surface is a good indication of strong heat generation in the fizz zone via NO_2 reduction, and that the catalytic effect involves NO_2; it is well known that NO_2 undergoes rapid oxidation reactions with C-H-O species. Those reactions are rapid even without catalysis.

H. Summary of Preceding Section

The gas phase reactions in the dark zone are accelerated slightly by the addition of super-rate burning catalysts. However, the luminous flame zone of a catalyzed double base propellant is displaced further from the burning surface than that of a noncatalyzed propellant despite the greatly increased burning rate in the former case. This result implies that (1) the occurrence of super-rate burning is not determined by the position of the luminous flame front, and (2) the heat feedback from the luminous flame to the burning surface is not instrumental in promoting the burning rate in the super-rate regime. Furthermore, mesa burning is not dependent on the luminous flame because the burning rate decreases even though the luminous flame approaches closer to the burning surface in the mesa-burning regime.

The results of the experimental observations described above indicate that the site of action of the catalyst in producing super-rate burning should be near the burning surface, i.e., in the fizz zone and/or at the burning surface and in the condensed phase (see Table 2).

The following two sections describe the catalyst behavior at the burning surface and in the gas phase near the burning surface.

---

*The experimental results (Ref. 12) indicates no significant NO reduction with either catalyzed or uncatalyzed double base propellants.

SECTION V

STUDIES ON THE CONDENSED PHASE REACTION ZONE AND THE REACTION AT THE BURNING SURFACE

It is well established that many small particles emanate from the burning surface when super-rate catalysts are added to double base propellants and, as described in the previous section, that behavior of the particles is different with each catalyst type. The search for the site of first action of catalysts thus must include the area of the burning surface. It is the purpose of this section to focus attention on the effects of the catalysts on the burning surface layers using the results obtained through high speed motion pictures and the results of the observation of propellant surfaces extinguished by rapid pressure decay.

A. Review of Findings of Previous Investigators

Several experimental studies of burning surface behavior have been made. Crawford and others[78] first found the existence, at low pressures, of a liquid-like layer on the burning surface of double base propellants. The layer was named the "foam zone" because it contained gaseous bubbles. However, such a foam zone has not been observed experimentally at high pressures. Heath and Hirst[82] observed burning surfaces by high speed (200 frames/sec) photographs and found that the burning surface was covered by numerous bright globular, hot spots, together with smaller black spheres. The lifetimes and the diameters of the hot spots on the surface decreased with increasing pressure. The diameters were found to vary between 0.01 and 0.03 mm. The lifetime of the black spheres coming from the surface appeared to be much longer than that of the hot spots. It is interesting to note the behavior of the hot spots and the black spheres as an aid in understanding the structure of the burning surface, although the composition of the hot spots and black spheres are unknown. A propellant of composition similar to that used by Heath and Hirst has been tested in this study and the results are discussed later in this section.

The burning surface structure of platonized propellants was observed by Brown and Chaille[90] using high speed cinemicrographs (3000 frames/sec). They obtained a significant result for the understanding of super-rate, plateau and mesa burning. Small globules, 30 ∿ 60 microns in diameter, were observed during burning at all pressures below the upper limit of plateau burning with propellants catalyzed by lead compounds. By careful analysis of the photographs, they found that the particles were formed on the surface and remained there, growing until they reached a certain size, and

then were released into the gas phase. The particles coming off the surface were trapped in a container cooled by dry ice and when analyzed were found to be lead metal.

When sodium chloride is added to a plateau type propellant, the super-rate and the plateau effects are diminished. Their observations show that, at all pressure ranges, particles of sodium chloride and lead chloride are present on the burning surface instead of molten lead metal. It is interesting to compare these results with those in Fig. 4 showing that lead chloride is ineffective in producing plateau burning. Evidently the sodium chloride reacts below or at the burning surface with the decomposing lead catalyst to form lead chloride. Once lead chloride is formed in the nitrate ester decomposition process, it is difficult to produce metallic lead or lead oxide, which are considered to be the key plateau producing agents.

A comprehensive study of the ignition of noncatalyzed and catalyzed double base propellants by means of laser and arc-image radiation sources has been carried out by several investigators at Princeton.[92] The results obtained indicate an essential difference between the ignition characteristics of noncatalyzed and catalyzed propellants. The transition from the transient ignition stage to steady burning is greatly influenced by the addition of catalysts, which decrease the pressure dependence of the process. High speed shadowgraph photography of the surface during ignition indicates the formation of a carbonaceous layer during the early phase of ignition of double base propellants catalyzed with PbSa and Pb2-EH. However, such a carbonaceous layer is not observed on the surface of a noncatalyzed propellant. This experimental result implies that the early stage of the decomposition process is influenced by lead compounds in double base propellants; recall the proportions of gaseous species are different in the ignition stage of a lead-catalyzed propellant, as observed by Dauerman and Tajima.[23]

Powling, et al[12] observed solid carbon formation on the surface of a burning propellant catalyzed by lead compounds; however, as pressure was increased into the mesa burning region, carbon was not seen on the surface. They believe that this complete disappearance of carbon is responsible for the appearance of the mesa (and, conversely, that the carbon itself is responsible for the super-rate) and that it is the result of accelerated oxidation by NO in the mesa pressure range. However no direct physical or chemical experimental evidence for this has been reported. Instead, one should consider the probability that the disappearance of solid carbon at high pressures is somehow connected with the disappearance of the molten lead metal on the surface as observed by Brown and Chaille. It is well known that many kinds of metal or metal oxides added to double base

propellants produce solid carbon at the burning surface. It seems possible that the extensive carbon formation which correlates with the super-rate occurs as a consequence of the presence of lead metal or lead oxide at the surface and that carbon is not formed when lead metal or lead oxide is not present on the burning surface.

B. Experimental Results of This Investigation

A description of the experimental equipment and techniques for taking photographs by a high speed camera is given in Appendix C-(4) and the specifications of all propellants used in this study are to be found in Appendix A.

(1) Burning Surface Structure

First, as a preliminary experiment to study particle behavior on the surface, the burning surface structure of a noncatalyzed NC/NG propellant which contained 0.75% of 15μ potassium nitrate (a flash suppressant) was studied. Figure 38 shows the surface to be covered by carbonaceous filaments and a few non-carbonaceous globules. The globular particles are believed to be agglomerates of K_2O coming from the KNO_3; they have no effect on burning rate or surface structure. Like a lead metal agglomerate,[90] after the particles reach a certain size, they lift off the surface as shown in Fig. 38. The stay time of the particles on the surface is calculated from the photographs and is approximately 0.01 sec. It is interesting to see that such particles can stay on the surface until they grow to a certain size, even though the burning rate is high, for example, 1.0 cm/sec at 70 atmospheres. There is a characteristic range of particle sizes corresponding to each burning rate.

The burning surface structures were also studied for four kinds of PNC/TMETN propellants: noncatalyzed, catalyzed by 1% CuSa, catalyzed by 1% PbSa, and catalyzed by 1% CuSa + 1% PbSa.

These observations of the burning surface have been carried out up to 80 atm, but the luminous flame comes too close to the burning surface at such high pressures; clear surface observations are only possible at less than 50 atm.

The overall results were as follows:

1. The noncatalyzed propellant burning surface is partially covered by carbonaceous fragments and filaments at low pressures, but under increased pressure the number of carbonaceous fragments decreases. Above 20 atm, the surface regresses smoothly and very few solid particles are ejected into the gas phase. The surface structure of PNC/TMETN propellant is found to be similar to that of NC/NG propellant (No. 6 propellant).

2. The burning surface of a propellant catalyzed by 1% CuSa is rough and produces large, apparently carbonaceous, fragments, which are ejected from the surface at low pressures; numerous visibly radiating spots are also seen on the surface. As pressure is increased the size of the pieces becomes smaller, and the number of pieces decreases; this entire effect of CuSa on the burning rate diminishes above 30 atm.

3. The burning surface of a propellant catalyzed by 1% PbSa is relatively smooth and similar to that observed in the case of noncatalyzed propellant. However, an essential difference that is observed is that many small brightly emitting spots appear on carbonaceous "fibers" projecting up to 80 microns above the surface; they subsequently disperse into the gas phase. The spots are very bright compared with the remainder of the "fibers"; the apparent diameter of the spots is approximately 50 microns. Figure 39 shows a typical photo of the surface structure of a propellant catalyzed by PbSa taken during the burning process.

4. The burning surface of a propellant catalyzed by 1% CuSa and 1% PbSa is rough, similar to the propellant catalyzed by 1% CuSa, at low pressures; it is relatively smooth at high pressures, producing very fine solid particles.

(2) Burning Surface Observations on Propellant Samples After Rapid Depressurization Extinguishment

For further observation of the burning surface of double base propellants, propellant samples extinguished at various pressures were prepared with the use of a rapid depressurization strand burner. The experimental process and the equipment are described in Appendix C-(5). The rate of depressurization is considered to be rapid enough for extinguishment in less than 0.001 sec (5×10^5 psia/sec at 500 psia). Merkle, Turk and Summerfield[91] measured the extinction boundary of the same kind of propellant used in this study and showed that depressurization rates over 3×10^4 psia/sec were fast enough to extinguish such a propellant burning at an initial pressure of 1000 psia; the extinction becomes easier with decreasing initial chamber pressure. The experiments in this study were conducted at pressures ranging from 90 to 915 psia.

Figure 40 shows the extinguished burning surface of a noncatalyzed NC/NG propellant stopped at different pressures. At low pressures the surface is covered rather irregularly by large size carbon particles; as pressure is increased the

size of the carbon particles decreases and their distribution becomes more uniform. Similar results were obtained from a catalyzed propellant which contained PbSa and Pb2-EH. Contrary to expectation, the surface of the catalyzed propellant did not reveal lead or lead oxide particles; it is possible they were present but were removed by the rapid extinguishment process.

Furthermore, several other investigators have made the observation that relatively large agglomerated metallic-lead particles (~ 60μ at 15 atm) appear on the burning surface at low pressures during super-rate burning. As the pressure is increased, the particle size decreases (~ 20μ at 80 atm) and the number of particles increases.[90] It is reported that these carbonaceous particles disappear above the mesa burning range. These experimental results indicate that the time available for agglomeration of metallic lead particles varies inversely with burning rate. When the burning rate is low, the residence time of the particles in the condensed phase and at the burning surface is long enough for formation of large agglomerated particles. However, as the burning rate increases, the residence time decreases and only small particles are formed before blow off occurs; hence the inverse dependence of particle size on burning rate.

This interesting trend could offer a partial explanation for the mesa-burning behavior of platonized propellants. It is possible that the metallic lead particles actually inhibit the gas-phase reaction as described in Section II-C-(3). At low pressures, when lead particles are large, this effect would be less pronounced than at high pressures when the ratio of surface area to volume of the lead particles is relatively large. However, this must be considered in the nature of a hypothesis, as there is presently no experimental evidence in support of such behavior.

SECTION VI

TEMPERATURE PROFILES OF CATALYZED AND NONCATALYZED PROPELLANT BURNING

The surface temperature during combustion is one of the most important physical values in the understanding of the actual physical and chemical picture of the double base propellant combustion process. All burning rate equations[36,37,1,15] require the burning surface temperature to describe the burning rate. Generally, this burning surface temperature is dependent on the pressure at which the propellant burns because the reactions in the gas phase where much of the heat is generated are a function of pressure; the amount of heat transferred from the gas phase to the solid phase strongly influences burning surface temperature. The temperature at any point in the combustion wave is a result of the balance of heat release at that point and the fluxes of heat through the point carried by conduction and convection. The temperature at the burning surface is most directly important for burning rate predictions but this is a consequence of the balance of fluxes near the surface. Examining the details of the temperature profile near (above and below) the surface can reveal how catalysts alter this profile and hence the burning rate.

A. Findings of Previous Investigators

Many previous investigators have measured the burning surface temperature by various experimental methods. Klein, et al[32] were the first to refine the measurement technique using fine thermocouples imbedded in a propellant sample; they obtained relatively reasonable burning surface temperatures at several different pressures.

Heller and Gordon[11] tried unsuccessfully to measure the burning surface temperature with an external thermocouple held onto the burning surface of a small propellant sample. The ends of the thermocouple terminals were pulled with a certain force to ensure that the bead of the thermocouple always touched the burning surface during propellant burning. They found the measured burning surface temperature was strongly dependent on the force applied to the thermocouple terminals. They also found the burning surface temperature to be very pressure dependent, increasing from 400°C at one atm to 1000°C at above 20 atm. This temperature obtained at high pressures is unrealistically high; it is doubtful that the thermocouple bead measured only the surface temperature in their experiments. However, their results do indicate that a higher temperature zone exists near the burning surface at elevated pressures.

Sabadell, Wenograd, and Summerfield[75] measured the burning surface temperature by a technique similar to that developed by Klein. They obtained credible surface temperatures at 150, 100, and 50 psig, of 268, 333, and 332°C, respectively.

The essential difficulty in a Klein-type thermocouple measurement is determining the position of the surface on the output record (millivolts vs time and, hence, distance) obtained as the junction proceeds through the combustion wave. Strittmatter, et al[93] tried to determine the exact position of the burning surface in the thermocouple output record by synchronizing the thermocouple output with a high speed microphotographic movie; they sought to observe the thermocouple bead emerging from the solid phase into the gas phase. By this means they obtained a burning surface temperature of 535°C at 200 psi.

Suh and others[94,95] measured the temperature profile in a double base propellant at low pressures with several different thermocouple wire sizes. They also synchronized their system with a microphotographic movie as did Strittmatter in his experiment. They measured burning surface temperatures of 300°C and 315°C at 5 and 10 psia respectively, and observed that plateau regions (in the temperature profile) occurred near the burning surface in the recorded temperature profile curves. They concluded that the plateau temperature regions were a consequence of the effect of thermocouple bead size; the smaller the bead size, the shorter the plateau temperature zone.

The burning surface temperature was estimated in a different way by Wilfong, Penner, and Daniels.[15] They observed that copper particles, smaller than 4μ, mixed with the propellant sample were melted into spheres on the quenched burning surface after a rapid pressure decay. Similar results were observed when finely powdered alkaline earth carbonates were incorporated in the propellant. From these observations they concluded that the burning surface temperature was above 1000°C. Although their results are similar to the results obtained by Heller and Gordon[11] by their thermocouple technique, their experimental results cannot be accepted without question. As discussed in Section V, the burning surface found after extinguishment by rapid depressurization is not flat but has an irregular shape and is usually covered with carbonaceous fragments even at high pressures. Therefore it is possible that the melted particles they observed were located on the projected fragments. Nevertheless, their observed results again indicate that there is a high temperature zone near the burning surface.

An optical technique was used by Powling and Smith[96] to measure the burning surface temperature. They showed the temperature was dependent on the composition of the double base propellant and lay between 320 and 400°C at atmospheric pressure. The technique is convenient for measuring solid surface temperatures, although here the surface roughness and projecting carbonaceous fragments may interfere with the measurement of the true burning surface temperature.

Zenin,[97] by means of fine thermocouples, and Aleksandrov and others,[98] by optical methods, measured the pressure dependency of the burning surface temperature. They found that the temperature increases almost linearly with the logarithm of pressure between 20 and 80 atm. Zenin found that the temperature increased from 380 to 415°C over this pressure range, while Aleksandrov and others found a similar increase from 350 to 410°C.

Results of all the available surface-temperature/pressure-dependence measurements which have been carried out by previous investigators are shown in Fig. 41. The general trend is that the burning surface temperature increases with increased pressure and burning rate. This is to be expected with the Arrhenius-type expression for propellant decomposition rate at the surface that occurs in the burning rate model used in this study and by other investigators.[36,37] From the figure, it can be concluded that the burning surface temperature of noncatalyzed double base propellants is approximately 300°C at one atmosphere (improved modern measurement techniques converge toward this level); similar, though somewhat higher temperatures at higher pressures are most credible. However, no burning surface temperatures for catalyzed propellants have been found in the literature.

The main purpose of the measurements of temperature profiles in this investigation is to obtain the surface-temperature/pressure dependence for the systematic series of propellant formulations studied here and to determine the region of the combustion zone responsible for the increased burning rate of catalyzed propellants over that of noncatalyzed propellants.

B. Experimental Results of This Investigation

The temperature distributions in noncatalyzed and catalyzed propellants have been measured at various pressures from 0.5 atmosphere to 22 atm by means of fine thermocouples imbedded in the propellants. The strand burner used in the thermocouple experiments at pressures above one atmosphere is the same as the strand burner described in Section III used to measure the burning rate. The strand burner used in

the measurement of the minimum burning pressures and the burning rate at subatmospheric pressures, as described in Section III, was also used for the thermocouple experiments at pressures below atmospheric.

Techniques have been developed for the fabrication, measurement, and handling of microthermocouples made from 2.5μ and 7.5μ diameter platinum and platinum-10% rhodium Wollaston wires*. The preparation of the thermocouples and of the propellant samples, and the instruments used to record the temperature profiles are described in Appendix C. The chemical compositions and properties of the propellants used in this experiment are listed in Appendix A.

Figure 42 represents a typical trace produced by an oscillograph of the distribution of temperature in the combustion wave. In all of the temperature traces it is possible to distinguish the following characteristic zones as shown in the figure.

Zone I is a non-reacting zone where only pure heat conduction occurs; it ends at a temperature of approximately 220°C as signalled by the beginning of small fluctuations in the temperature curve.

Zone II is defined as the subsurface reaction zone, extending from the end of Zone I until the start of the relatively large fluctuations in temperature signalling the burning surface.

Zone III is defined as the fizz zone, which extends from the burning surface to the region which temperature gradient becomes small.

Zone IV is defined as the dark zone, which extends from the end of the fizz zone to the point at which the temperature starts increasing rapidly.

Zone V is defined as the flame zone, which extends from the point of rapidly increasing temperature.

Figure 43 shows an oscillogram of a temperature trace in which the fluctuations in Zones II and III are seen more clearly.

Zone II was not observed in the temperature traces with larger-size thermocouples (∿ 25μ) because the zone is very narrow; the response of such a large thermocouple to the temperature fluctuations was consequently poor. Zone V was

---

*The thermocouple bead size corresponding to the wire size is discussed in Appendix C-(6).

only observed above 7 atmospheres and only when larger-size thermocouples were used, because the smaller-size thermocouples ($\sim$ 2.5μ) are too weak at high temperatures to withstand the flow of hot gas. Zone V is located at a great distance from the surface and Zone IV is elongated so that it is much larger than the other zones. Zone IV, the dark zone, has a rather mild temperature gradient; therefore, energy transfer by conduction to the solid from Zone V is negligible. For this reason, interest was centered on the temperature distribution measurements near the burning surface, i.e., in Zones I, II and III. Zone IV and V were examined optically as described in Section V.

The peak temperature in the dark zone varies from 700°C at 0.6 atm to 800°C at atmospheric pressure. It increases to 900°C at 7 atm, and to approximately 1200°C above 20 atm. Further increases in pressure will eventually result in the collapse of the dark zone at about 200 $\sim$ 300 atmospheres but will bring about only a slight increase in maximum temperature in the dark zone until then. So far, no experimental measurement of this increase has been reported.

The thickness of the fizz zone (i.e., Zone III) is actually dependent on the chemical kinetics of the gaseous species evolved at the burning surface which in turn is dependent on pressure. Figure 44 shows the variation with pressure of the fizz zone thickness of a noncatalyzed propellant. The thickness decreases with increased pressure, resulting in an increased temperature gradient (and increased final temperature as noted above). Therefore, the rate of heat input by conduction from the gas phase to the solid phase increases with increasing pressure. Figure 45 shows the fizz zone thickness variation with pressure for a catalyzed propellant. The pressure-dependence and the temperature profiles are all similar to those of a noncatalyzed propellant. However, the thickness of the fizz zone of the catalyzed propellant is less than that of the fizz zone of the noncatalyzed propellant, therefore the temperature gradient dT/dx is larger in the former than in the latter case, as shown in Figs. 46, 47, and 48. Therefore, the heat feedback from the gas phase to the solid phase of the catalyzed propellant is clearly larger than that of the noncatalyzed propellant; it is evident that the reactions in the fizz zone of the catalyzed propellant are accelerated by the effect of catalysts in the regime of super-rate burning. This acceleration is even more marked when one notes that the fizz zone of the catalyzed propellants is shortened despite the greatly increased gas velocity through this zone during super-rate burning.

Figure 49 shows the temperature profiles of a propellant containing burning rate suppressants and noncatalyzed propellants at subatmospheric pressures, measured by means of 7.5μ-

diameter thermocouples. When 3% ammonium polyphosphate, $(NH_4)_2(PO_3H)_m$, is added to a noncatalyzed propellant as a burning suppressant, the temperature profile in the fizz zone is decreased. The burning rate is decreased approximately 20% even though the minimum burning pressure is lowered by the solid carbon which is generated at the burning surface by the addition of the ammonium polyphosphate (this carbon protects the burning surface from heat loss as described in Section III). The same trend is observed when 5% of oxamide, $(CONH_2)_2$, is added to the noncatalyzed propellant. Evidently the suppressants work in essentially the opposite way of the super-rate catalysts, slowing rather than accelerating fizz zone reactions.

C. Discussion of Experimental Results

The "temperature inflection method" is commonly used for the determination of the position of the burning surface in the recorded temperature profile curves; it assumes no heat release in the condensed phase and takes the inflection point of the log $(T - T_0)$ vs distance plots as indicating the burning surface. The method is described in Appendix C-(6)-(b). However, during low pressure burning ($\sim$ 1 atm) of double base propellants, the subsurface reaction Zone II is stretched out in time, with the result that the log $(T - T_0)$ vs distance plots do not show a clear inflection point. In such a case, the surface position is detected by a change in the amplitude of the temperature fluctuations or by a clear inflection point appearing in the original recorded temperature profile curve. Surface temperature determinations via the inflection method are shown in Fig. 50. The pressure dependency of the measured surface temperature is shown in Fig. 51. The burning surface temperature of the noncatalyzed propellant and propellants catalyzed by PbSa and CuSa show similar trends of increasing temperature with increasing pressure. The temperature of the catalyzed propellant is higher than that of the noncatalyzed propellant by approximately 25°C at 1 atm and 30°C at 21 atm. The average surface temperature for the noncatalyzed propellant is 285, 305 and 345°C at 1, 8 and 21 atmospheres, respectively; for the catalyzed propellant, it is 310, 330 and 375°C at 1, 8 and 21 atmospheres, respectively.

At low pressures (less than 1 atm), the heat required to maintain steady burning is generated mainly at the burning surface; therefore, the heat conducted from the gas phase to the burning surface is of secondary importance in controlling the burning rate. Generally, the surface reaction is of zero-order with respect to the pressure.[1,36] Consequently, the burning rate becomes constant at low pressures ($\sim$ 1 atm), as described in Section III. The measured temperature gradient and burning surface temperature provide some order-of-

magnitude estimates of the quantities comprising the steady state energy integral from minus infinity to the surface:

$$\rho_p r c_p (T_s(r) - T_0) = \lambda_g \left(\frac{dT}{dx}\right)_{s,g} + \rho_p r Q_s \qquad \text{(VI-1)}$$

At a pressure of 0.52 atm, $(dT/dx)_g$ at the burning surface of a noncatalyzed propellant was measured and found to be about 0.62×10^4 °C/cm, with T_s = 270°C, r = 0.045 cm/sec and T_0 = 25°C. The estimation of λ_g is rather difficult, but based on the gas composition analysis[12] and on the value used by a previous investigator,[75] λ_g is assumed 1.2×10^{-4} cal/cm-sec-°C.[99] $\lambda_g(dT/dx)_g$ is then given as 0.74 cal/cm^2-sec. However, the first term of the energy balance equation, $r\rho_p c_p(T_s - T_0)$, is about 5.9 cal/cm^2-sec; therefore, as expected the heat conducted from the gas phase to the burning surface is a small contribution; thus the estimation of λ_g and the accuracy of the measurement of $(dT/dx)_g$ is not significant. Finally, Q_s is found to be about 75 cal/g, which is of the same order as that measured by Zenin[100] and Sabadell, et al.[75] No significant differences in Q_s were obtained when the propellant was catalyzed with a combination of lead and copper compounds at low pressures, where the super-rate burning is less pronounced. At high pressures, the temperature gradient in the fizz zone is large enough to control the burning rate; however, the heat feedback from the gas phase could not be reliably calculated because the strong temperature-dependence of λ_g renders the feedback term too indefinite. Rough estimates of the magnitude of the fizz zone temperature gradient are shown in Figs. 47 and 48. By means of the latter data, the heat-release Q_s at the burning surface was calculated (Eq. VI-1) and found to increase from 75 cal/g at 1 atm to 100 cal/g at 21 atm (i.e., where pronounced super-rate burning occurred). This trend is shown in Fig. 52.

The observations of steep temperature gradients just above the burning surface of noncatalyzed propellants, i.e., in the fizz zone, are in agreement with results of previous investigators.[32,75,101] The most important result of this experiment is that the temperature gradients become steeper when a propellant is catalyzed to produce super-rate burning. The temperature of the dark zone is not greatly affected by the addition of the catalysts.

The heat generated in the fizz zone is transferred by conduction to the low-temperature upstream reaction region. Such a physical picture can be studied in terms of a flame sheet model, which is the extreme case of the reaction occurring only at the maximum temperature. Such a model has been applied to double base propellant combustion by Rice and Ginell,[36] as described in Section II. Merkle, Turk and

Summerfield,[91] as well as Ohlemiller and Summerfield[102] used a similar method to obtain the heat feedback from the gas phase to the burning surface of a solid propellant. A mathematical model that uses these observations will be developed in Section VII.

The results of the temperature measurements in the fizz zone show that the temperature increases almost linearly with distance for an appreciable distance above the burning surface (a fact that will be utilized later); the temperature gradient becomes low only near the end of the fizz zone. Therefore, it seems that some exothermic reaction begins to occur at the burning surface and that the heat input from gas phase to the burning surface does not take place only through heat conduction from the highest temperature end of the zone, as in a flame sheet model. The implication is that the activation energy in the gas phase, appropriate to an overall reaction rate expression, $\exp(-E_g/RT_g)$, is not large and that the rate of reaction is, as a consequence, more dependent upon the concentration of unreacted gas as well as the temperature.

The steeper temperature gradient in the fizz zone of a propellant catalyzed by lead compounds implies greater heat feedback from the gas phase to the burning surface and an increase in burning rate. This provides good evidence that the site of the accelerated reaction is in the fizz zone. On the other hand, as described in Section IV and V, strong carbon formation was observed at the burning surface of a propellant catalyzed by lead compounds. This experimental result indicates that the initial effect of lead compounds could be in the condensed phase, as concluded by Dauerman and Tajima.[23] Therefore, some active species could be generated when solid carbon is formed at the burning surface by the action of lead compounds, with the active gaseous species yielding a higher rate of chemical reaction in the fizz zone. Thus, a picture of the catalyst action is emerging in which the initial effect is to alter the decomposition process at and below the surface; products of this altered decomposition then yield their greatest effect by accelerating the reactions in the fizz zone. The accelerated fizz zone reactions increase the conductive feedback to the surface, boosting its temperature and the burning rate.

SECTION VII

DISCUSSION OF SUPER-RATE COMBUSTION MODELS PRESENTED BY OTHER WORKERS AND THE MODEL PROPOSED IN THIS STUDY

A systematic experimental program, as described in Sections III to VI, has been undertaken to determine the actual site of the catalytic action that produces super-rate, plateau and mesa burning. In this section the results of these experimental tests are compared with the trends predicted by the super-rate, plateau and mesa burning models of previous investigators. The respective mechanisms on which these models are based are represented pictorially in Fig. 53. A super-rate burning model is presented, which differs from the models of previous workers. In addition, simplified mathematical models of the burning of noncatalyzed and catalyzed propellants are discussed in this section.

A. Discussion of Super-Rate Combustion Models in Light of Available Experimental Evidence

As described in Section II-D, the combustion models proposed by previous investigators are quite different from one another. The models used by previous investigators cannot explain all the experimental results; moreover, some investigators neglected the experimental results of other investigators. The validity of each of the models is discussed below in light of the experimental observations of this and of other investigations.

The photosensitized reaction model proposed by Camp and others[66] agrees qualitatively with certain aspects of the behavior of super-rate burning observed in their own experiments; however it falls short of explaining several other experimental results. This has been checked by mathematical modeling studies based on the UV radiation hypothesis; see Appendix B.

If, as suggested in the model, super-rate burning is initiated by radiation from the luminous flame, it is difficult to explain tripling of the burning rate at 2 atmospheres by the addition of 4% PbO, since, as described in Section III-A, no visible or ultraviolet light is emitted from the gas phase at this pressure.[103]

As a more direct test of this UV radiation hypothesis, Ohlemiller and Summerfield[102] measured the burning rate with and without external radiation. The burning rate increased, as expected with increasing radiation flux but no difference in burning rate was observed when equivalent radiant fluxes with and without ultraviolet (and blue) radiation were used. The increased burning rate was due to the increase in the total heat flux into the burning surface.

Finally, it was observed in this study from temperature profile measurements that the fizz zone reaction is accelerated and the burning rate increased by the addition of lead compounds in the pure fizz-burning pressure range, i.e., in the range where there is total absence of a luminous flame (see Section VI-B). On the basis of the above observations and discussion, the photosensitized model is not confirmed.

The carbon catalysis model proposed by Powling, et al[12] is the only model in which an attempt is made to explain the overall burning behavior, including the super-rate, plateau and mesa-burning phenomena. The model is based on the increased reduction of nitric oxide by carbon in the fizz zone to produce a greater heat flux to the surface. As noted in Section II-A-(4), Powling placed relatively little emphasis on the NO_2 produced in the initial decomposition of the nitrate esters. He preferred to consider the steep temperature gradient in the fizz zone as being due to the exothermic reduction of NO to N_2 in this region. However, if this is what occurs, there should be a significant concentration of N_2 at the beginning of the dark zone; this is not borne out by, for example, the investigations outlined in references 12 and 11. Therefore, the present author feels that the magnitude of the fizz zone temperature gradient is more likely due to the exothermic reduction of NO_2 to NO, and that the reduction to N_2 occurs subsequently in the flame zone.

Powling and co-workers proposed that the super-rate effect is due to the catalysis of the NO reduction in the fizz zone by lead compounds acting in conjunction with the extensive carbon on the burning surface; in the present study, however, it is suggested that the lead acts (indirectly) on the NO_2 in the fizz zone rather than on the NO, in producing super-rate burning. This is supported by Dauerman and Tajima.[23]

The solid carbon generated at the burning surface by the addition of lead compounds plays an important part in the Powling carbon catalysis model, but the model does not account for the reaction step in which the carbon is formed. It is important to include some description of the carbon-formation step because the initial action of lead compounds probably takes place in the condensed phase (as seen in this study). Powling, et al referenced the experimental observation (at low pressures) by Watts[68] that the reaction between carbon and NO is catalyzed by lead; this reaction purportedly produces the mesa by rapidly removing the surface carbon above some pressure level. However, it is also assumed in this model that super-rate burning is caused by catalyzed NO reduction (oxidizing gaseous species, not surface carbon), the catalyst being some combination of the lead and carbon on the burning surface. But this catalytic-reaction process has not been observed in independent experiments; the Watts reference does not support it as Powling seems to imply.

Furthermore, according to the experimental results obtained by Watts,[68] the reaction between carbon and NO catalyzed by copper is faster than the reaction between carbon and NO catalyzed by lead. The present experimental results on propellant behavior show that copper compounds increase the burning rate but not nearly to the same extent as lead compounds above about 6 atm. The appearance and disappearance of solid carbon on the burning surface occurs at about the same time as the appearance and disappearance of metallic-lead globules on the burning surface.[90] Consequently, it appears that the carbon-formation mechanism is in some way connected to the formation of the metallic lead. Therefore, it is felt that the mechanism of the disappearance of the carbon at pressures higher than the mesa-burning range may be more directly related to the simultaneous disappearance of the metallic lead from the burning surface(the two events signalling a return to a more normal, non-carbon forming degradation of the condensed phase). This seems more likely than a sudden onset of rapid oxidation by nitric oxide of carbon that is still trying to form, as proposed in the model of Powling, et al. (It is possible, of course, that all these events, including NO oxidation of carbon, occur in some coupled sequence; there is, as yet, not enough experimental evidence to pin down the likely cause of mesa burning.)

Note again that Powling, et al base their model on two key reaction schemes, one involving the accelerated reduction of NO by solid carbon and lead as catalysts, and the other involving the oxidation of the solid carbon by NO, the latter catalyzed by lead alone. Their hypothesis is that the former reaction occurs in the super-rate burning regime, and that the mesa-burning behavior is due to the dominance of the latter reaction in the mesa-burning pressure range. We have indicated above certain objections to this model based on the present study and those of others.[90] It should be noted that Adams[1] has expressed related objections: there is no evidence to support the suggestion that the reaction involving the oxidation of solid carbon (and, hence, its rapid removal) should occur only in the mesa-burning pressure range, and it seems unlikely that the reaction should suddenly become dominant in this region, especially in view of the fact that it is probably a first-order reaction (Watts[68]) whereas the reaction between NO and other gaseous species is higher than second order. Furthermore, assuming Powling's hypothesis to be correct, it is not clear why the oxidation of solid carbon should cause mesa-burning behavior, (i.e., reduction in burning rate) when the reaction is accompanied by the formation of N_2 with a consequently high heat release.

It should be noted that other investigators have put forth qualitative explanations of super-rate burning. For example, Steinberger[55] proposed a reaction scheme in the gas phase whereby accelerated burning could occur; however, this scheme offers no explanation of mesa or even plateau burning.

As a conclusion to this subsection, the points of disagreement between experimental observations and the models of Camp and Powling will be summarized. Camp's model, based on photosensitized subsurface reactions, due to ultraviolet radiation feedback from the flame zone, is contradicted by the observation of Ohlemiller and Summerfield that ultraviolet radiation from an external source has no significant effect on burning rate, and by the fact that super-rate burning occurs at low pressures, when the flame zone emits no visible or ultraviolet radiation. Powling's model, based on heat feedback from the fizz zone due to the exothermic reduction of NO to N_2 in this region, is at variance with the results of Powling himself, who found the concentration of N_2 in the dark zone to increase only slightly during super-rate burning and in any case, to be of the order of a few percent at most. In light of these criticisms, the author feels the controlling mechanism during super-rate burning to be the exothermic reduction of NO_2 to NO with the accompanying oxidation of C-H-O species to H_2O, CO, CO_2 etc in the fizz zone rather than either of the mechanisms mentioned above.

B. Super-Rate Burning Model Proposed in This Study

The theoretical models used to predict the normal burning rate behavior of double base propellants in terms of the chemical and physical properties of the propellants have been discussed in Section II-D. These models can describe the normal burning rate behavior at various pressures when reasonable values of physical and chemical parameters are inserted. However, a mathematical model capable of predicting super-rate, plateau and mesa burning has not been presented. As described in Section II-D, several qualitative, phenomenological explanations of plateau burning have been presented, but it has been difficult to construct mathematical models from these phenomenological explanations because of the indistinct discussions and insufficient experimental data on super-rate and plateau burning behavior.

The only previous mathematical modeling of catalyzed propellants was done by Ohlemiller and Summerfield.[102] They formulated and solved an approximate version of the photochemical reaction model described in Section II-D, which was originally presented by Camp.[66] They introduced a photodegradation reaction in the subsurface region which is controlled by radiation penetrating from the luminous flame. Their calculated results show that super-rate burning can occur as a result of extra heat release in the subsurface zone or acceleration of the fizz zone induced by photochemical reaction. However, the degree of super-rate burning decreases gradually with increased pressure; the pressure index does decrease as desired, but no negative pressure index has been obtained in their model which is described in Appendix B; furthermore, the discussion of Section VII-A casts serious doubt on the validity of the basic photochemical hypothesis.

In the present section, we will formulate and examine the predictions of a new model of super-rate burning. First, however, it will be useful to recall some of the experimental observations as to catalyst behavior in the combustion wave and begin to present a rationale for this behavior. We will then develop an approximate mathematical representation of this behavior.

(1) Catalyst Behavior in Condensed Phase and at the Burning Surface

The experimental burning surface observations show evidence of catalytic action in the condensed phase (generation of carbonaceous material), which is diminished as the burning rate is increased; this is found for propellants catalyzed by lead or copper compounds. The diminishing catalytic action is most easily explained as the consequence of a purely physical effect: the available time for catalyst action in the condensed phase decreases with higher rate of the surface regression because the thermal wave becomes thinner. To define available time in the condensed phase, a characteristic time is introduced which describes the length of time required for a molecule to pass through the temperature wave in the solid. This characteristic time is given as $\tau_p = \alpha_p/r^2$ where r is the burning rate and α_p is the thermal diffusivity of the propellant; it is evident, then, that the available time for catalyst action in the condensed phase decreases rapidly as burning rate is increased. It is obvious experimentally that the catalytic effect disappears at high burning rate. We will, then, incorporate this effect in our model by assuming that the fractional amount of the propellant affected by the catalyst in the condensed phase is a function of the available time for catalysis. The fraction affected by catalyst decomposes and produces active gaseous species and solid carbon at the burning surface. On the other hand, the fractional part which is not affected by the catalyst in the condensed phase decomposes along the normal pathway, which is assumed to be the same pathway of decomposition as in noncatalyzed propellants.

(2) Catalyst Behavior in Gas Phase

In the approximate mathematical model to be developed here, the active gaseous species generated by the catalyst at the burning surface are assumed to react by an independent path in the gas phase. It is assumed that the reaction of the active species is rapid enough to control the overall gas phase reaction rate when their fractional amount is large. However, by the physical mechanism above, the increased burning rate with increased pressure decreases their fractional amount; then the fractional amount which is not affected by the catalyst in the condensed phase becomes dominant in the gas phase reaction, i.e., the burning process returns to normal.

As described in Section V, it is observed that carbonaceous particles are formed on the burning surface when super-rate burning occurs. This correlates well with the experimental results observed by Dauerman and Tajima.[23] Their measurements revealed that the ratio of (C-H-O species)/(NO_3) or (C-H-O species)/(NO_2) decreases when lead stearate is added to a normal double base propellant (see Section (IV-B). (The C-H-O species contain a large fraction of aldehydes which are taken here to be representative.) When solid carbon formation on the burning surface is induced by the lead stearate, aldehyde (RCHO) concentration decreases without necessarily affecting the concentration of NO_2 (recall that aldehydes and NO_2 are generally believed to be the first stage decomposition products in nitrate ester propellant flames as described in Section II-A-(1)).

Now, the burning rates of gaseous mixtures of formaldehyde (HCHO) and NO_2 and acetaldehyde (CH_3CHO) and NO_2 are strongly dependent on mixture ratio.[26,7] As the ratio of (HCHO)/(NO_2) or (CH_3CHO)/(NO_2) approaches the stoichiometric ratio from the fuel rich side, the reaction rate and hence the burning rate increase rapidly as described in Section II-A-(2).

The experimental temperature profiles in Section VI clearly show that the gas phase reaction rate in the fizz zone is accelerated when lead compounds are added to the propellant. At the same time, a greatly increased amount of carbon appears on the burning surface and the propellant burning rate increases.

On the basis of these observations and the above discussion of NO_2 aldehyde flame speed versus stoichiometric ratio, we suggest the following ordering of events which results in super-rate burning. The lead containing catalyst, in some thermally altered form (possibly PbO), acts below and at the burning surface to promote solid carbon formation in the degradation of the nitric esters. The extent of this carbon promotion reaction is proportional to the amount of catalyst present and the time available as the molecules pass through the thermal wave in the condensed phase. Formation of solid carbon implies that the remaining molecules forming at the burning surface have available a relatively greater proportion of the oxidant NO_2; the equivalence ratio of these gases is shifted nearer stoichiometric and their reaction rate is greatly accelerated. It is this accelerated reaction rate immediately above the surface which boosts the conductive heat input to the surface and hence the burning rate. Note that the amount of heat release above the surface is not controlling here but rather the rate of heat release; it increases the heat feedback (increased $\lambda_g(dT/dx)_{g,s}$) from the gas phase to the burning surface. (Carbon formation on the burning surface need not contribute to heat release in the fizz

zone but rather may reduce the total heat release in the fizz zone.) However, as burning rate increases with pressure, the time available for the catalyst to alter the nitric ester degradation decreases as discussed above. Consequently, as pressure increases, carbon formation decreases, the equivalence ratio of the gases above the surface shifts away from stoichiometric and the burning rate returns to normal. The combustion process discussed above is shown schematically in Fig. 54. Note that this sequence accounts for super-rate burning and its disappearance. It is the latter that reduces the propellant pressure exponent but, as we shall see, this sequence does not yield a negative exponent, or mesa burning.

It is interesting to note that this picture of super-rate burning is consistent with the fact, pointed out by Preckel[52] and Camp,[67] that the effectiveness of lead compounds in producing super-rate burning decreases as the energy of the basic propellant increases. The interpretation here is that since a high energy noncatalyzed propellant contains a greater percentage of NG or more highly nitrated NC; then, like the catalyzed propellant, its surface gasification products contain a higher concentration (more nearly stoichiometric) of NO_2. For example, at a pressure of 100 atm, the burning rate of the propellant which has a heat of explosion of 850 cal/g is 0.71 cm/sec, while the burning rate of the propellant which has a heat of explosion of 1440 cal/g is 2.20 cm/sec at the same pressure.[52] Consequently, the concentration ratio of (C-H-O species)/(NO_2) of the high energy propellant is not significantly affected by the addition of lead compounds (decreased carbon formation on the surface), and only slight super-rate burning is observed. There is also less capacity for additional increases when lead compounds are added; presumably, if a propellant reaches its stoichiometric mixture ratio, the lead compounds would have no effect or even a negative effect.

In the following subsection, a mathematical reaction model is described which utilizes the concept of two, independent gas phase reaction paths as an approximation of the catalyst behavior discussed above. The first gas phase reaction path is not affected by the catalyst; the second gas phase reaction path is induced by the catalyst. It predicts super-rate burning at low pressures and the disappearance of super-rate burning at high pressures.

C. General Equations for Double Base Propellant Burning

The basic assumptions in the following description of the burning rate model are

1. One-dimensional burning*
2. Steady burning at a fixed pressure
3. Negligible radiation from the luminous flame to the burning surface.

With reference to Fig. 3 and the list of symbols at the end of the text, the energy and the species equations are:

condensed phase energy equation:

$$\frac{d}{dx}\left(\lambda_p \frac{dT}{dx}\right) - \rho_p r c_p \frac{dT}{dx} + \mathcal{R}_p Q_p = 0 \qquad \text{(VII-1)}$$

condensed phase species equation for species j:

$$\frac{d}{dx}\left(\rho_p D_{p,j} \frac{d\varepsilon_j}{dx}\right) - \rho_p r \frac{d\varepsilon_j}{dx} - \mathcal{R}_{p,j} = 0 \qquad \text{(VII-2)}$$

fizz zone energy equation:

$$\frac{d}{dx}\left(\lambda_g \frac{dT}{dx}\right) - \rho_g u_g c_g \frac{dT}{dx} + \mathcal{R}_g Q_g = 0 \qquad \text{(VII-3)}$$

fizz zone species equation for species i:

$$\frac{d}{dx}\left(\rho_g D_{g,i} \frac{d\varepsilon_i}{dx}\right) - \rho_g u_g \frac{d\varepsilon_i}{dx} - \mathcal{R}_{g,i} = 0 \qquad \text{(VII-4)}$$

Several additional assumptions are applied to the above equations: (1) no endothermic or exothermic reaction is involved within the condensed phase (below the surface), however, some thermally neutral chemical reaction can be included, (2) the luminous flame zone does not contribute to the

---

*It is emphasized that the carbon formation does not violate the spirit of the one-dimensional assumption. In all compositions, at pressures above two atmospheres, the surface carbon is a friable ash whose density is a small fraction of the propellant density. The surface is not covered by a layer of sufficient mass or depth to substantially invalidate the idealized picture of planar surface regressing under the influence of a one-dimensional feedback flux from the fizz zone.

conductive heat feedback from the gas phase to the burning surface, (3) no species diffusion in the condensed phase or in the fizz zone. Assumption 1 is acceptable for propellants burning in the normal rocket operating pressure as described in Section VI-C. Assumption 2 is valid below 100 atmospheres as described in Section IV-E and Section VI-C. Assumption 3 is not examined experimentally in this study; it is essentially a mathematical expedient, similar to that used by Parr and Crawford[37] which should not greatly affect the qualitative behavior of the model. (It is recognized that a further mode of burning rate acceleration by carbon formation at the surface is possible. Carbon has a substantially higher thermal conductivity than the hot gases above the surface. It is possible, then, that heat feedback along the carbon filaments could locally raise the temperature of the gases coming off the surface and accelerate their rate of reaction. This mechanism may well be operative to some extent but it is probably much less important than the stoichiometric shift mechanism proposed here; in general, the amount of carbon available for boosting the conductive feedback is small.) Equations (VII-1) and (VII-2) are then simplified as follows:

for the condensed phase:

$$\frac{d}{dx}\left(\lambda_p \frac{dT}{dx}\right) - \rho_p r c_p \frac{dT}{dx} = 0 \qquad \text{(VII-1a)}$$

$$- \rho_p r \frac{d\varepsilon_j}{dx} - \mathcal{Q}_{p,j} = 0 \qquad \text{(VII-2a)}$$

The treatment of the fizz zone reaction, which determines the heat feedback from the gas phase to the condensed phase, $\lambda_g (dT/dx)_{s,g}$, is the basic point which leads to the burning rate equation. Krier, T'ien, Sirignano and Summerfield[111] obtained a heat feedback model (KTSS model) by assuming a heat release in the gas phase which is a step function that has a positive constant value $\mathcal{Q}$. In this study, we will examine the validity of using this KTSS model for the fizz zone reaction. The experimental measurement results which are described in Section VI-B and C are used to examine this point.

The model represents the heat feedback from the gas phase to the condensed phase by the integration of the energy equation in the gas phase [Eq. (VII-3)] with the boundary condition that heat flux at infinity must be zero,

$$\lambda_g \frac{dT}{dx}\Big)_{g,s} = \frac{\lambda_g \mathcal{Q} Q_g}{\rho_p c_g r}\left\{e^{-\rho_p r c_g x_i/\lambda_g} - e^{-\rho_p r c_g x_g/\lambda_g}\right\} \qquad \text{(VII-5)}$$

where $\mathcal{R}$ is a positive constant for $x_i < x \leq x_g$ and is zero elsewhere, and $\mathcal{R}$ should be considered an average value for the real reaction rate occurring in the fizz zone.

In general, reaction rates are strongly dependent on the temperature when the activation energy is high. In the case of reactions involving NO_2 in the fizz zone, it is reported that the activation energy is low[26] (Rice and Ginell[36] assumed zero activation energy). Therefore the reaction rate is not strongly influenced by the temperature as described in Section VI-C. Thus it is assumed that the two major effects on the reaction rate -- temperature and concentration of reactant -- tend to cancel each other; as the reaction proceeds the temperature increases but the concentration of the reactants decreases. Furthermore, it is assumed that the resulting constant rate of reaction occurs from the burning surface ($x_i = 0$) throughout the fizz zone (the temperature gradients above the burning surface are approximately constant up to about 50% of the fizz zone as shown in Fig. 44, which indicate some heat release even right above the burning surface).

Equation (VII-5) becomes, under these approximations,

$$\lambda_g \left(\frac{dT}{dx}\right)_{s,g} = \frac{\lambda_g \mathcal{R} Q_g}{\rho_p c_g r}\left\{1 - e^{-\rho_p r c_g x_g/\lambda_g}\right\} \qquad \text{(VII-6)}$$

$$= \frac{\lambda_g \mathcal{R} Q_g}{\rho_p c_g r}\left\{1 - e^{-x_g/L^*}\right\} \qquad \text{(VII-6a)}$$

where L^* is a characteristic length.

Using the values obtained by the temperature measurements described in Section VI, the term in the exponent in Eq. (VII-6) is evaluated as follows: $c_g = 0.4$ cal/g°C $\rho_g = 1.54$ g/cm^3, $\lambda_g = 4 \times 10^{-4}$ cal/cm-sec°C

p	atm	1.2	8	20	100
r	cm/sec	0.046	0.158	0.821	1.05
x_g	$\times 10^{-4}$ cm	200	170	120	80
L^*	$\times 10^{-4}$ cm	140	41	7.9	6.2
x_g/L^*		1.4	4.1	15	13

The term in the exponent is quite large above 1 atm so that Eq. (VII-6) becomes approximately,

$$\lambda_g \left.\frac{dT}{dx}\right)_{s,g} = \frac{\lambda_g \mathcal{R} Q_g}{\rho_p c_g r} \qquad \text{(VII-7)}$$

This asymptote occurs whenever the heat transferred back to the solid is small compared to the heat released in the gas phase, which implies that x_g/L^* is large enough.

We realize that Eq. (VII-7) is not precise, however, the equation permits the behavior of super-rate burning to be studied without introducing mathematical complexities that are inconsistent with the uncertainty in the transport and reaction parameters.

The boundary conditions for the energy equations in the condensed phase, at the burning surface, respectively, are given as:

$$T = T_0 \quad \text{at} \quad x = -\infty$$

$$\lambda_p \frac{dT}{dx} = \lambda_g \left.\frac{dT}{dx}\right)_{s,g} + \rho_p r Q_s \quad \text{at} \quad x = 0$$

The integrated energy equation obtained from utilizing Eq. (VII-1a) and the boundary conditions is:

$$\rho_p r c_p (T_s - T_0) = \lambda_g \left.\frac{dT}{dx}\right)_{s,g} + \rho_p r Q_s \qquad \text{(VII-8)}$$

Generally, the reaction rate of a one-step reaction

$$\sum_{i=1}^{N} \nu_i' M_i \xrightarrow{k} \sum_{i=1}^{N} \nu_i'' M_i \qquad \text{(VII-9)}$$

is given as

$$\mathcal{R}_i = \rho_g \frac{d\varepsilon_i}{dt} = \rho_g u_g \frac{d\varepsilon_i}{dx} = (\nu_i'' - \nu_i') k \prod_{\ell=1}^{N} (\rho_g \varepsilon_\ell)^{\nu_\ell'} \qquad \text{(VII-10)}$$

Therefore the heat feedback from the gas phase to the burning surface is, from Eqs. (VII-4), (VII-7) and (VII-10):

$$\lambda_g \left.\frac{dT}{dx}\right)_{s,g} = \frac{\lambda_g}{\rho_p c_g r} \sum_{i=1}^{N} Q_{g,i} (\nu_i'' - \nu_i') k \Pi (\rho_g \varepsilon_\ell)^{\nu_\ell'} \qquad \text{(VII-11)}$$

Then, combining Eq. (VII-8) with Eq. (VII-11), and solving for r we get:

$$r = \sqrt{\frac{\lambda_g}{\rho_p^2 c_p c_g (T_s - T_0 - Q_s/c_p)} \sum_i^N Q_{g,i} (\nu_i'' - \nu_i') k \Pi (\rho_g \varepsilon_\ell)^{\nu_\ell'}} \qquad \text{(VII-12)}$$

Equation (VII-12) is the simplified burning rate equation. If the rates of the reactions in the fizz zone are known, the burning rate is given in terms of gas density (pressure), burning surface temperature, initial propellant temperature and physical properties of propellant.

The burning surface temperature is related to the burning rate by an Arrhenius equation which assumes first order decomposition reactions for each reaction species at the burning surface.

$$r = \sum_{j=1}^{M} \varepsilon_j Z_{s,j} \exp(-E_{s,j}/RT_s) \qquad \text{(VII-13)}$$

where M is the number of assumed parallel, independent gasification reaction paths in the condensed phase.

Equations (VII-12) and (VII-13) can be combined, then the burning rate and the burning surface temperature can be obtained for any given set of conditions.

D. Normal and Super-Rate Burning Model Based on Assumed Reaction Paths in the Fizz Zone Representing Stoichiometric Shift

Like previous investigators who modeled normal double base propellant combustion,[36,37,1] we assume that such normal burning is adequately described by a single, overall, first-order surface decomposition reaction followed by a single, overall second-order reaction in the fizz zone.

NONCATALYZED REACTION SCHEME

$$A \longrightarrow A_1^* \longrightarrow X_1 + Y_1 \longrightarrow X_1' + Y_1' \longrightarrow \text{LUMINOUS FLAME}$$

CONDENSED PHASE SURFACE FIZZ ZONE DARK ZONE

Now, translation of the proposed accelerated fizz zone reactions, which yield super-rate burning, into mathematical terms presents a problem. In the proposed model this accel-

eration is attributed to a shift in the stoichiometry of the gases but this cannot be put in mathematical terms without a detailed knowledge of the elementary reactions. Lacking this knowledge, we seek to simulate the acceleration effect in the simplest possible way. To do this, we assume that the catalyst introduces a second decomposition path in the condensed phase yielding more highly reactive species in the fizz zone (and also carbon at the surface). As before, the amount of propellant passing through this new pathway is proportional to the amount of catalyst present and the available time for catalyst action in the condensed phase.

CATALYZED REACTION SCHEME

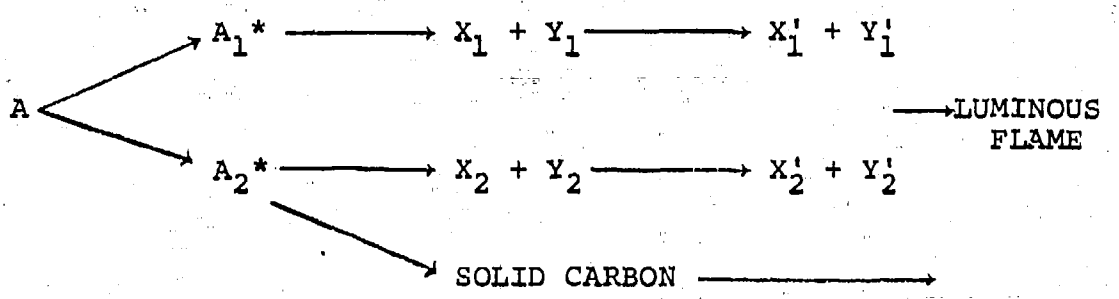

CONDENSED PHASE | SURFACE | FIZZ ZONE | DARK ZONE

The burning rate equations based on the above reaction schemes are derived below from the simplified burning rate model described in the previous subsection.

(1) Burning Rate Model for Noncatalyzed Propellant

Generally the gas phase reactions in flame models for premixed gases and the gas phase reactions of propellant burning are assumed to be bimolecular and hence of second order. For noncatalyzed propellant burning a single overall second order reaction in the fizz zone is assumed. Then we can express Eq. (VII-12) as

$$r = \sqrt{\frac{\lambda_g Q_g k_1 \epsilon_1^{*2} \rho_g^2}{\rho_p^2 c_p c_g (T_s - T_0 - Q_s/c_p)}} \qquad \text{(VII-14)}$$

The reaction rate constant, k_1, is a function of temperature expressed as;

$$k_1 = Z_1 \exp(-E_1/RT_g) \qquad \text{(VII-15)}$$

The perfect gas law is also used to relate the assumed spatially constant density to p and T_g:

$$\rho_g = p/RT_g \qquad \text{(VII-16)}$$

Equations (VII-15) and (VII-16) are substituted into (VII-14), then, the burning rate equation for noncatalyzed propellant is given as

$$r = \sqrt{\frac{\lambda_g Q_1 \varepsilon_1^{*2} Z_1 \exp(-E_1/RT_g)}{\rho_p^2 c_p c_g (T_s - T_0 - Q_s/c_p)\cdot(RT_g)^2}}\; p \qquad \text{(VII-17)}$$

where T_g is given as

$$T_g = T_0 + Q_s/c_p + Q_1/c_g$$

The burning surface decomposition rate, i.e., burning rate, is given from Eq. (VII-13) as:

$$r = Z_{s,1} \exp(-E_{s,1}/RT_s) \qquad \text{(VII-13a)}$$

The nonlinear character of the algebraic equations, (VII-17) and (VII-13a), implies the need for an iteration solution. In practice, the normal burning rate at a given p and T_0 is solved by a single variable Newton-Raphson iteration.

(2) Burning Rate Model for Catalyzed Propellant

For catalyzed propellant burning the reaction path in the condensed phase takes two paths; one is not affected by the burning catalyst added to the propellant and the other one is affected by the catalyst; the latter generates "active" species in the condensed phase, however this catalyst reaction is assumed to have a negligible reaction heat. In general such catalytic reactions may be heterogeneous (if the catalyst is undissolved) or homogeneous, however, the actual reaction mechanism is not clear at present. Therefore in this analysis a homogeneous type reaction is assumed in the condensed phase. The concentration of "active" species A_2^* at the burning surface is derived as follows:

$$\frac{d[A_2^*]}{dt} = r\frac{d[A_2^*]}{dx} = k_p [A][\beta C] \qquad \text{(VII-18)}$$

k_p is given by the same type of Arrhenius expression as Eq. (VII-15). Then

$$\frac{d[A_2^*]}{[A_0 - A_2^*]} = \frac{1}{r} Z_p \exp(-E_p/RT)\cdot[\beta C]dx \qquad \text{(VII-19)}$$

Pure heat conduction is assumed in the condensed phase, therefore, from the temperature profile at the burning surface one gets

$$\frac{dx}{dT} = \frac{\alpha_p}{r} \frac{1}{T_s - T_0} \tag{VII-20}$$

The chemical reaction occurs mainly very near the burning surface, therefore Eq. (VII-20) is substituted i to (VII-19) and integrated by using the Zeldovich-Frank Kamenetskii approximation.[104] Then the mass fraction of "active" species ε_2^* at the burning surface is

$$\varepsilon_2^* = 1 - \exp\left\{ - \frac{\alpha_p}{r^2} \frac{Z_p[\beta C]}{T_s - T_0} \frac{RT_s}{E_p} \exp(-E_p/RT_s) \right\} \tag{VII-21}$$

and

$$\varepsilon_1^* = 1 - \varepsilon_2^* \tag{VII-22}$$

The gas phase reaction scheme consists of two independent reaction pathways in the fizz zone. For reaction path 1, the chemical reaction mechanism is completely the same as in the case of noncatalyzed propellant burning. A second order reaction is assumed and the gaseous reactant fractions X_1 and Y_1 equals ε_1^* at the burning surface. Via reaction path 2, the more reactive gaseous species X_2 and Y_2 which are produced by the catalytic effect in the condensed phase react faster than X_1 and Y_1. This reaction is also assumed to be second order.

The total rate of reaction in the fizz zone is expressed as follows:

$$\mathcal{R}_g = k_1[X_1][Y_1] + k_2[X_2][Y_2] \tag{VII-23}$$

The reaction rate constants, k_1 and k_2, are expressed by the same type of Arrhenius expressions as Eq. (VII-15). Thus, the burning rate equation for burning with catalysis is given from Eqs. (VII-12) and (VII-23),

$$r = \sqrt{\frac{\lambda_g (H_1 + H_2)}{\rho_p^2 c_p c_g (T_s - T_0 - Q_s/c_p)(RT_g)^2}}\, p \tag{VII-24}$$

$$H_1 = Q_1 Z_1 \varepsilon_1^{*2} \exp(-E_1/RT_g) \tag{VII-25-1}$$

$$H_2 = Q_2 Z_2 \varepsilon_2^{*2} \exp(-E_2/RT_g) \qquad \text{(VII-25-2)}$$

where T_g is given as:

$$T_g = T_0 + Q_s/c_p + (Q_1\varepsilon_1^* + Q_2\varepsilon_2^*)/c_g \qquad \text{(VII-26)}$$

The burning surface decomposition rate, i.e., burning rate, is given from Eq. (VII-13) as:

$$r = Z_{s,1}\varepsilon_{s,1}^* \exp(-E_{s,1}/RT_s) + Z_{s,2}\varepsilon_{s,2}^* \exp(-E_{s,2}/RT_s) \qquad \text{(VII-13b)}$$

A solution to this set of equations, (VII-13) and (VII-24), is obtained iteratively at any particular pressure by assuming a trial value of T_s in Eq. (VII-13). If the calculated value of T_s does not correspond to the initially assumed value, the procedure is repeated with a new value of T_s until sufficiently close agreement is obtained.

E. Discussion of the Models for Noncatalyzed and for Catalyzed Burning

One of the main objectives in presenting mathematical burning rate models for noncatalyzed and catalyzed propellants is to check the proposed qualitative mechanism for super-rate, plateau and mesa burning; this check is useful even though it requires considerable simplification of the actual reaction mechanism. The burning-rate models described in this section still involve a number of parameters relating chemical kinetics to the burning rates. However, as described in Section III, the detailed structure of the chemical-reaction paths in the narrow zone around the burning surface are not well known. Therefore, the numerical calculations carried out with the models are only approximate; of main interest, then, are the qualitative trends in their predictions. The necessary physical and chemical values used in the burning rate models were selected from the results of previous investigators.

The results of the model calculations are shown in Figs. 55, 56, and 57. The values assumed for the physical constants and reaction kinetics are listed at the end of the text. Figure 55 shows the results for noncatalyzed and catalyzed propellant burning-rates. The predicted burning rate for the noncatalyzed propellant increases with increasing pressure; the pressure index also increases from 0.35 at one atmosphere to 0.85 over 20 atmospheres, when the initial propellant temperature is 323°K. Other observations are that the predicted burning rate increases with an increase in the initial temperature of the propellant, and that the predicted temperature sensitivity, σ_p, defined as $\sigma_p = \partial \log r/\partial T$

(at constant pressure) is large at low pressures and decreases with increasing pressure. These general predicted trends of burning rate behavior agree fairly well with real propellants.

Figure 55 also shows the super-rate burning behavior predicted by the burning-rate model. The greatest super-rate burning occurs in the low-pressure region, and the effect decreases with increasing pressure. Above about 100 atmospheres, the super-rate burning has essentially disappeared. The behavior of the temperature sensitivity is different from the behavior of that of a noncatalyzed propellant: here the temperature sensitivity decreases gradually with increasing pressure, then increases as the super-rate effect begins to disappear. This predicted qualitative behavior of the burning rate and of the temperature sensitivity are in good agreement with experimental observations. It is also observed that the predicted temperature sensitivity of the propellant catalyzed with lead compounds decreases as pressure index decreases, as reported by Preckel.[52]

Figure 31 shows the behavior that underlies the appearance and disappearance of the super rate. The fraction, ϵ_2^*, of propellant mass affected by the catalyst is at a maximum at very low pressures and thus the fizz zone reactions receive their maximum acceleration. However, since, at these very low pressures, surface heat release is most important for the burning rate, the super-rate may actually be somewhat less than at higher pressures where ϵ_2^* is very slightly less but the fizz zone is more important. For still higher pressures, the decay of ϵ_2^* with increasing pressure becomes dominant and the super-rate begins diminishing. (Recall that the catalytic effect in the condensed phase diminishes as pressure and hence burning rate increases.) The relative heat contributions from the two reaction paths are shown in Fig. 56 in terms of the ratio of the reaction parameters defined by the equations, (VII-25-1) and (VII-25-2).

One sees that the heat generated by path 2 is largely dominant throughout the super-rate burning range and that the heat generated by path 1 dominates in the high-pressure range.

The calculated burning-surface temperature and the temperature at the end of the fizz zone of noncatalyzed and catalyzed propellants are compared in Fig. 57. It is observed that the burning-surface temperatures of the noncatalyzed and catalyzed propellant increase gradually with increasing pressure. The temperature of catalyzed propellant is higher than that of the noncatalyzed propellant throughout super-rate burning range; the difference between the two is reduced as the super-rate effect decreases. During super-rate burning, the temperature at the end of the fizz zone of the cata-

lyzed propellant is higher than that of the noncatalyzed propellant. As the super-rate effect diminishes, the order is reversed owing to the lower heat release at the burning surface of the catalyzed propellant assumed in this example (in accord with results of Lenchitz[76] - see Section IV).

The burning rate model described above, which is based on experimental observations of the gradual disappearance of super-rate, fails to explain the mechanism of mesa-burning and only partially accounts for the plateau. The burning rate model describes qualitative burning-rate behavior which indicates that the burning rate at high pressures is largely dependent on the gas-phase reaction. Therefore, plateau and mesa burning are also considered to be largely a consequence of some type of effect on the gas phase reaction.

It is clear from Eq. (VII-24) that the term under the square-root sign must vary inversely with pressure in the mesa-burning regime. This behavior is most likely to be due to a pressure dependence of the H_1 and H_2 terms in order to get mesa-burning, i.e., to an inhibiting reaction occurring in the fizz zone, which could not be specified in this analysis for lack of experimental evidence.

As discussed in Section II-C-(3), it is well known that the addition of lead compounds inhibits both the gas phase reactions of nitrate esters[1] and hydrocarbon oxidation.[64,65] Therefore, it is possible that the burning rate decreases and a zero or negative pressure index appears with increasing pressure owing to the inhibition by lead of reactions analogous to pathway 2 in the fizz zone in the super-rate burning model. At higher pressures, the reaction pathway 1 dominates the burning rate and the burning rate therefore returns to normal. However, the mechanism of combustion inhibition by lead compounds is not sufficiently well understood at this point to justify its inclusion in the burning rate model presented here. The combustion model discussed above is shown schematically in Fig. 58.

F. Summary of the Discussion of Combustion Models

The validity of combustion models presented by other workers has been discussed in Section VII-A. It was pointed out in this section that none of the models offers satisfactory explanations of the observed experimental trends. The models of Camp and Powling are compared in Table 3 with that of the author, on a basis of the effect of the respective zones in the combustion region on the super-rate and mesa-burning phenomena. In Table 4, the theoretical trends of the 3 models are listed together with the experimental evidence supporting these trends. It is observed that the trends predicted by the author's model are in closer agreement with experimental results than are the trends predicted by the models of Camp and Powling.

SECTION VIII

SUMMARY OF OBSERVATIONS

In this section, we summarize the observations that were used to develop the new model of super-rate burning presented in this study.

A. Major Experimental Observations of this Study and Their Implications

1. At a given pressure, the temperature gradient in the fizz zone just above the burning surface during super-rate burning of a catalyzed propellant is greater than that of a noncatalyzed propellant. This implies that the heat feedback from the gas phase to the solid phase is increased by the addition of catalysts. (Section VI-B.)

2. The heat-release at the burning surface of a catalyzed propellant is approximately the same as that of a noncatalyzed propellant at low pressures. This implies that an increased exothermicity causing super-rate burning does not occur in the condensed phase (at least at low pressure and probably high pressure). (Section VI-C.)

3. During super-rate burning of a catalyzed propellant the luminous flame is displaced further from the burning surface than the luminous flame of noncatalyzed propellants. In the mesa-burning pressure range, the luminous flame zone approaches closer to the burning surface with increasing pressure. This implies that the reactions beyond the fizz zone do not affect the burning rate. (Section IV-E.)

4. The structure of the burning surface of a double base propellant is significantly affected by the addition of catalysts. (The effect is less pronounced at high burning rates than it is at low burning rates.) It is inferred from these observations that the catalysts act on the decomposition of the condensed phase and this action of the catalysts is related to the residence time in the condensed phase, during which catalysis takes place. (Section V-B.)

B. Supporting Observations

(1) Observations of This Study

1. The structure of the burning surface of a propellant catalyzed with PbSa is smooth and produces finely-divided particles ($\sim$ 50μ in diameter), which are ejected into the gas phase during super-rate burning. (Section V-B.)

2. CuSa increases the burning rate at low pressures and slightly decreases it at high pressure, however, when combined with the super-rate-producing additive PbSa, it enhances the super-rate burning, at low pressures. (Section III-A.)

3. The temperature at the burning surface of a propellant catalyzed with a mixture of PbSa and CuSa is approximately 25°C higher than that of a non-catalyzed propellant in the range of pressures below 20 atmospheres, in which super-rate burning occurs; in both cases, the surface temperature increases with increasing pressure. At twenty atmospheres, the temperature at the burning surface of a catalyzed propellant is about 375°C, while that at the surface of a noncatalyzed propellant is about 345°C. (Section VII-C.)

4. The overall order of the chemical reaction in the dark zone is approximately 2.5 and is not affected by the addition of burning rate catalysts. (Section IV-E.)

5. The length of the dark zone can be correlated theoretically with the pressure index of the burning rate and with the order of the chemical reaction in the dark zone. The correlation is of the form $L_d = C/p^{n-m}$ where L_d is the length of the dark zone, p the pressure, m the pressure index, n the overall order of the reaction and C a constant. (Section IV-C.)

6. The burning-rate behavior of PNC/TMETN-type double base propellants is similar to that of NC/NG propellants in so far as temperature sensitivity, super-rate, plateau and mesa burning are concerned. Accordingly, the results of studies of PNC/TMETN propellants are directly applicable to studies of NC/NG propellants. (Section III-A.)

(2) Observations from Other Investigators

1. The rate of oxidation of C-H-O species by NO_2 increases when lead stearate is added to a propellant. Upon initial decomposition, the ratio (C-H-O species/NO_2), for a catalyzed propellant is less than that for noncatalyzed propellant (Dauerman[23]).

2. The reaction rate between NO_2 and aldehydes is strongly dependent on the mixture ratio of the two species (Pollard[26]). This suggests that the increasing solid carbon content on the surface increases the heat feedback by increasing the concentration of oxidizing species at the surface. The excess carbon is oxidized downstream of the fizz zone.

3. In the super-rate range, the ratio of carbon dioxide to carbon monoxide is higher for a catalyzed propellant than that for a noncatalyzed propellant. However, the ratio is less than that of a noncatalyzed propellant in the plateau and mesa-burning regimes (Lenchitz[76]).

4. High energy propellants (containing a higher concentration of nitroglycerin) are less susceptible to super-rate burning by the addition of lead compounds, even when sufficient lead compounds are added to significantly lower the caloric value of the propellant. Furthermore, the burning rate at high pressure does decrease. This suggests that there is not a simple connection between the super-rate and mesa mechanisms (Preckel,[51] Camp[67]).

5. For propellants catalyzed with lead compounds, small globules of lead or lead oxide are observed during burning at all pressures below the upper limit of plateau burning. The size of globules decreases as burning rate increases and the number of globules increases with burning rate. However, such globules are not seen above mesa burning pressures (Brown[90]).

SECTION IX

CONCLUSIONS OF THIS STUDY

In relating the conclusions of this study to the super-rate burning process, firstly, the important physical changes attributed to the lead compounds are summarized and, secondly, the combustion zone interactions which produce super rate and eventually lead to plateaus and mesas are briefly recapitulated. The parenthetical references used here are the experimental observations summarized in Section VIII.

The regions affected directly by lead compounds are the condensed phase just below the burning surface and the burning surface itself (a distance less than 100μ at 1 atm and 20μ at 20 atm), where the lead compounds decompose ultimately into finely-divided metallic lead or lead oxide particles. The decomposition products of the lead catalyst react with the nitrate esters in this surface reaction layer where the chemical degradation leads to NO_2, aldehydes, etc., altering their normal thermal decomposition paths so as to produce an increased amount of solid carbon (VIII-A-4 and VIII-A-2), at the burning surface of the catalyzed propellant. Despite this chemical pathway alteration, the net exothermicity of the surface reaction layer is not significantly changed (VIII-A-2).

Most importantly, the presence of lead compounds results in a strong acceleration of the fizz zone reactions, i.e., those in the gas phase close to (100μ) the surface (VIII-A-1). Acceleration of the reactions in the subsequent dark zone or in the luminous flame zone is not significant (VIII-A-3). The result of the fizz reaction rate acceleration is an increased heat feedback (e.g., increases as large as 100% to the surface) which produces super-rate burning.

Consequently, we conclude that this action of the lead compounds to produce increased carbon and the acceleration of the fizz zone reactions are directly coupled as follows. The portion of decomposed organic molecules which appears at the surface in the form of carbon rather than readily oxidizable aldehydes could reduce the effective fuel/oxidizer (aldehyde/NO_2) ratio (VIII-B-(2)-1). This increased NO_2 proportion constitutes a shift in equivalence ratio toward the stoichiometric value. Such a shift for NO_2/aldehyde mixtures results in a greatly accelerated reaction rate (VIII-B-(2)-2). The excess carbon is oxidized downstream of the fizz zone. This is the proposed mechanism of fizz zone reaction rate acceleration.

The action that results in the plateau effect is as follows. As the burning rate increases (resulting both from increased pressure and addition of lead compounds), the time

available for the initial catalytic action in the surface reaction layer decreases (e.g., 0.2 sec at 1 atm and 0.002 sec at 20 atm) (VIII-A-4 and VIII-B-(2)-5). Thus, the fraction of the reactants affected by the lead compounds (and higher concentration of NO_2) decreases in the fizz zone with increasing burning rate. Consequently, the reaction rate in the fizz zone approaches the normal reaction pathway, and, then, the increased burning rate, i.e., super-rate burning, diminishes as pressure increases. The rate of disappearance of super-rate with increased pressure determines the slope of the burning rate plateau.

The burning rate model resulting from this study differs from previous comprehensive models with respect to at least two major points. In the pressure range of our experiments, our evidence did not support Camp's theory of photosensitized subsurface reactions. While Powling, et al, hypothesized that carbon catalyzed the NO reduction in the fizz zone, evidence in this study supports the conclusion that lead compounds act instead to increase the proportion of NO_2 entering the fizz zone which in turn accelerates the gas phase reactions there which utilize NO_2, not NO, as the oxidizer.

The research reported here resulted in a reasonable explanation of super-rate burning. However, no firm explanation was found for the abrupt termination of super-rate effects at the pressure where plateaus and mesas are measured, nor is there any experimentally-supported explanation in the literature. The unfinished task of explaining the plateau and mesa effects is a very important one which should receive additional attention.

As a result of this study, research on other combustion processes and characteristics of practical interest (e.g., ignition, combustion instability, temperature sensitivity, hazard classification, extinction) can be undertaken with an improved level of understanding.

LIST OF SYMBOLS

			Units
a	-	constant in Vieille's burning rate law, ap^m	
c	-	specific heat	cal/g K
d	-	dark zone index, $d = m - n$	
k	-	reaction rate constant	
m	-	pressure exponent (or pressure index) in Vieille's burning rate law, ap^m	
n	-	order of chemical reaction	
p	-	pressure	atm, kg/cm^2
r	-	burning rate normal to surface	cm/sec
u	-	velocity	cm/sec
x	-	distance from propellant surface (Fig.3)	cm,mm,μ
A	-	designation of chemical species produced in condensed phase by normal pathway	
A*	-	designation of chemical species produced in condensed phase by catalyzed pathway	
C	-	designation of catalyst	
D	-	diffusion coefficient	cm^2/sec
E	-	activation energy	cal/mole
H	-	reaction parameter used in burning equation (Eq. VII-25)	
L	-	dark-zone length	cm,mm
M	-	designation of an arbitrary chemical species	
Q	-	energy of reaction per unit mass	cal/g
R	-	universal gas constant, 1.987	cal/mole-°K
$\mathscr{R}$	-	reaction rate	$mole/cm^3$-sec
T	-	temperature	K,C
T_0	-	initial propellant temperature	K,C

X - designation of chemical species in fizz zone

X' - designation of chemical species in dark zone

Y - designation of chemical species in fizz zone

Y' - designation of chemical species in dark zone

Z - pre-exponential factor

α - thermal diffusivity cm^2/sec

β - coefficient of catalysis in condensed phase (Eq. VII-18)

ε - mass fraction

η_d - catalyst activity in dark zone, (Eq. IV-13)

λ - thermal conductivity cal/cm-sec-C

ν_i' - stoichiometric coefficient for species i appearing as a reactant

ν_i'' - stoichiometric coefficient for species i appearing as a product

ρ - density g/cm^3

σ_p - temperature sensitivity of burning rate at constant pressure $(d \ln r/dT_0)_p$ K^{-1}

τ - reaction time sec

Subscripts

1 - reaction path 1

2 - reaction path 2

c - catalyzed

d - dark zone

f - luminous flame zone

g - gas phase

i - species i

j - species j

n - noncatalyzed

p - condensed phase

s - burning surface

LIST OF ABBREVIATIONS*

Propellants

NC	- Nitrocellulose
NG	- Nitroglycerine
PNC	- Plastisol nitrocellulose (Naval Ordnance Station).
TMETN	- Trimethylolethane trinitrate (Trojan Powder Co.)
TEGDN	- Triethylene glycol dinitrate (Trojan Powder Co.)
EC	- N,N' - Diethylcarbanilide (Eastman Organic Chemical).
DPA	- Diphenylamine
DBP	- Dibutylphthalate
DEP	- Diethylphthalate
NDA	- 2-Nitrodiphenylamine
CW	- Candelilla wax
AP	- Ammonium perchlorate

Catalysts

PbSa	- Normal lead salicylate (National Lead Co.)
Pb2-EH	- Lead 2-ethylhexoate (National Lead Co.)
PbO	- Lead oxide (Allied Chemical Corp.)
Pb	- Lead powder (Alcan Metal Powders)

---

*More complete description of the ingredients is included in Section 2 of Appendix D.

CuSa	- Monobasic cupric salicylate (National Lead Co.)
Cu	- Copper powder (Alcan Metal Powders)
Sa	- Salicylic acid (Fisher Scientific Co.)
C	- Carbon powder (Columbian Carbon Co.)
PHOSCHEK-30	- Ammonium polyphosphate (Monsanto Co.)
OXAMIDE	- (Eastman Organic Chem. Dept.)

LISTING OF PHYSICAL CONSTANTS AND PARAMETERS FOR BURNING RATE MODEL CALCULATION

The following numerical values were assumed as typical of double base propellants in the calculations:

$c_p = 0.35$ cal/g C

$c_g = 0.40$ cal/g C

$\alpha_p = 0.00093$ cm^2/sec

$\lambda_g = 0.0002$ cal/cm-sec C

$\rho_p = 1.54$ g/cm^3

$E_s = 17 \times 10^3$ cal/mole

$A = 5 \times 10^5$ cm/sec

$Q_1 = 330$ cal/g

$Z_1 = 1 \times 10^9$ $cm^3/g\text{-}sec$

$E_1 = 17 \times 10^3$ cal/mole

The chemical kinetic parameters for the plateau burning rate model are assigned the following reasonable values; these values are not the result of experiment but rather are deduced:

$E_{s,2} = 17 \times 10^3$ cal/mole

$Z_{s,2} = 5 \times 10^5$ cm/sec

$E_2 = 7.7 \times 10^3$ cal/mole

$E_p = 5 \times 10^3$ cal/mole

$Z_2 = 1 \times 10^9$ $cm^3/g\text{-}sec$

$Z_p = 5 \times 10^6$ $cm^3/g\text{-}sec$

$Q_2 = 360$ cal/g

$[\beta C] = 0.01$

REFERENCES

1. Adams, G. K. and Wiseman, L. A., "The Combustion of Double Base Propellants," Selected Combustion Problem., Butterworth's Scientific Publications, London, 1954, pp. 277-288.

2. Powling, J., Smith, W. A. W. and Thynne, J., "The Flame Decomposition of Some Substituted Ethyl Nitrates," Combustion and Flame, Vol. 4, No. 8, 1960, pp. 201-211.

3. Hicks, J. A., "The Low Pressure Decomposition Flame of Ethyl Nitrate," Eighth Symposium (International) on Combustion, Williams Wilkins, Baltimore, 1962, pp. 487-496.

4. Adams, G. K. and Bawn, C. E. H., "The Homogeneous Decomposition of Ethyl Nitrate," Trans. Faraday Soc., Vol. 45, 1949, pp. 494-499.

5. Levy, J., "The Thermal Decomposition of Nitrate Esters," J. Amer. Chem. Soc., Vol. 76, 1954, pp. 3254-3257.

6. Levy, J. B., "A Kinetic Study of the Thermal Decomposition of Ethyl Nitrate," U.S. Naval Ordnance Laboratory, NAVORD Report 2313, June, 1952.

7. Powling, J. and Smith, W. A. W., "The Combustion of the Butane-2, 3- and 4-Diol Dinitrates and Some Aldehyde-Nitrogen Dioxide Mixtures," Combustion and Flame, Vol. 2, No. 2, 1958, pp. 157-170

8. Adams, G. K., "The Chemistry of Solid Propellant Combustion: Nitrate Ester or Double Base Systems," Proceedings of the Fourth Symposium on Naval Structual Mechanics, Purdue University, April 1965, pp. 117-147.

9. Huggett, C., "Combustion of Solid Propellants," Combustion Processes, High Speed Aerodynamics and Jet Propulsion Series, Vol. 2, Princeton University Press, Princeton, 1956, pp. 514-574.

10. Crawford, B. L., Huggett, C. and McBrady, J. J., "Observations on the Burning of Double-Base Powders," National Defense Research Committee Armor and Ordnance Report No. A-268 (OSRD No. 3544), April, 1944.

11. Heller, C. A. and Gordon, A. S., "Structure of the Gas Phase Combustion Region of a Solid Double Base Propellant," J. Phys. Chem., Vol. 59, 1955, pp. 773-777.

12. Hewkin, D. J., Hicks, J. A., Powling, J. and Watts, H., "The Combustion of Nitric Ester-Based Propellants: Ballistic Modification by Lead Compounds," Combustion Science and Technology, 1971, Vol. 3 pp. 307-327.

13. Dickson, A. D., Crawford, B. L., and Rotenberg, D. L., "Infrared Spectra of Propellant Flames," Industrial and Engineering Chemistry, Vol. 48, 1956, pp. 759-761.

14. Robertson, R. and Napper, S. S., "The Evolution of Nitrogen Peroxide in the Decomposition of Guncotton," J. Chem. Soc., Vol. 91, 1907, pp. 764-786.

15. Wilfong, R. E., Penner, S. S. and Daniels, F., "An Hypothesis for Propellant Burning," J. Phys. & Colloid Chem., Vol. 54, No. 6, 1950, pp. 863-872.

16. Rideal, E. K. and Robertson, A. J. B., "The Spontaneous Ignition of Nitrocellulose," Third Symposium (International) on Combustion, The Williams & Wilkins Co., Baltimore, 1949, pp. 536-544.

17. May, I. W., Private Communication, Dec. 1972.

18. White, K. J. and Morgan, C. U., "Radical Mechanisms in the Ignition of Propellants," 2nd Review of AMC Research on Ignition Phenomena Program, Ballistic Research Laboratories, Nov. 1972.

19. Gelernter, G., Browning, L. C., Harris, S. R. and Mason, C. M., "The Slow Thermal Decomposition of Cellulose Nitrate," J. Phys. Chem., Vol. 60, 1956, pp. 1260-1264.

20. Shafizadeh, F. and Wolfram, M. L., "The Controlled Thermal Decomposition of Cellulose Nitrate. IV. C^{14} Tracer Experiments," J. Amer. Chem. Soc., Vol. 80, 1958, pp. 1675-1677.

21. Dauerman, L., Salser, G. E. and Tajima, Y. A., "Evidence for Nitrogen Trioxide in the Combustion of a Double Base Propellant," J. of Phys. Chem., Vol. 69, 1965, pp. 3668-3669.

22. Dauerman, L., Salser, G. E. and Tajima, Y. A., "Characteristics of Volatilized Species from Solid Propellants," AIAA J., Vol. 5, No. 8, Aug. 1967, pp. 1501-1503.

23. Dauerman, L. and Tajima, Y. A., "Solid-Phase Reactions of a Double-Base Propellants," AIAA J., Vol. 6, No. 4, 1968, pp. 678-683.

24. Pollard, F. H. and Wyatt, R. M. H., "Reactions Between Formaldehyde and Nitrogen Dioxide; Part I. The Kinetics of the Slow Reaction," Trans. Farad. Soc., Vol. 45, No. 320, 1949, pp. 760-767.

25. Pollard, F. H. and Woodward, P., "Reactions Between Formaldehyde and Nitrogen Dioxide: Part II. The Explosive Reaction," Trans. Farad. Soc., Vol. 45, No. 320, 1949, pp. 767-770.

26. Pollard, F. H. and Wyatt, P. M. H., "Reactions Between Formaldehyde and Nitrogen Dioxide; Part III. The Determination of Flame Speeds," Trans. Farad. Soc., Vol. 46, No. 328, 1950, pp. 281-289.

27. McDowell, C. A. and Thomas, J. H., "Oxidation of Aldehyde in the Gaseous Phase; Part IV. The Mechanism of the Inhibition of the Gaseous Phase Oxidation of Acetaldehyde by Nitrogen Peroxide," Trans. Farad. Soc., Vol. 46, No. 336, 1950, pp. 1030-1039.

28. Sawyer, R. F. and Glassman, I., "The Reactions of Hydrogen with Nitrogen Dioxide, Oxygen, and Mixtures of Oxygen and Nitric Oxide," 12th Symposium (International) on Combustion, 1969, pp. 469-479.

29. Cummings, G. A. McD., "Effect of Pressure on Burning Velocity of Nitric Oxide Flames," Nature, No. 4619, May, 1958, p. 1327.

30. Strauss, W. A. and Edse, R., "Burning Velocity Measurements by the Constant Pressure Bomb Method," 7th Symposium (International) on Combustion, 1958, pp. 377-385.

31. Sawyer, R. F., "The Homogeneous Gas Phase Kinetics of Reactions in the Hydrazine-Nitrogen Tetroxide Propellant System," Ph.D. Thesis, Princeton University, 1965.

32. Klein, R., Mentser, M., von Elbe, G. and Lewis, B., "Determination of the Thermal Structure of a Combustion Wave by Fine Thermocouples," J. Phys. & Colloid Chem., Vol. 54, No. 6, 1950, pp. 877-884.

33. Boys, S. F. and Corner, J., "The Structure of the Reaction Zone in a Flame," J. Proc. Roy. Soc., London, Vol. A197, No. 1048, 1949, pp. 90-106.

34. Corner, J., "The Fffect of Diffusion of the Main Reactants on Flame Speeds in Gases," J. Proc. Roy. Soc., London, Vol. A198, No. 1054, 1949, pp. 388-405.

35. Corner, J., Theory of the Interior Ballistics of Guns, Wiley, 1950.

36. Rice, O. K. and Ginell, R., "Theory of Burning of Double-Base Rocket Propellants," J. Phys. & Colloid Chem., Vol. 54, No. 6, 1950, pp. 885-917.

37. Parr, R. G. and Crawford, B. L., "A Physical Theory of Burning of Double-Base Rocket Propellants," J. Phys. & Colloid Chem., Vol. 54, No. 6, 1950, pp. 929-954.

38. Geckler, R. D., "The Mechanism of Combustion of Solid Propellants," Selected Combustion Problems, Butterworth's Scientific Publications, London, 1954, pp. 289-339.

39. Spalding, D. B., "The Theory of Burning of Solid and Liquid Propellants," Combustion and Flame, Vol. 4, No. 1, 1960, pp. 59-76.

40. Preckel, R. F., "Ballistics of Catalyst Modified Propellants," Bulletin of Fourth Meeting of the Army-Navy Solid Propellant Group, Armour Research Foundation, Illinois Institute of Technology, Chicago, 1948, pp. 67-71.

41. Camp, A. T., Preckel, R. F., "Castable Homogeneous Propellant Systems Containing Polymerizable Materials," Allegany Ballistics Laboratory, ABL/p-14, April, 1950.

42. Zmachinski, S. and Preckel, R. F., "Strand Rate Ballistic Studies of Plateau Type Propellants," Allegany Ballistics Laboratory, ABL/P-19, Nov., 1950.

43. Zmachinski, S. and Preckel, R. F., "Strand Rate Ballistics Studies of Plateau-Type Propellants; Rate-Controlling Characteristics of Carbon Black and Other Additives," Allegany Ballistics Laboratory, ABL/P-21, May, 1951.

44. Godsey, J. H. and Preckel, R. F., "Strand Rate Ballistic Studies of Plateau-Type Propellants; Characteristics of Various Ballistic Modifiers," Allegany Ballistics Laboratory, ABL/ -25, April, 1955.

45. Preckel, R. F., "Gas Producing Charges", U. S. Patent 3,033,716, May, 1962 (filed March 7, 1955).

46. Preckel, R. F., "Gas Producing Charges," U. S. Patent 3,033,715, May, 1962 (filed March 7, 1955).

47. Preckel, R. F., "Gas Producing Charges," U. S. Patent 3,033,717, May, 1962 (filed April 14, 1955).

48. Preckel, R. F., "Gas Producing Charges," U. S. Patent 3,033,718, May, 1962 (filed April 14, 1955).

49. Camp, A. T., "Solventless Processed Nitrocellulose Propellants Containing Lead Compounds," U. S. Patent 3,088,858, May, 1963 (filed April 30, 1953).

50. Camp, A. T. and Crescenzo, F. G., "Nitrocellulose Gas Producing Charges Containing Copper and Lead Salts and Aluminum," U. S. Patent 3,138,499, June 1964, (filed May 28, 1958).

51. Preckel, R. F., "Plateau Ballistics in Nitrocellulose Propellants," ARS J., Vol. 31, No. 9, 1961, pp. 1286-1287.

52. Preckel, R. F., "Plateau Ballistics in Nitrocellulose Propellants," AIAA J., Vol. 3, No. 2, 1965, pp. 346-347.

53. Camp, A. T. and Haussmann, H. K., "Numerical Evaluation of Super-Rate Burning of Extruded Double-Base Propellants and the Related Importance of the Chemical Structure of Burning-Rate Modifiers," U. S. Naval Ordnance Test Station, NAVORD Report 5870, Jan. 1959.

54. Crawford, B. L., Huggett, C. and McBrady, J. J., "Double-Base Powders with Catalyzed Nitrocellulose," University of Minnesota Report No. 18, Aug. 1944.

55. Steinberger, R. and Carder, K. E., "Mechanism of Burning of Nitrate Esters," Bulletin of the Tenth Meeting of the JANNAF Solid Propellant Center, Dayton, June, 1954, pp. 173-187.

56. Steinberger, R. and Carder, K. E., "Mechanism of Burning of Nitrate Esters," Fifth Symposium (International) on Combustion, Reinhold, New York, 1955, pp. 205-211.

57. Whittaker, A. G., Williams, H. and Rust, P. M., "Burning-Rate Studies; Part 5. A Liquid-Propellant System Showing the Negative Pressure-Coefficient Phenomenon," U. S. Naval Ordnance Test Station, NAVORD Report 1999, Sept. 1955.

58. Adams, G. K. and Lloyd, G. O., "The Effect of Lead Acetylsalicylate on the Combustion of Nitric Esters," Explosives Research and Development Establishment, ERDE Report No. 10/R/53, Mar. 1953.

59. Adams, G. K., Parker, W. G. and Wolfhard, H. G., "Radical Reaction of Nitric Oxide in Flames," Discussions Faraday Soc., Vol. 14, 1953, pp. 97-103.

60. Ellis, W. R., Smythe, B. M. and Theharne, E. D., "The Effect of Lead Oxide and Copper Surfaces on the Thermal Decomposition of Ethyl Nitrate Vapor," Fifth Symposium (International) on Combustion, Reinhold, New York, 1955, pp. 641-647.

61. Chamberlain, H. N., Hoare, D. E. and Walsh, A. D., "The Mode of Action of Lead Tetraethyl as an Inhibitor of Combustion Processes," Discussions Faraday Soc., Vol. 14, 1953, pp. 89-97.

62. Bardwell, J., "Inhibition of Combustion Reactions by Inorganic Lead Compounds," Combustion and Flame, Vol. 5, No. 1, 1961, pp. 71-75.

63. Hoare, D. E., Walsh, A. D. and Li, T. M., "The Oxidation of Tetramethyl Lead and Related Reactions," 13th Symposium (International) on Combustion, 1971, pp. 461-469.

64. Lewis, B. and von Elbe, G., Combustion Flames and Explosions of Gases, Academic Press Inc., New York, 1961.

65. Ashmore, P. G., Catalysis and Inhibition of Chemical Reactions, Butterworths, London, 1963.

66. Camp, A. T., Haussmann, H. K., McEwan, W. S., Henry, R. A., Olds, R. H. and Besser, E. D., "A Decade of Progress in the Understanding of Certain Ballistic Properties in Double-Base Propellants," U. S. Naval Ordnance Test Station, NAVORD Report 5824, Jan. 1958.

67. Camp, A. T., Carton, C. H. and Haussmann, H. K., "Possible Catalytic Mechanisms in Double Base Propellant Burning," Bulletin of the Tenth Meeting of the JANNAF Solid Propellant Group, Wright Air Development Center, Dayton, June, 1954, pp. 81-106.

68. Watts, H., "The Oxidation of Charcoal by Nitric Oxide and the Effect of Some Additives," Trans. Faraday Soc., Vol. 54, 1957, pp. 93-105.

69. Steinberger, R., "Plateau Propellants; Mechanism of the Plateau Effect," Bulletin of the Eighth Meeting of the JANNAF Solid Propellants Group, 1952, pp. 157-172.

70. Mellor, J. W., "Inorganic and Theoretical Chemistry," Longmans, Green and Co., Vol. VII, p. 577, 679. Cited in Ref. 69.

71. Shinha, S. L. and Patwardhan, W. D., "Burning of Platonized Propellants," Explosivestoffe, No. 10, 1968, pp. 223-225.

72. Camp, A. T., "Nitrocellulose Plastisol Propellants," Propellants Manufacture, Hazards, and Testing, Advances in Chemistry, Series 88, American Chemical Society, Wash. D.C., 1969, pp. 29-35.

73. Steinz, J. A., Stang, P. L. and Summerfield, M., "The Burning Mechanism of Ammonium Perchlorate-Based Composite Solid Propellants," Aerospace and Mechanical Sciences Report No. 830, Princeton University, Feb. 1969.

74. Steinz, J. A., Stang, P. L. and Summerfield, M., "The Burning Mechanism of Ammonium Perchlorate-Based Composite Solid Propellants," High Speed Photographs Presented at AIAA 4th Propulsion Joint Specialist Conference, Cleveland, Ohio, June 1968.

75. Sabadell, A. J., Wenograd, J. and Summerfield, M., "Measurement of Temperature Profiles through Solid Propellant Flames Using Fine Thermocouples," AIAA J., Vol. 3, No. 9, 1965, pp. 1580-1584.

76. Lenchitz, C. and Haywood, B., "Determination of the Role of the Ballistic Modifier in Propellant Combustion Using the Heat of Explosion Test," Combustion and Flame, Vol. 10, No. 2, 1966, pp. 140-145.

77. McEwan, W. S. and Jenkins, H. P., "Heat of Explosion

of Solid Propellants Containing Metalic Additives," U. S. Naval Ordnance Test Station, NAVORD Report 1934, Dec. 1951.

78. Crawford, B. L., "Studies on Propellants," University of Minnesota, UM/FR (OSRD 6374), Oct. 1945.

79. Maltsev, V. M. and Summerfield, M., "Investigation of the Spectral Radiation Characteristics of the Flame-jet of Nitrate-Ester Propellants Containing Platonizing Catalysts," to be published.

80. Sotter, J. G., "Chemical Kinetics of the Cordite Explosion Zone," Tenth Symposium (International) on Combustion, The Combustion Institute, 1965, pp. 1405-1411.

81. Maltsev, V. M., Law, R. J., Ryan, N. W., Bare, A. D. and Summerfield, M., "On the Mechanical Effect of the Catalytic Additives PbSa and CuSa in the Combustion of Double-Base Propellants," Unpublished paper, Jan. 1972.

82. Heath, G. A. and Hirst R., "Some Characteristics of the High Pressure Combustion of Double-Base Propellants," Eighth Symposium (International) on Combustion, The Williams & Wilkins Co., Baltimore, 1962, pp. 711-720.

83. Laidler, K. J., Chemical Kinetics, McGraw-Hill Inc., New York, 1965.

84. Penner, S. S., Chemistry Problems in Jet Propulsion, Pergamon Press, New York, 1957.

85. Hinshelwood, C. N., The Kinetics of Chemical Change, Oxford University Press, Oxford, 1950.

86. Hinshelwood, C. N. and Green, T. E., "The interaction of Nitric Oxide and Hydrogen and the Molecular Statistics of Termolecular Gaseous Reactions," J. Chem. Soc., 1926, pp. 730-739.

87. Pannetier, G. and Souchay, P., Chemical Kinetics, Elsevier Publishing Co., New York, 1967.

88. Crawford, B. L., Huggett, C. and McBrady, J. J., "The Mechanism of the Burning of Double-base Propellants," J. Phys. & Colloid Chem., Vol. 54, No. 6, 1950, pp. 854-862.

89. Schuyler, F. L., "Analytical Investigation of Com-

bustion Instability in Solid Propellant Rockets," IIT Research Institute Report ITTRI-A6002, Chicago, 1963.

90. Brown, L. M. and Chaille, J. L., "The Role of the Metal in Mesa Catalysis," Bulletin of the Twelfth Meeting of the JANNAF Solid Propellant Group, 1956, pp. 275-286.

91. Merkle, C. L., Turk, S. L. and Summerfield, M., "Extinguishment of Solid Propellants by Rapid Depressurization," Aerospace and Mechanical Sciences Dept. Report No. 880, Princeton University, July, 1969.

92. Summerfield, M., Ohlemiller, T. J., Caveny, L. H. and DeLuca, L., "Rate Controlling Processes in Double Base Propellant Ignition," 1st Review of AMC Fundamentals of Ignition Task, Ballistic Research Laboratories, Nov. 1971; Also see DeLuca, L., Caveny, L. H. and Summerfield, M., "A Comparative Study of Radiative Ignition Characteristics of Different Classes of Solid Propellants," AIAA 11th Aerospace Sciences Meeting, Washington, D.C., AIAA preprint 72-176, Jan. 1973.

93. Strittmater, R. C., Holmes, H. E. and Watermeier, L. A., "Measurement of Temperature Profiles in Burning Solid Propellant," Ballistic Research Laboratories, Memorandum Report No. 1737, March 1966.

94. Suh, N. P., Tsai, C. L., Thompson, C. L. and Moore, J. S., "Ignition and Surface Temperatures of Double Base Propellants at Low Pressure: Thermocouple Measurements," AIAA J., Vol. 8, No. 7, 1970, pp. 1314-1321.

95. Tsai, C. L., Woodward, E. C. and Suh, N. P., "The Surface Temperature of M-2 Double Base Propellants at Low Pressures," A Progress Report to Picatinny Arsenal, University of South Carolina, 1969.

96. Powling, J. and Smith, W. A. W., "Measurement of the Burning Surface Temperatures of Propellant Compositions by Infra-red Emission," Combustion and Flame, Vol. 6, No. 3, 1962, pp. 173-181.

97. Zenin, A. A., "Structure of Temperature Distribution in Steady-State Burning of a Ballistite Powder," Fizika Goreniya iVzryva, Vol. 2, No. 3, 1966, pp. 67-76.

98. Aleksandrov, V. V., Konev, E. V., Mikheev, V. F. and Khlevnoi, S. S., "Surface Temperature of Burning

Nitroglycerine Powder," Fizika Goreniya i Vzryva, Vol. 2, No. 1, 1966, pp. 68-73.

99. Schach, A., Industrial Heat Transfer, John Wiley & Sons, Inc., 1965.

100. Zenin, A. A., "Burning of Nitroglycerine Powder in Vacuum and at Subatmospheric Pressures," Fizika Goreniya i Vzryva, Vol. 2, No. 1, 1966, pp. 74-78.

101. Kubota, N., Caveny, L. H. and Summerfield, M., "Temperature Sensitivity of Double Base Propellants," Proceeding of Eighth JANNAF Combustion Meeting, Naval Post-Graduate, Monterey, Sept. 1971, pp. 387-401.

102. Ohlemiller, T. J. and Summerfield, M., "A Study of the Mechanism of Super-Rate Burning in Platonized Double Base Propellants," Unpublished Paper, Guggenheim Laboratories, Princeton University, Mar. 1971.

103. Maltsev, V. M., Private Communication, Jan. 1972.

104. Frank-Kamenetskii, D. A., Diffusion and Heat Exchange in Chemical Kinetics, Princeton University Press, Princeton, N.J. translated from Russian edition, 1955.

105. Kubota, N., Caveny, L. H. and Summerfield, M., "Combustion Processes of Double Base Propellants," Fifth Fall Technical Meeting, The Eastern Section of the Combustion Institute, Waterloo, Aug. 1971.

106. Seleznev, V. A., Pokhil, P. F., Maltsev, V. M. and Bavykin, I. B., "An Optical Method of Measuring the Burning Surface Temperature of Condensed Systems," Combustion and Flame, Vol. 13, 1960, pp. 139-142.

107. Hunt, M. H., Heller, C. A. and Gordon, A. S., "Surface Temperature of Burning Double Base Propellant," U. S. Naval Ordnance Test Station, NAVORD Report 2079, Jan. 1954.

108. Davis, B. E., "The Kinetics and Mechanism of Solid, Double-Base, Rocket Propellant Combustion," Ph.D. Thesis, University of Sheffield, 1970.

109. Shook, G. B., "Measurement of Some Properties of Solid Propellants Pertinent to Ignition and Combustion Studies," U. S. Naval Ordnance Test Station, NAVORD Report 1949, Mar. 1952.

110. Hildenbrand, D. L., Whittaker, A. G. and Euston, C. B., "Measurement of the Temperature Distribution in Burning Liquid Strands," U. S. Naval Ordnance Test Station, NAVORD Report 1999, Part 4, May 1955.

111. Krier, H., T'ien, J. S., Sirignano, W. A. and Summerfield, M., "Nonsteady Burning Phenomena of Solid Propellants: Theory and Experiments," AIAA J., Vol. 6, No. 2, 1968, pp. 278-285.

Table 1

Overall Reaction Order n in Dark Zone
Determined from Burning Rate Index m and Dark Zone Index d.

PROPELLANT TYPE	CATALYST	PRESSURE RANGE, ATM	m	d	n	REFERENCE
PNC/TMETN NO. 1026	NO CATALYST	15 - 60	0.80	-1.69	2.49	KUBOTA
PNC/TMETN NO. 1029	1% CuSa 1% PbSa	15 - 60	0.45	-1.96	2.41	KUBOTA
PNC/TMETN NO. 1031	1% CuSa 1% PbSa	15 - 60	0.28	-2.27	2.55	KUBOTA
NC/NG	NO CATALYST	20 - 100	0.56	-1.95	2.51	HEATH REF. 82
NC/NG	NO CATALYST	11 - 35	0.60	-2.20	2.80	HELLER REF. 11
NC/NG	NO CATALYST	17 - 41	0.45	-2.00	2.45	CRAWFORD REF. 10

Table 2

Reaction Steps That Have Been Proposed
in Double Base Propellant Burning

1. Subsurface reaction and reaction at burning surface

$$R\text{-}ONO_2 \longrightarrow NO_2 + R'\text{-}CHO \quad \text{species}$$

$$\left\{\begin{matrix} NC \\ NG \end{matrix}\right\} \qquad \left\{\begin{matrix} HCHO \\ CH_3CHO \\ HCOOH \\ \text{etc.} \end{matrix}\right\}$$

This reaction is endothermic.
(Ref. Adams,[1] Adams,[8] Crawford[10] and Wilfong[15])

2. Reaction at surface and in fizz zone (establishes a rapid temperature rise in the gas phase and a net heat release at burning surface).

$$NO_2 + R'\text{-}CHO \quad \text{species} \longrightarrow NO + C\text{-}H\text{-}O \quad \text{species}$$

$$\left\{\begin{matrix} HCHO \\ CH_3CHO \\ HCOOH \\ \text{etc.} \end{matrix}\right\} \qquad \left\{\begin{matrix} CO,\ CO_2 \\ CH_4,\ H_2O \\ H_2,\ \text{etc.} \end{matrix}\right\}$$

Probably some small amount of reaction involving NO.
(Ref. Adams,[1] Schuyler[89] and Crawford[10])

For example,

$$NO_2 + HCHO \rightarrow NO + H_2O + CO, \quad \Delta H \sim 43 \text{ kcal/mole}$$

$$2NO_2 + HCHO \rightarrow 2NO + H_2O + CO_2, \quad \Delta H \sim 97 \text{ kcal/mole}$$

less likely

$$NO_2 + HCHO \rightarrow 1/2\ N_2 + H_2O + CO_2, \quad \Delta H \sim 132 \text{ kcal/mole}$$

$$2NO + HCHO \rightarrow N_2 + H_2O + CO_2, \quad \Delta H \sim 81 \text{ kcal/mole}$$

3. Reactions in dark zone
(slow, yielding mild temperature changes; involving NO).

$$NO + C\text{-}H\text{-}O \quad \text{species} \longrightarrow N_2,\ CO_2,\ CO$$

$$\left\{\begin{matrix} CO,\ H_2 \\ CH_4,\ \text{etc.} \end{matrix}\right\} \qquad H_2O,\ \text{etc.}$$

Such reactions occur mostly above 1000 C
(Ref. Sotter,[80] Davis,[108] Sawyer,[28] Sawyer,[31] and Powling[12]).

4. Reactions in luminous flame zone
(steep temperature gradient coincides with luminous flame front; final flame and final combustion products are produced).

$$NO + \begin{Bmatrix} CO,\ H_2 \\ CH_4,\ \text{etc.} \end{Bmatrix} \text{ species} \longrightarrow N_2,\ CO_2,\ CO,\ H_2O,\ \text{etc.}$$

(Ref. Adams,[1] Crawford,[10] Sotter,[80] Davis,[108] and Powling[12]).

For example,

$$NO + H_2 \longrightarrow 1/2\ N_2 + H_2O,\ \Delta H \sim -79\ \text{kcal/mole}$$

$$NO + CO \longrightarrow 1/2\ N_2 + CO_2,\ \Delta H \sim -89\ \text{kcal/mole}$$

The reactions in this zone do not include NO_2 reactions.

Table 3

Summary of Combustion Models in Terms of Processes Considered in the Several Flame Zones

MECHANISM	UV RADIATION (CAMP)	CATALYTIC CARBON (POWLING)	THIS STUDY (KUBOTA)
SUPER-RATE BURNING MECHANISM			
FLAME ZONE	INCREASED UV RADIATION FROM Pb	NO EFFECT	NO EFFECT
DARK ZONE	NO EFFECT	NO EFFECT	NO EFFECT
FIZZ ZONE	NO EFFECT	Pb + CARBON CATALYTIC REDUCTION NO	INCREASED RATE NO_2 + C-H-O SPECIES
SURFACE	NO EFFECT	CARBON FORMATION	CARBON FORMATION, DECREASED [C-H-O SPECIES]
SUBSURFACE	NC + Pb + UV RADIATION → SENSITIZE	NO EFFECT	Pb CHANGES REACTION PATHWAY
RATE CONTROL	FLAME ZONE & SUBSURFACE	FIZZ ZONE	FIZZ ZONE & SUBSURFACE
MESA BURNING MECHANISM			
FLAME ZONE	SATURATED UV RADIATION	NO EFFECT	NO EFFECT
DARK ZONE	NO EFFECT	NO EFFECT	NO EFFECT
FIZZ ZONE	NO EFFECT	OXIDATION OF CARBON BY CATALYZED NO	INHIBITION REACTION INVOLVING Pb
SURFACE	UV RADIATION BLOCKED BY LEAD METAL	SOLID CARBON DISAPPEARS	SOLID CARBON DECREASES
SUBSURFACE	SENSITIZATION DECREASES	NO EFFECT	Pb EFFECT DECREASES
RATE CONTROL	SURFACE	FIZZ ZONE	FIZZ ZONE

TABLE 4

EXPERIMENTAL EVIDENCE IN SUPPORT OF PROPOSED THEORETICAL MECHANISMS

A = UV Radiation Mechanism proposed by Camp

B = Carbon catalytic mechanism proposed by Powling

C = Mechanism proposed by Kubota

○ = Theory supported by experiment

× = Theory not supported by experiment

EXPERIMENTAL SUBJECT	A	B	C	EXPERIMENTER
FIZZ ZONE TEMP. GRAD.		○	○	Kubota
DARK ZONE TEMP.		×	○	Powling; Kubota
FLAME ZONE TEMP.	○		○	Maltsev Lenchitz
BURNING SURFACE TEMP.	○	○	○	Kubota
RADIATION FROM FLAME ZONE	○			Maltsev
HEAT OF EXPLOSION		×	○	Lenchitz
DARK ZONE COMPOSITION		○	○	Powling
DARK ZONE LENGTH			○	Kubota
FINAL PRODUCTS				Lenchitz
GAS PHASE REACTION TIME		×	○	Kubota
CARBON ADDITION	○			Preckel; Kubota
METALLIC Aℓ EFFECT	○			Camp
INCREASED LEAD CONTENT		○	○	Preckel; Kubota
OTHER ADDITIVES				
PARTICLE SIZE	○		○	Camp; Kubota
MIXING CONDITION	○		○	Kubota

TABLE 4 (Continued)

EXPERIMENTAL SUBJECT	A	B	C	EXPERIMENTER
CARBON UV ABSORBER EFFECT	O			Camp
CARBON CATALYTIC EFFECT				
ARTIFICIAL UV EFFECT	×			Ohlemiller
UV ABSORBER EFFECT	O			Camp
HEAT RELEASE AT SURFACE	×	O	O	Kubota
MINIMUM BURNING PRESSURE	×			Kubota
BURNING SURFACE STRUCTURE	O	O	O	Brown; Kubota
CARBON AT SURFACE		O	O	Powling; Kubota
LEAD AT SURFACE	×		O	Brown; Kubota
INITIAL DECOM. PRODUCTS	O		O	Dauerman
FIRST STAGE LEAD ACTION	O		O	Steinberger; Dauerman
HIGH ENERGY PROP. COMP.			O	Preckel Camp
TEMPERATURE SENSITIVITY			O	Camp; Kubota

Camp (66, 67)
Powling (12)
Lenchitz (79)
Ohlemiller (102)
Brown (90)
Maltsev (79)
Preckel (51, 52, 43, 44)
Dauerman (23)
Steinberger (69)

( ) Denotes Reference Number

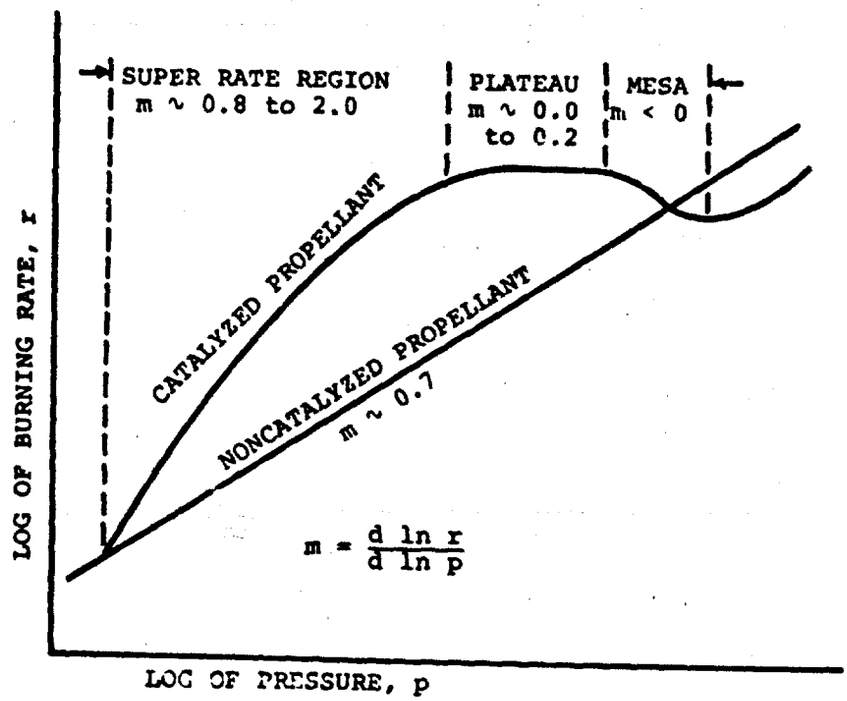

Fig. 1. Definition of super rate, plateau and mesa-burning.

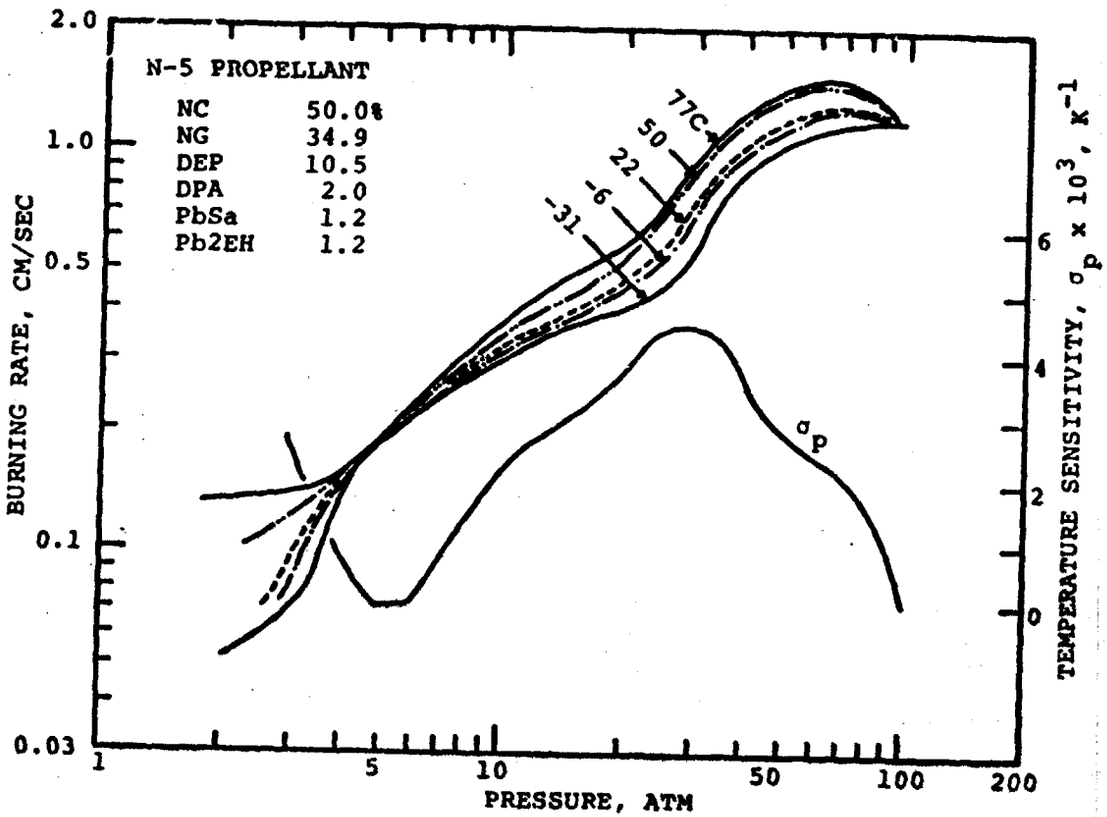

Fig. 2. Plateau propellant burning rate and temperature sensitivity of widely used propellant.

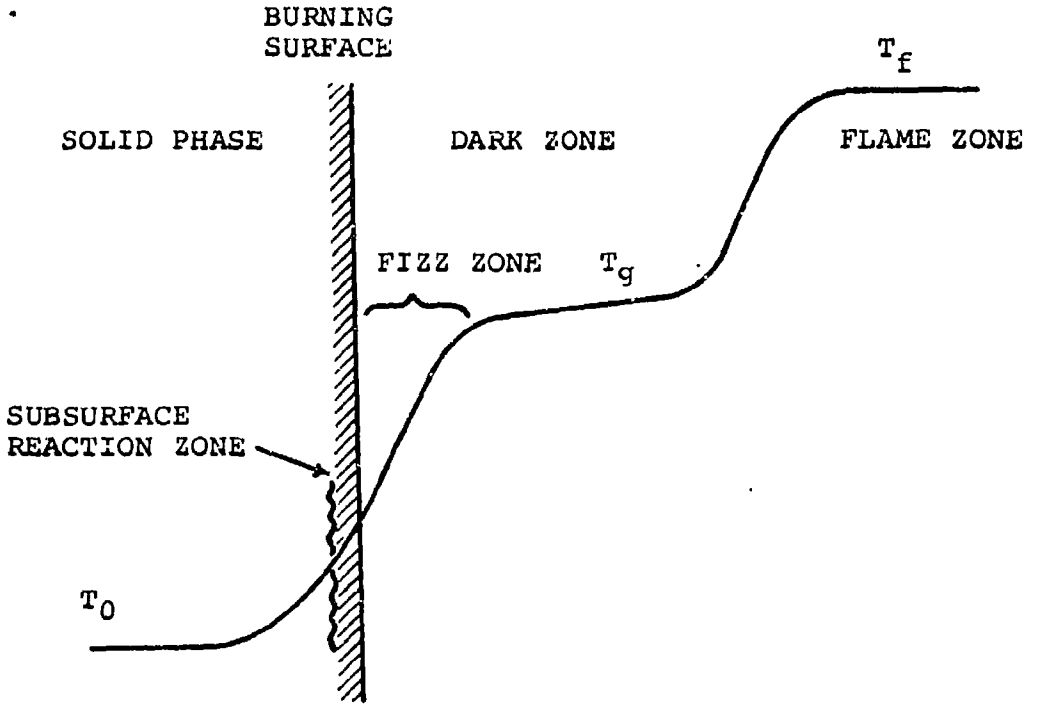

Fig. 3. Combustion zones and processes of double base propellant.

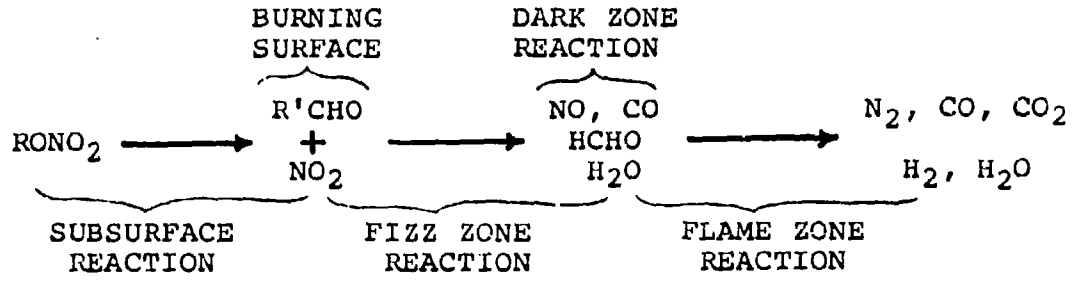

Fig. 3A. Reaction scheme of combustion processes of double base propellants.

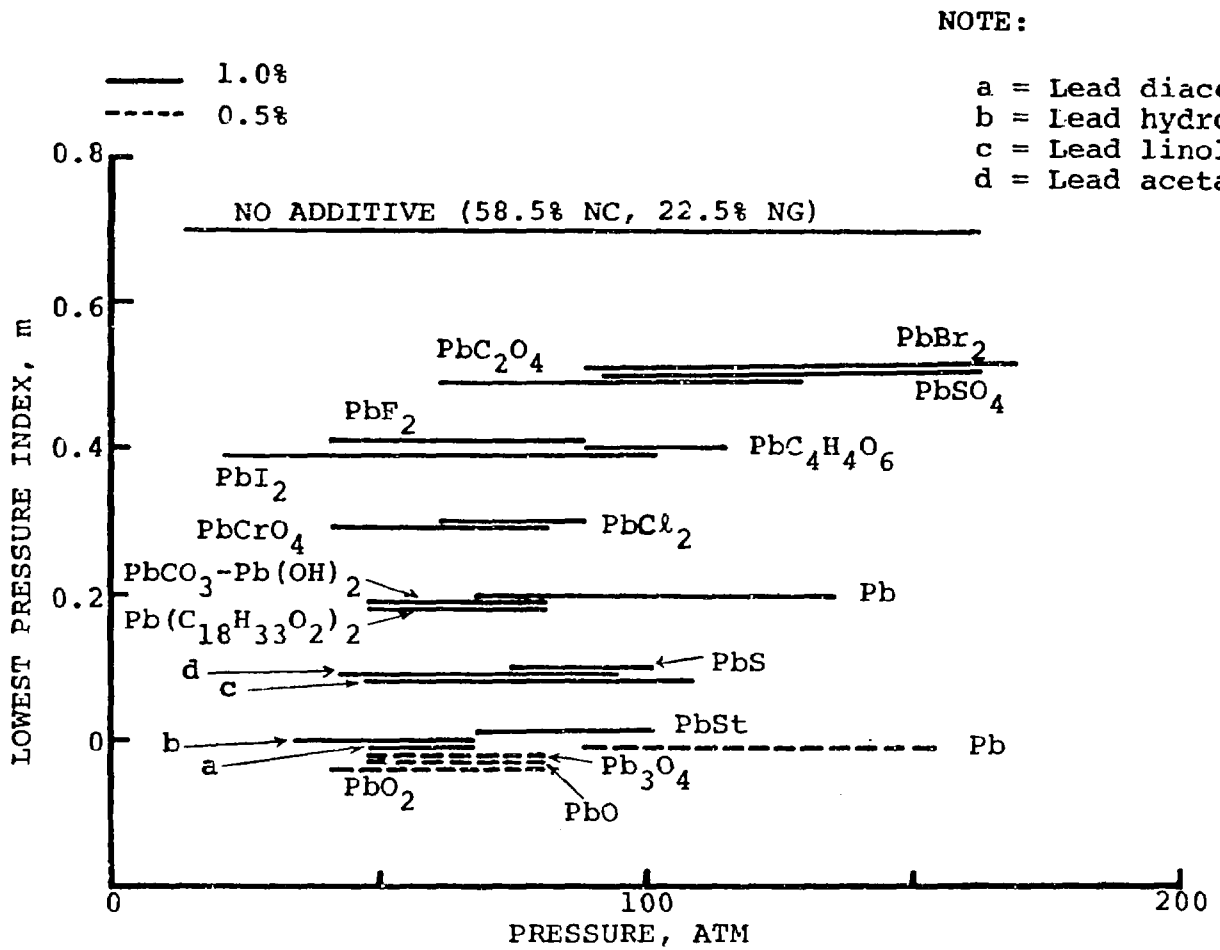

Fig. 4. Effect of various lead compounds added to basic propellant on the lowest pressure index and pressure range of plateau burning (based on results of Preckel (ref. 45)).

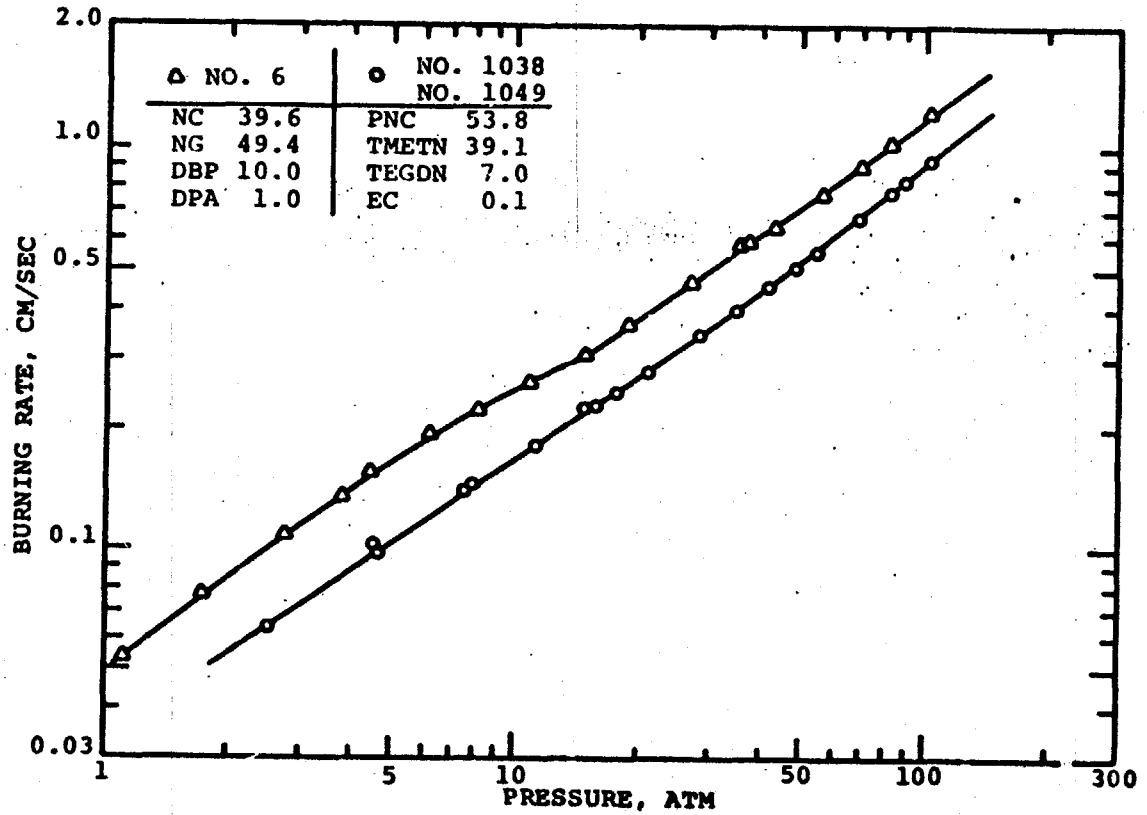

Fig. 5. Comparison of burning rates of NC/NG and PNC/TMETN propellants showing that the pressure indices are about the same.

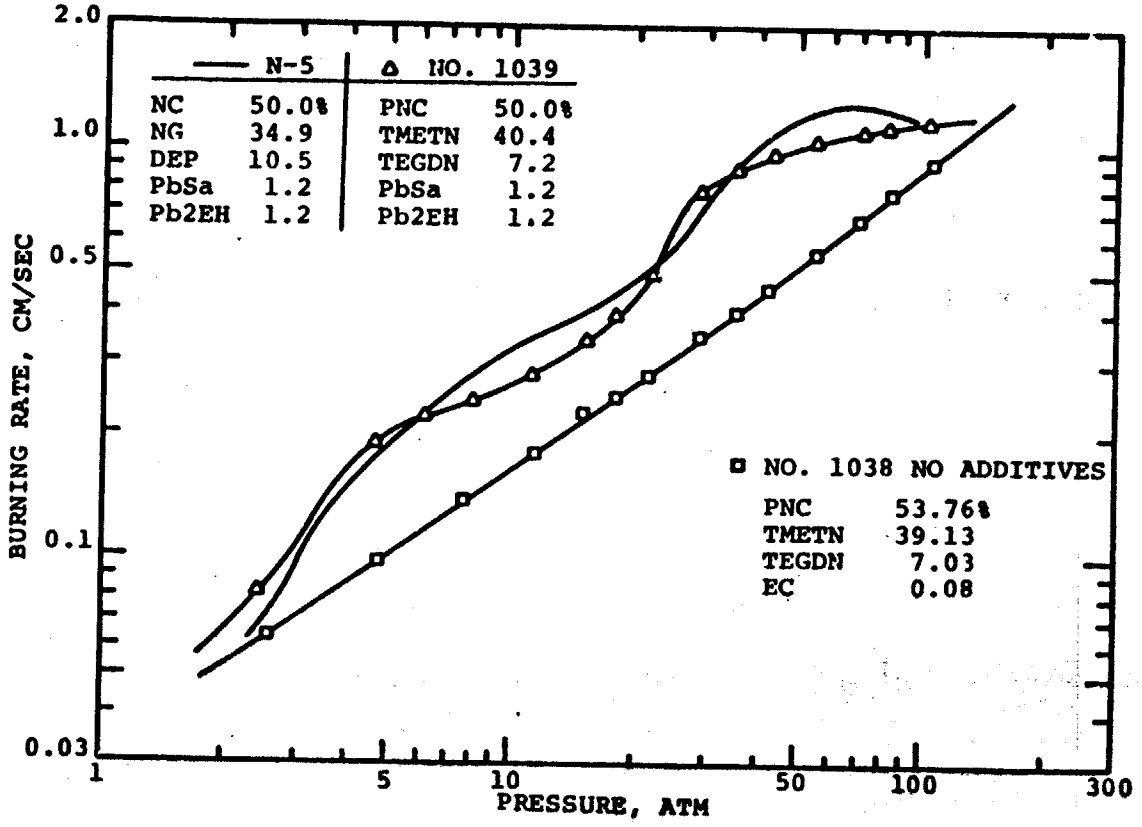

Fig. 6. Comparison of plateau burning rate of NC/NG and PNC/TMETN propellants showing that the super rate characteristics are comparable when TMETN replaces NG.

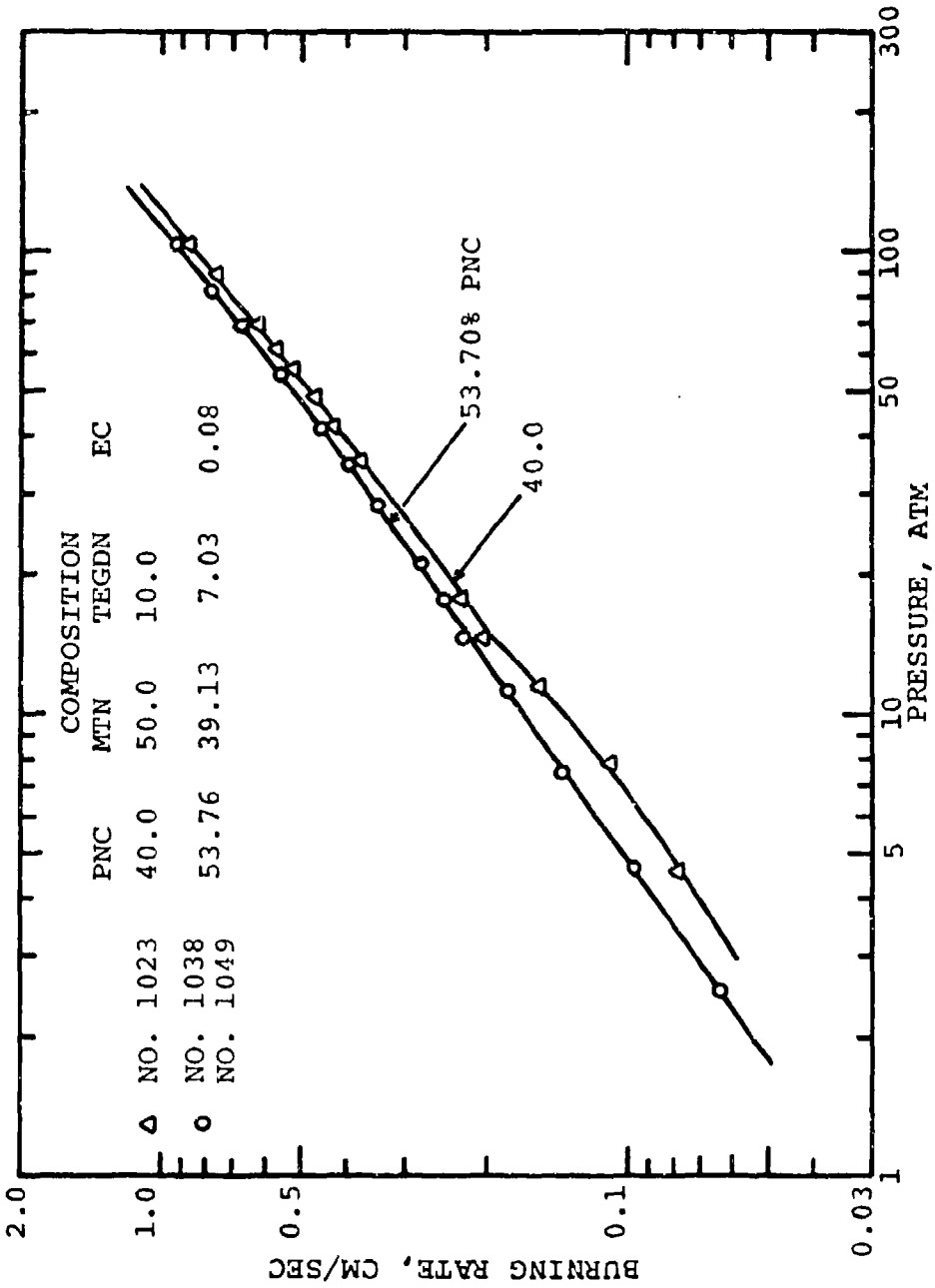

Fig. 7. Increase in burning rate corresponding to increase in PNC.

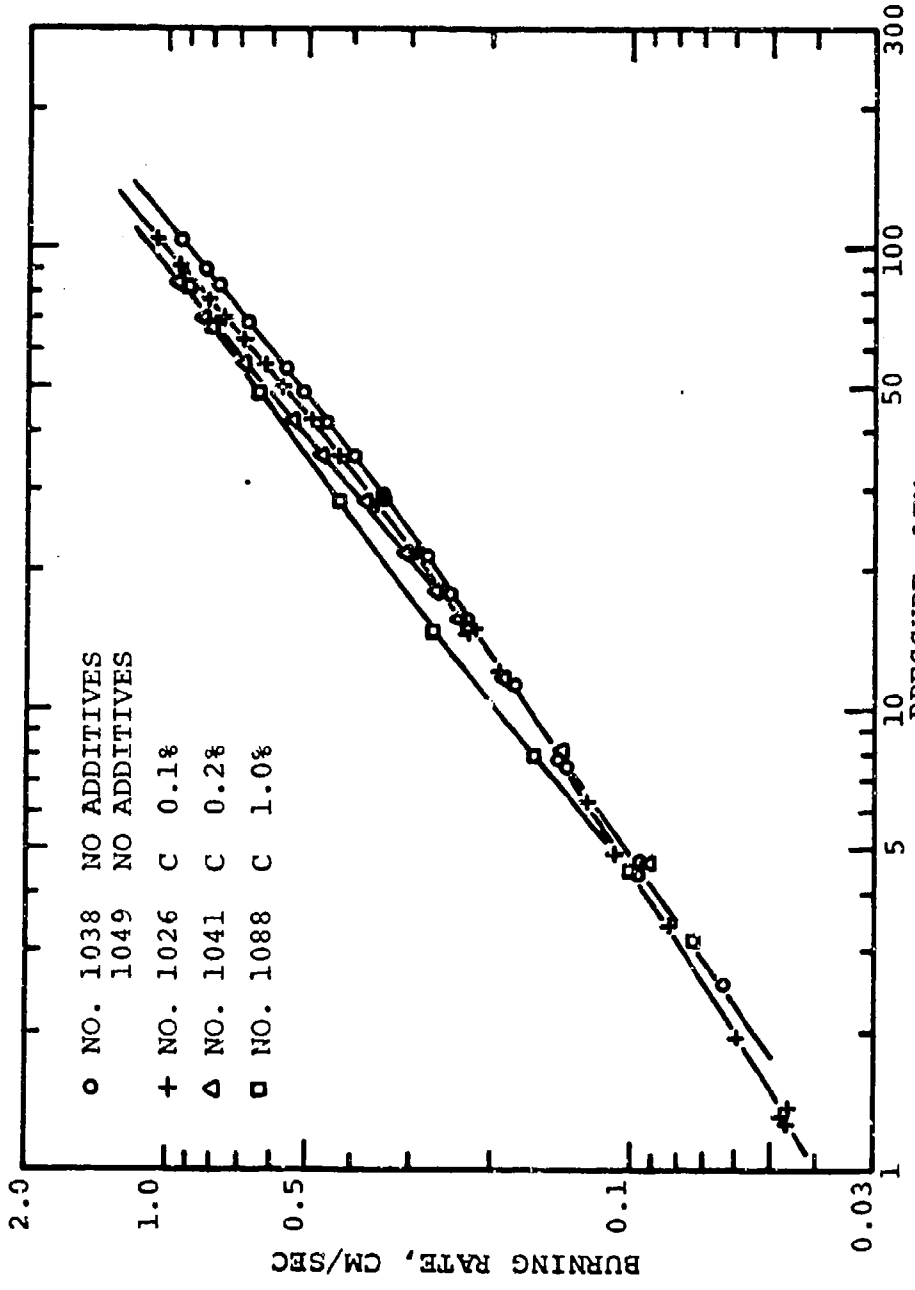

Fig. 8. Carbon powder addition increasing burning rate of PNC/TMETN propellants.

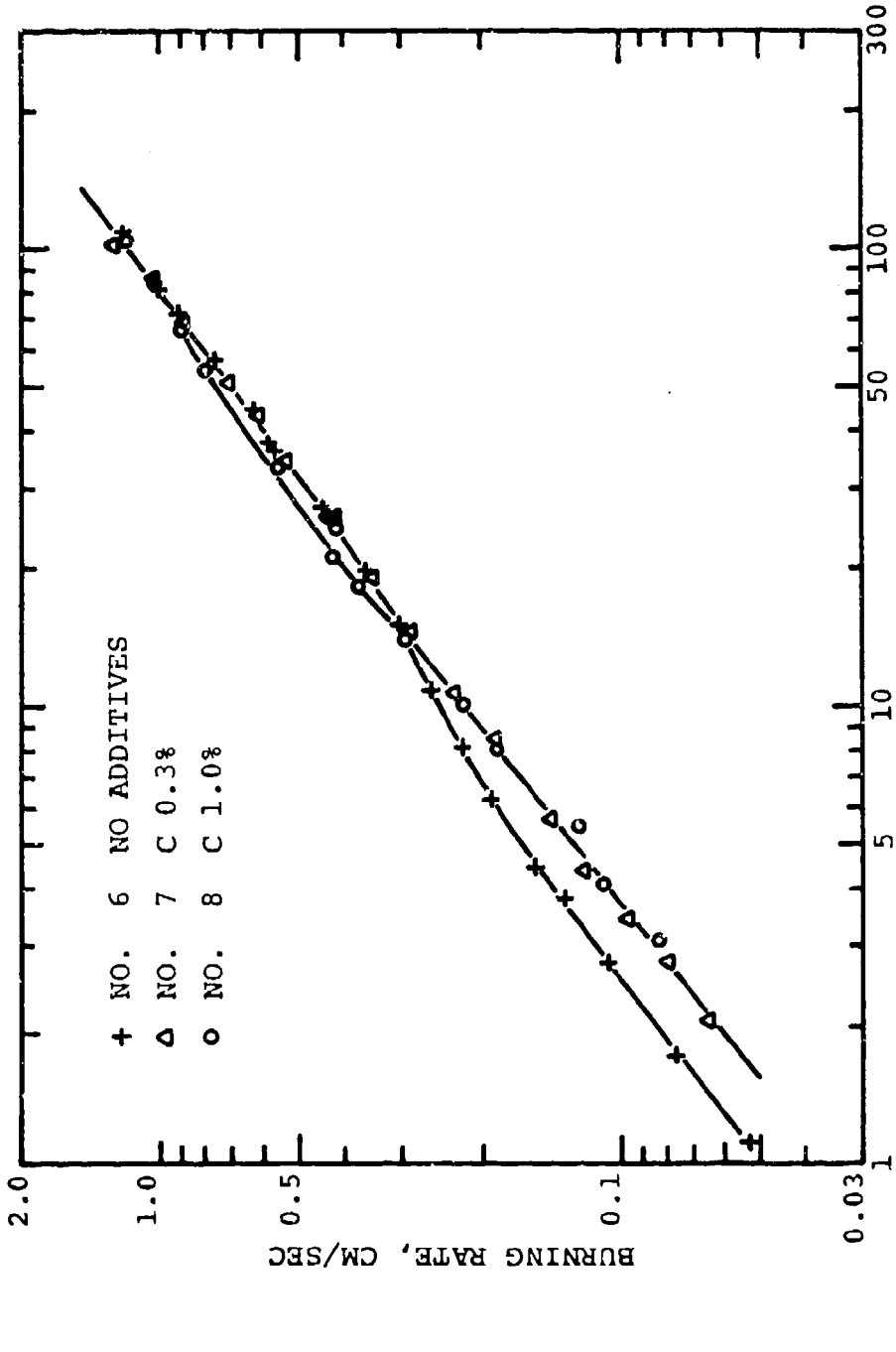

Fig. 9. Pressure dependence and carbon powder concentration effects on NC/NG propellant burning rate.

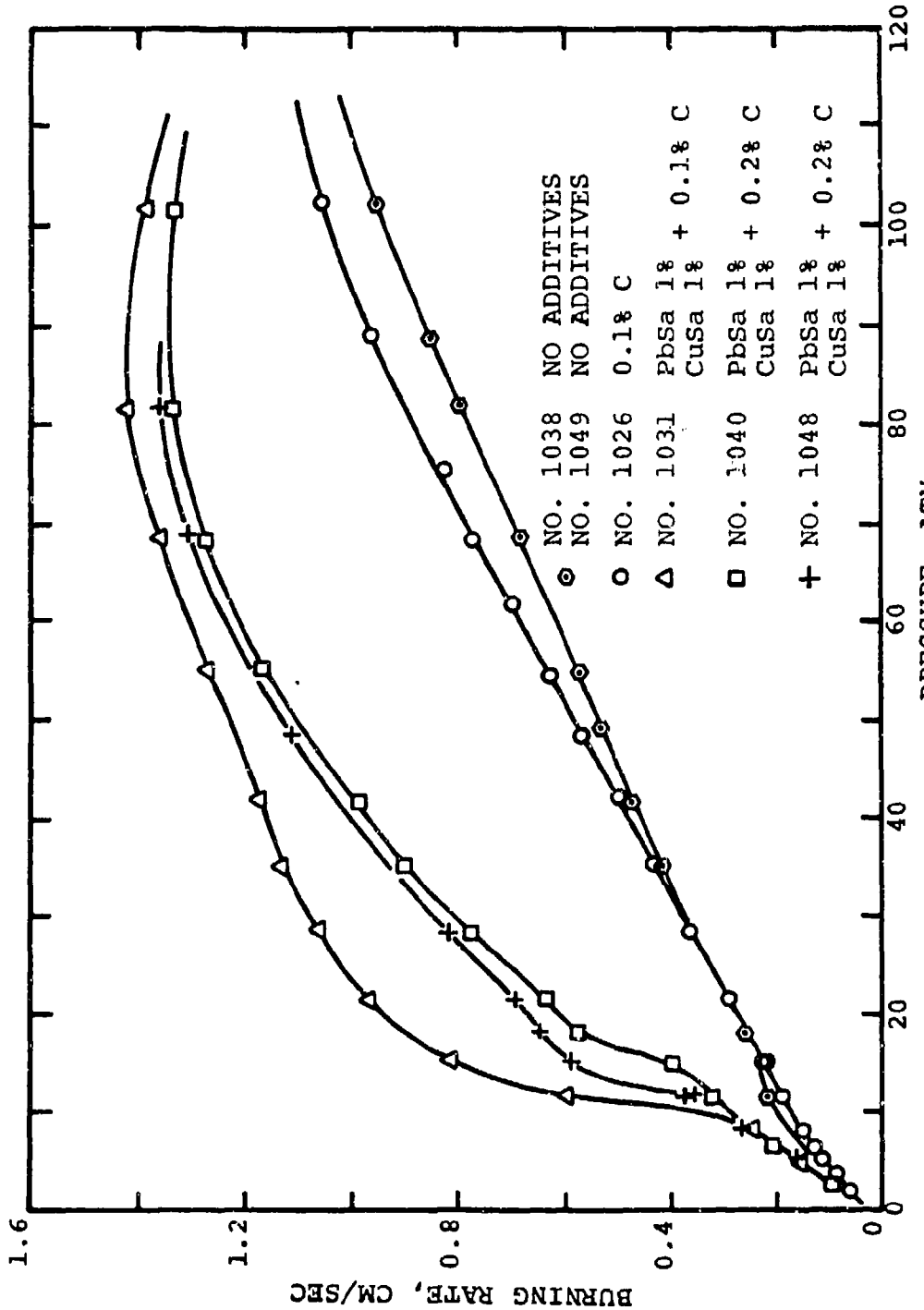

Fig. 10. Addition of carbon powder to plateau propellants diminishing super rate.

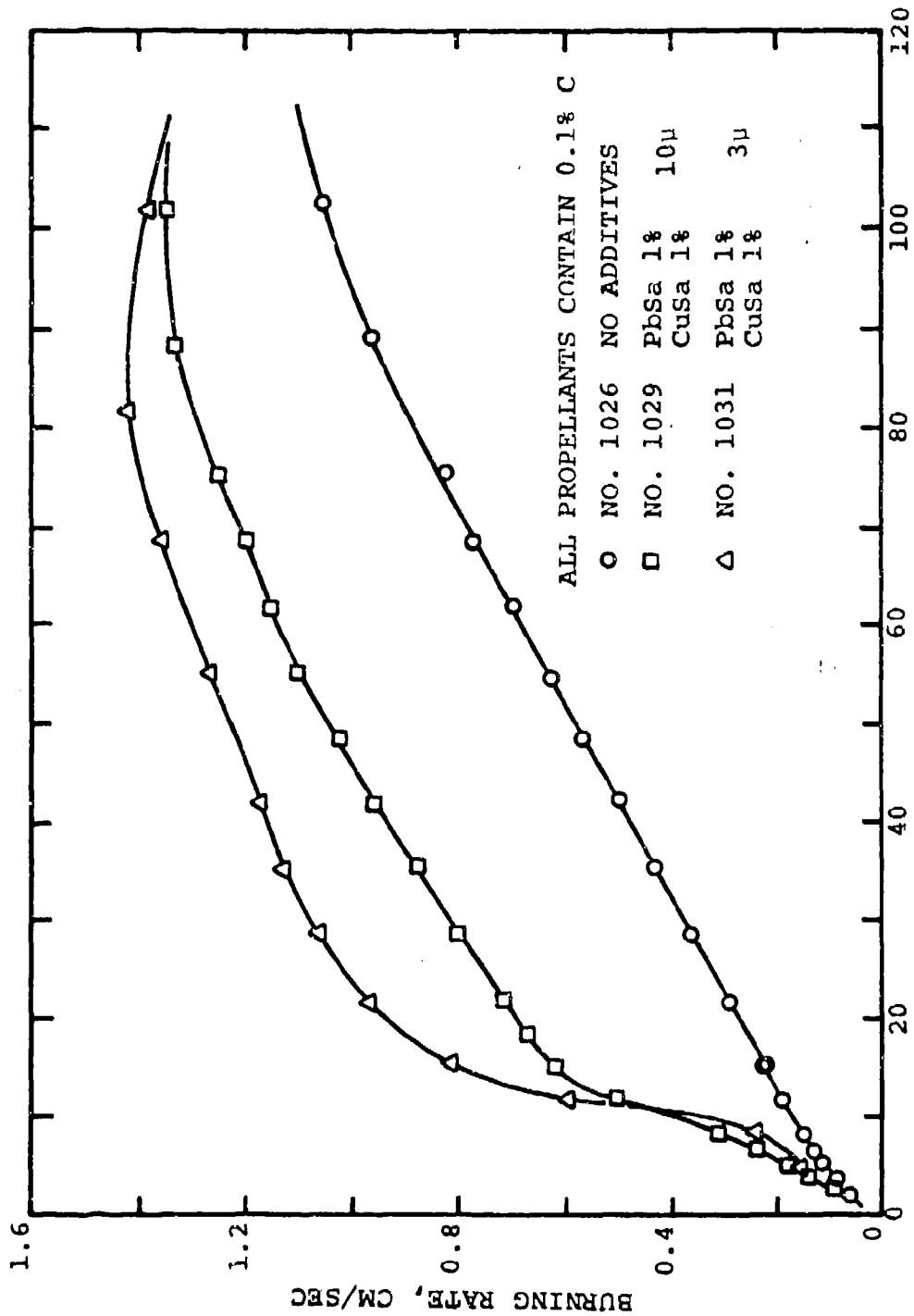

Fig. 11. Effect of catalyst particle size on burning rate showing that smaller granulations are more effective.

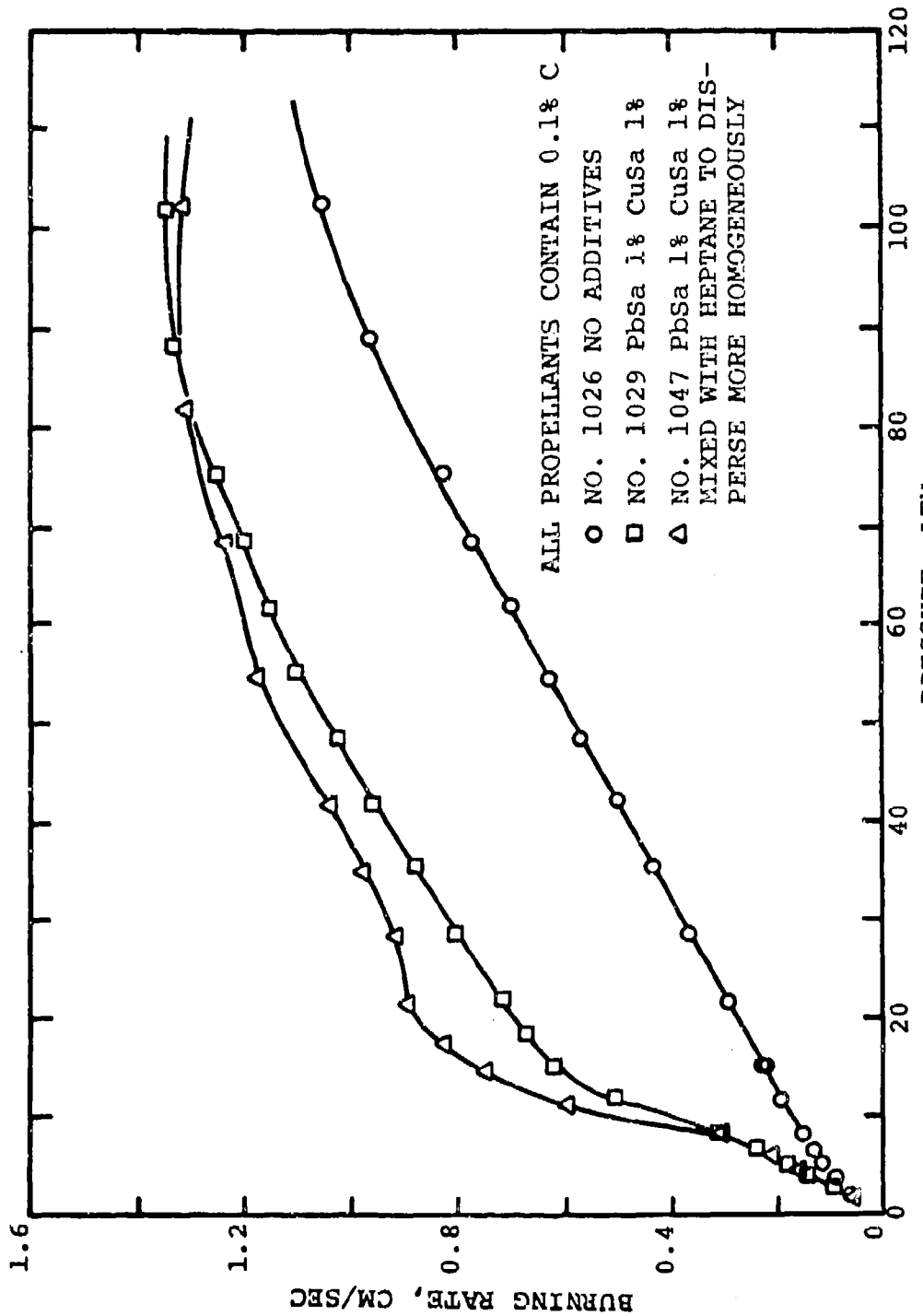

Fig. 12. Effect of additive dispersion on burning rate showing that improved dispersion increases catalyst effectiveness.

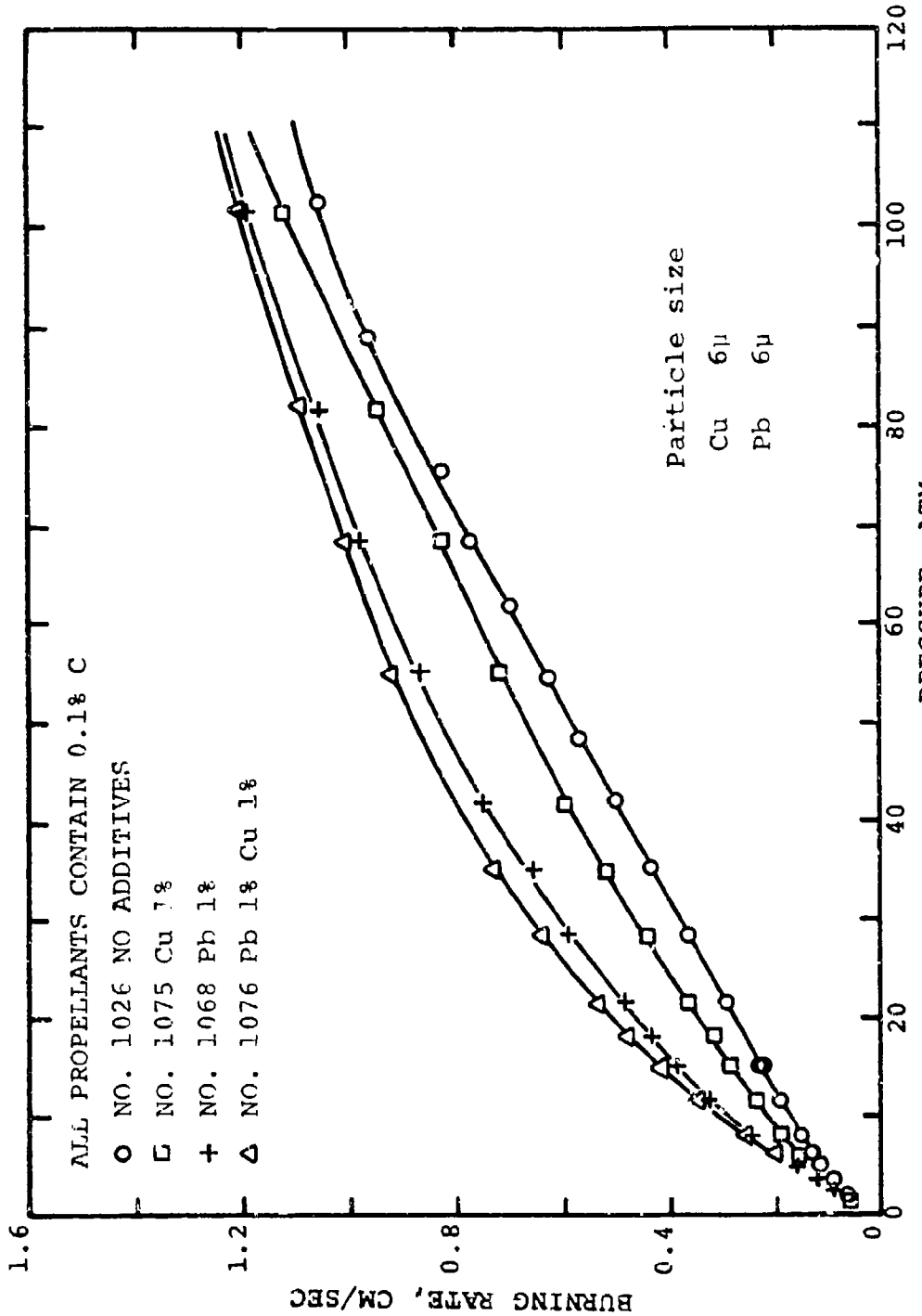

Fig. 13. Effect of elemental lead and copper powder on burning rate showing that lead is more effective than copper.

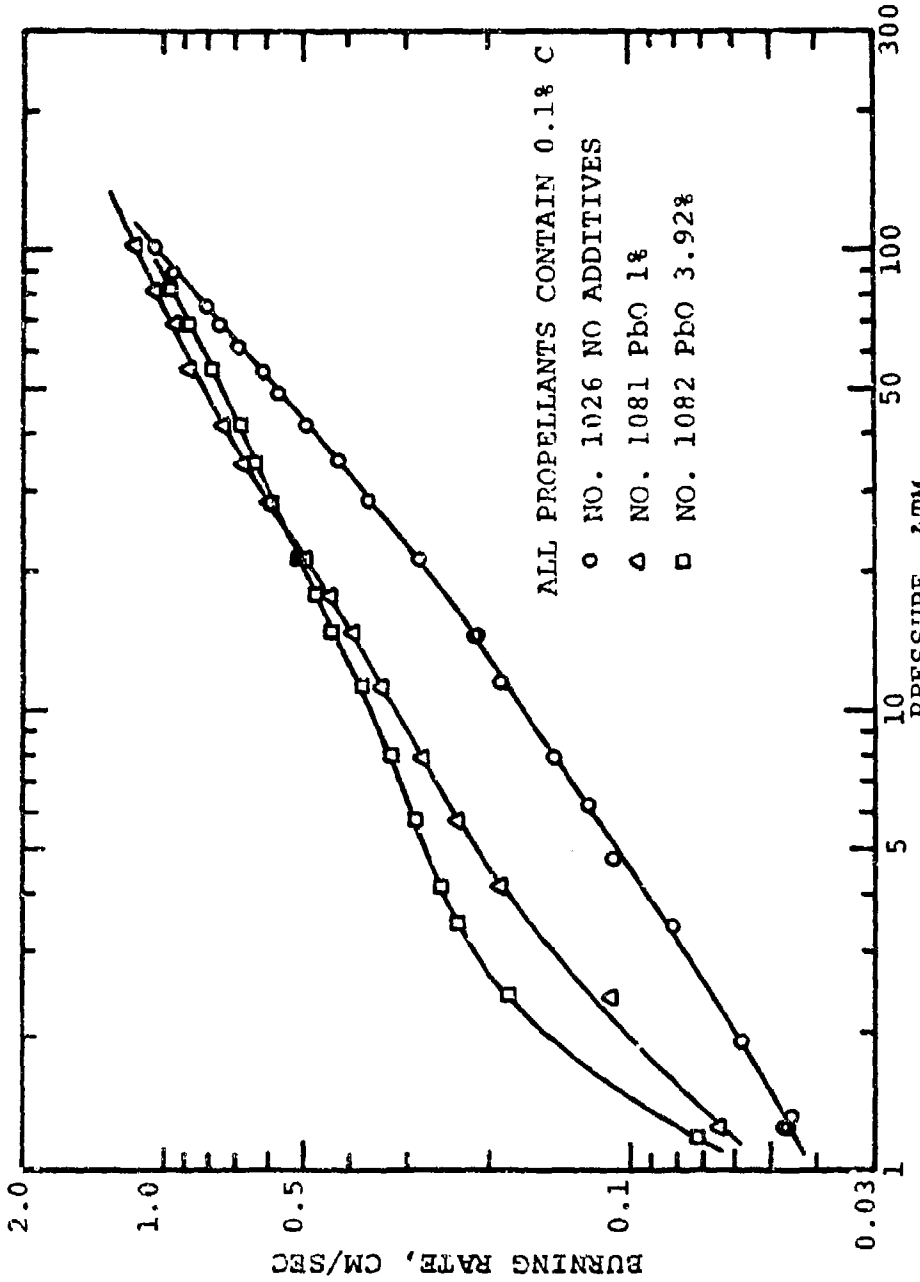

Fig. 14. Increasing PbO percentage is most effective at lower pressures.

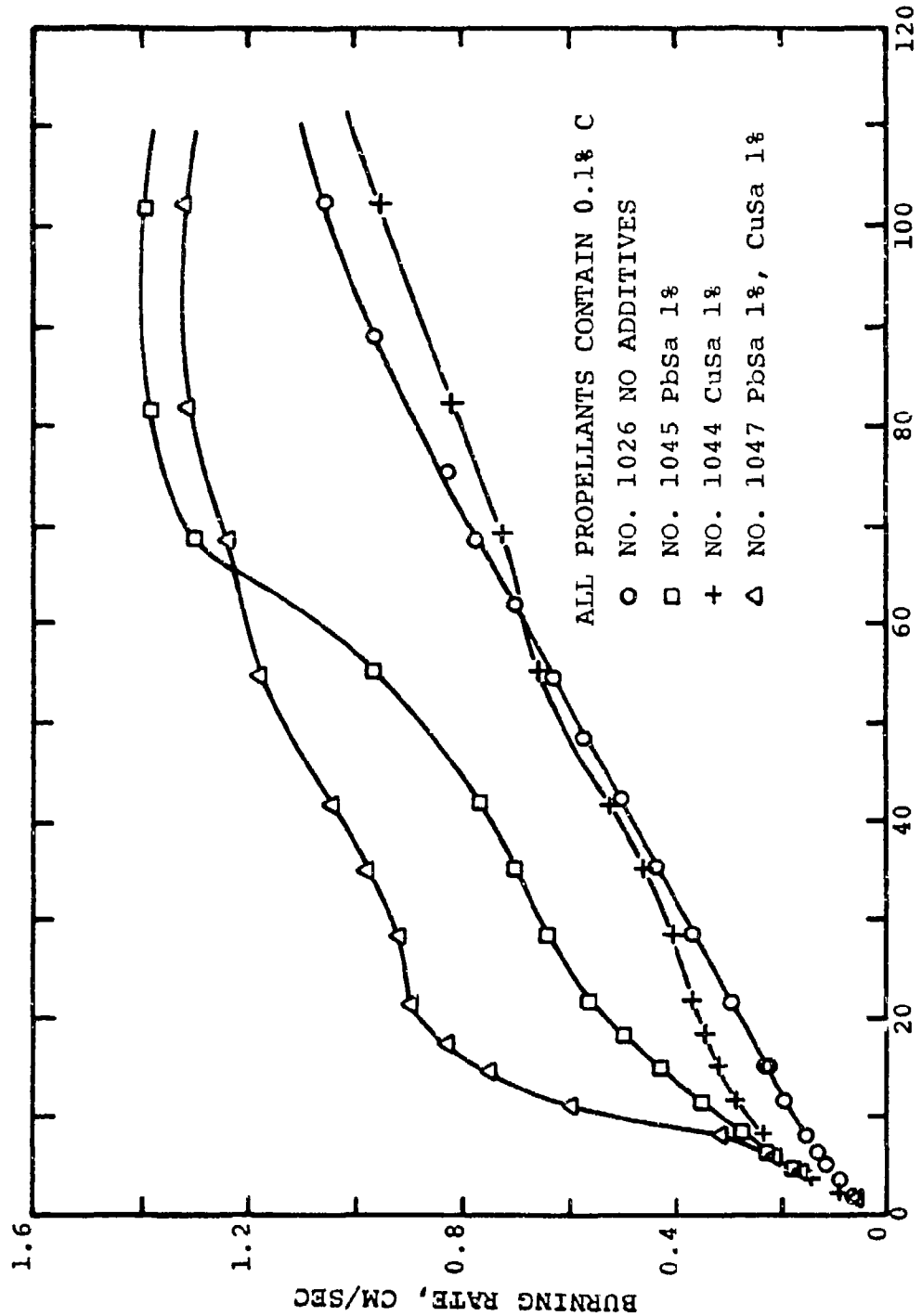

Fig. 15. Additive effect of PbSa and CuSa on burning rate at higher pressures (showing synergistic effect that extends plateau range to lower pressures).

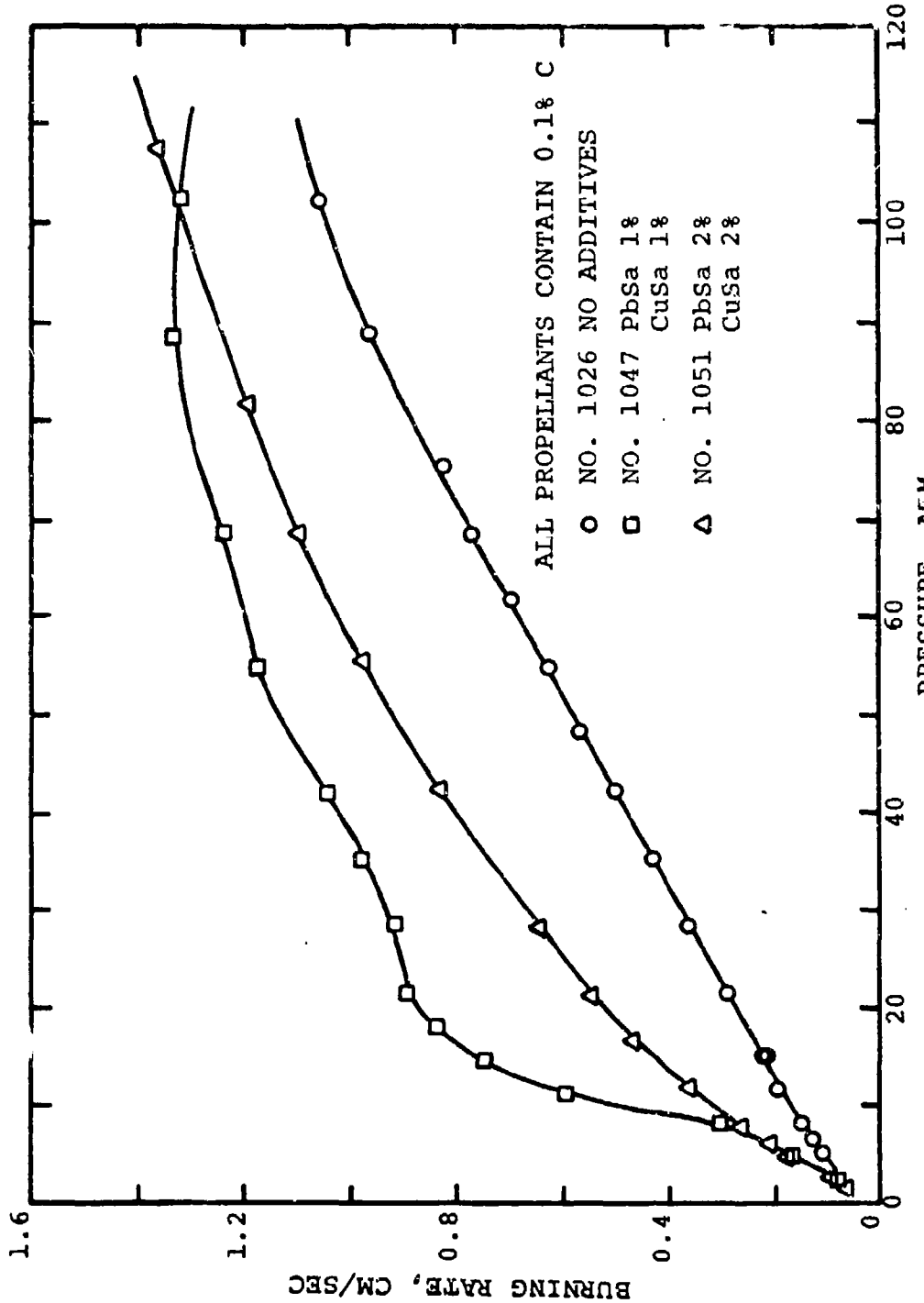

Fig. 15A. Effect of catalyst content on burning rate showing that adding catalyst beyond a certain level decreases super rate.

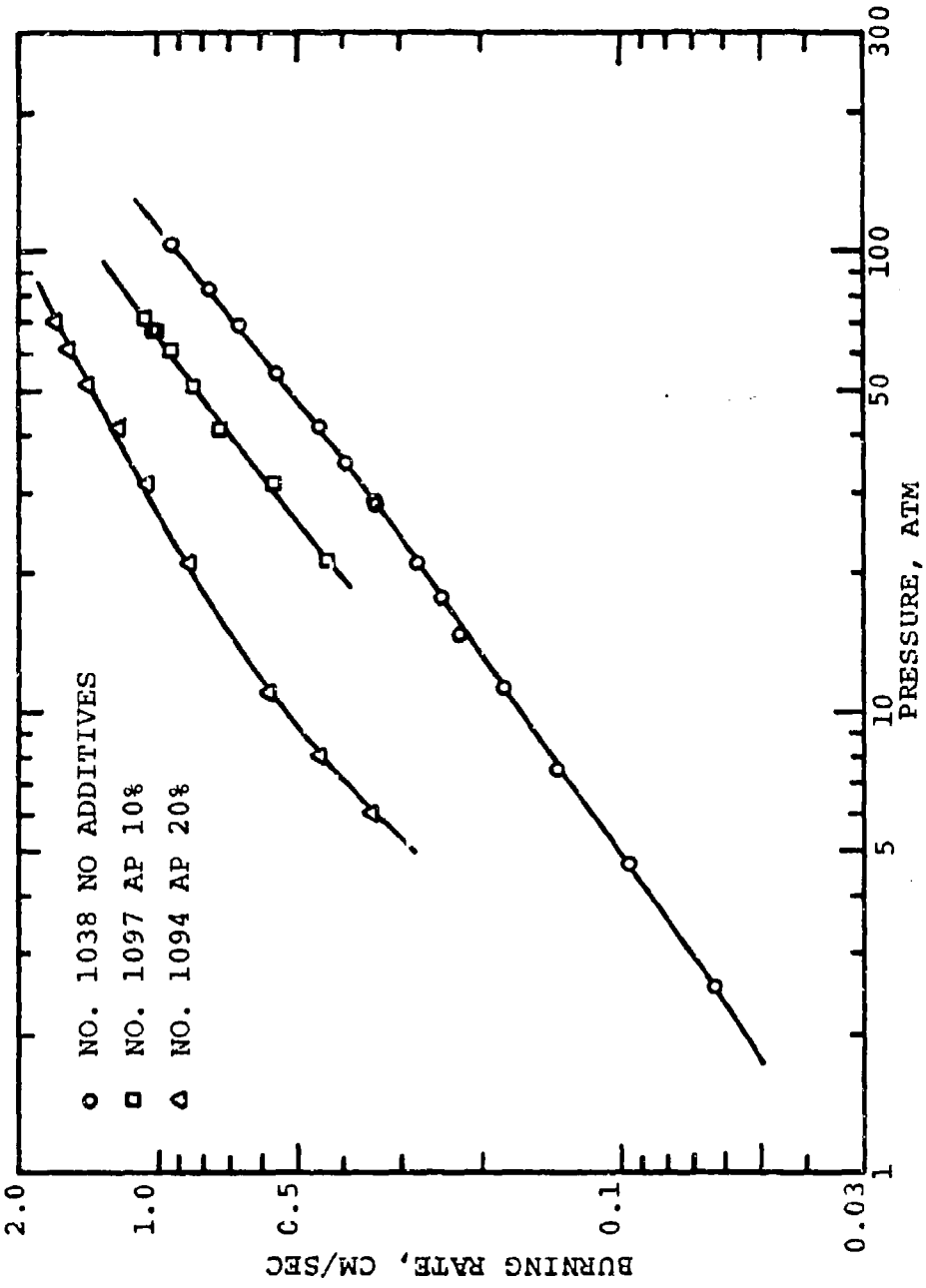

Fig. 16. Increase in burning rate with increasing AP content.

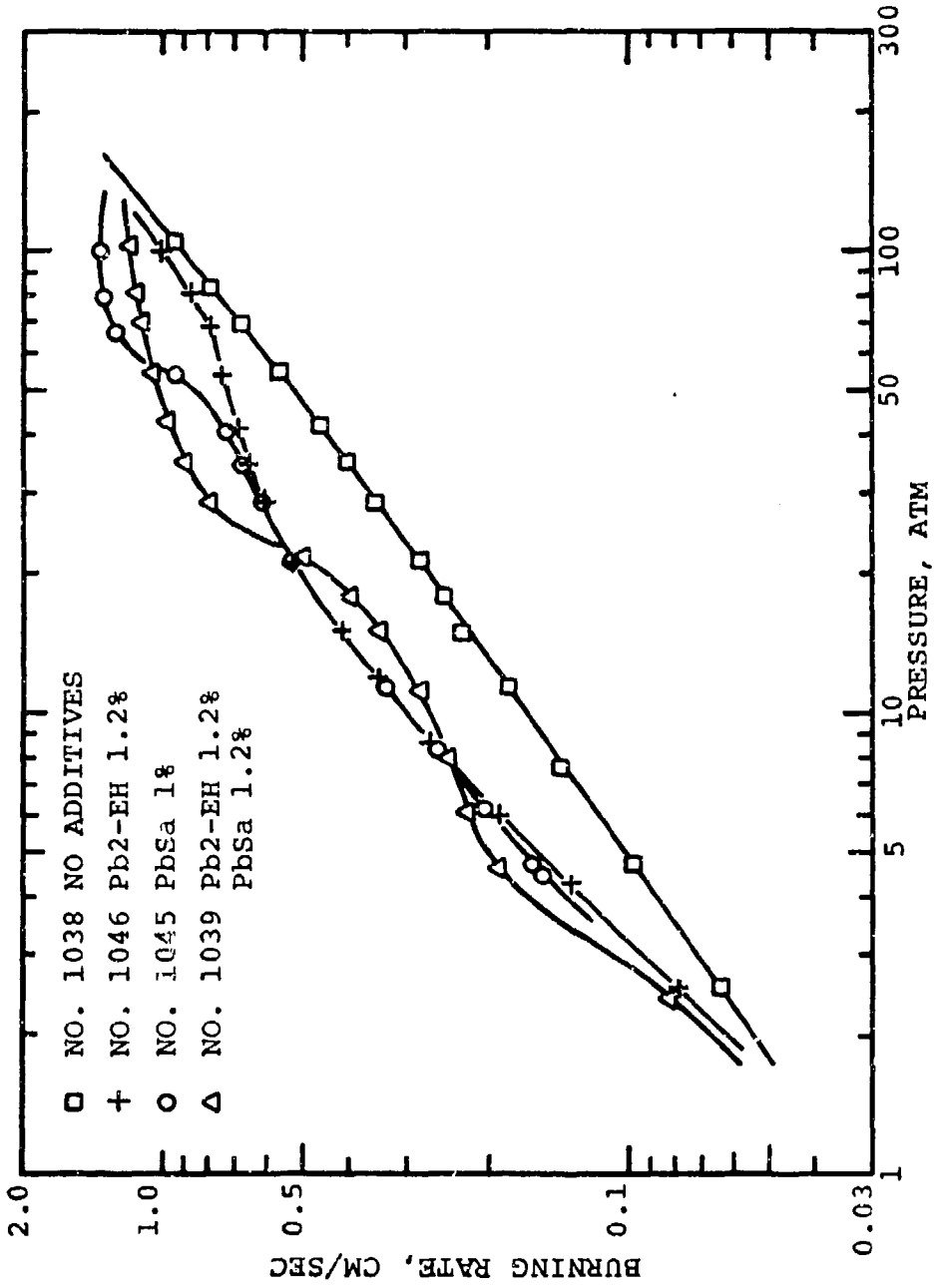

Fig. 17. Combined effect of PbSa and Pb2-EH on burning rate.

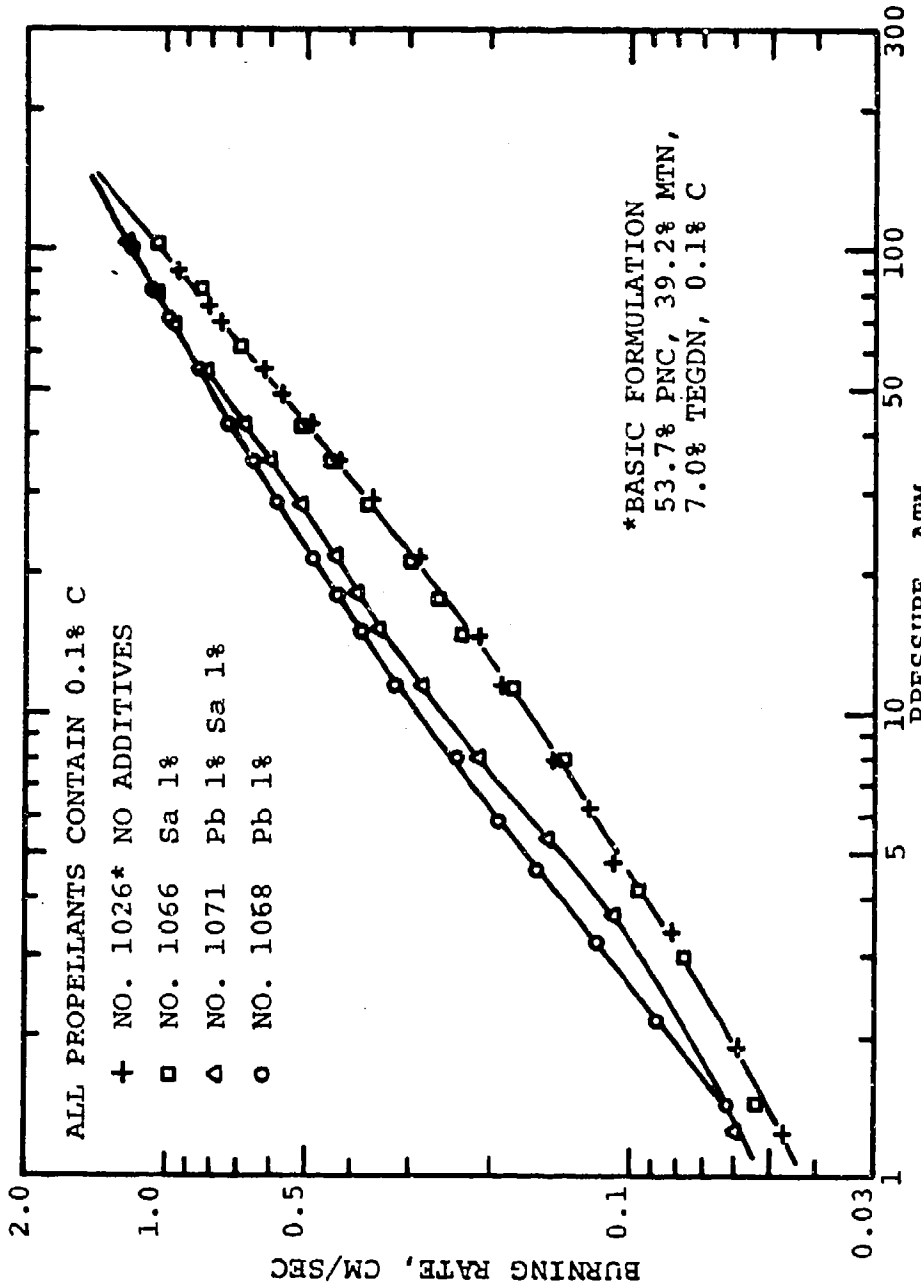

Fig. 18. Comparison of catalyst components shows that organic part of lead salt (used alone) has no effect on burning rate.

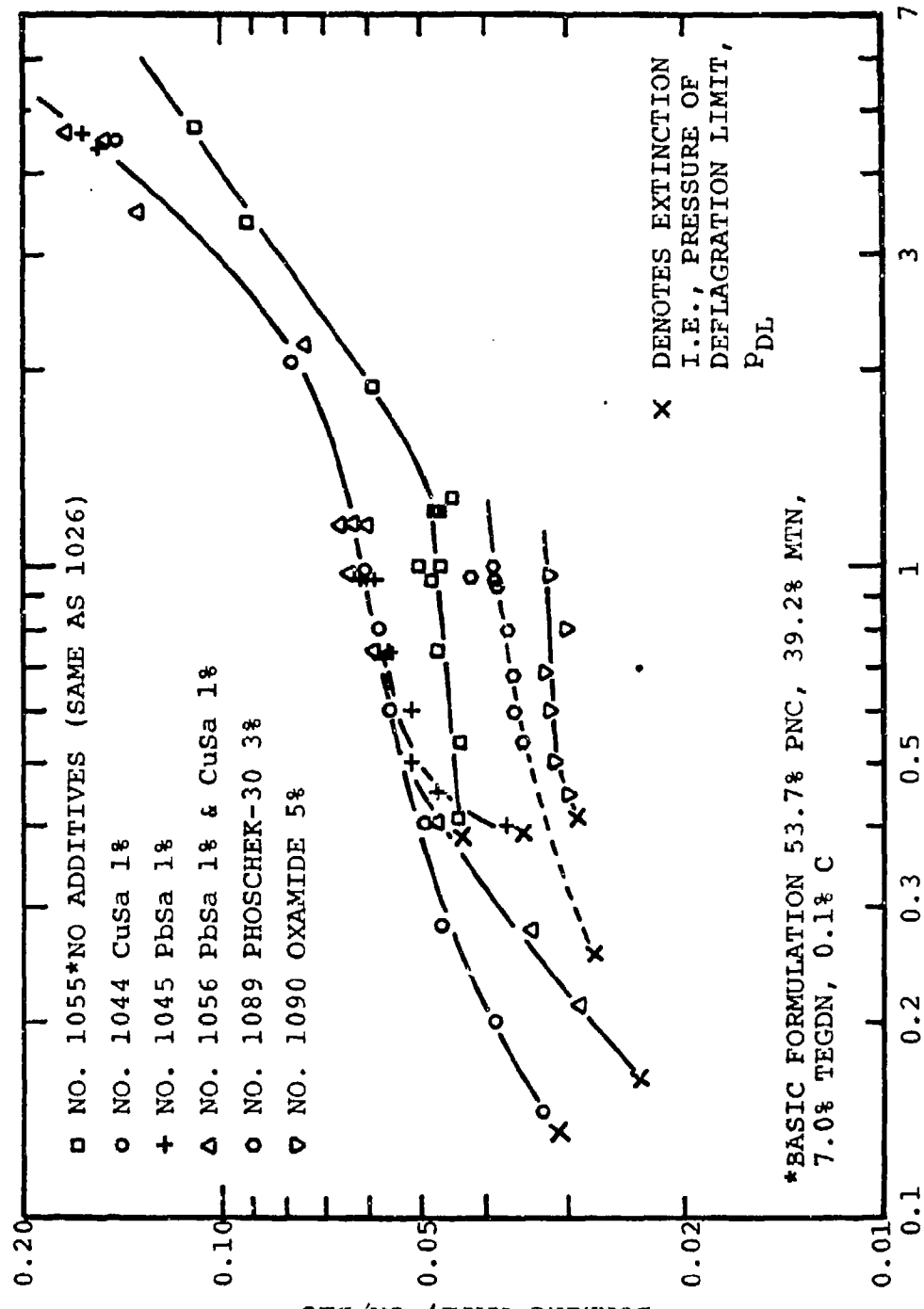

Fig. 19. Effect of additives on burning rate and on deflagration limit pressure in N_2.

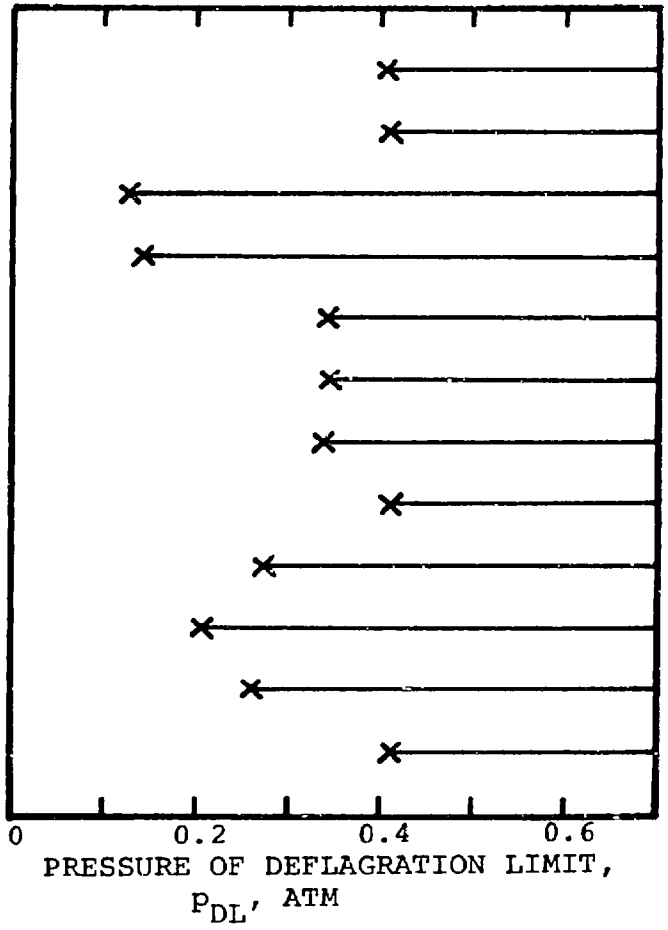

PROP. NO.	ADDITIVE
1055*	NO ADDITIVE (SAME AS 1026)
1045	PbSa 1%
1044	CuSa 1%
1056	PbSa 1% CuSa 1%
1068	Pb 1%
1075	Cu 1%
1076	Pb 1% Cu 1%
1081	PbO 1%
1082	PbO 4%
1085	PbO 7%
1089	PHOSCHEK-30 3%
1090	OXAMIDE 5%

*Basic formulation 53.7% PNC, 39.2% MTN, 7.0% TEGDN, 0.1% C

Fig. 20. Effect of additives to PNC propellants on pressure of deflagration limit in N_2.

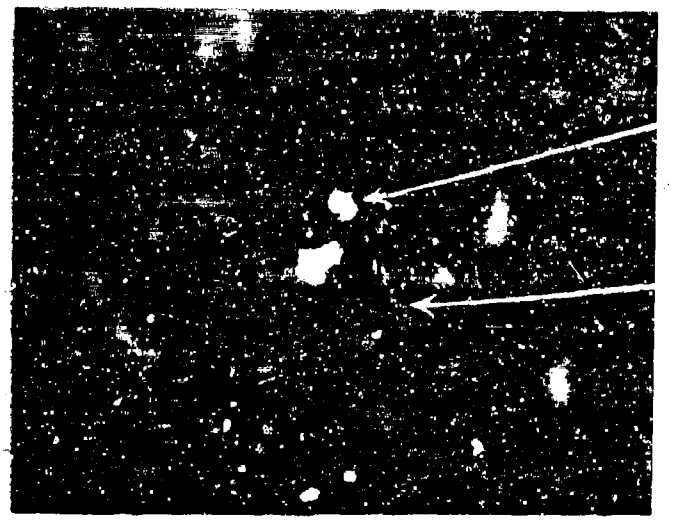

NO. 1044 CuSa 1%
p = 0.2 ATM

Fig. 21. Microphotograph of residue of propellant burning showing crystalline particles and carbonaceous particles.

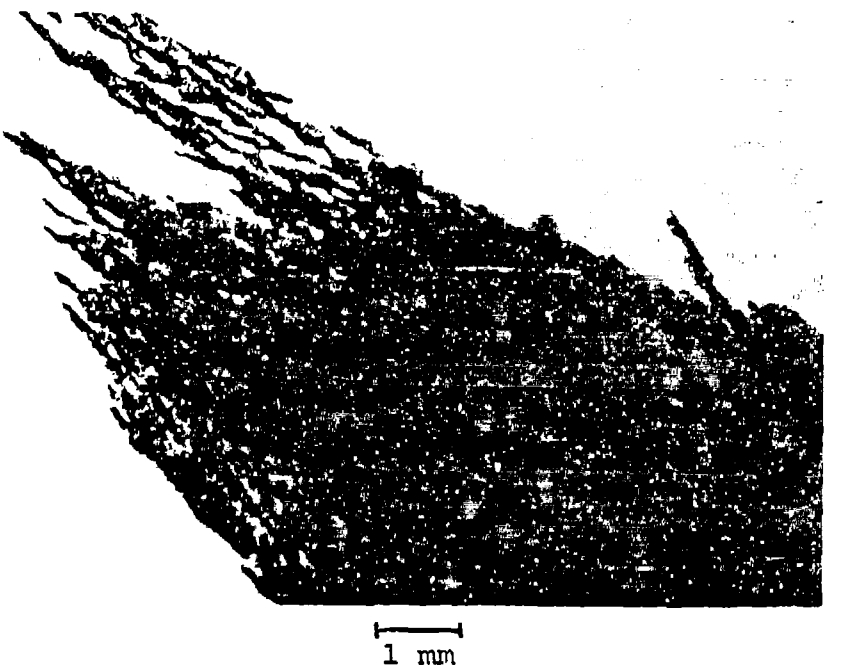

NO. 1089 PHOSCHEK-30 3%
p = 1 ATM in N_2

Fig. 22. Photograph of solid carbon on the burning surface of propellant modified by a phosphorus containing compound. (This very extensive carbon formation is an anomalous behavior not typical of other propellants.)

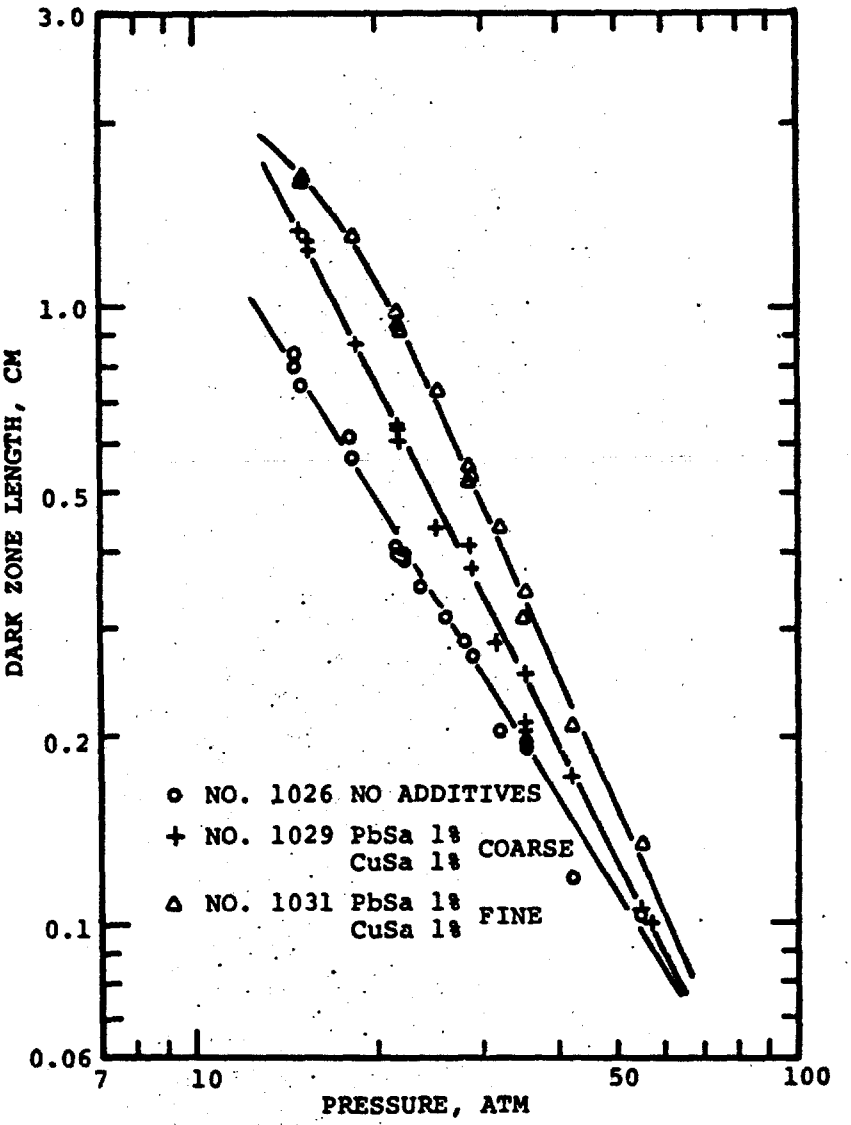

Fig. 23. Effect of catalyst on dark zone length showing increased length with finer granulation of PbSa and CuSa.

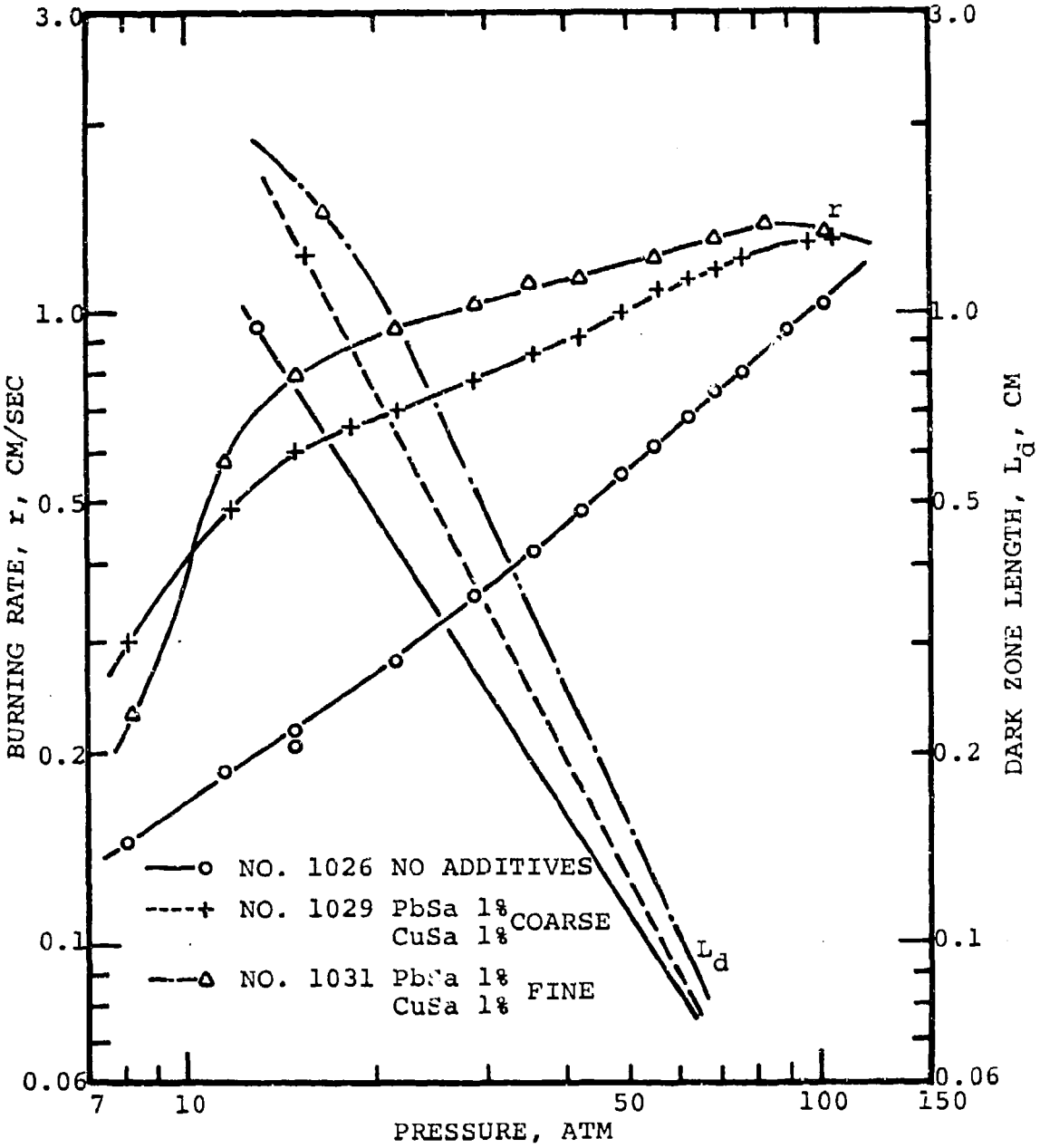

Fig. 24. Effect of burning rate on dark zone length showing lengthening of dark zone with higher burning rates.

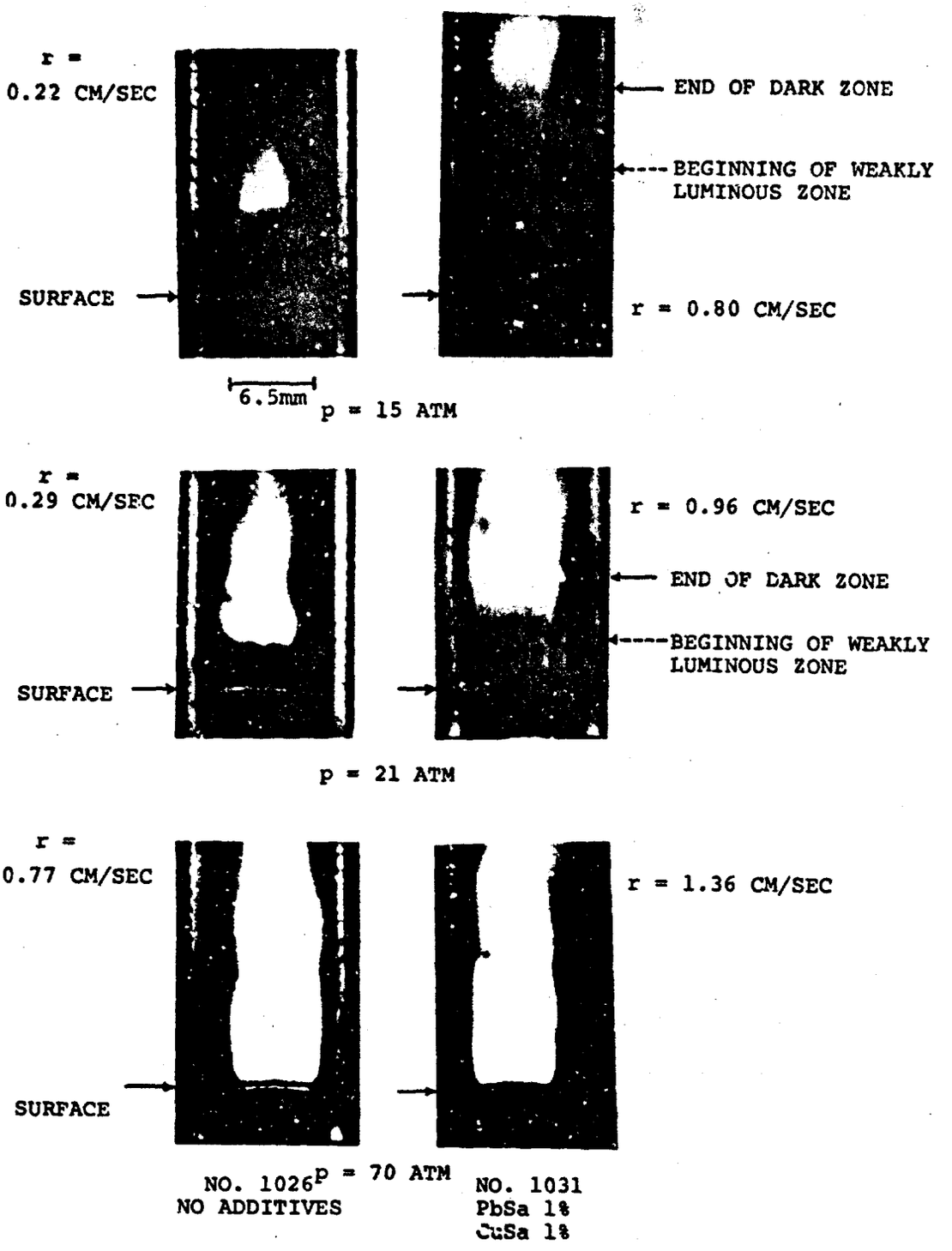

Fig. 25. Comparison of dark zone lengths of catalyzed and noncatalyzed propellants showing distended luminous flame with increased burning rate.

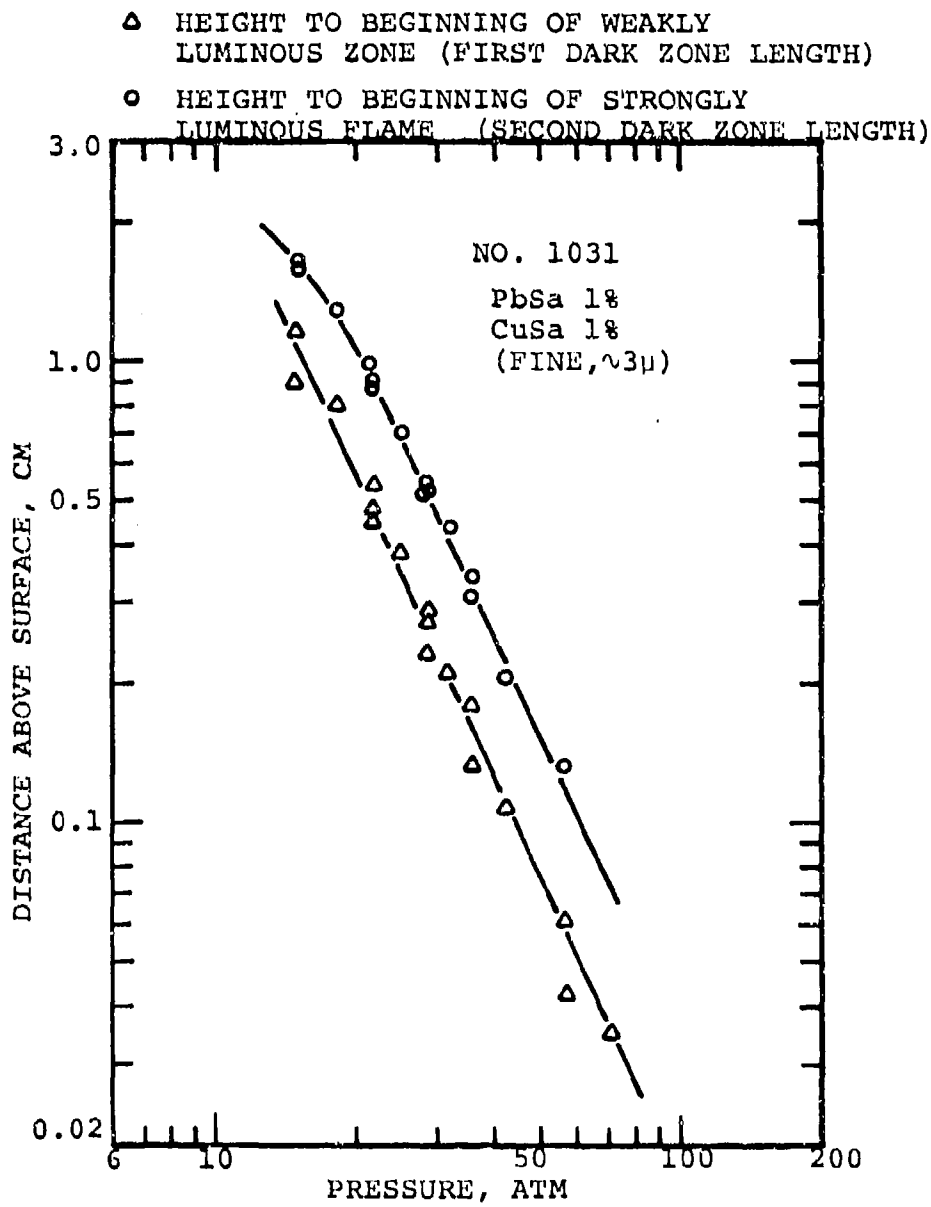

Fig. 26. Effect of pressure on the two "dark zone" lengths observed in the presence of PbSa and CuSa.

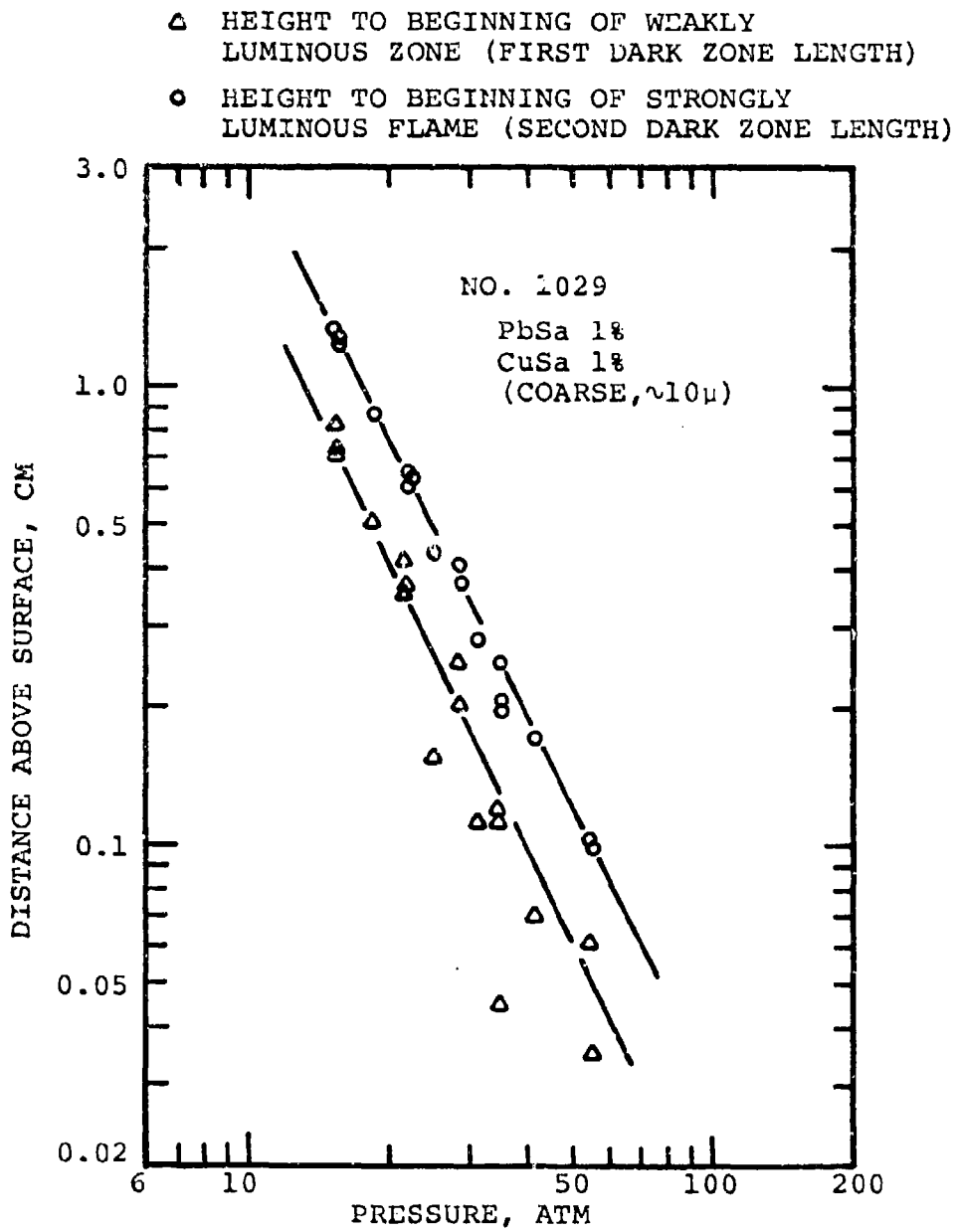

Fig. 27. Effect of pressure on the two "dark zone" lengths observed in the presence of PbSa and CuSa.

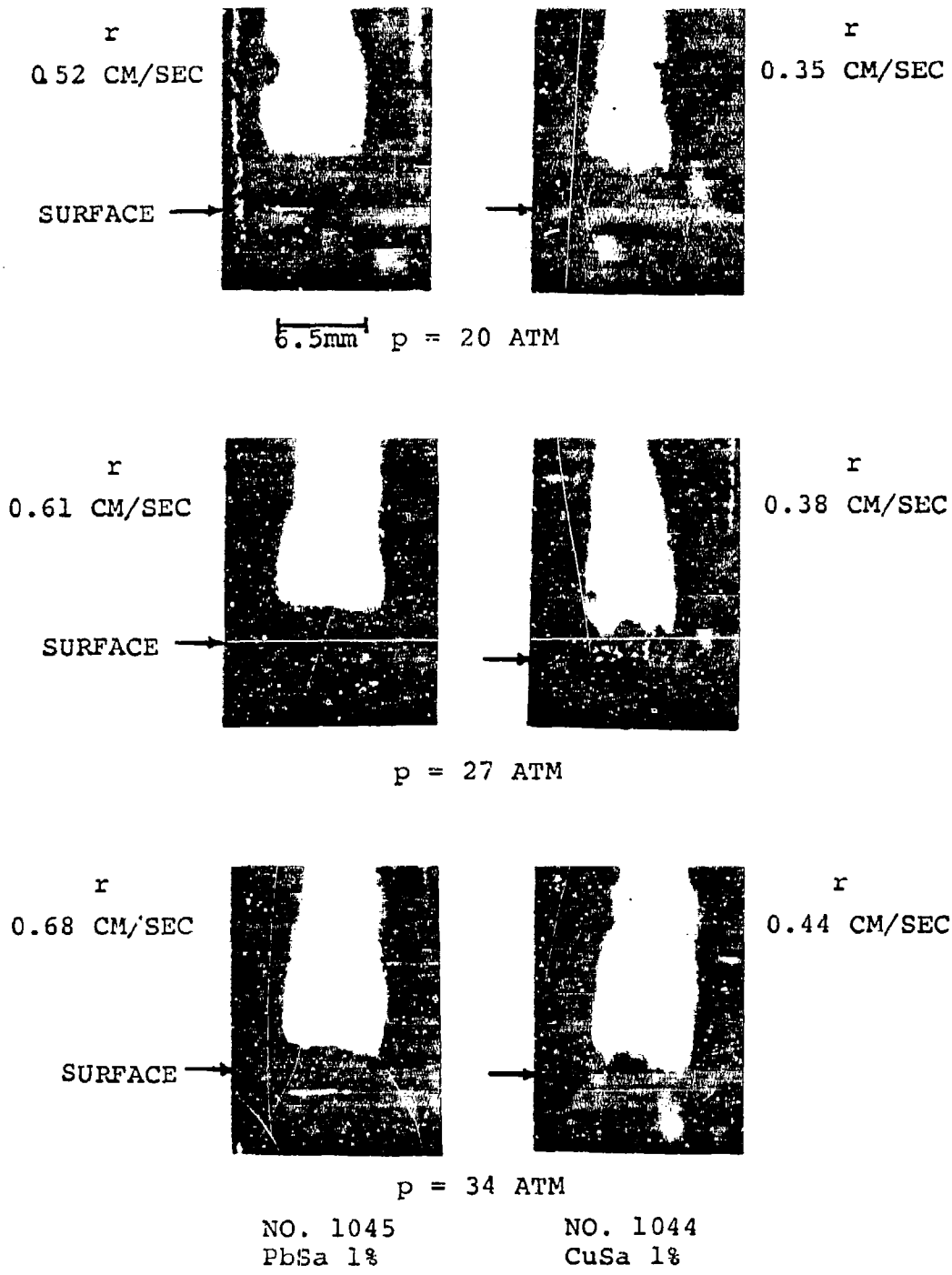

Fig. 28. Comparison of PbSa and CuSa effects on flame structure; PbSa alone cause a faint weak-luminosity zone while CuSa does not; CuSa, however, generates large carbonaceous particles which disrupt the normally planar high luminosity flame zone.

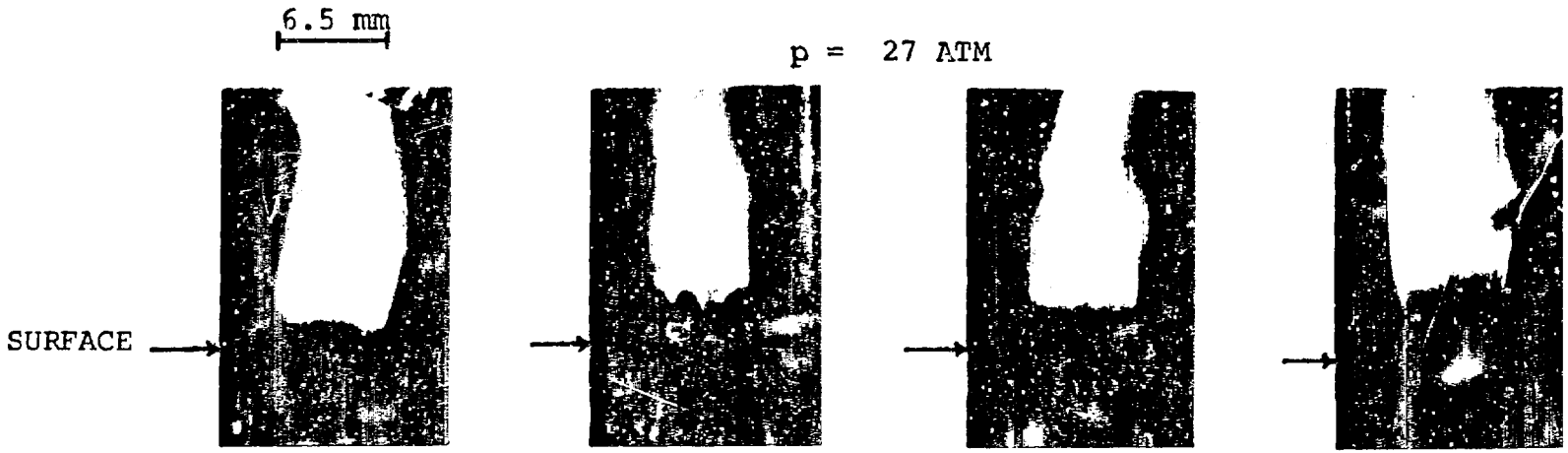

	NO. 1026 NO ADDITIVES	NO. 1044 CuSa 1%	NO. 1045 PbSa 1%	NO. 1031 PbSa 1% CuSa 1%
r CM/SEC	0.35	0.38	0.61	1.05
L_d CM	0.29	0.60	0.55	1.25

Fig. 29. Effect of catalyst on flame structure and burning rate (p = 27 atm) showing that CuSa produces a rough carbonaceous layer on surface; the further addition of PbSa eliminates this effect but introduces a considerable weak luminosity zone.

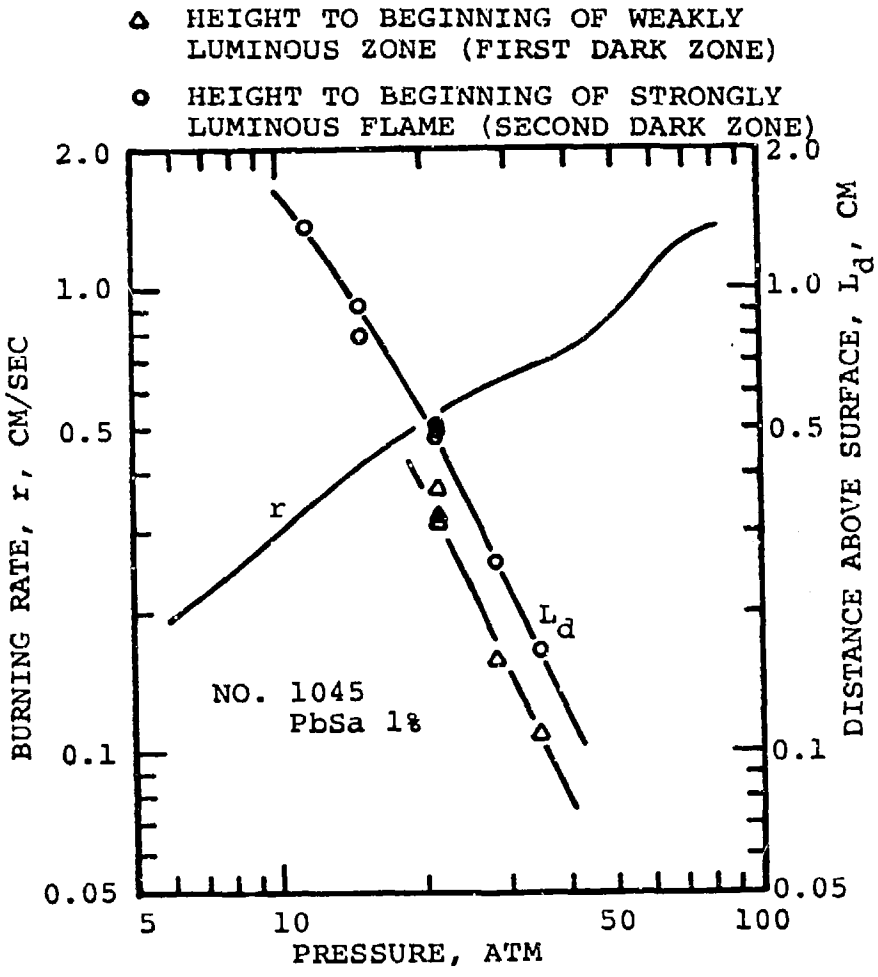

Fig. 30. Pressure vs burning rate and dark zone length showing the existence of weakly luminous zone by the addition of PbSa.

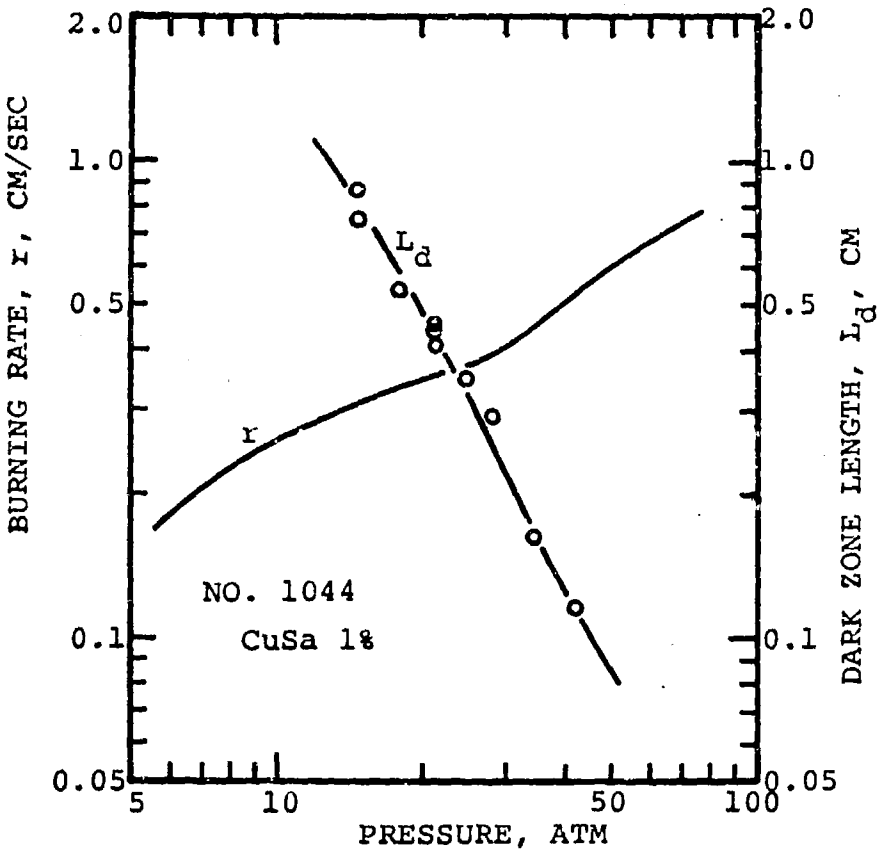

Fig. 31. Pressure vs burning rate and dark zone length.

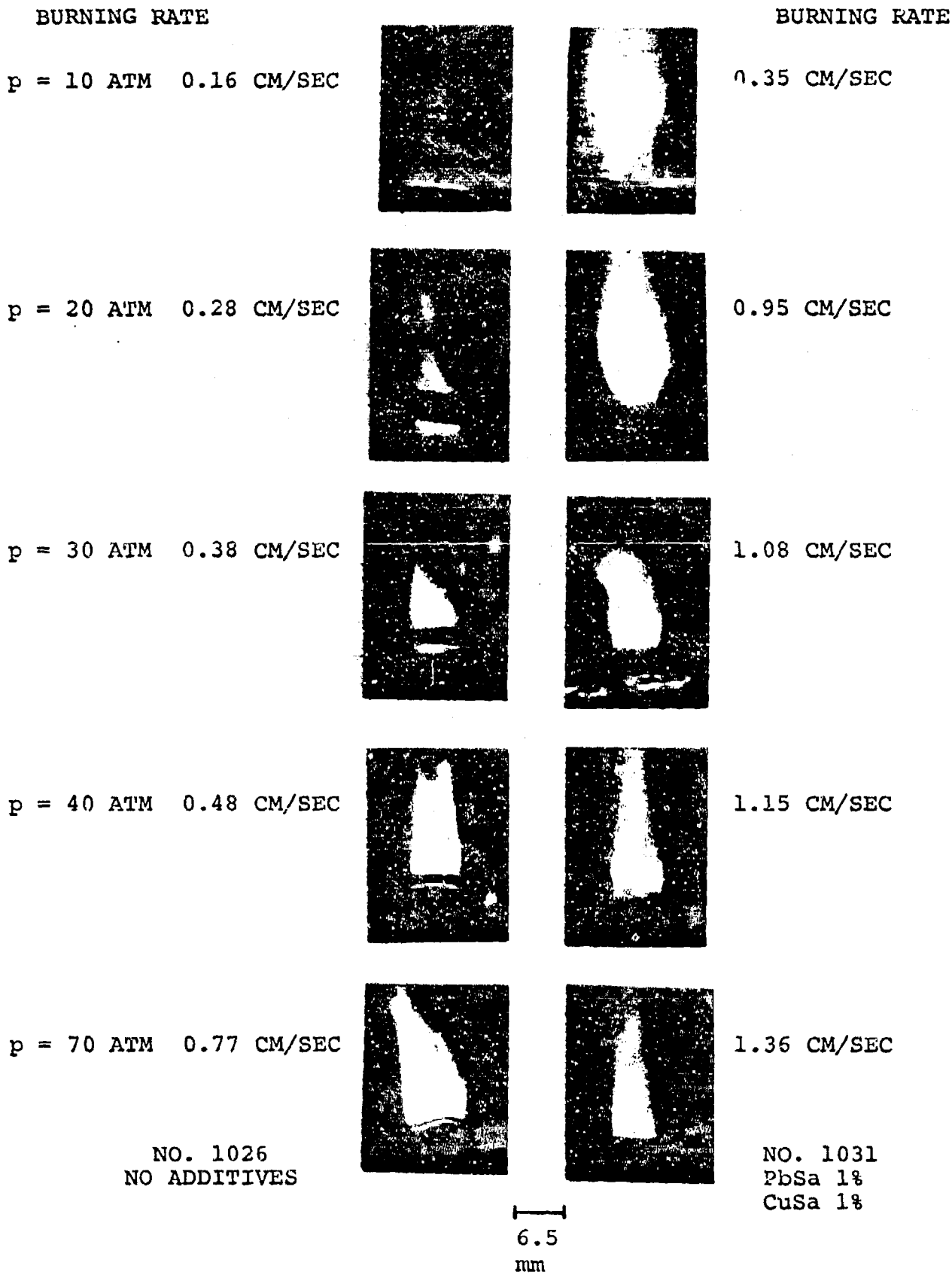

Fig. 32. Infra-red photographs of noncatalyzed and catalyzed propellant flames showing that catalyst addition increases infra-red emission in dark zone.

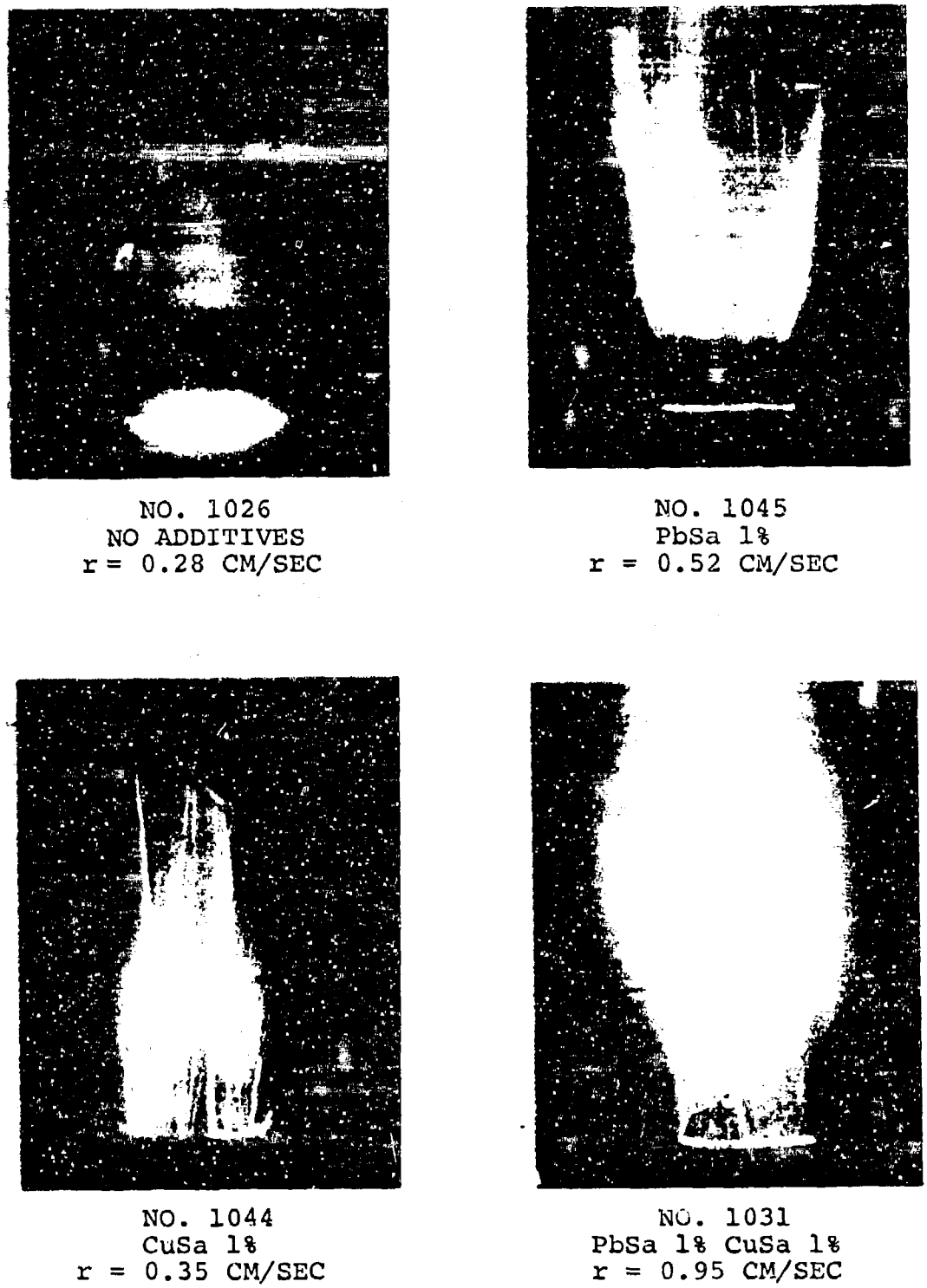

p = 20 ATM
NOTE: PHOTOGRAPHIC PROCESS SAME IN ALL CASES.

Fig. 33. Effect of catalyst on flame structure showing ejected particles from burning surface of catalyzed propellant (photographed using IR film).

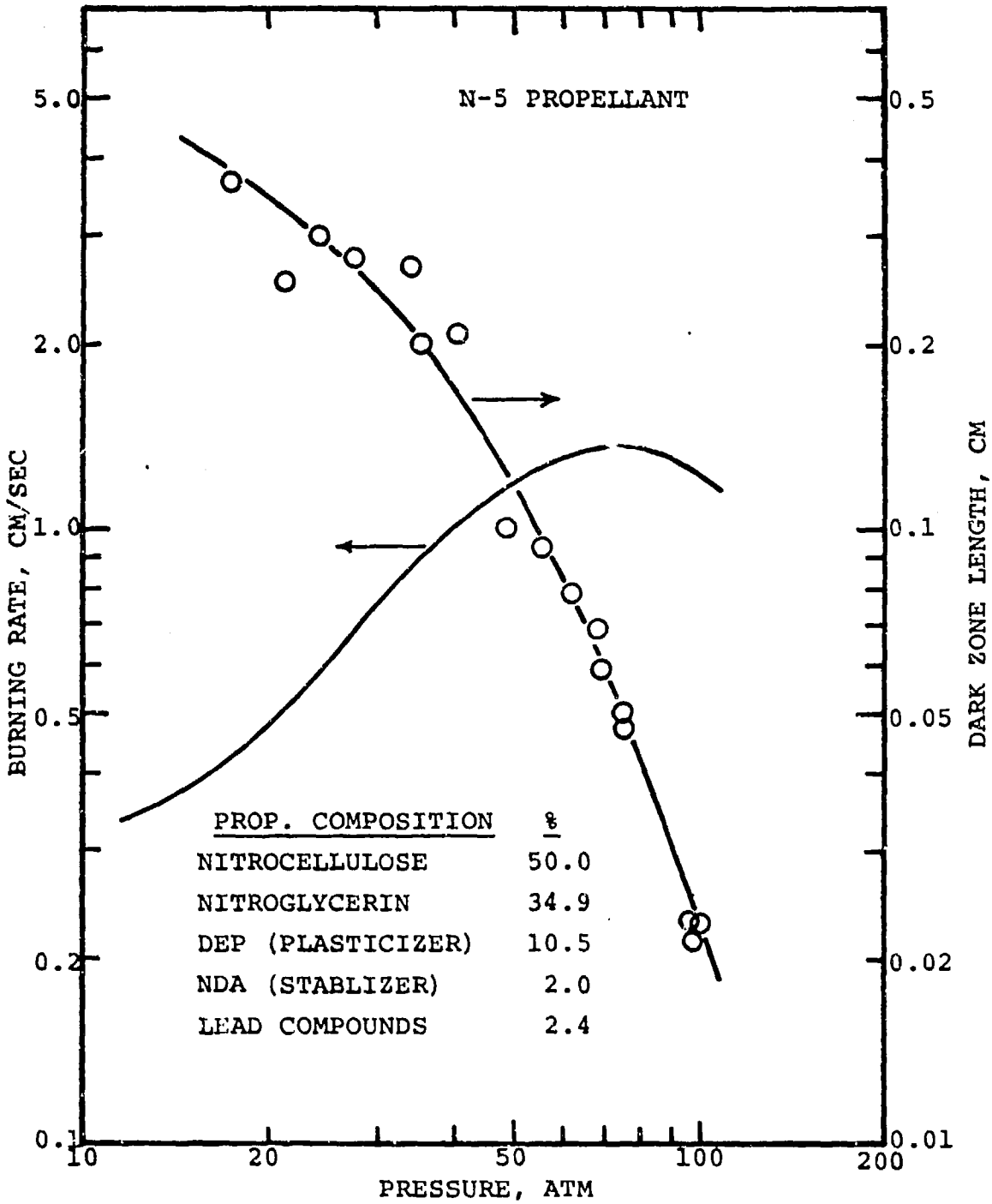

Fig. 34. Variation of dark zone length with pressure of plateau, mesa propellant showing rapidly decreasing dark zone length with increasing pressure in mesa region.

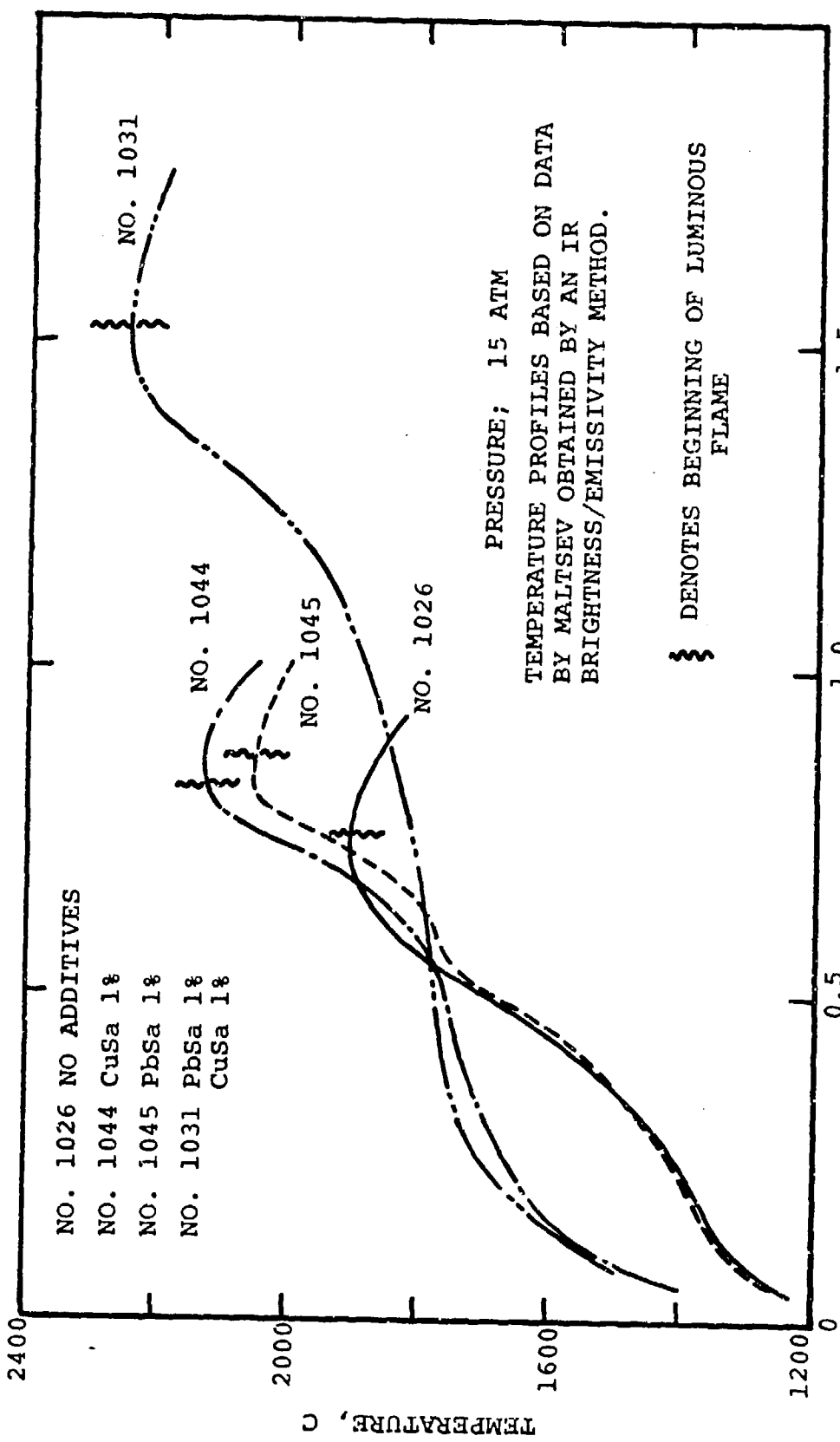

Fig. 35. Temperature profiles in gas phase (including beginning of luminous flame).

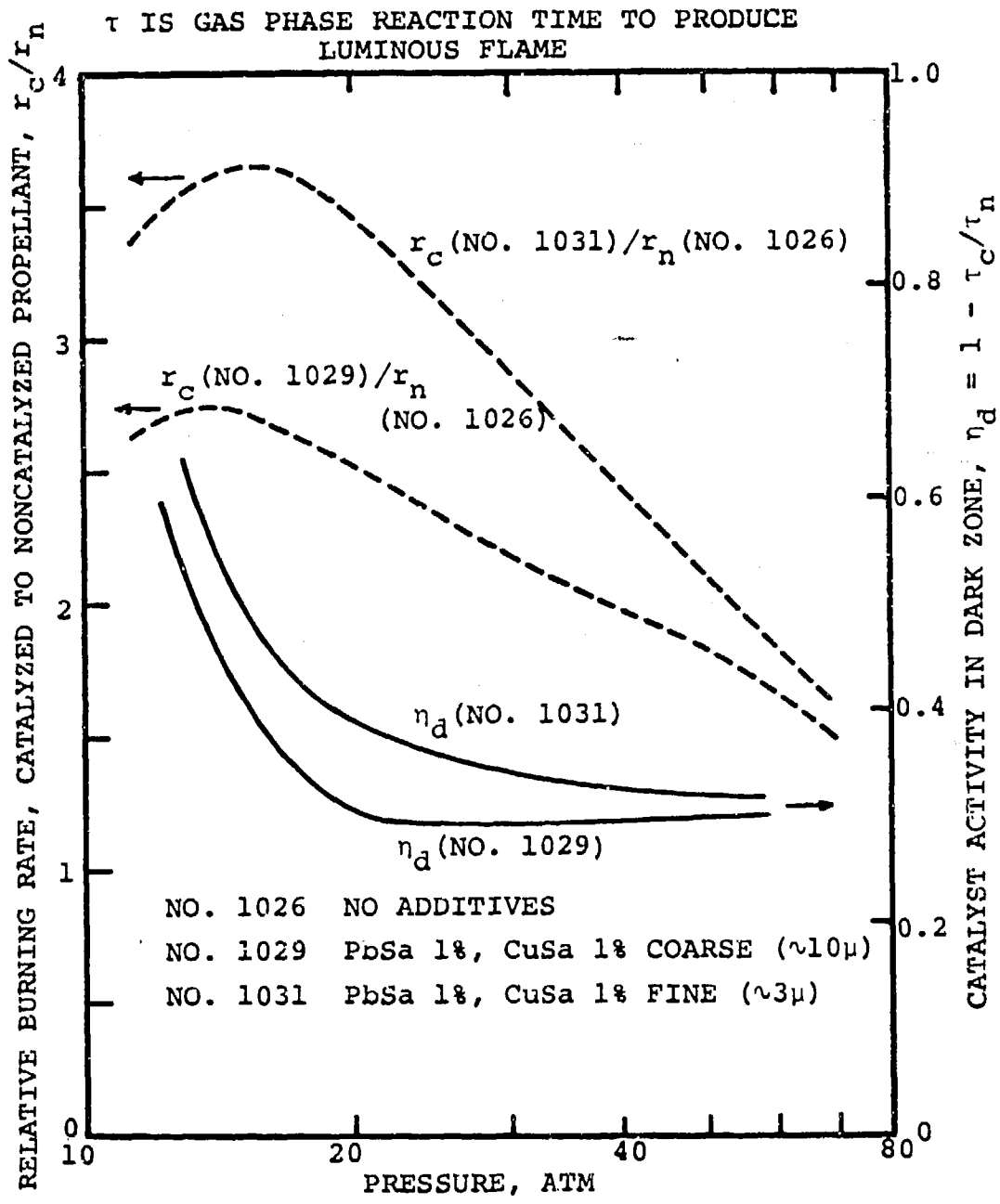

Fig. 36. Catalyst "activity" in dark zone and relative increase in burning rate as functions of pressure; the parameter is catalyst particle size.

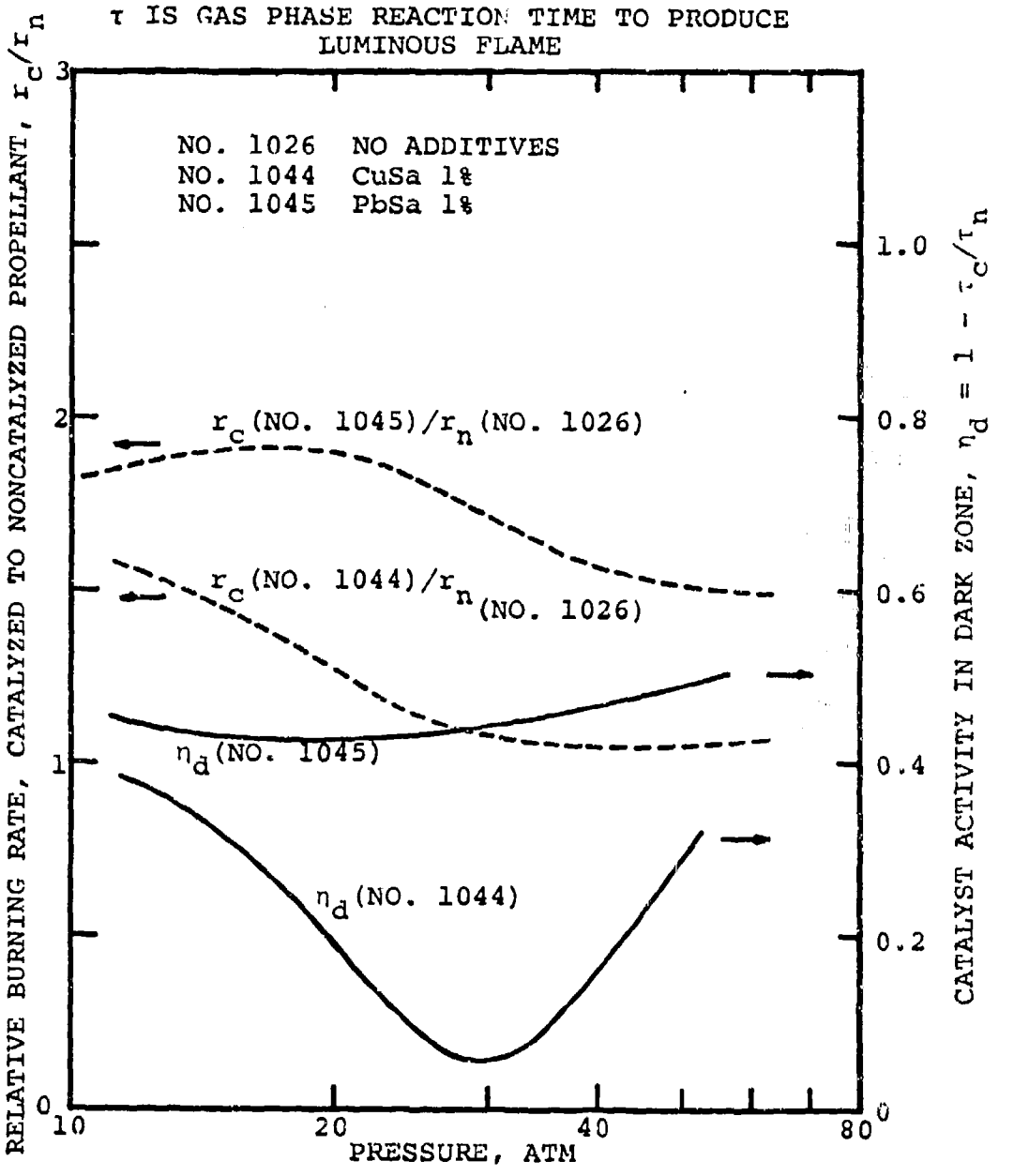

Fig. 37. Catalyst "activity" in dark zone and relative increase in burning rate as functions of pressure; the parameter is catalyst type.

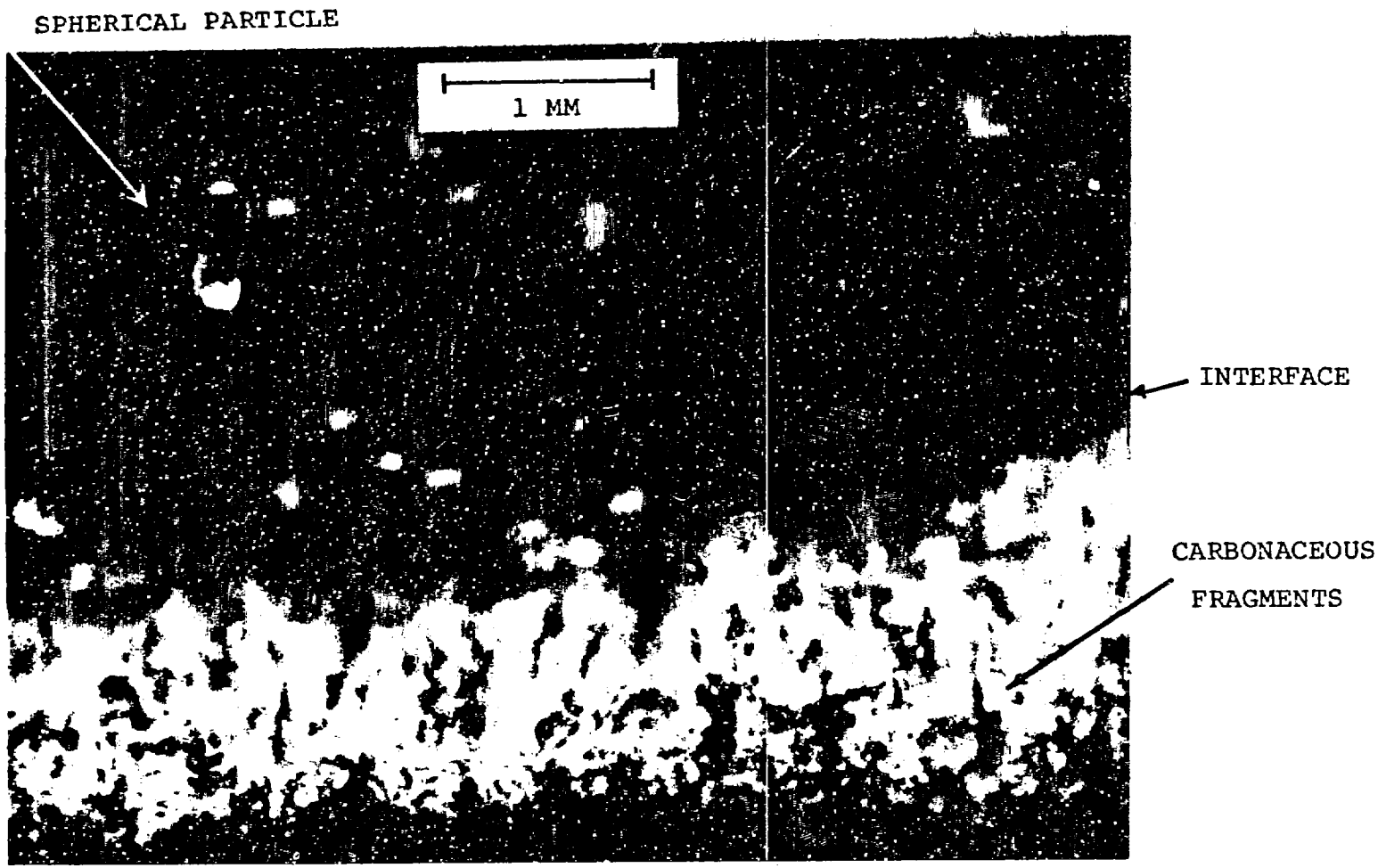

PROPELLANT NO. 6 KNO_3 0.75%
P = 15 ATM, r = 0.31 CM/SEC

Fig. 38 Photomicrograph of burning surface structure showing carbonaceous fragments and a spherical particle (probably K_2O) leaving the surface.

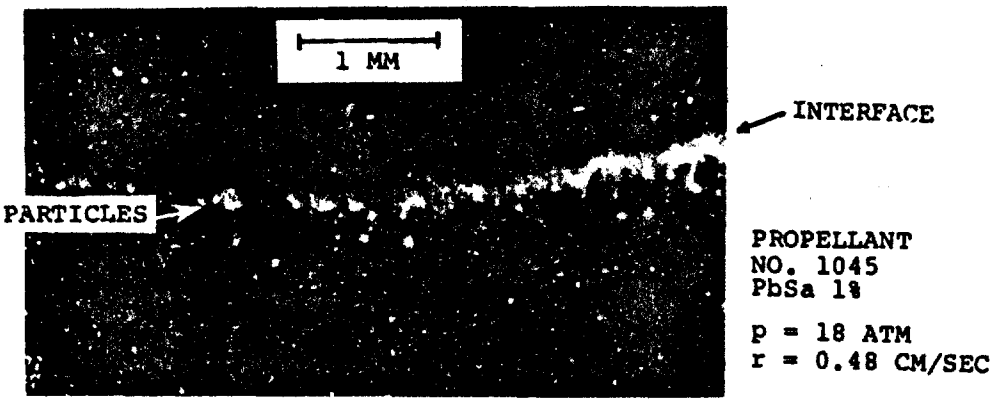

Fig. 39. Photomicrograph of surface during burning showing the appearance of brightly emitting spots on carbonaceous filaments when PbSa is added (this is not observed with the basic propellant).

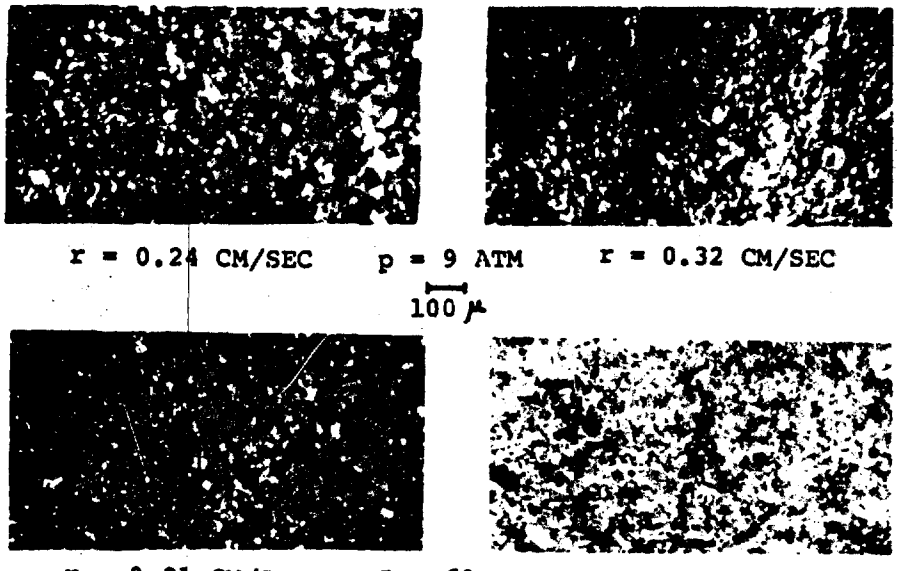

NO. 6 NONCATALYZED				N-5			
NC	39.6%	DPA	1.0	NC	50.0%	PbSa	1.2
NG	49.4	DBP	10.0	NG	34.9	Pb2-EH	1.2
				DED	10.5		

Fig. 40. Photomicrographs of extinguished (by rapid depressurization) burning surface of noncatalyzed and catalyzed propellant samples showing decreasing amount of and size of carbon particles on the surface with increasing pressure.

WORKER	METHOD	T/C SIZE, μ	YEAR	REF.
⊖ KLEIN	T/C	12.5	1950	32
◎ WILFONG	MELTING PT. OF METAL		1950	15
⧋ GORDON	T/C	76	1954	107
● HELLER	T/C	7.6 & 12.5	1955	11
□ POWLING	INFRA-RED RADIOMETER		1962	96
× SABADELL	T/C	7.6	1965	75
○ ZENIN	T/C	5 x 300	1966	97
⊡ ALEKSANDROV	T/C	5 x 60	1966	98
▽ STRITTMATTER	T/C	5 x ?	1966	92
+ SELEZNEV	RADIOMETER		1969	106
△ TSAI	T/C	12.5	1969	95
⬡ SUH	T/C	12.5 & 25.4	1970	94
◉ KUBOTA	T/C	7.6	1971	105

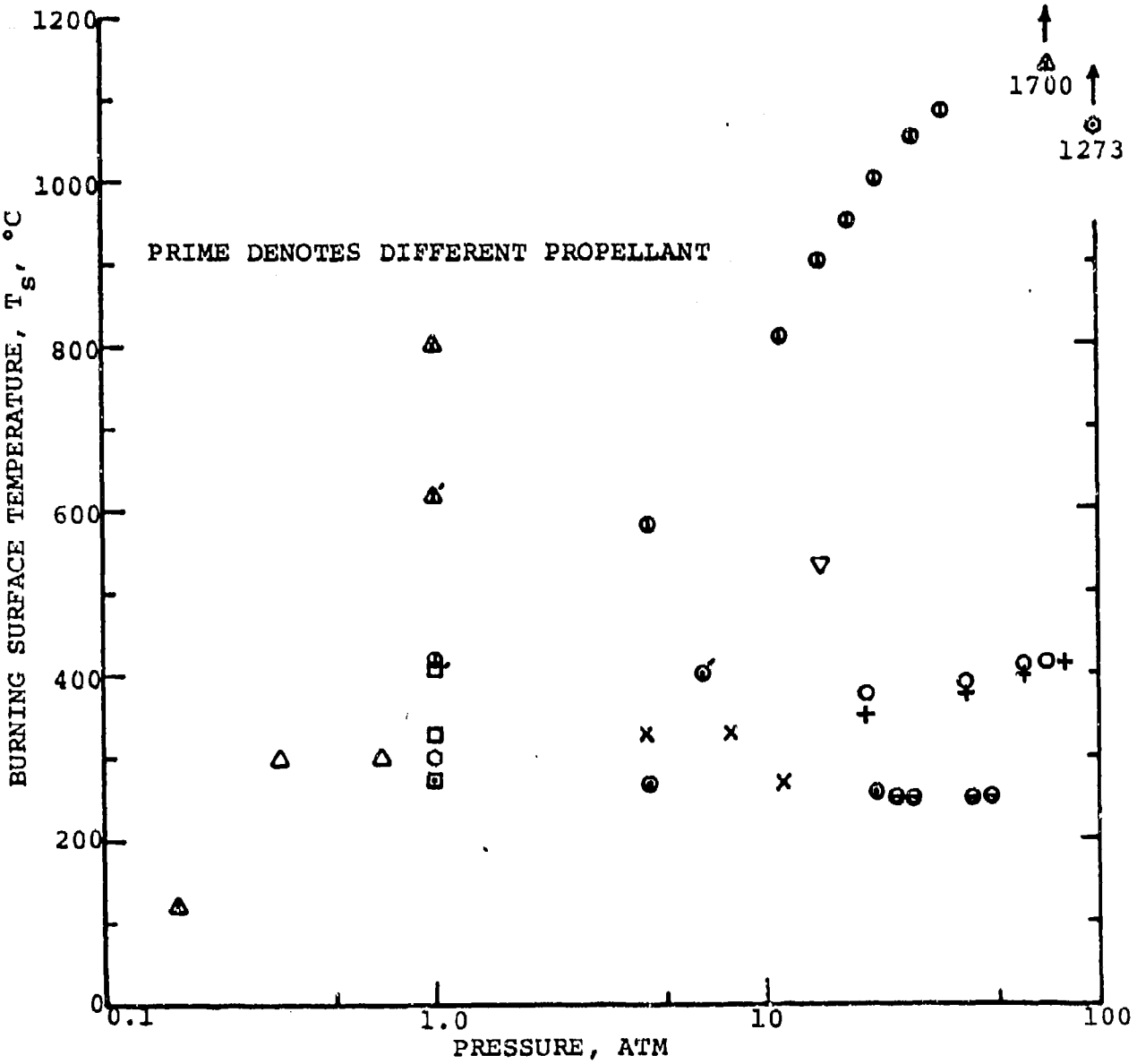

Fig. 41. Burning surface temperature of double base propellants vs pressure as measured by previous investigators.

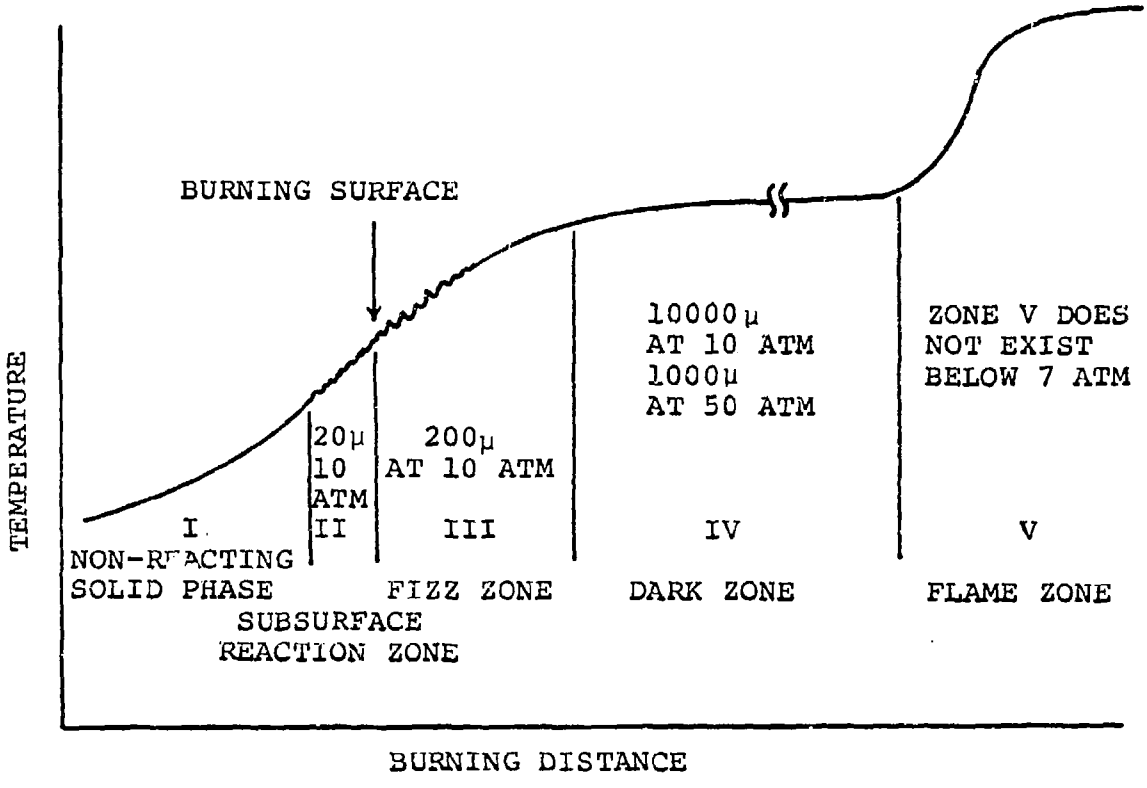

Fig. 42. General features of a typical temperature profile in catalyzed and noncatalyzed propellants combustion.

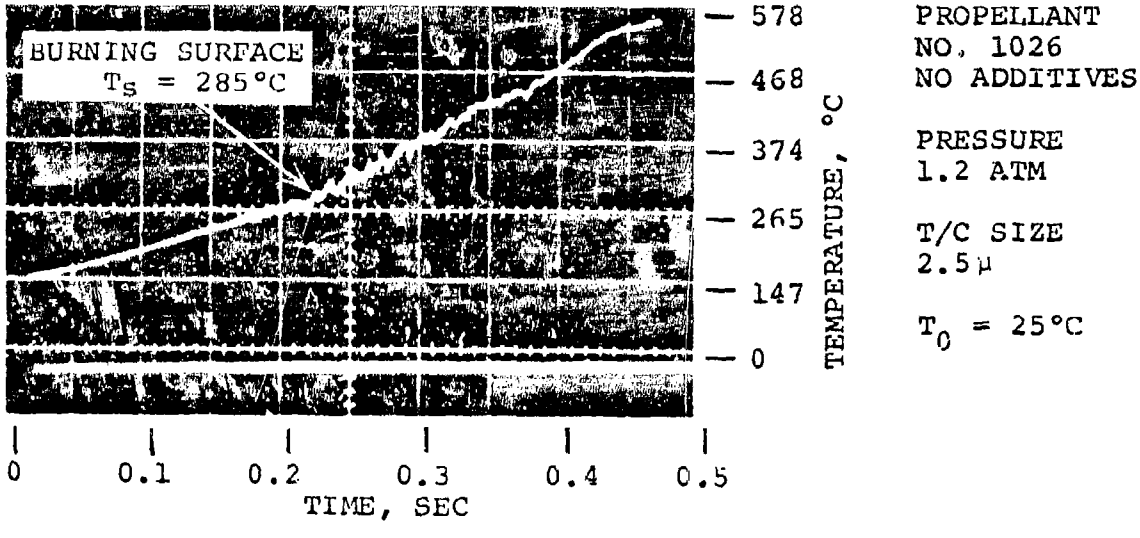

Fig. 43. Oscillogram of temperature profile showing voltage fluctuations near point where surface arrives at thermocouple.

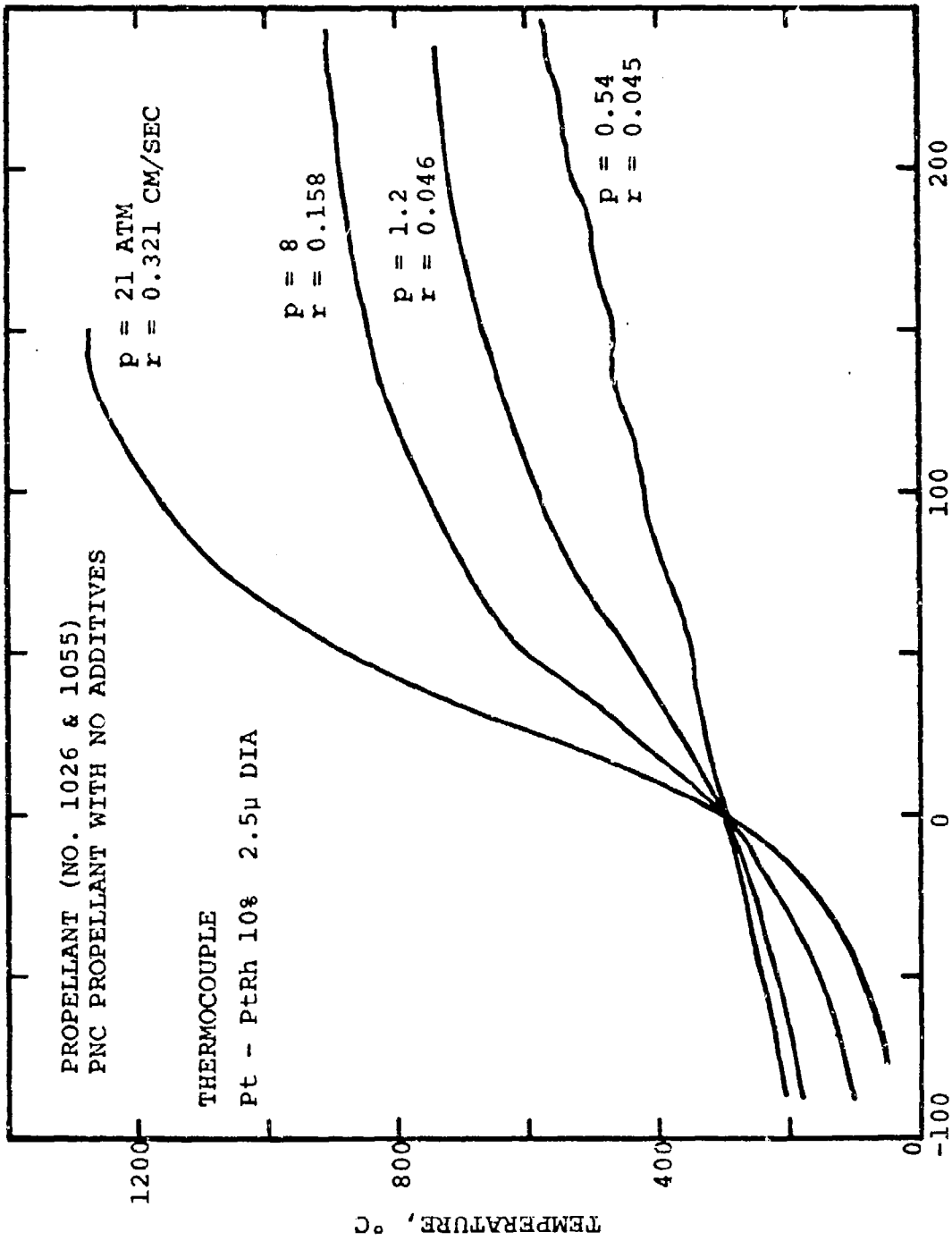

Fig. 44. Measured temperature vs distance in condensed phase and gas phase showing increasing temperature gradients and dark zone temperatures with increasing pressure, noncatalyzed propellant.

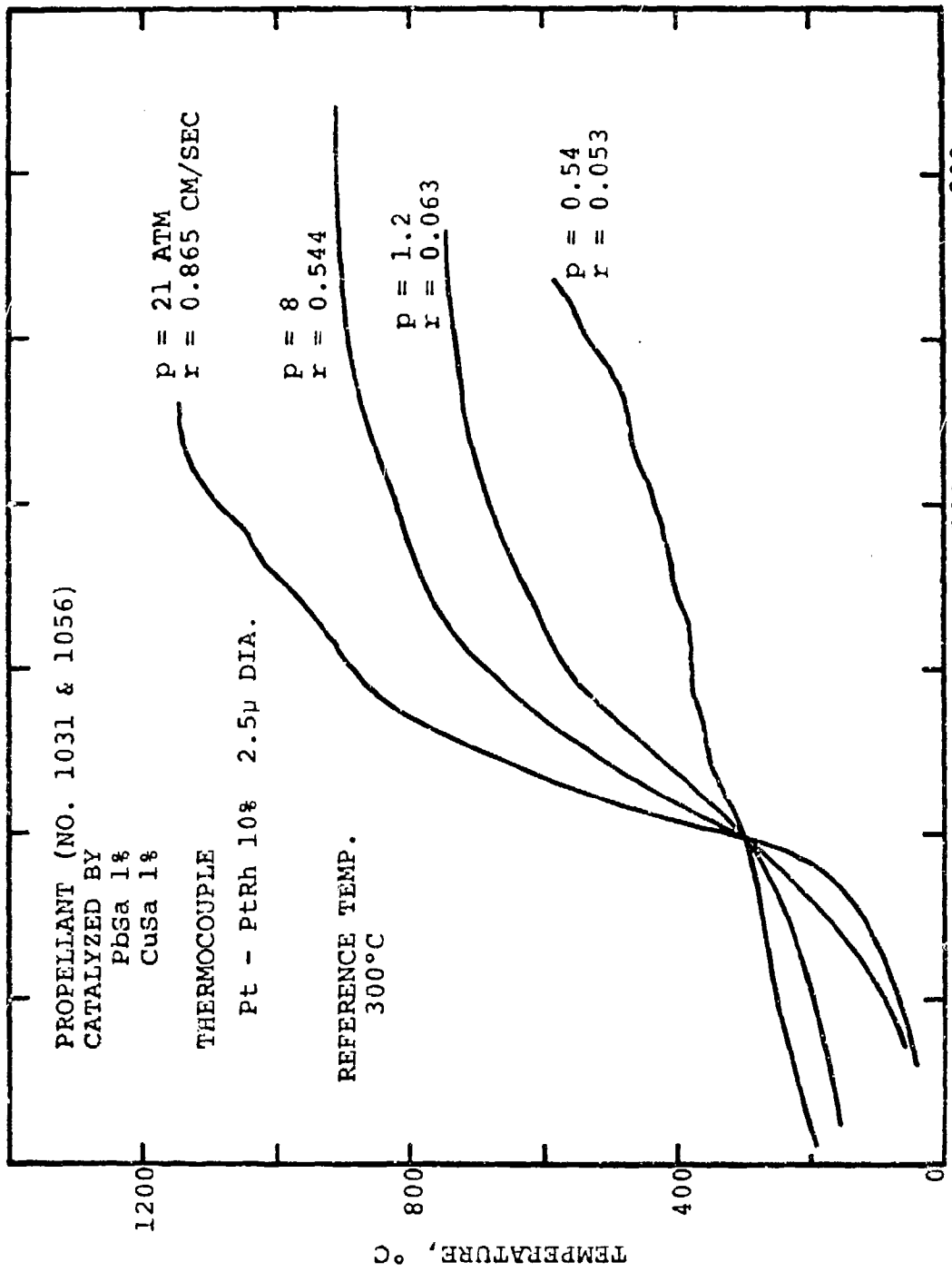

Fig. 45. Measured temperature vs distance in condensed phase and gas phase showing increasing temperature gradients and dark zone temperatures with increasing pressure; catalyzed propellant.

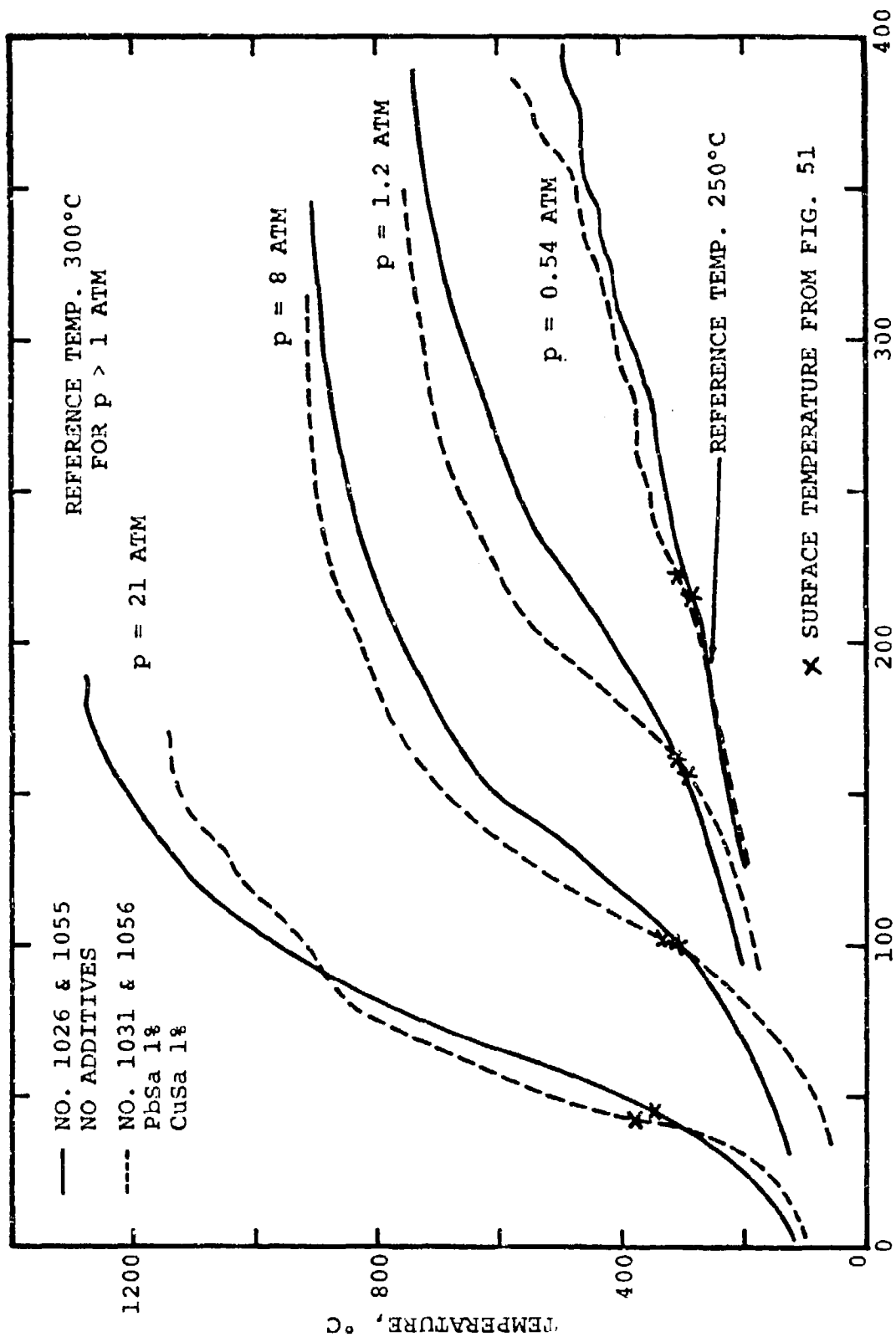

Fig. 46. Comparison of temperature profiles in fizz zone between noncatalyzed and catalyzed propellants.

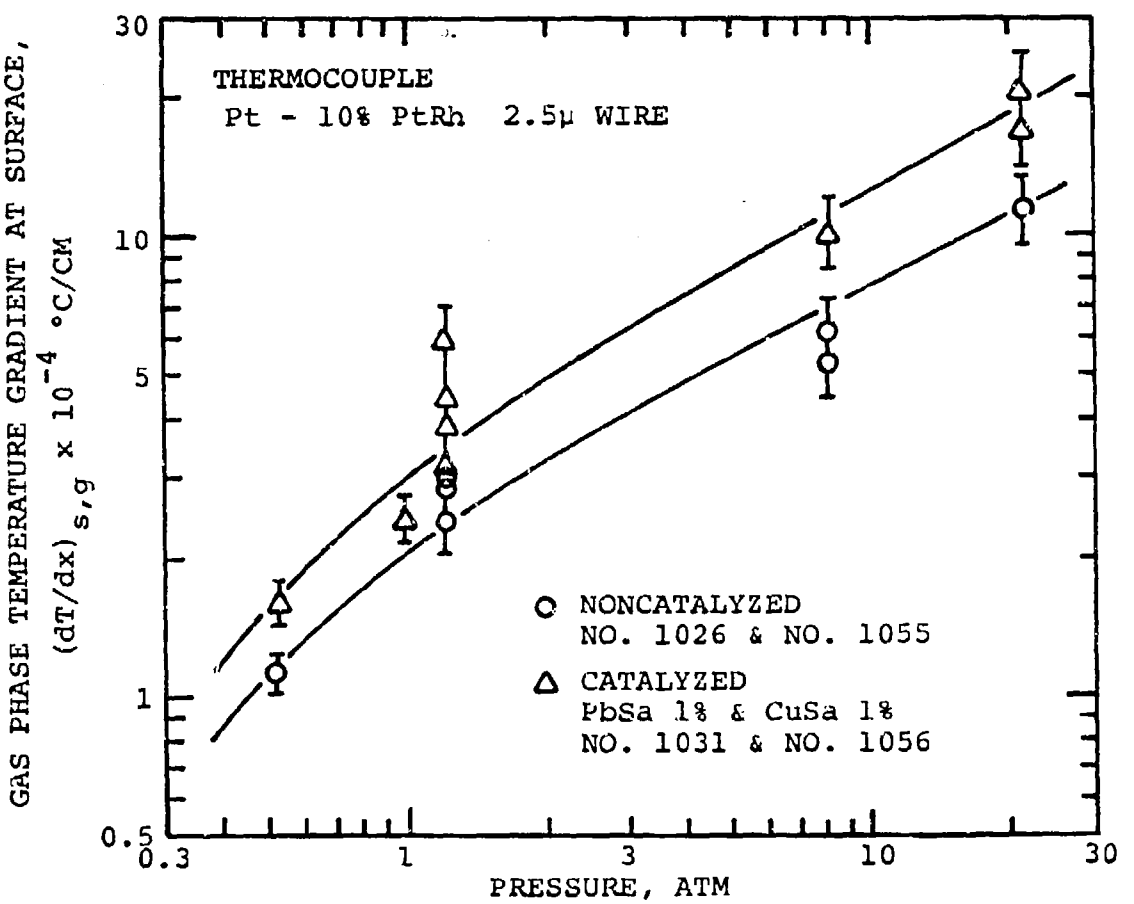

Fig. 47. Temperature gradient of the gas phase on burning surface vs pressure showing higher rate of heat feedback from gas phase to condensed phase when propellant is catalyzed.

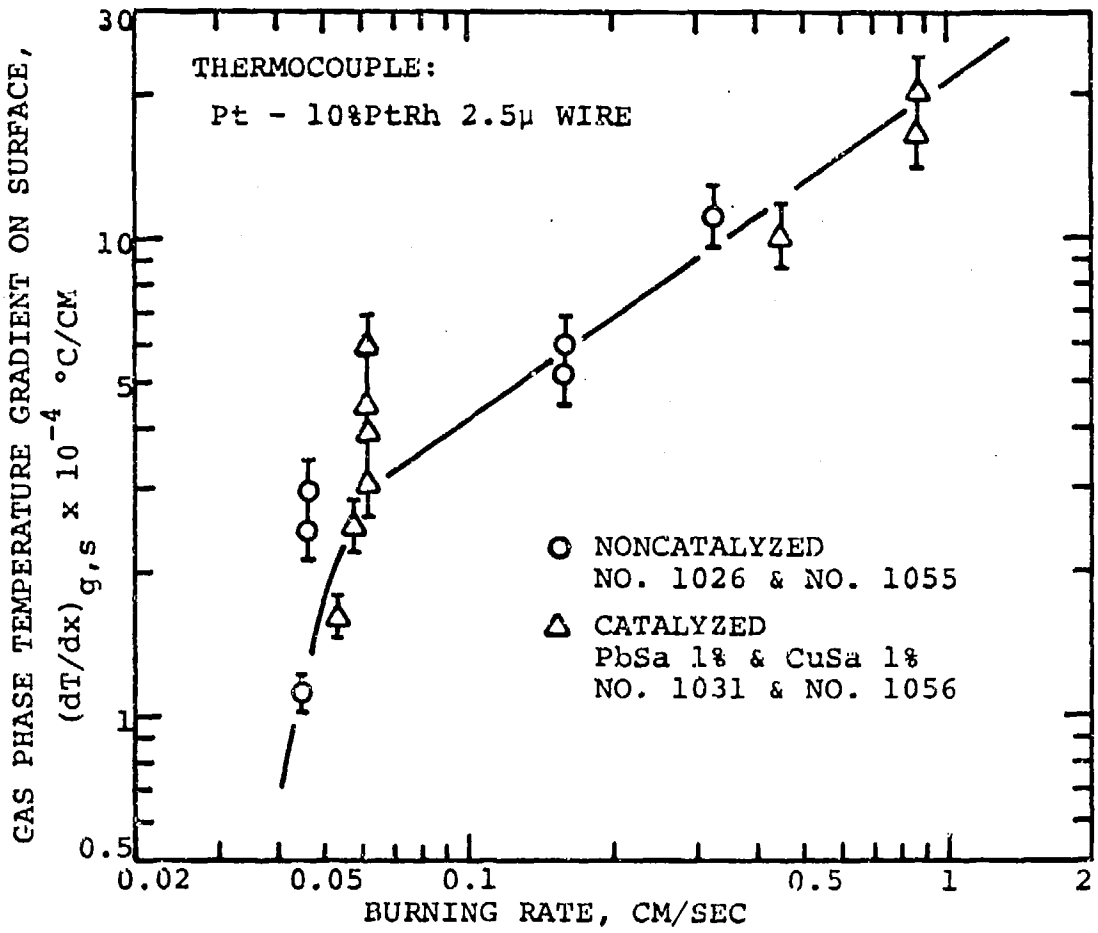

Fig. 48. Temperature gradient of the gas phase on burning surface vs burning rate showing rapidly decreased heat feedback from gas phase to condensed phase at low pressures.

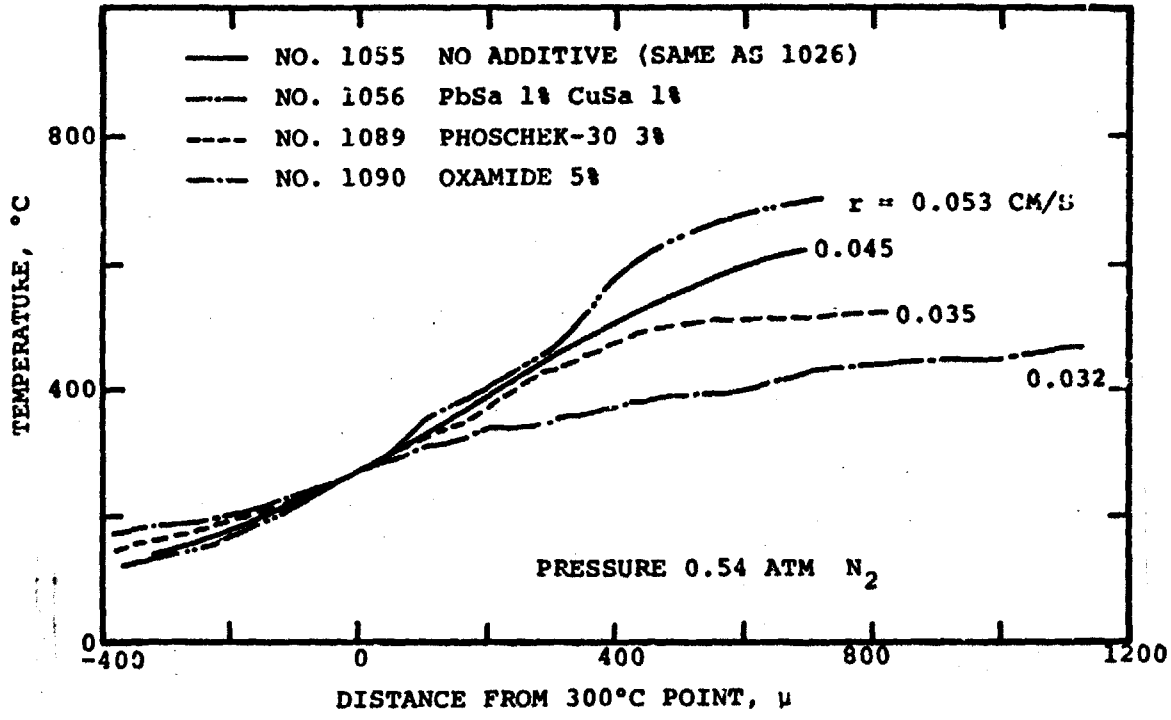

Fig. 49. Measured temperature vs distance in condensed phase and gas phase showing how flammability retarding additives reduce temperature gradients and fizz zone temperatures.

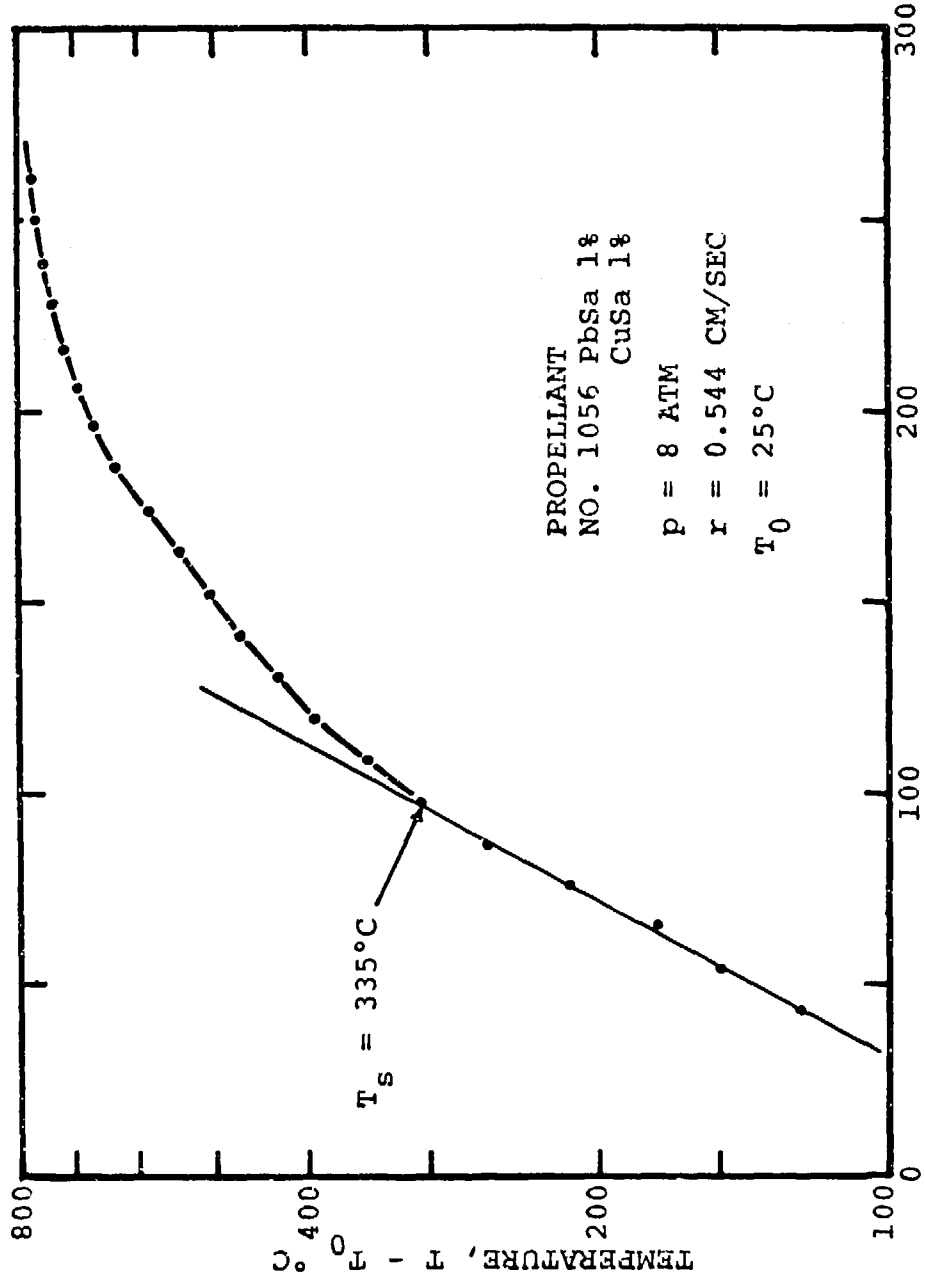

Fig. 50. Surface temperature determined by temperature inflection method (propellant 1056 at 8 atm).

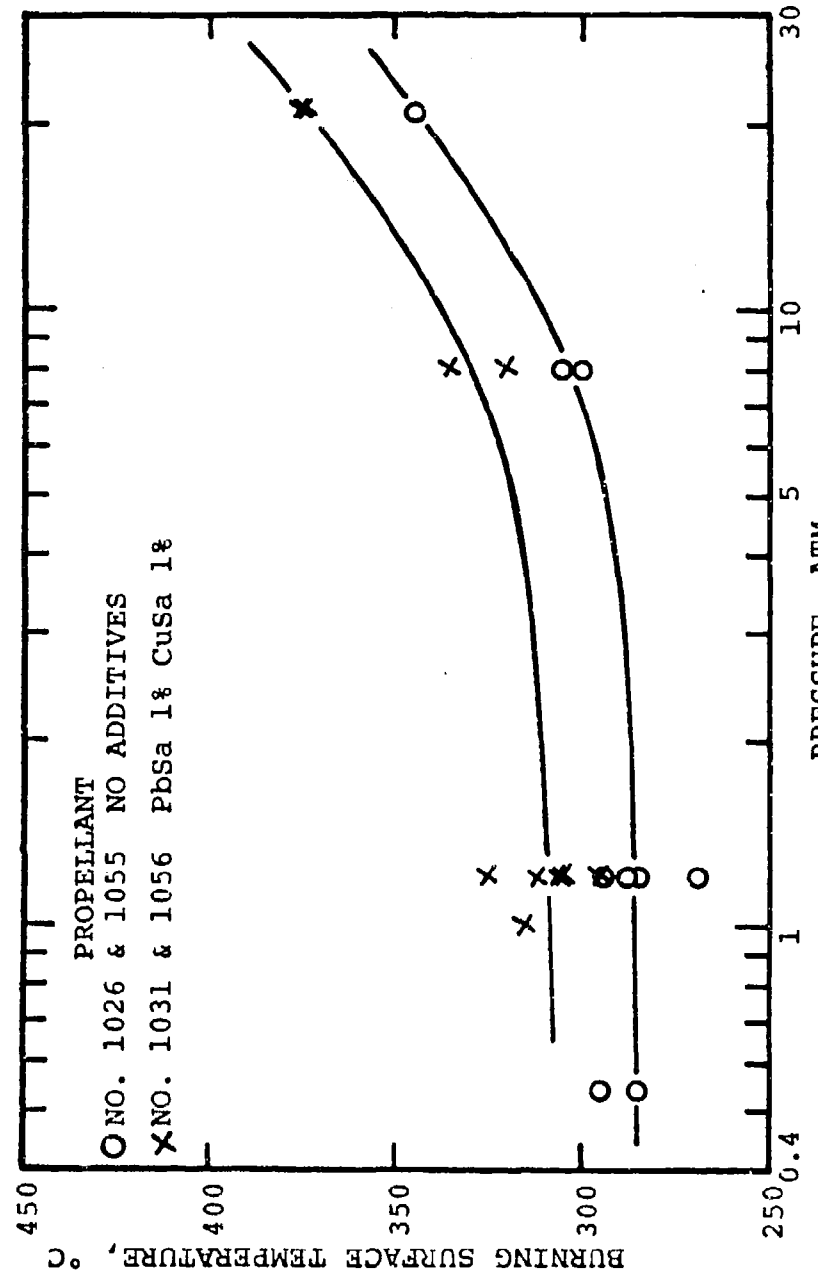

Fig. 51. Dependence of burning surface temperature on pressure and comparison of burning surface temperature of catalyzed and noncatalyzed propellant.

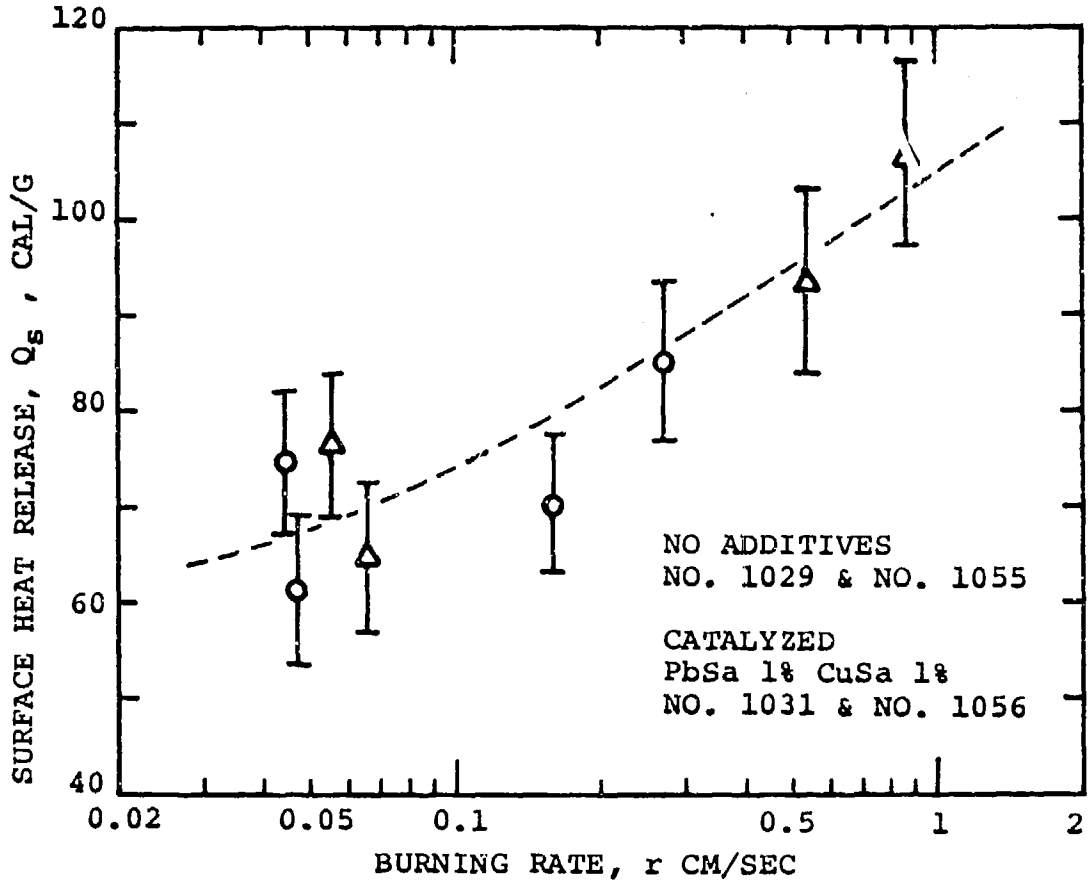

Fig. 52. Relationship between the surface heat release and the burning rate showing no detectable difference of Q_s between noncatalyzed and catalyzed propellants.

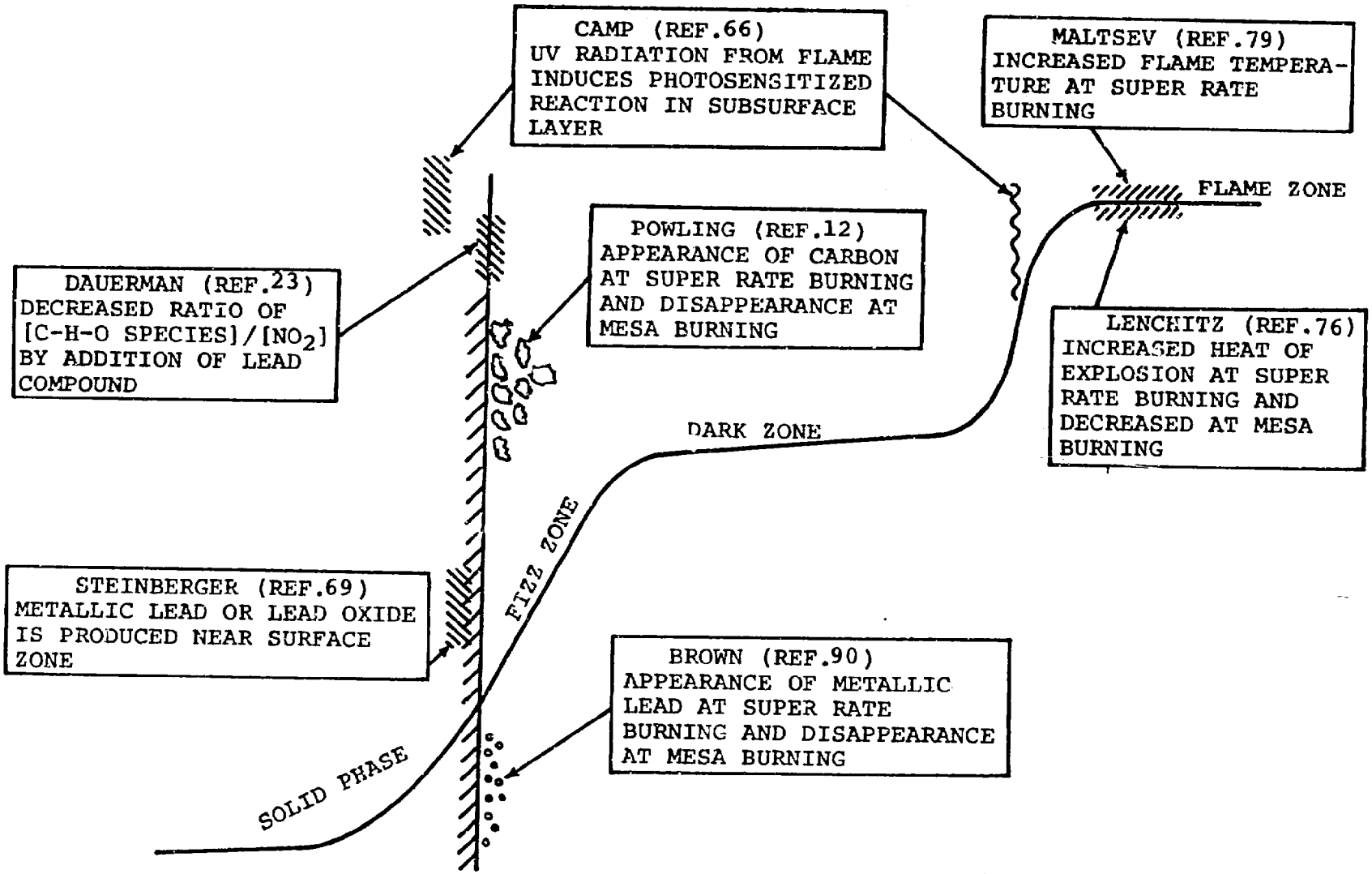

Fig. 53. Zones emphasized by previous investigators

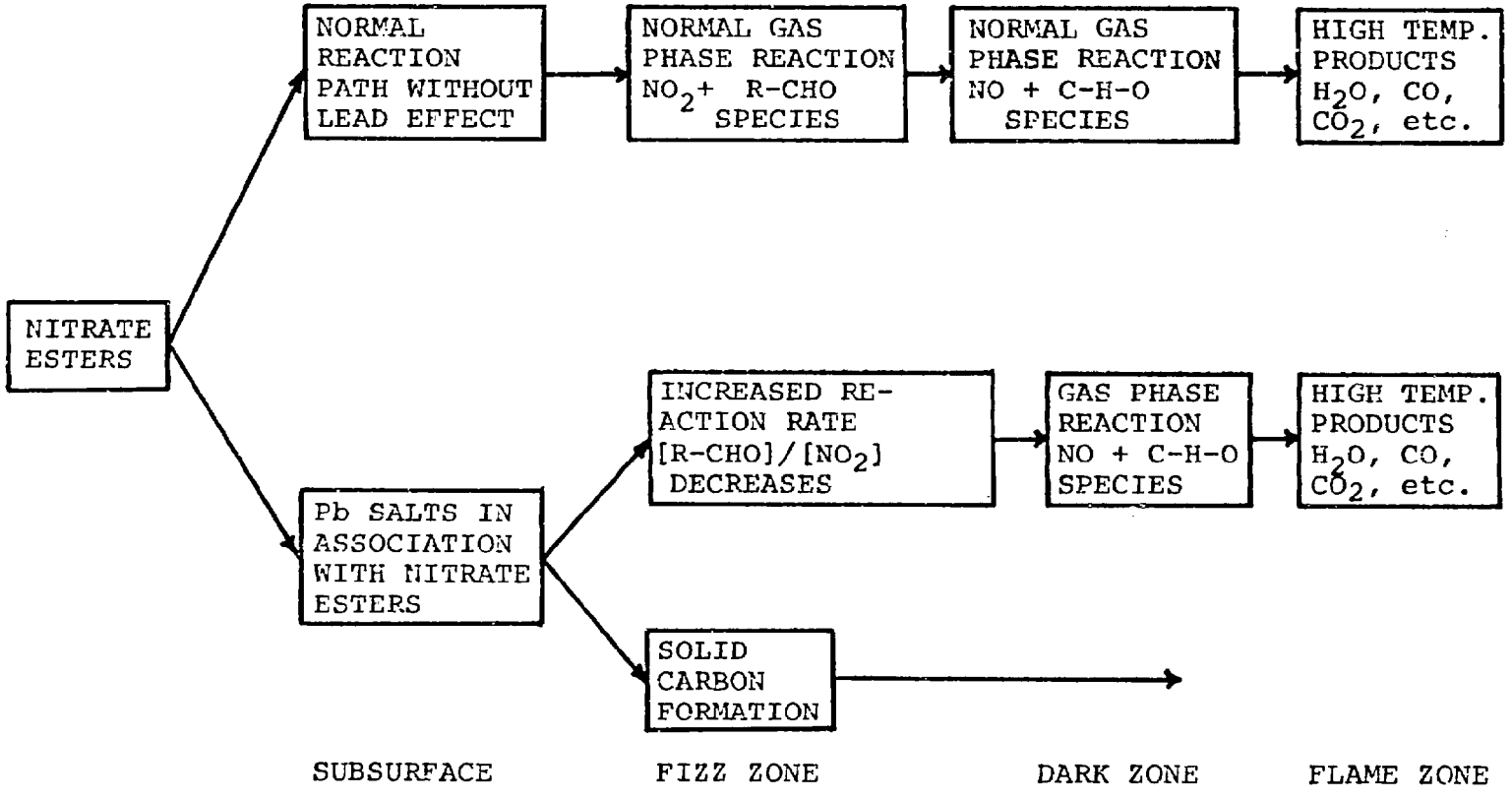

Fig. 54. Proposed reaction pathways for super-rate burning

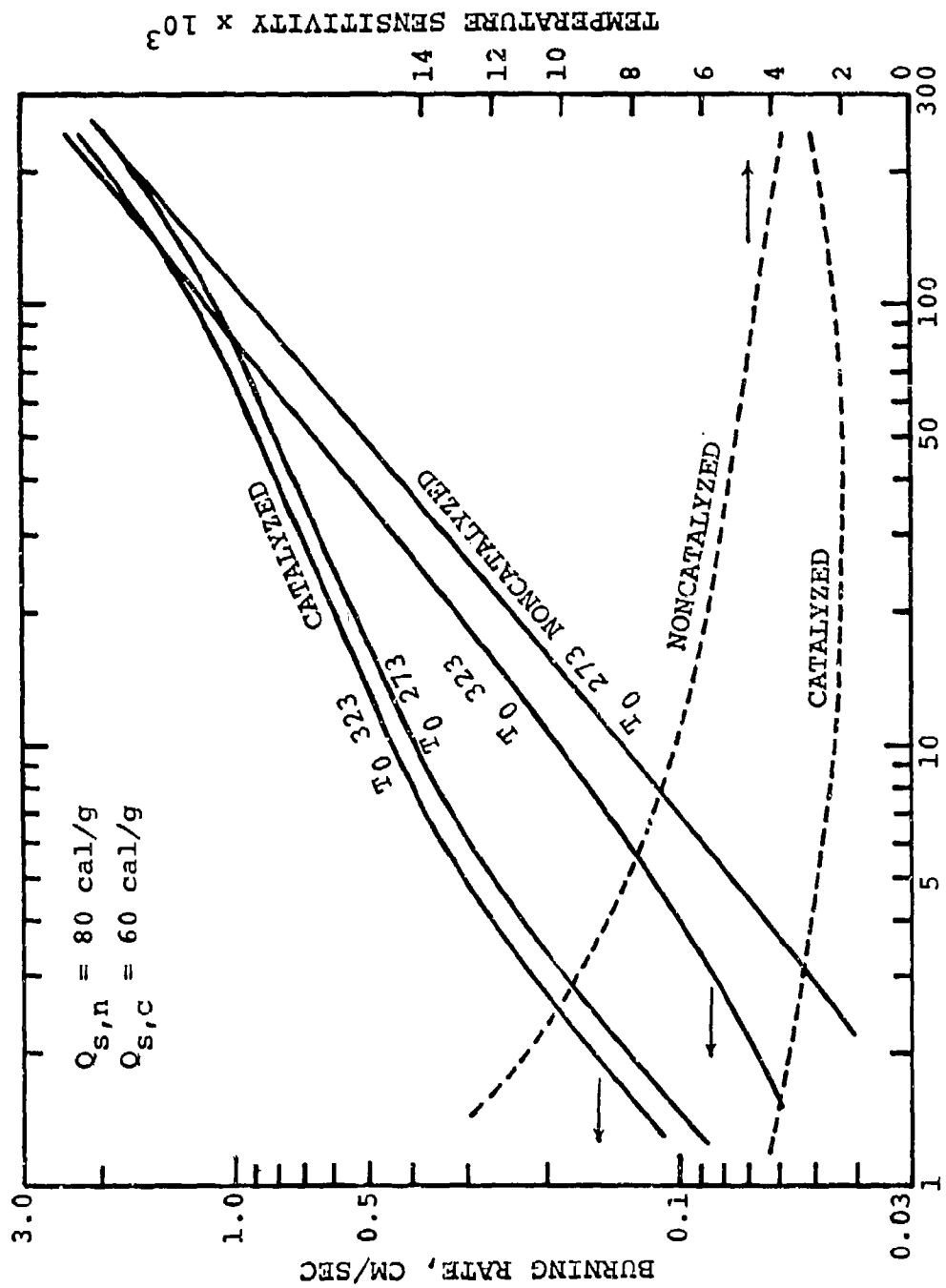

Fig. 55. Calculated burning rate and temperature sensitivity vs pressure of noncatalyzed and catalyzed propellant.

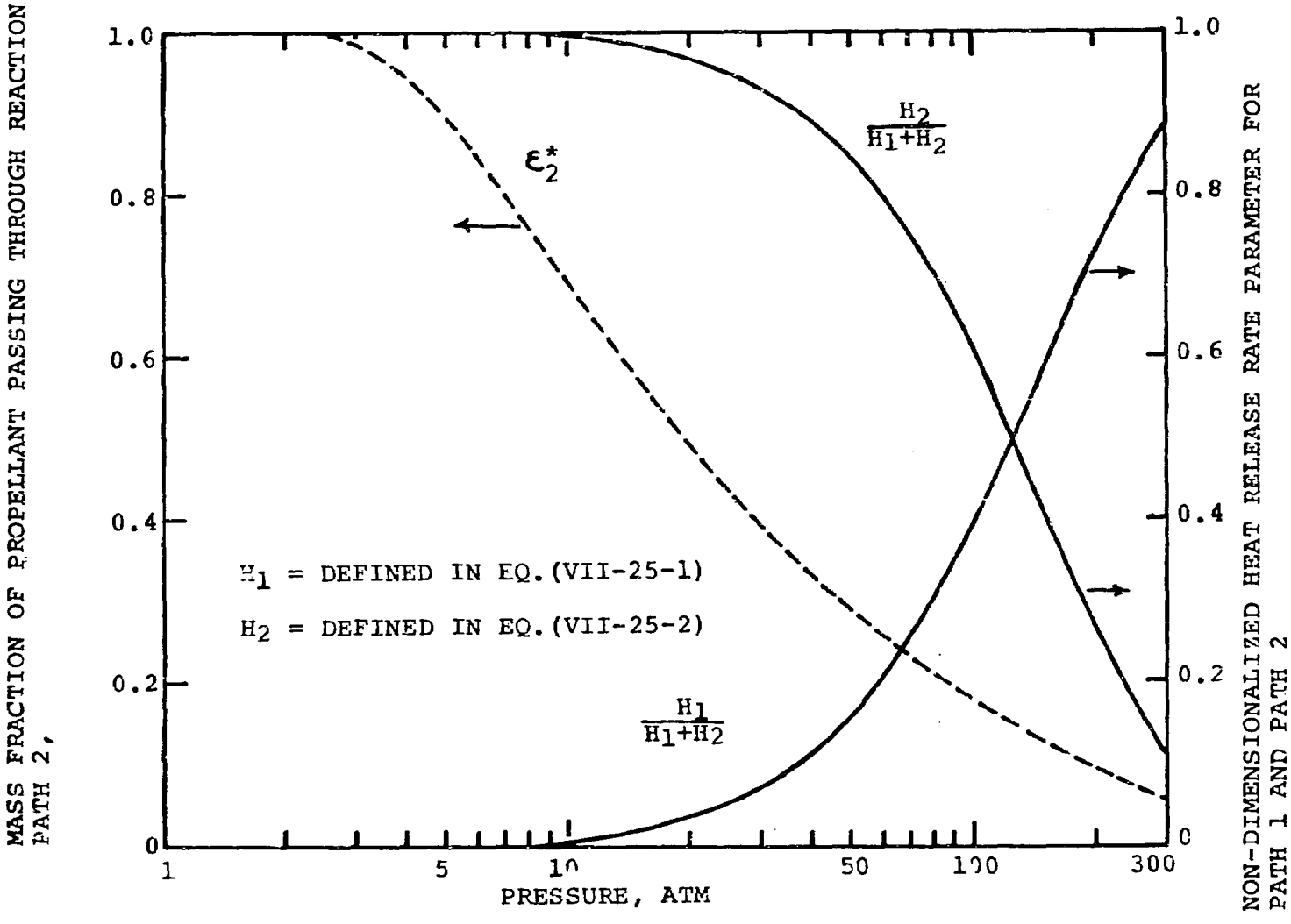

Fig. 56. Calculated mass fraction of propellant passing through reaction path 2 and non-dimensionalized heat release rate parameter for path 1 and path 2.

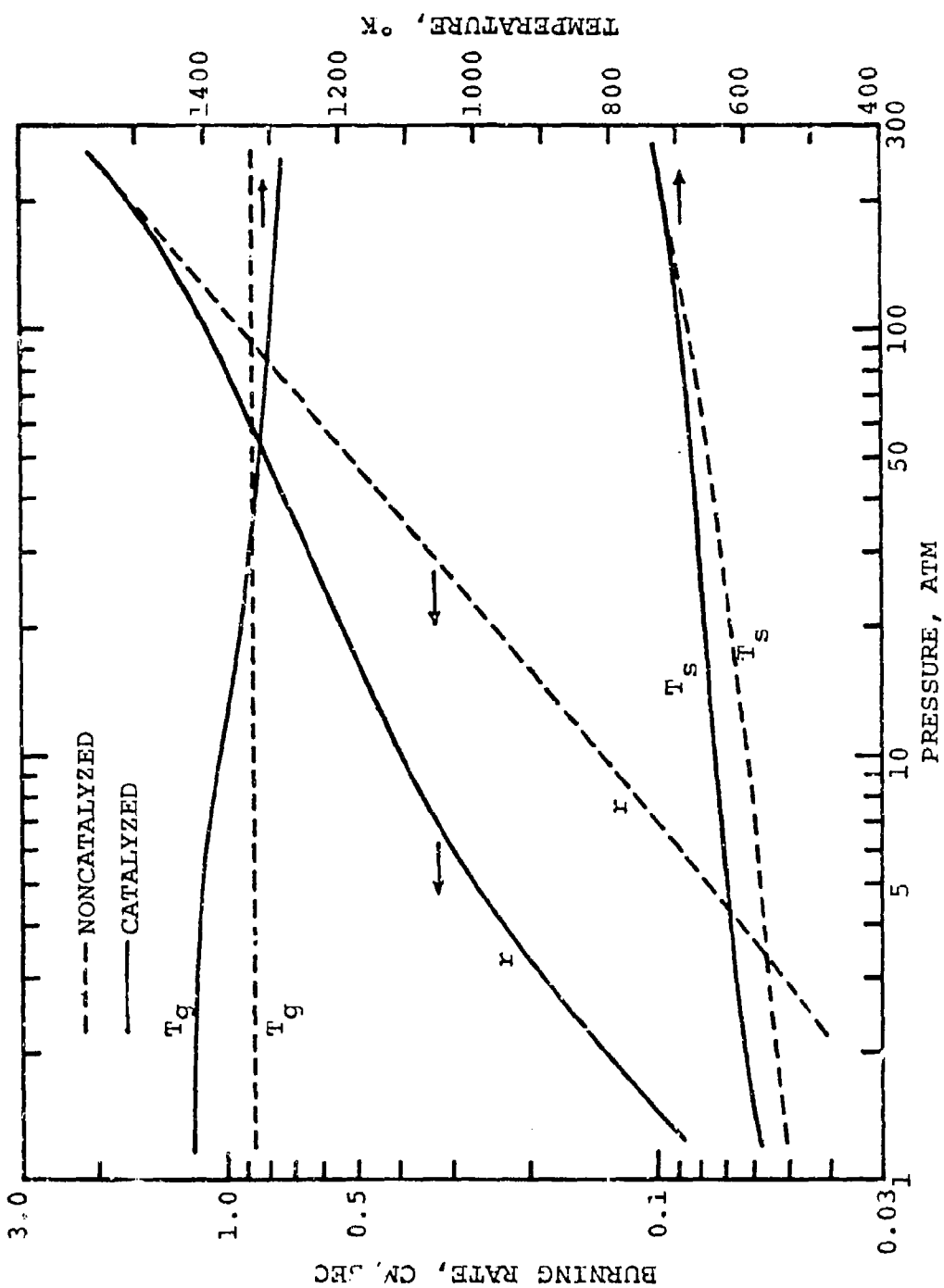

Fig. 57. Calculated burning rate, burning surface temperature, and dark zone temperature vs pressure for noncatalyzed and catalyzed propellants.

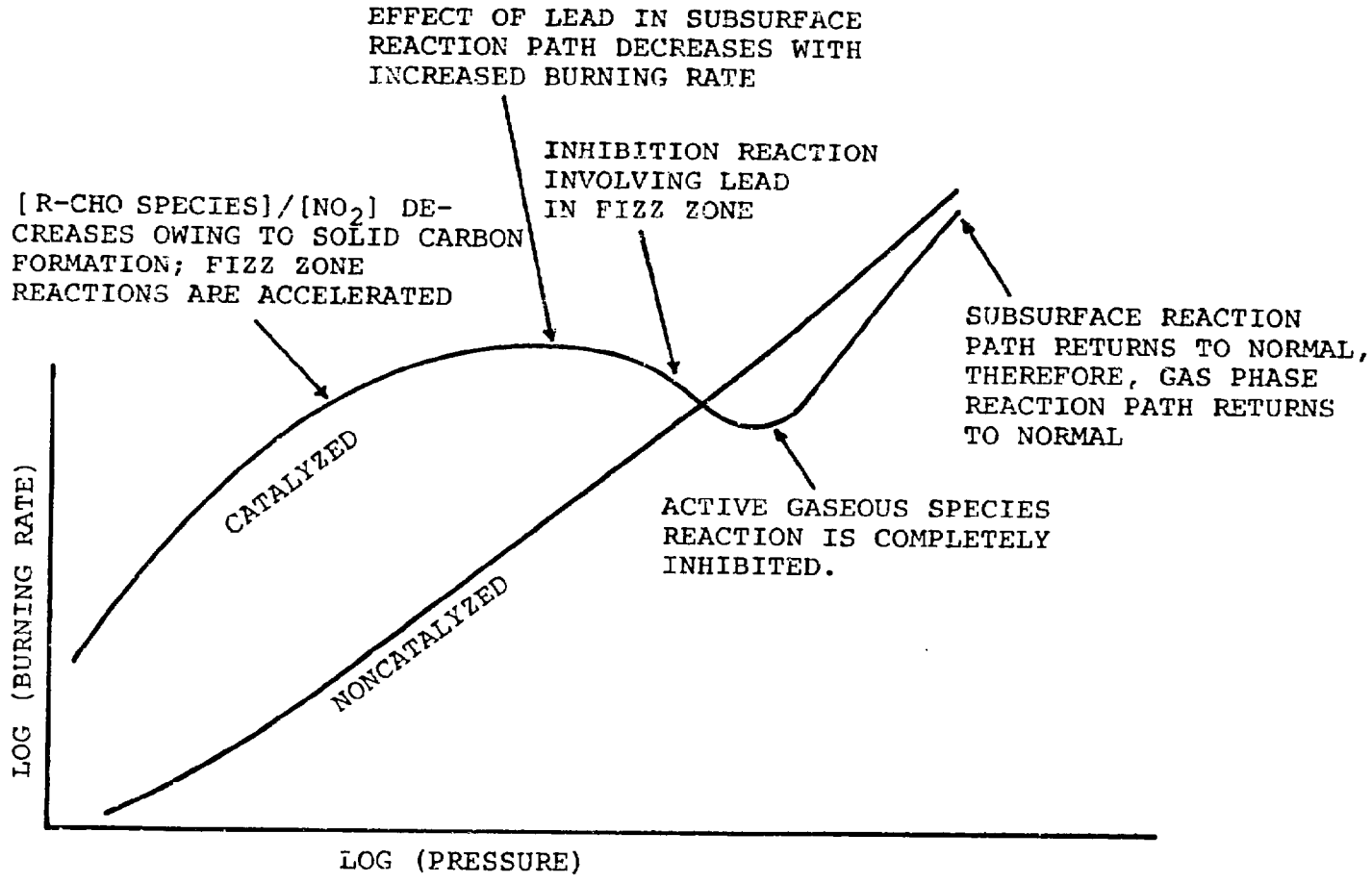

Fig. 58. Postulated plateau burning rate model

APPENDIX A

SPECIFICATIONS OF ALL PROPELLANT FORMULATIONS USED IN THIS INVESTIGATION

The composition of the propellant used in this investigation are listed in Table A-1 and A-2 of this Appendix. The propellants in Table A-1 are PNC/TMETN type propellants manufactured at Princeton. The manufacturing process is described in Appendix D. The density of the propellants was measured by a method similar to that used by Steinz[73]. In each case, the density of the propellant strands was found to be approximately the same as that calculated. For example, the density of the noncatalyzed propellant, No. 1026, was found to be 1.543 g/cm^3 (99.94% of the theoretical value, the calculation being based on an assumption of no chemical reaction between the propellant ingredients); the density of the catalyzed propellant, No. 1029, was found to be 1.542 g/cm^3 (99.86% of the theoretical value).

The NC/NG type propellants used in this study are listed in Table A-2. The propellants of batch number from 6 to 9 are manufactured at Feltman Research Laboratories, Picatinny Arsenal. The latter are castable-type double base propellants comprising spherical-shaped NC particles ($\sim$80 microns in diameter). N-5 propellant is a standard U.S. Navy propellant (a JANNAF reference propellant) catalyzed to produce plateau and mesa-burning.

TABLE A-1

SPECIFICATIONS OF ALL PNC/TMETN PROPELLANT FORMULATIONS USED FOR THIS STUDY.

BATCH NO.*	BASIC COMPOSITION %				ADDITIVES %			COMM.
	PNC	TMETN	TEGDN	EC	C	PbSa	CuSa	
1023	40.00	50.00	10.00					
1026	53.70	39.10	7.02	0.08	0.10			
1029	52.65	38.33	6.88	0.08	0.10	0.98	0.98	L
1031	52.65	38.33	6.88	0.08	0.10	0.98	0.98	S
1038	53.76	39.13	7.03	0.08				
1039	50.00	40.40	7.02		PbSa 1.20 Pb2EH 1.20			H
1040	52.55	38.33	6.88	0.08	0.20	0.98	0.98	S
1041	53.60	39.10	7.02	0.08	0.20			
1044	53.29	38.70	6.85	0.08	0.10		0.98	S
1045	53.29	38.70	6.85	0.08	0.10	0.98		S
1046	50.70	40.90	7.20		Pb2-EH 1.20			H
1047	52.65	38.33	6.88	0.08	0.10	0.98	0.98	LH
1048	52.55	38.33	6.88	0.08	0.20	0.98	0.98	S
1049	53.76	39.13	7.03	0.08				
1051	51.60	37.56	6.74	0.08	0.10	1.96	1.96	L
1055	53.70	39.10	7.02	0.08	0.10			
1066	53.29	38.70	6.85	0.08	0.10	Sa 0.98		
1068	53.29	38.70	6.85	0.08	0.10	Pb 0.98		
1071	52.65	38.33	6.88	0.08	0.10	Pb 0.98 Sa 0.98		
1075	53.29	38.70	6.85	0.08	0.10	Cu 0.98		
1076	52.65	38.33	6.88	0.08	0.10	Pb 0.98 Cu 0.98		
1081	53.29	38.70	6.85	0.08	0.10	PbO 0.98		
1082	51.60	37.56	6.74	0.08	0.10	PbO 3.92		
1089	52.09	37.93	6.80	0.08	0.10	PHOSCHEK-30 3.00		
1090	51.01	37.14	6.67	0.08	0.10	OXAMIDE 5.00		
1094	43.01	31.31	5.62	0.06	AP(5μ) 20.00			
1097	48.38	35.22	6.33	0.07	AP(5μ) 10.00			

NOTE: L denotes unground additives (PbSa ∿ 10μ and CuSa ∿ 10μ).
S denotes ground additives (PbSa ∿ 3μ and CuSa ∿ 3μ).
H denotes additives mixed with heptane.
Pb powder particle size ∿ 6.0μ.
Cu powder particle size ∿ 5.4μ.
PbO powder particle size ∿ 5μ.

*Propellants manufactured at the Guggenheim Laboratories of Princeton University.

TABLE A-2

SPECIFICATIONS OF ALL NC/NG PROPELLANT FORMULATIONS USED FOR THIS STUDY

BATCH NO.	BASIC COMPOSITION %				ADDITIVES %		COMM.
	NC	NG	DPA	DBP	C	KNO_3	
6	39.60	49.40	1.00	10.00			
7	39.40	49.30	1.00	10.00	0.30		
8	39.10	48.90	1.00	10.00	1.00		
9	39.25	49.00	1.00	10.00		0.75	
N-5	50.0	34.9	DEP 10.5 NDA 2.0 PbSa 1.2 Pb2-EH 1.2 CW 0.2				

NOTE: Propellants batch number 6 to 9 are manufactured at Feltman Research Labolatories, Picatinny Arsenal for this study. The propellants are manufactured by cast with ball powder of nitrocellulose (~80 microns).

N-5 propellant is a standard JANNAF propellant manufactured by U.S. NAVY (using solventless-extruded double base propellant).

APPENDIX B

SUMMARY OF OHLEMILLER AND SUMMERFIELD'S PLATEAU MODELLING WORK BASED ON THE CAMP UV RADIATION HYPOTHESIS

A. A Preliminary Model of Super-Rate Burning Based on Photochemically Assisted Degradation in the Condensed Phase*

The following is a description of a preliminary model for the steady burning of a platonized double base propellant. The basic premise of the model is that the primary site of action of the ballistic modifiers which produce super-rate burning and hence plateau behavior is in the condensed phase. It is assumed that ultraviolet radiation originating from the hot flame gases is absorbed in depth below the regressing propellant surface and there induces photochemical reactions whose net effect is a considerable increase in the propellant burning rate. The amount of this super rate (or elevation above the burning rate of the unmodified propellant) is itself dependent on the absolute burning rate since this parameter dictates the time available for reactions in the condensed phase; it is the decrease in super rate with increased burning rate which yields plateau burning behavior.

Certain elements of the model discussed here are, at present, necessarily arbitrary but it is, of course, the overall objective of the concomitant experimental research program to eliminate the ambiguous points and quantify the overall model as much as possible. The emphasis at this stage is on laying out in detail a plausible approximate model which can account for the most salient features of plateau burning. Computer solutions will be sought both as a check on the validity of the basic ideas and as guides for further model refinement and experimental tests. The flame zone is envisioned schematically as shown in Fig. B-1. The processes at and below the surface are idealized to consist of a few basic steps, thermal and photochemical degradation of the large, complex molecules to small fragments and then, at the surface, gasification of these fragments. The net process, the transformation of the cold unreacted propellant entering the flame zone at the initial temperature T_0 to small molecules leaving the surface at temperature T_s may be exothermic or endothermic. It should be noted that a variation in this net

---

*The basic idea for this model is contained in NAVORD Rept. 5824, "A Decade of Progress in the Understanding of Certain Ballistic Properties of Double Base Propellants," A. T. Camp, et al, Jan., 1958; the hypothesis is discussed briefly in Section II of this report.

heat of gasification is one possible source for super-rate burning effects; however, until this point is checked experimentally it will be assumed that the net gasification heat is constant.

In accord with the usual assumption in flame theory that a set of highly complex reactions is describable by a small set of controlling reactions, it is assumed that the processes in the condensed phase can be described as follows:

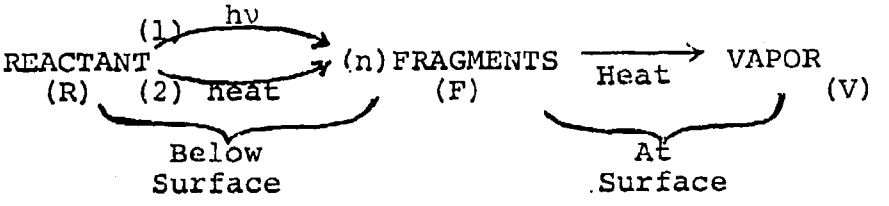

The details of path 1 might be

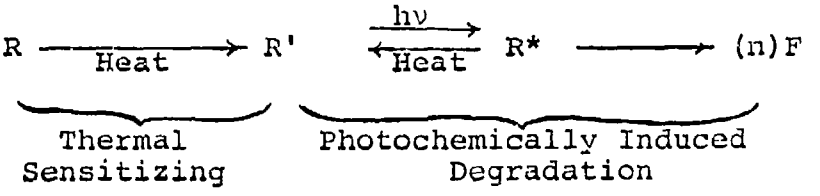

The upper sequence illustrates the basic hypothesis that the ultraviolet flame radiation absorbed below the propellant surface yields a parallel path by which the reactants are degraded; the lower sequence shows in more detail the possible steps in such a parallel path. There are certain conceptual simplifications here for the purpose of modelling. In the real propellant what is here termed reactant, comprises for the most part both nitrocellulose and nitroglycerin. It has been suggested that the actual primary absorber of the UV radiation in this photochemical chain is the ballistic modifier which then serves as a photosensitizer for the degradation of the nitrate esters. In the second sequence above, then, it would perhaps be more realistic if R', the thermally sensitized nitrate ester, was converted to the photo-activated form R* by interaction with the excited modifier molecule. It is felt, however, that the above simplified sequence as a first approximation, preserves the essential physical elements and facilitates assessment of the overall model. The importance of the parallel photochemical path in the context described here is that it constitutes an essentially temperature insensitive

way to go from reactant to fragment molecules; i.e., this path is uncoupled from the temperature wave in the condensed phase and degradation proceeds at a rate dependent on the local radiant flux and reactant concentration. Energetic photons instead of thermal agitation surmount the activation energy barrier to reaction; the thermodynamic limitations on reaction rates still exist, of course, and the net endothermicity or exothermicity of the degradation is, again, assumed to be unchanged.

The second sequence above shows that the photochemical degradation path is not necessarily completely independent of local temperature. First, the photochemical pathway may need to be thermally sensitized; i.e., the reactant may need to be at some sufficient temperature above ambient before photon absorption leads to appreciable further reaction. This is, at present, an open point and requires further investigation. Second, it is possible that the photochemical production of an activated reactant species is countered by a temperature sensitive deactivation; this provides one possible reason for the disappearance of super rate effects at low absolute burning rates, as will be seen below. The inclusion or noninclusion of these thermal effects constitutes an option in the modelling process since plausible alternative explanations exist for those elements of propellant behavior.

It should be noted that a necessary assumption in hypothesizing a photochemical scheme such as that discussed here is that there exists a large multiplication factor in the reaction sequence. The absolute flux of ultraviolet radiation feedback from the flame is not yet known but it is certainly small compared to the conductive feedback flux; the direct thermal heating effects of flame radiation are assumed to be negligible in the present discussion. However, the highly energetic nature of the ultraviolet photons makes a considerable difference when conditions are such that the free radicals produced by photon absorption can yield a branching chain sequence of reactions. It has been suggested that the first net effect of photon absorption is scission of an NO_2 radical; this is captured by the stabilizer but leaves behind a alkoxy radical which may subsequently produce an extensive reaction chain. A single absorption event ultimately leads to the production of a large number of molecular fragments; the quantum efficiency of the process is much greater than unity.

B. Results of Model Studies

The differential equations which properly describe the above models have only a single coordinate dependence, that is, distance along the axis perpendicular to the propellant surface. To reduce the equations to an approximate alge-

braic description of the model, it is necessary to integrate out this coordinate dependence by making use of the fact that an Arrhenius temperature dependence usually collapses the reaction zone nearly to a sheet.

Consider first the energy equation for the gas phase flame (recall that only the first stage is considered).

$$\lambda_g \frac{d^2T}{dx^2} - \dot{m}c_g \frac{dT}{dx} + \rho_g Q_f \dot{\varepsilon} = 0$$

where

$$\dot{\varepsilon} = Z_g \rho_g \varepsilon^2 \exp(-E_g/RT)$$

(See the attached nomenclature table.) This can be formally integrated to:

$$\dot{q}(0) = -\lambda_g \left(\frac{dT}{dx}\right)_0 = -Q_f \int_0^{-\infty} \rho_g \dot{\varepsilon} \exp\left(\frac{\dot{m}c_g}{\lambda_g} x\right) dx$$

where $\dot{q}(0)$, the conductive feedback to the surface, is the real quantity of importance to the model. With the assumption that the flame is essentially a sheet $\dot{\varepsilon}$ is replaced by a delta function and the entire heat release occurs at a distance x_f above the surface approximately equal to:

$$x_f \simeq \left(\frac{\dot{m}}{\rho_g}\right)\tau = \frac{\dot{m}}{\rho_g^2 Z_g \bar{\varepsilon}^2 \exp(-E_g/RT_f)}$$

Then, the conductive feedback to the surface can be expressed as

$$\dot{q}(0) = r\rho_s Q_f \exp(-ar^2/p^2)$$

The lumped constant a is a measure of flame thickness; it is a function of flame temperature and gas phase activation energy.

Now an energy balance at the surface gives the following:

$$\dot{m}c_g(T_s - T_R) - \dot{m}c_s(T_0 - T_R) = \dot{m}Q_s + \dot{m}Q_f \exp(-ar^2/p^2) \quad \text{(B-1)}$$

where the last term is the flame feedback just estimated. The second term on the left accounts for deviations of initial propellant temperature from the reference tempera-

ture for chemical energy (such deviations also affect flame temperature and hence the lumped constant a). The only fundamental unknowns here are T_s and r so if one more equation relating these two variables is available, the model is complete. For normal burning the usual assumption of a pyrolysis term at the surface is used.

$$r = A_3 \exp(-E_3/RT_s) \qquad (B-2)$$

Consider next the subsurface conservation equation for the final active complex of the photochemical scheme that is to yield super-rate burning.

$$\frac{\dot{m} d[R]}{\rho_s dx} + \mu\phi I_{UV}(x)[M]A_5 e^{-E_5/RT} - A_6[R]e^{-E_6/RT} = 0$$

Here diffusion of the complex is neglected. In an effort to keep the model as simple as possible, the photochemical pathway leading to the active complex is written as a single reaction proportional to the UV intensity, ballistic modifier concentration, and local temperature; degradation of the complex is via a first order temperature dependent reaction.

The equation is integrated throughout in the condensed phase from the burning surface ($x = 0$) to $x = \infty$.

$$\int_0^\infty \frac{m}{\rho_s}\frac{dR}{dx}\,dx + \int_0^\infty \mu\phi I_{UV}[A]A_5 e^{-E_5/RT}dx - \int_0^\infty [R]A_6 e^{-E_6/RT}\,dx = 0$$

It is assumed that all the reactions occurs, near the burning surface and $I_{uv} \simeq I_0$, $[A] \simeq$ constant and $[R] \simeq R_0$.

Then, we get

$$-\frac{m}{\rho_s}R_0 + \mu\phi I_0[A]A_5 \int_0^\infty e^{-E_5/RT}\,dx - R_0A_6 \int_0^\infty e^{-E_6/RT}\,dx = 0$$

Next, approximate the Arrhenius integrals by Zeldovich/Frank-Kamenetski approximation with assumed pure heat conduction in the condensed phase near the burning surface;

$$\frac{dx}{dT} = \frac{\alpha_p}{r}\frac{1}{T_s - T_0}$$

$$- \frac{m}{\rho_s} R_0 + \mu\phi I_0 [A] A_5 \frac{\alpha/r}{T_s - T_0} e^{-E_5/RT_s} \left(\frac{RT_s^2}{E_5} \right)$$

$$- R_0 A_6 \frac{\alpha/r}{T_s - T_0} e^{-E_6/RT_s} \left(\frac{RT_s^2}{E_5} \right) = 0$$

$$\dot{R} = \frac{m}{\rho_s} R_0 = \frac{\mu\phi I_0 [A] A_5 \frac{\alpha/r}{T_s - T_0} \left(\frac{RT_s^2}{E_5} \right) e^{-E_5/RT_s}}{1 + A_6 \frac{\alpha/r^2}{T_s - T_0} \left(\frac{RT_s^2}{E_6} \right) e^{-E_6/RT_s}} \qquad \text{(B-3)}$$

Now, in accord with the qualitative ideas about the mode and site of action of the active complex discussed above, one can use this expression to pose approximate models of super-rate burning. Suppose first that the net effect of the action of this complex is to create a pathway for degradation of the condensed phase which has a negligible activation energy but the same energetics as in normal burning. The fraction of the condensed phase degraded along this pathway will be proportional to the flux of the active complex. We assume that in the condensed phase at least the normal and super rate pathways proceed in parallel with relative independence so that Eq. (B-2) is replaced by

$$r = A_3 \exp(-E_3/RT_s) + (\gamma/\rho_s)\dot{R} \qquad \text{(B-4)}$$

The super rate model then consists of Eqs. (B-1), (B-3), and (B-4) which specify r and T_s as functions of pressure and initial temperature. We assume that the photochemical pathway not only lowers the activation energy barrier but also yields a more exothermic decomposition at and below the surface. The only additional specification for such a model is the dependence of surface heat release on the two pathways.

$$Q_s = (r_1 Q_1 + r_2 Q_2)/(r_1 + r_2)$$

$$r_1 = A_3 \exp(-E_3/RT_s)$$

$$r_2 = (\gamma/\rho_s)\dot{R}$$

These, plus Eqs. (B-1), (B-3), and (B-4) specify the model. Solutions are obtained in the same way as was described previously.

Typical burning behavior is shown in Fig. B-2; it is assumed there that the photochemical pathway produces twice the surface heat release of normal burning. The pressure regime has been extended to 4000 psig to show that the super rate does indeed tend to vanish at high pressures. Unfortunately, this is about the only aspect of the super rate behavior which is consistent with experimental results. The most flagrant inconsistency with experiment is the tendency for super rate to be greatest at the lowest pressure and the highest T_0. This, however, is inherent in this model because the increased surface heat release counters the flame blow away tendency (which would decrease the burning rate) best when the flame is of least importance, i.e., at low pressures and high initial temperatures. This model is an improvement over the first version but still inadequate. The viability of the basic ideas of the model is not necessarily disproved by this result. Conceivably, a more exact representation of such important factors as the flame feedback could yield more reasonable behavior; this possibility should be pursued in future work.

We turn finally to the possibility that the active complex has no influence on the condensed phase but rather tends to accelerate the gaseous flame (the first stage of the two stage flame). Then the more likely way to view the active complex is as a catalyst, presumably solid particles of dimension small relative to the 1st stage flame zone. A very approximate but reasonable way to account for such effects is to assume that the effective activation energy in the gas is a mass averaged value of those for normal and catalyzed burning.

$$E_g = \frac{r_{CAT}}{r_{TOT}} E_{CAT} + \left(1 - \frac{r_{CAT}}{r_{TOT}}\right) E_{NORMAL}$$

$$r_{CAT} = (\gamma/\rho_s)\dot{R}$$

These, plus Eqs. (B-1), (B-2), and (B-3) specify the model.

Typical results are shown in Fig. B-3; it is assumed there that the catalytic pathway has an activation energy which is 70% of that for normal burning. Here, obviously, is a very sensitive mechanism; there are no fundamentally

conflicting tendencies except those present in normal burning. As the activation energy decreases the increased flame feedback increases the surface temperature and hence the burning rate; a new balance is reached when flame speed matches the increased blowing velocity from the surface. Note that the overall qualitative behavior is more consistent with experiment. True plateau (slope $\approx$ 0) or mesa (slope $<$ 0) behavior is not predicted, however.

(C) Nomenclature for Appendix B

- c - specific heat
- m - mass burning rate = $r\rho_s$
- p - pressure
- r - burning rate
- x - distance from propellant surface
- A_3 - frequency factor for surface pyrolysis
- A_5 - frequency factor for lumped photochemical pathway to final active complex
- A_6 - frequency factor for thermal deactivation of complex
- E - activation energy
- I_{UV} - UV radiation intensity
- $[M]$ - ballistic modifier concentration
- Q - heat release
- R - universal gas constant
- $[R]$ - concentration of final active complex
- T - temperature
- Z_g - frequency factor of gas phase flame reaction
- γ - multiplicative factor for active complex effectiveness ($\gamma\phi$ gives the overall quantum efficienty)
- ε - fraction of unconsumed gaseous reactant
- λ - thermal conductivity
- μ - UV absorption coefficient of propellant
- ρ - density
- τ - reaction time of gas phase flame
- ϕ - quantum efficiency of photochemical reaction

Subscripts

g - flame zone

f - end of fizz zone

s - burning surface

1 - reaction pathway 1

3 - reaction pathway 3

5 - reaction pathway 5

6 - reaction pathway 6

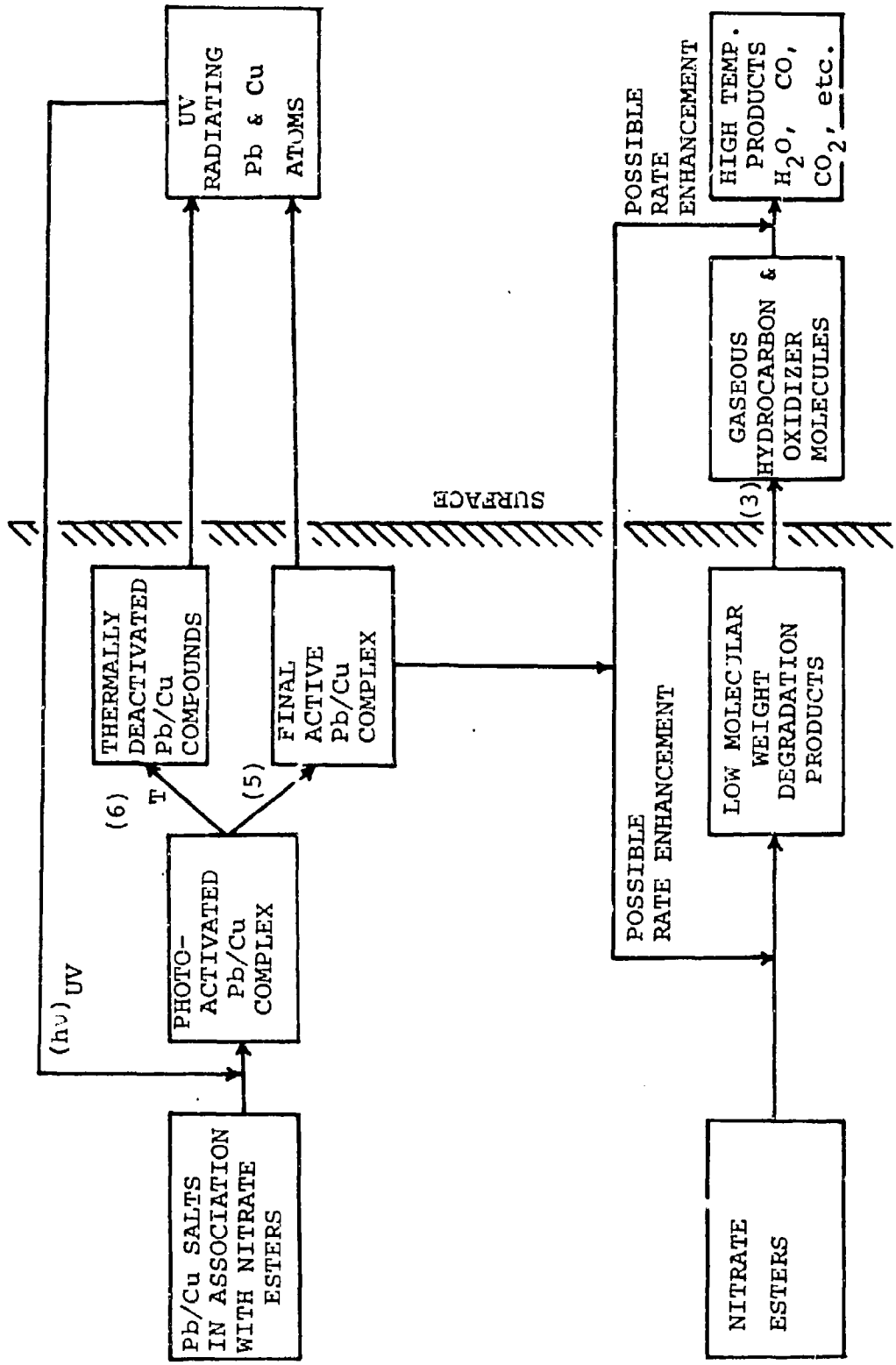

Fig. B-1. Proposed reaction pathways for platonized propellants.

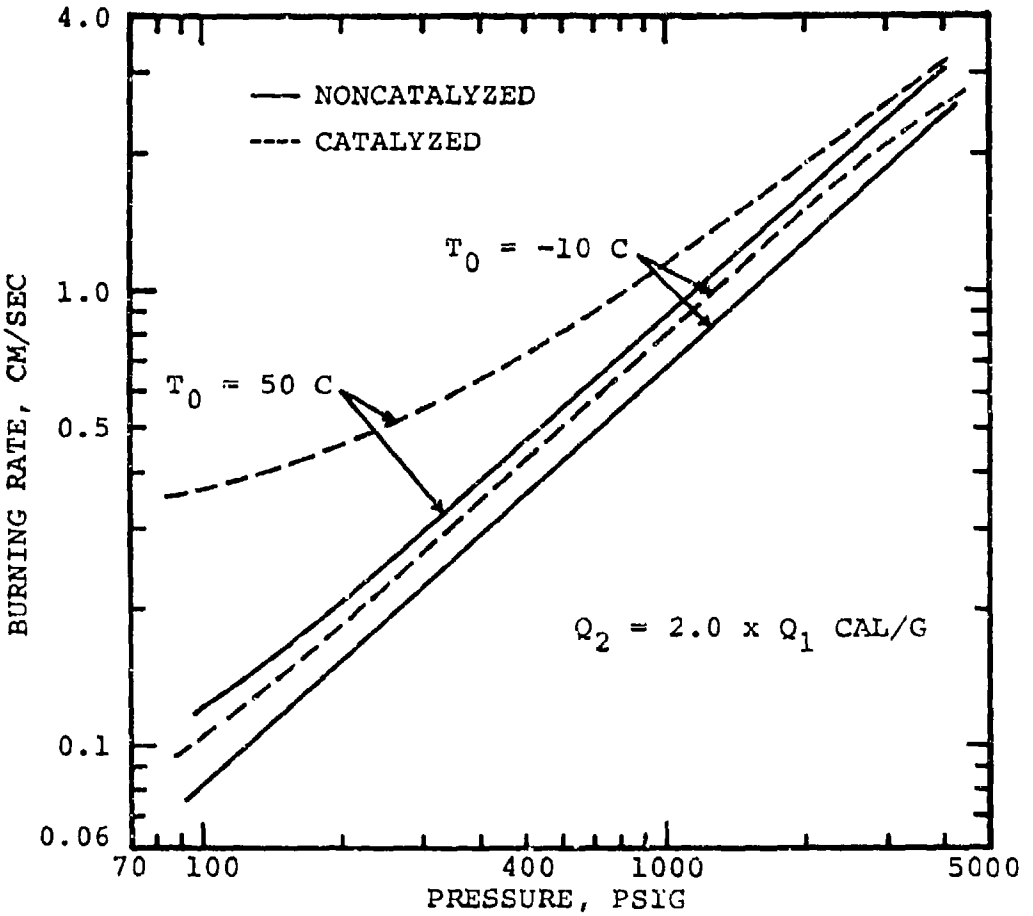

Fig.B-2. Calculated burning rates for catalyzed and noncatalyzed propellants (for this case, catalysis is assumed to accelerate the surface zone reactions and double their exothermicity).

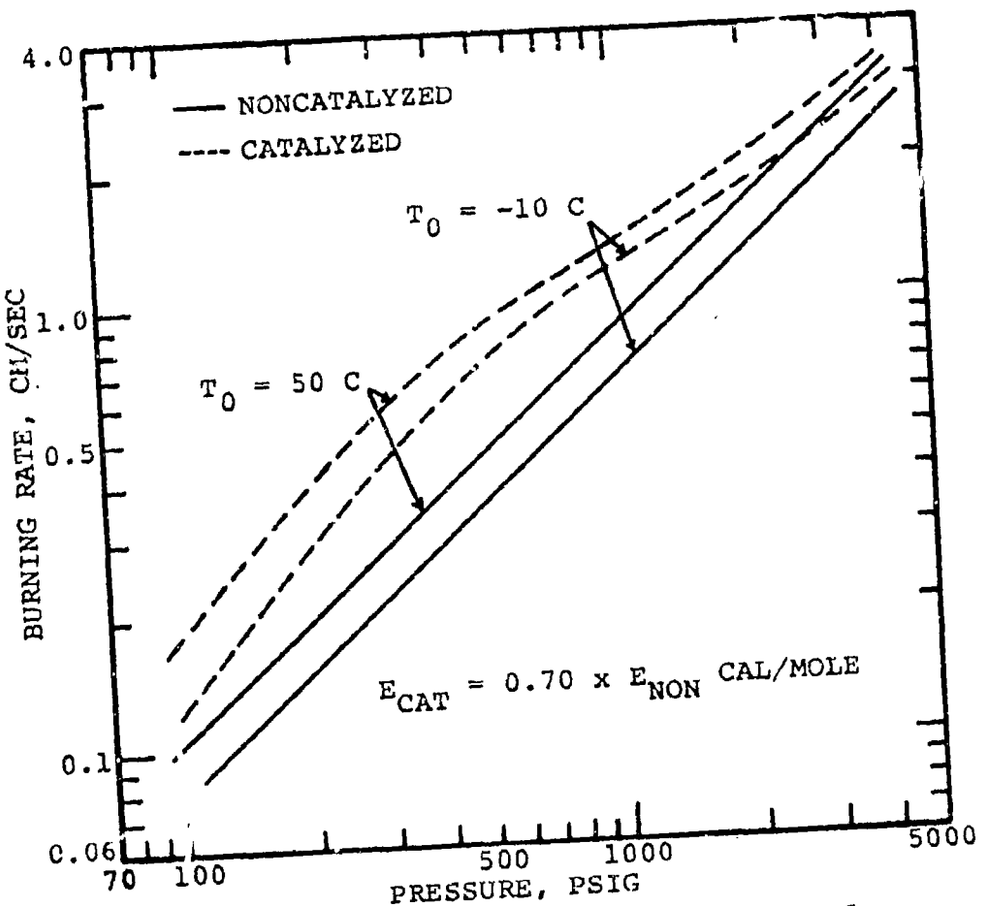

Fig.B-3. Calculated typical burning rates for catalyzed and noncatalyzed propellants (for this case, catalysis is assumed to decrease the gas phase activation energy only; no thermal effects are assumed).

APPENDIX C

EXPERIMENTAL PROCEDURE AND MEASUREMENTS

In this study, a wide range of experimental measurement techniques were used to investigate the combustion mechanisms of double base propellants. In this appendix, the description of the experimental procedures and apparatus are categorized as follows: (1) burning rate measurements in the range 1 - 100 atmosphere (discussed in Section III), (2) burning rate and minimum burning pressure measurements at subatmospheric pressures (Section III), (3) gas phase observations (Section IV), (4) burning surface observations during propellant burning (Section V), (5) extinguished propellant burning surface observations by rapid depressurization (Section V) and (6) temperature profile measurements through combustion processes by embedded thermocouples (Section VI).

1. Burning Rate Measurements in the Range 1 - 100 atm.

(a) Experimental Apparatus

Figure C-1 shows the propellant strand in position between two electrical terminal posts. Ignition is accomplished by passing a current through a nichrome wire threaded through the top end of the strand. Burning rates are measured by determining the instant of melting of each of 7 low melting-point fuse wires of lead metal, 0.25 mm in diameter threaded through the strand at accurately known separation distances (1.27 cm). These 7 fuse wires, each in series with a resistor, form 7 parallel arms of an electrical circuit, the output voltage changes discontinuously as soon as a fuse wire melts. The temperature of the strand is measured by a calibrated copper-constantan thermocouple threaded through the strand and the bead of the thermocouple is placed in the center of the strand. The signal is read by the same equipment that is used at nitrogen gas flow temperature measurement.

Also shown in Fig. C-1 are a Dynisco PT-76U-2M (1 - 136 atm) strain-gauge pressure transducer and thermocouples placed in the nitrogen flow and in the strand. The outputs of the pressure transducer, the two thermocouples, and the fuse wire circuit are amplified separately (using Dana DC amplifier models 3420 and 2200). These amplified signals are recorded continuously by a high response multi-channel galvanometer recorder (Honeywell Visicorder model 1508 with type M-3300 Galvanometers).

As shown in the exploded view of Fig. C-2, the pressure chamber consists of a long 1-5/8 inch internal diameter stainless steel tube. Nitrogen and combustion products es-

cape to the atmosphere via a choked orifice at the upper end of the tube and enters through a long coil immersed in anti-freeze. Nitrogen gas flow temperature is controlled by the liquid temperature which is controlled by an electric heater to heat up or dry-ice to cool down. These temperatures are measured by calibrated chromel-alumel thermocouples placed below the strand in the strand burner and in the liquid. The signals are amplified (by a Dana model 2200A DC amplifier) and measured by a digital voltmeter (Digitec model 201 manufactured by United Systems Corp.).

The steady-state chamber pressure during a burning rate measurement test is measured by one of two bourdon gauges (manufactured by Heise and with guaranteed accuracy of 0.1% of full-scale), depending on the pressure: below 14.5 atm (200 psig), a 1 - 18 atm (0-250 psig) gauge with 0.5 psi graduations was used, and the range 14.5 - 103 atm (200-1500 psig), a 1 - 136 atm (0 - 2000 psig) gauge with 2.0 psig graduations was used. Figure C-3 shows an overall view of the instrumentation and control panels.

(b) Effect of Nitrogen Purge Rate

The effect of nitrogen purge rate on burning rate was investigated at three different pressure levels between 150 and 1200 psia (10 to 82 atm). This was done by varying the exhaust orifice diameter of the strand burner. Figure C-4 shows the effect of nitrogen purge rate on the burning rate. The two dotted lines in the figure show the nitrogen purge rate four and forty times the propellant gas generation rate. At those flow rate levels, the burning rate is almost independent of the nitrogen flow rate. However, there are indications that reverse flow of the hot combustion gases when the nitrogen mass flow rate becomes comparable to the mass flow rate generated by the burning propellant. This sometimes causes the fuse wires to melt before the burning surface reaches the fuse wires.

(c) Temperature Sensitivity Measurements

For the temperature sensitivity measurements, (i.e., $r(p,T_0)$ determinations), a constant N_2 flow, preconditioned to the desired temperature maintained the strand at the desired initial temperature. Low temperature conditions were obtained by passing the N_2 through an ethylene glycol and water bath cooled by dry-ice. High temperature conditions were obtained by heating the same bath with electric heaters. The conditioning temperature of the strand was monitored by a thermocouple threaded through the strand.

2. Burning Rate and Minimum Burning Pressure Measurements at Subatmospheric Pressures

(a) Apparatus

The apparatus used for the measurements of the burning rates, the minimum burning pressures, and the temperature profiles at subatmospheric pressures consists of a chamber with four quartz windows. The chamber is connected directly to a large surge tank which is evacuated by a vacuum pump, as shown in Fig. C-5. The pressures are measured by means of a mercury manometer and are controlled by a pressure regulator. A needle-valve is used to control the amount of gas flow. Nitrogen was used for the adjustment of the chamber pressure. As experimental results show, burning rates are not affected by gases such as nitrogen and argon[94,76]. Figure C-6 shows a close-up view of the propellant strand in position on the holder.

(b) Experimental Procedure

The propellant strands used in the experiment were 7 mm square and 40 mm long; each strand has a thin nichrome wire threaded through it for electrical ignition. The measurements of burning rate and of minimum burning pressure were obtained by means of five fuse wires, 0.12 mm in diameter, which were threaded through each strand at accurately-measured (5.0 mm) intervals along its length. The fuse wires, each in series with a resistor were connected up so that the output of an electrical circuit was changed discontinuously when the receding burning surface melted a wire and broke the circuit. The amplified signals were recorded by means of Honeywell model 1508 Visicorder (see Fig. C-3) with a type M-3300 galvanometer.

The photographic technique used by Steinz[73] for burning rate measurements of composite propellants at subatmospheric pressures was considered. However, the burning surface could not be observed clearly on the photographs since double base propellants (especially platonized propellants) form carbon residues on the surface of the strand and evolve large quantities of smoke during burning.

The procedure used in this experiment was as follows: the strand was mounted vertically on the holder and the ignition wire and five fuse wires connected to their appropriate terminals. The chamber was then evacuated once to approximately 10 mm Hg and thoroughly purged with nitrogen to the desired pressure. The pressure during the test was read from a mercury manometer.

The minimum burning pressures were measured by the

same experimental procedure and same size of propellant strands as used in the measurements of burning rates. The propellant strands were prepared without fuse wires to avoid the heat loss as the burning surface encounters the fuse wires. (The heat loss may influence the minimum burning pressure.) The minimum burning pressures were examined by changing the orientation of the propellant samples. It was observed that there were some differences of the minimum burning pressures. Therefore, for consistency, all the measurements were done with vertical propellant strands burning on the top surface.

The temperature profiles were measured by means of platinum and 10% platinum-rhodium thermocouples, 2.5 or 7.5 microns in diameter. The thermocouples were imbedded in the propellant samples as described in Appendix C- 6 - (a).

(c) Effect of Fuse Wires

The effect of the presence of fuse wires on the burning rate was determined in the subatmospheric pressure range where the effect is expected to be large. Because the heat required to melt the fuse wire may cause a disturbance of steady propellant burning. However, no fuse wire effect could be discerned from comparison of photographically determined burning rates. The comparisons were made for noncatalyzed propellants with relatively clean burning surfaces. Near the point of low pressure extinction, the burning rates were significantly influenced by the presence of the fuse wire. So, burning rates determined by use of fuse wires near the extinction pressures must be used with caution. For example, a noncatalyzed propellant will be affected when the pressure is within 0.4 atm of the extinguishment pressure.

3. Strand Burner for Gas Phase Observations

(a) Apparatus

The strand burner for gas phase observations consisted of a chamber with two quartz windows mounted on the side of the chamber wall. A small cylinder 20 mm in diameter is mounted vertically inside and connected to the base of the chamber. Two transparent glass plates are mounted on the side of the cylinder as shown in Fig. C-7. The cylinder is used to maintain a flow of nitrogen gas around the burning strand for the purpose of keeping the glass plates free of smoke deposits. The N_2 gas is supplied through the base of the chamber and the flow rate is adjusted by changing the size of the orifice mounted on the top of the burner. The adjustment is similar to that of the strand burner described in Appendix C-1-(a).

High speed photographs of the dark zone and of the flame zone were obtained using two cameras. A Fastax 16 mm high-speed camera, with extension rings, was used to photograph the higher burning rates corresponding to the higher pressures. The Fastax was operated at 1000 frames per second. A Bollex 16 mm movie-camera, also with extension rings, was used to photograph at low pressures lower burning rates corresponding to the lower pressures. The Bollex was operated at 64 or 32 frames per second. The overall view of the apparatus is shown in Fig. C-8. (The optical line of the spectroscope which is seen in the figure is not adjusted to the observation window of the strand burner.) To find the location of the burning surface from the photographs during measurements of the dark zone length, the propellant strand was illuminated from outside of the strand burner by a tungsten lamp. The camera was focused carefully on the propellant strand through the quartz window of the chamber and through the glass plate mounted on the cylinder guiding the flow of nitrogen gas.

(b) Preparation of Propellant Strand Samples

The propellant strands used in the gas phase and flame zone observations were of a 7 mm square cross-section and 40 mm in length. The sides of the strands were coated with an inhibitor. In such applications, it is desirable that the inhibitor be consumed so as to maintain a flat burning surface. Accordingly, the inhibiting techniques were perfected to that the inhibitor burns at the same speed as the propellant strand, and produces no solid residues at the sides of the strand. The inhibitor is a mixture of 50% cellulose acetate, 25% ethylalcohol, and 25% toluene. The ignition system used was similar to that used in the burning rate measurements.

(c) Data Reduction

The photographs obtained during the test were projected, frame by frame, onto a screen and the length of the dark zone measured from each frame. The length of the dark zone was taken to be the distance from the burning surface to the place where the brightness increased sharply.

4. Strand Burner for Observations of the Burning Surface

As shown in Figs. C-9 and C-10, the strand burner for the burning surface observations consisted of a conical-shaped cylinder with two quartz windows. The two windows are mounted opposite each other on the cylinder wall, and are inclined at 45 degrees with respect to the axis of the burner. One window is used for the illumination of the propellant surface by means of a tungsten lamp, and the other

is used for observations by a high speed camera (i.e., Fastax 16 mm high-speed camera). Ignition-wire leads are passed through the bottom of the burner; the propellant-sample holder is mounted on the bottom of the burner. The bottom of the strand burner is provided with an inlet for purge gases to ensure that the windows and the optical path are not obscured by the combustion gases. The nitrogen purge rate is controlled by an orifice mounted at the exhaust pipe on the top of the burner. The orifice is selected to allow five times as much gas to escape to the atmosphere as is generated by the propellant. The choice of flow rate was based on reasoning similar to that described previously in the discussion of the burning-rate measurements with the strand burner.

5. Extinction of Burning by Rapid Depressurization

As shown in Fig. C-11, the burner for rapid depressurization extinguishment consists of a cylindrical section with two exhaust nozzles. The bottom of the chamber supports the propellant strand sample, which, in this study, were 7 mm by 7 mm by 5 cm in length. The sides of the samples were coated with inhibitor. The open end of the chamber is closed off by a pair of diaphragms. Rapid depressurizations were obtained by bursting the two diaphragms by suddenly reducing the pressure between them.

The experiment is conducted by placing the propellant sample at the bottom of the chamber as shown in Fig. C-12. The two diaphragms are positioned as shown, and the cavity between them is pressurized to about one-half of the burning chamber pressure. The propellant is ignited by means of an electrically heated wire. The exhaust gases initially pass through a small nozzle which is situated in the side wall of the double-diaphragm apparatus; this nozzle controls both the flow and the chamber pressure as long as the diaphragms remain intact. The diaphragms are chosen to be strong enough to withstand the differential in pressure between the combustion chamber and the pre-pressurized cavity, but not strong enough to withstand the differential between the chamber pressure and atmospheric pressure. Consequently, when the propellant has reached the desired steady state burning, the pressurized space between the two diaphragms is vented so that the chamber pressure causes both diaphragms to shear cleanly at the wall and the chamber pressure drops rapidly. Sheet aluminum of four different thicknesses ranging between 0.020" and 0.040" was used for the diaphragms. The small nozzles ranged between 0.063 inches and 0.116 inches in diameter were used to maintain the desired steady-state pressure during the burning of the propellant strand.

The chamber pressure was measured by means of a trans-

ducer flush mounted in the chamber wall. A Dynisco, model Pt76 transducer was used and its output was recorded on a Visicorder at a paper speed of 60 in/sec. Also, the steady state chamber pressure was measured by means of a bourdon gauge manufactured by Heise (Range 1 to 136 atm).

6. Temperature Profile Measurements

(a) Thermocouple Production Technique and Preparation of Propellant Samples

One of the primary objectives during the development of the manufacturing techniques was to obtain reproducible bead sizes as small as possible to minimize the thermal lag. For these experimental measurements, wires 2.5 microns and 7.5 microns in diameter were used. The Wollaston wires consist of a silver sheath over the platinum and 10% platinum-rhodium (Pt-10% PtRh) thermocouple wires. Pieces of Pt and 10% PtRh wires are cut into roughly 4 cm lengths. The silver is removed by immersing the wires in a solution of 1 part nitric acid and 1 part distilled water for about 15 minutes. Thereafter, the wires are placed across the two arms of a micromanipulator and are fixed by means of magnets.

The micromanipulator, made by the Zeiss Company, has three degrees of freedom with which to adjust the wire position. The bare tips of the wires are positioned under a "Stereozoom" microscope, manufactured by Bausch and Lomb Company. The arms of the micromanipulator are brought together until the tips of the wires are touching and form an included angle of about 60 degrees. The tips of the wires are examined very carefully through the microscope to ensure contact and an ohmmeter is used to ensure that the positive and negative ends are connected to the arms of the micromanipulator. In this study, the junction of the wires was welded by means of Misco acetylene-oxygen microtorch with a tip number 000; the latter provides a flame approximately one half a millimeter wide and one millimeter long.

The welded thermocouple beads were carefully studied under a high magnification microscope (Nikon Microflex Model EFM x 100) and their sizes measured. Only those of size less than approximately 4 microns, for wire 2.5 microns in diameter, and 10 microns, for wire 7.5 microns in diameter, were selected for the experiments.

The propellant samples, of 7 mm x 7 mm cross-section and 3 cm in length were cut in half lengthwise; one of the pieces of the sample was placed under the thermocouple held on the arms of the micromanipulator. The propellant

sample was slowly lifted until its surface touched the thermocouple, whereupon acetone was applied to the surface of the propellant sample to imbed the thermocouple on the surface. After the acetone had dried, the two magnets holding down the ends of the wires were removed and the sample containing the thermocouple is removed from the manipulator. Acetone was applied to the surfaces of both samples, which were then pressed together on all sides. Over fifty percent of the thermocouples were destroyed during the latter step; however the squeezing of the samples is necessary to ensure uniform contact between the sample and the thermocouple; otherwise, many small bubbles are observed at the mating plane. After the continuity of the wires had been checked by means of a voltmeter, the samples were kept for 4 days at 50°C in an electrically-heated furnace. Thereafter, the surfaces of the samples were inhibited with Hot Fuel Proof Dope, manufactured by the Testor Corp. After the inhibiting, the strands with embedded thermocouples were considered ready for use.

(b) Determination of the Burning Surface Temperature from the Recorded Temperature Profile by the "Temperature Inflection Method"

The determination of the burning surface temperature by the temperature inflection method is based on a correlation of the experimental data with the one-dimensional steady state energy-balance equation applied at the burning surface[32,75]. The steady state energy equation is

$$\frac{d}{dx}\left(\lambda\frac{dT}{dx}\right) - \rho r c\frac{dT}{dx} + \mathcal{R}Q = 0 \qquad \text{(C-1)}$$

Assuming that no heat release occurs below the surface reaction layer and that the propellant properties are constant, that integrating Eq. (C-1) across the solid phase yields:

$$T - T_0 = (T_s - T_0)\exp(r\rho_p c_p x/\lambda_p) \qquad \text{(C-2)}$$

Thus the temperature profile is straight line plot of $\log(T - T_0)$ versus x. The point of departure from linearity, the inflection point in the $\log(T - T_0)$ versus x curve, is taken to be the burning surface temperature. If the propellant properties such as ρ_p, c_p, λ_p, are dependent on the temperature, the energy, Eq. (C-1), when integrated will not have a simple form. However, the results of Shook[109] show that these properties are almost independant of the temperature between 25°C and 100°C. It should be noted that the temperature inflection method is not applicable to the determination of the burning surface

temperature during burning at low pressures, since the subsurface reaction layer is stretched out below the surface and the inflection point is not well defined.

(c) Catalytic Effects of the Platinum Thermocouple Wire on the Chemical Reactions during Double Base Propellant Burning.

Thermocouples coated with silica or with some other inert material are commonly used to measure the gas temperatures to avoid incorrect readings of the temperature resulting from catalytic effects at the thermocouple surfaces. The thermocouples used in this investigation were not coated. The basis for the decision not to coat the thermocouples was the experimental evidence[11,75,94,110] that no catalytic effects have been detected when platinum wires are used to measure double base propellant temperature profiles. Furthermore, coatings increase the thermal lag of the thermocouples not only because of the resultant increase in bead size, but also because of the low thermal conductivity of the coating (e.g., the thermal conductivity of silica is about one fiftieth of that of platinum).

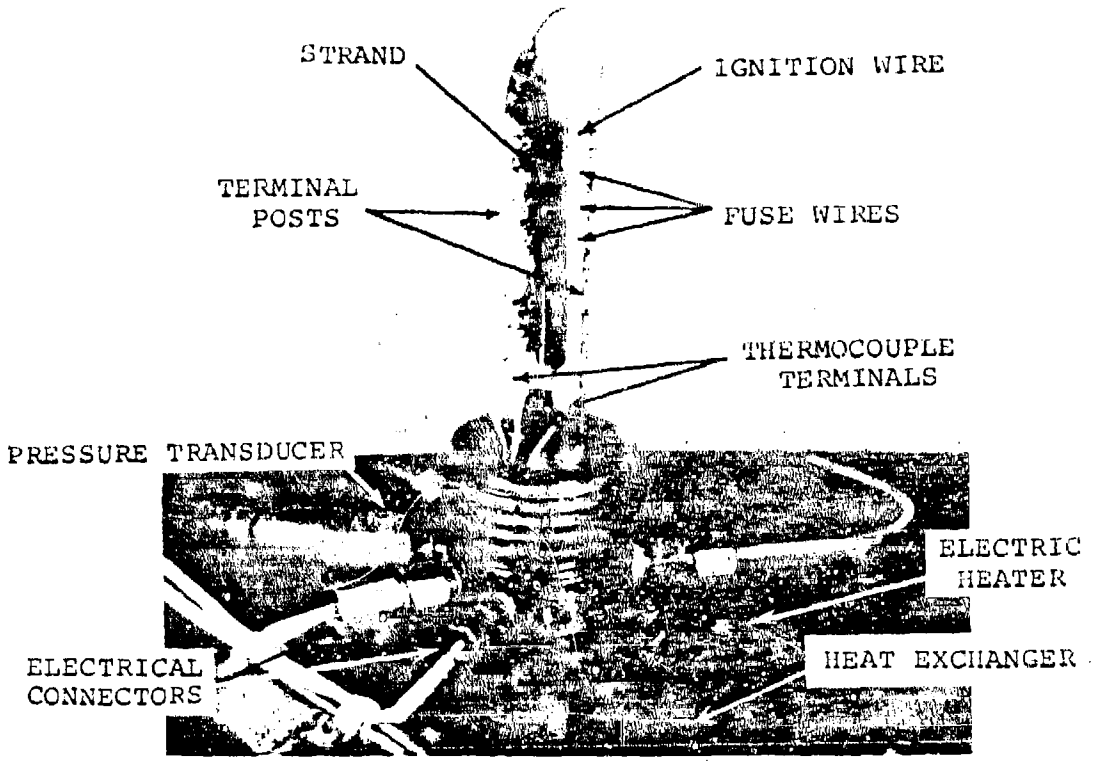

Fig. C-1. Close-up of strand holder prior to test (1 - 100 atm strand burner).

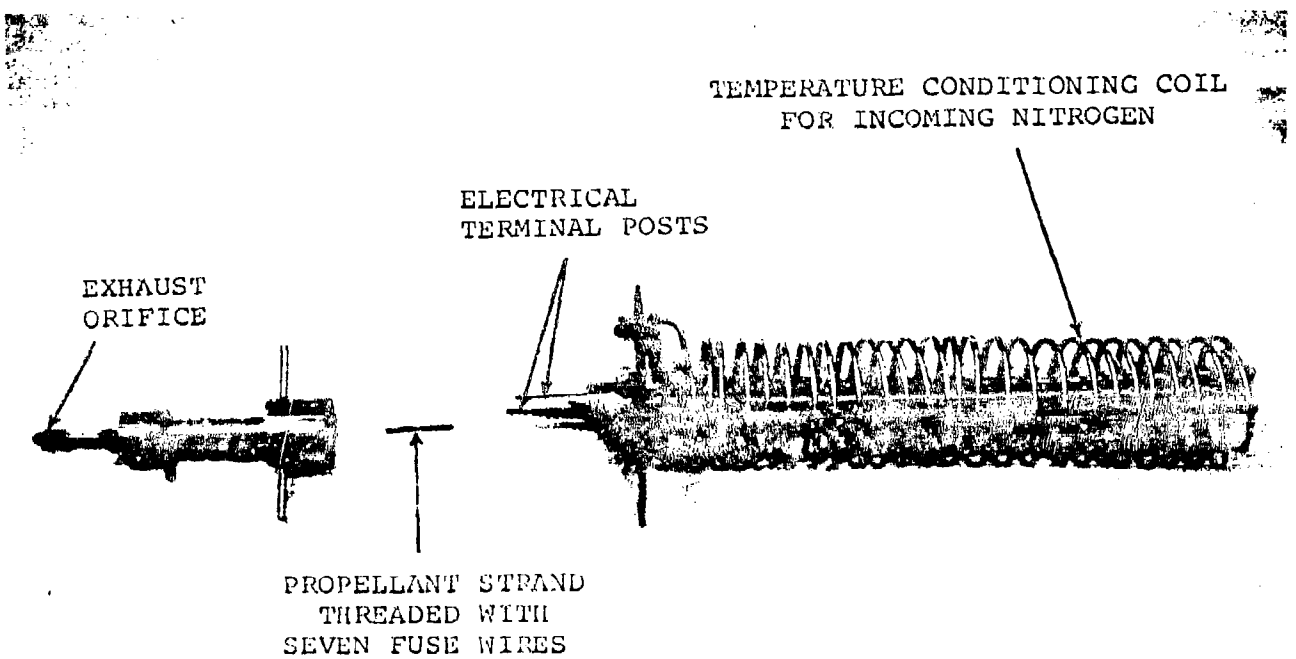

Fig. C-2. Exploded view of strand burner for measuring burning rates in 1 - 100 atm range.

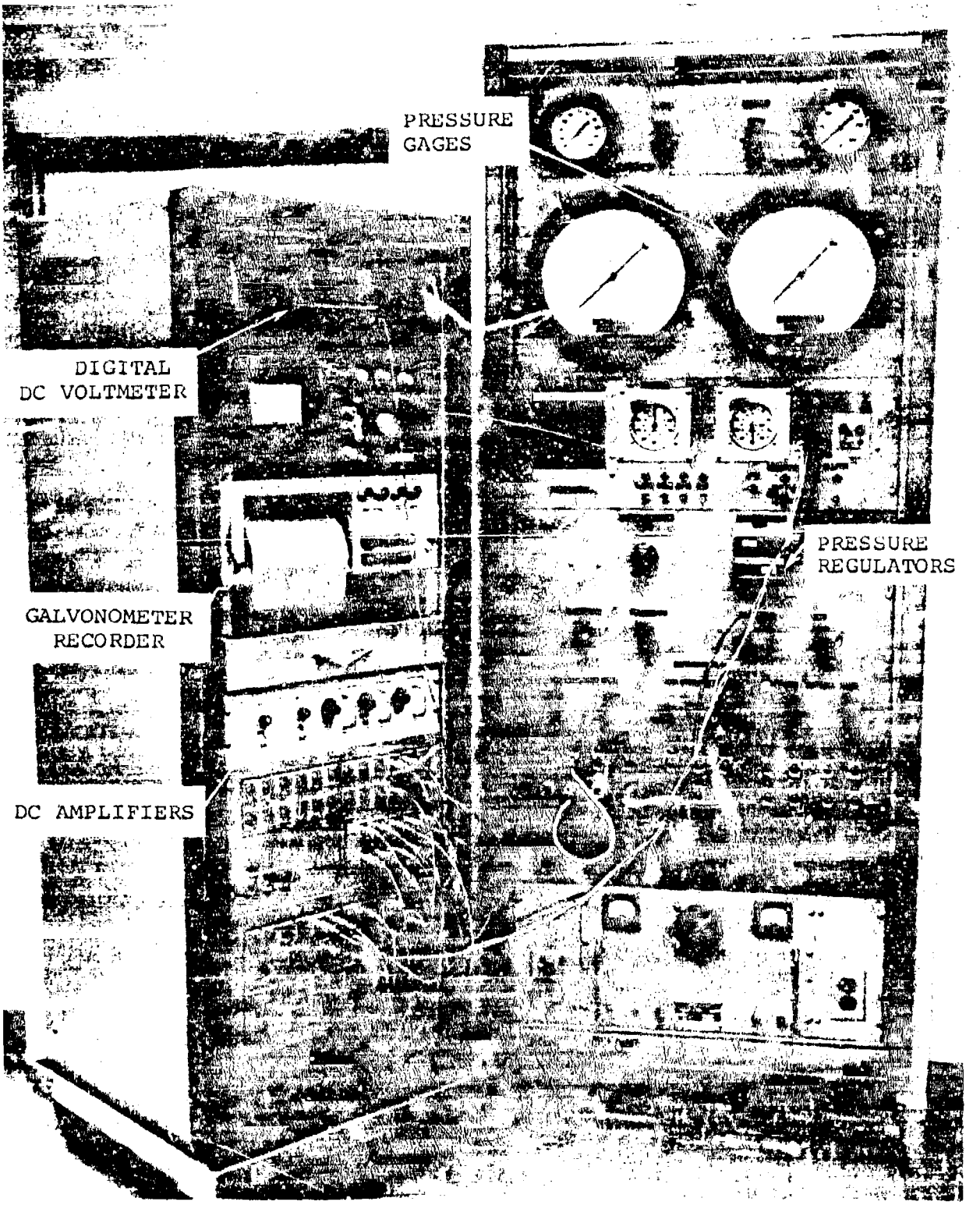

Fig. C-3. Instrumentation for measuring burning rates and temperature profiles in 1 - 100 atm range.

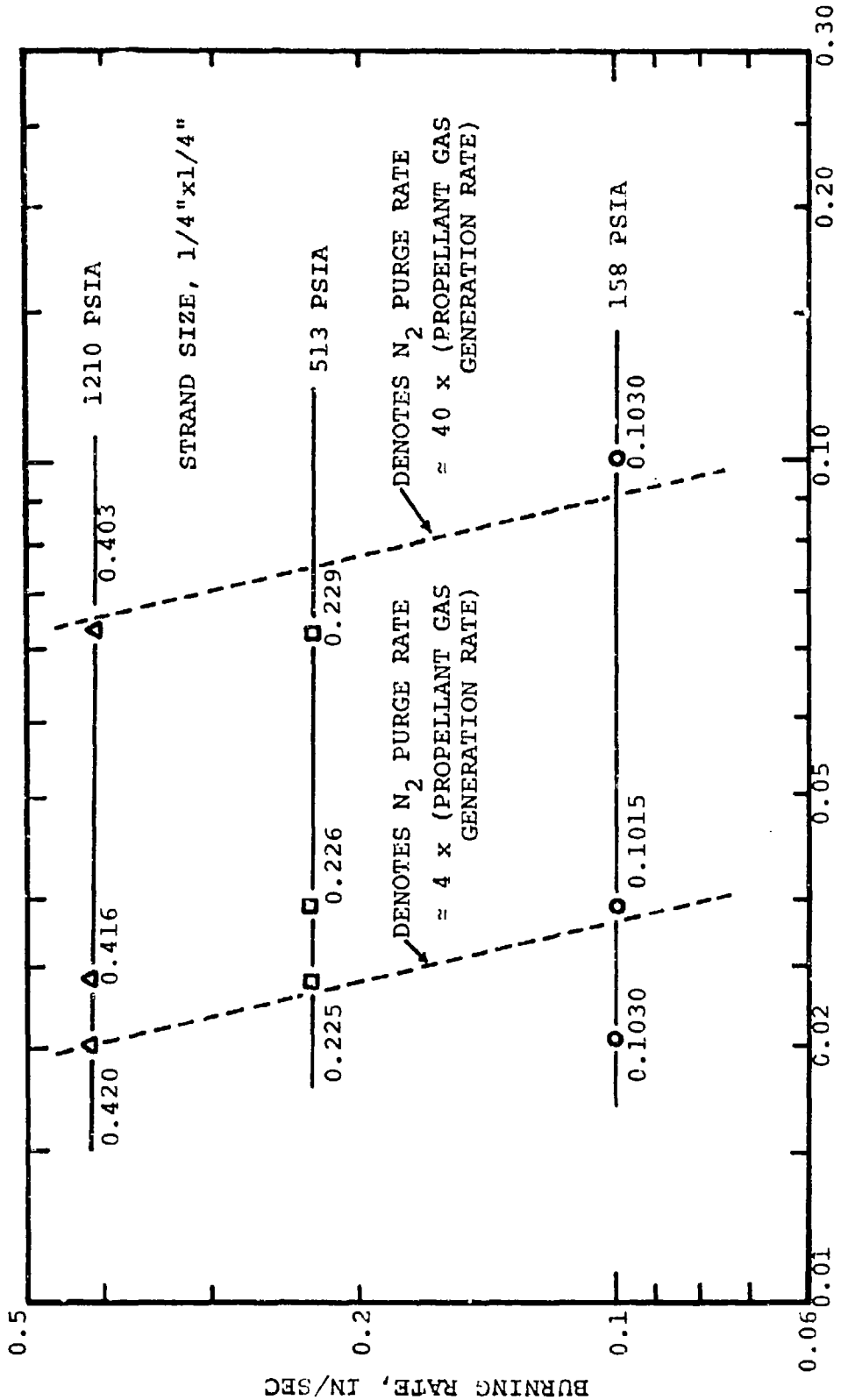

Fig. C-4. Insensitivity of burning rate of double base propellant on N_2 purge gas rate.

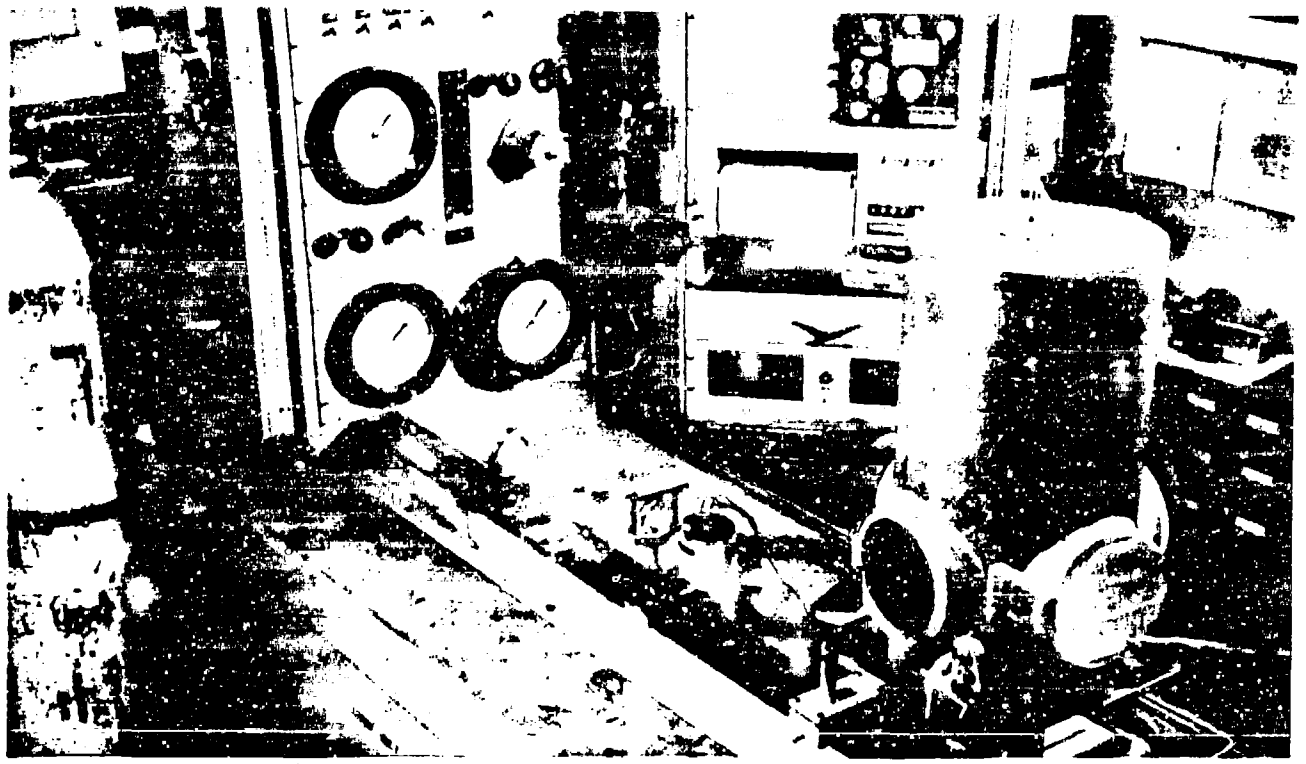

Fig. C-5. Apparatus for measuring burning rates and temperature profiles at subatmospheric pressures.

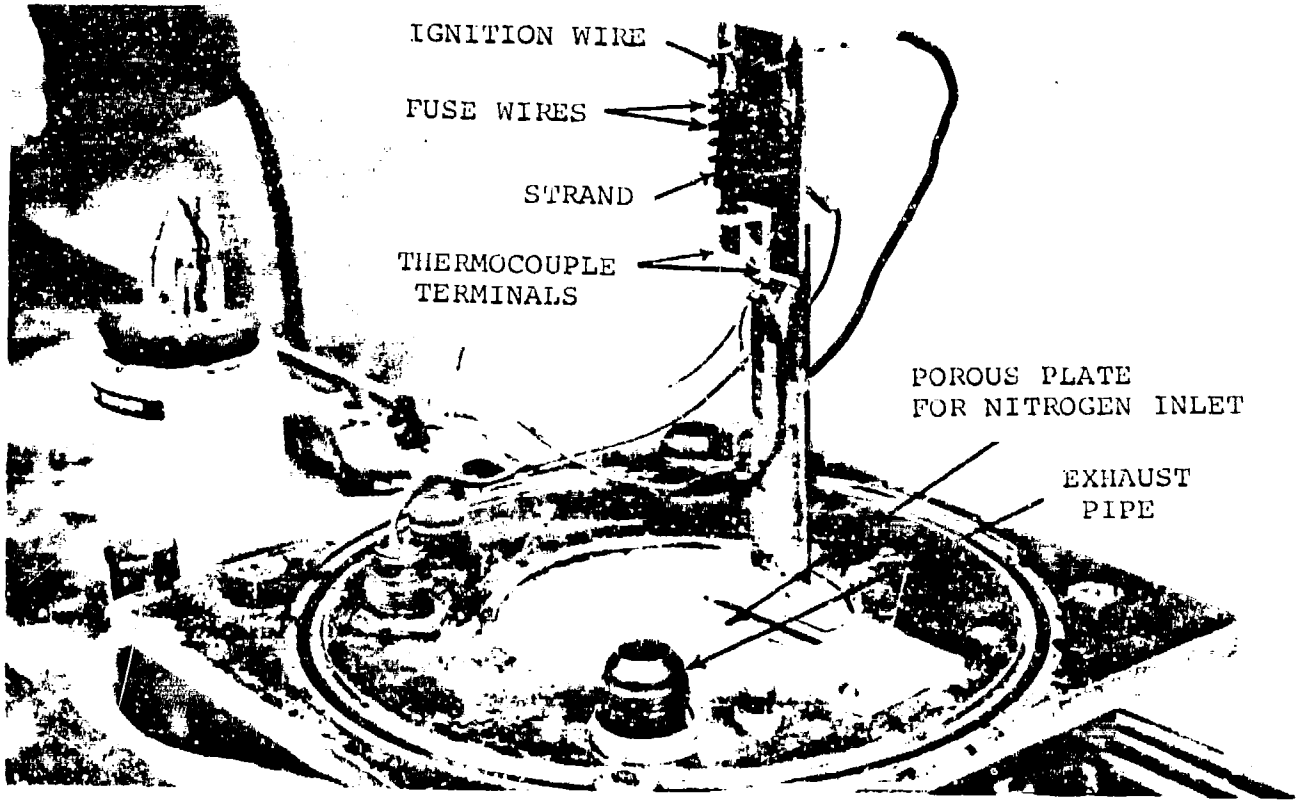

Fig. C-6. Close-up of strand burner for measuring burning rates at subatmospheric pressures.

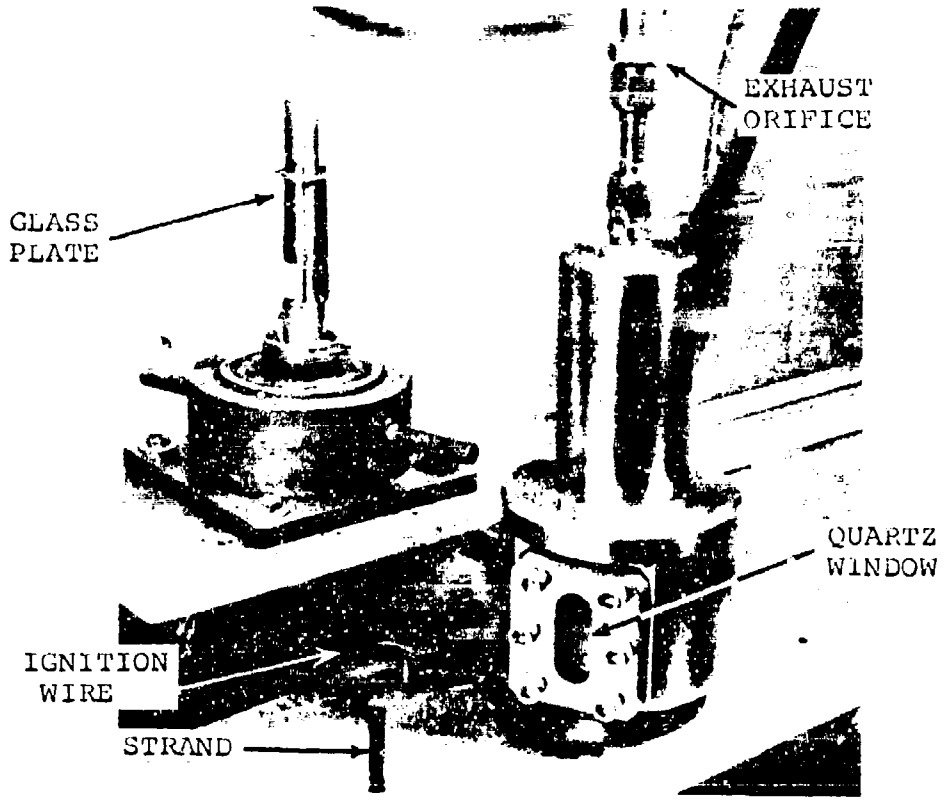

Fig. C-7. Strand burner for gas phase observations.

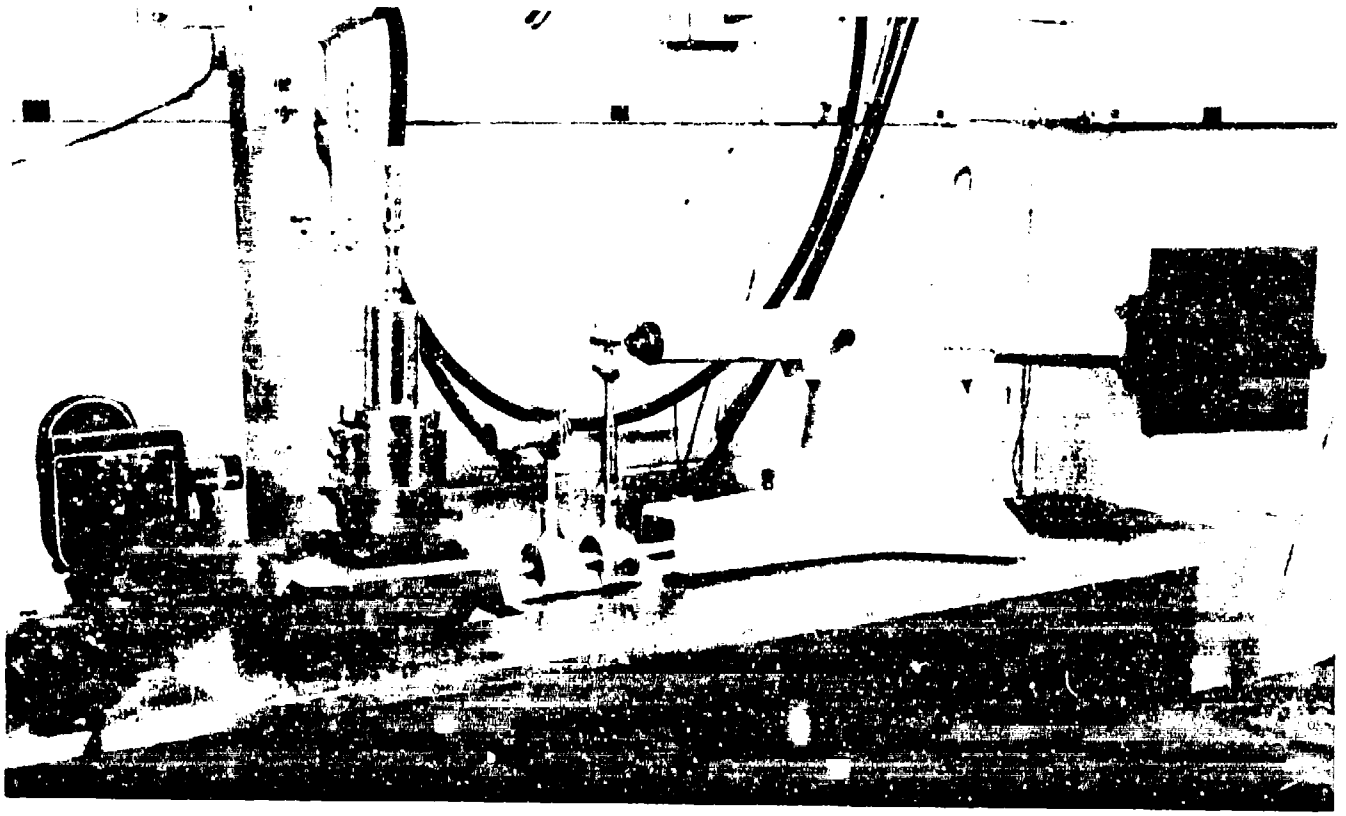

Fig. C-8. Photograph of assembled strand burner for gas phase observations.

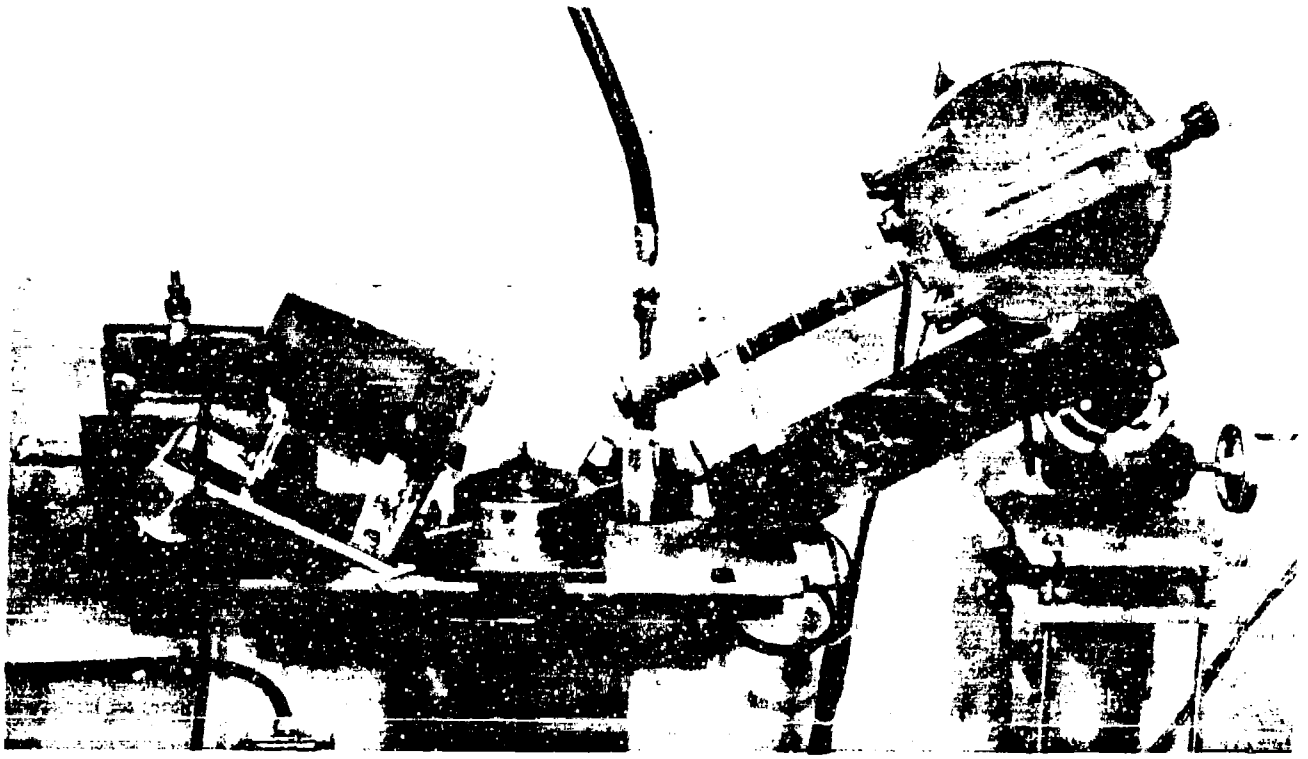

Fig. C-9. Photograph of assembled strand burner for burning surface observations.

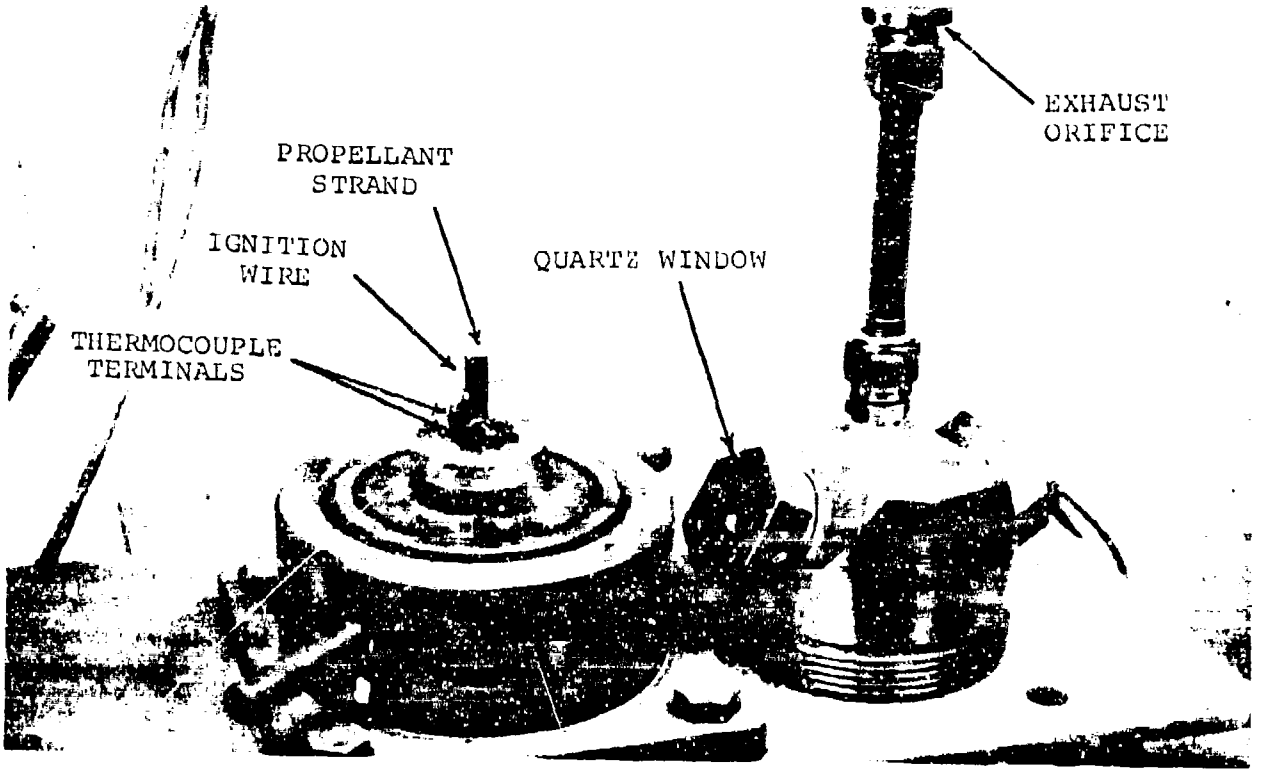

Fig. C-10. Close-up of strand burner for burning surface observations.

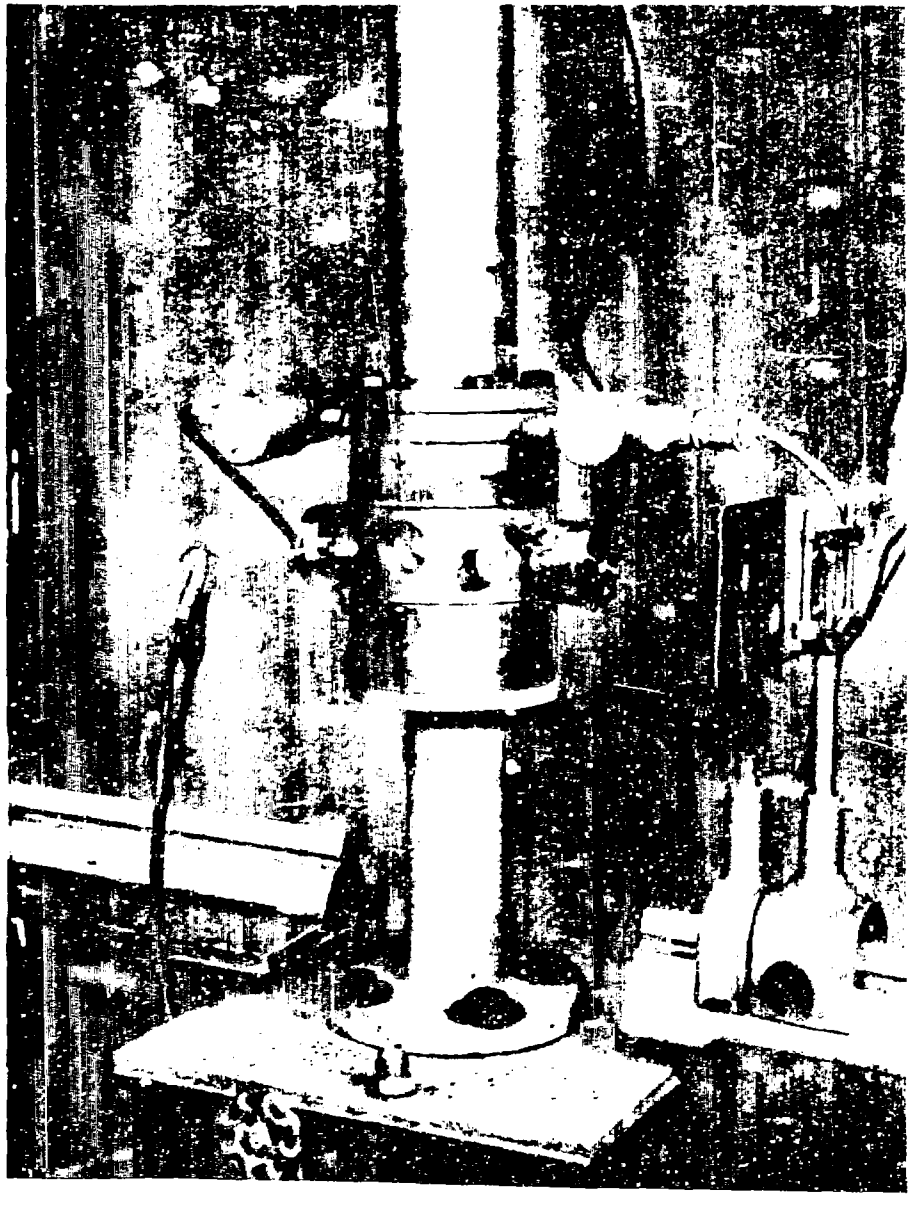

Fig. C-11. Photograph of assembled strand burner used for extinction of propellant burning by rapid depressurization.

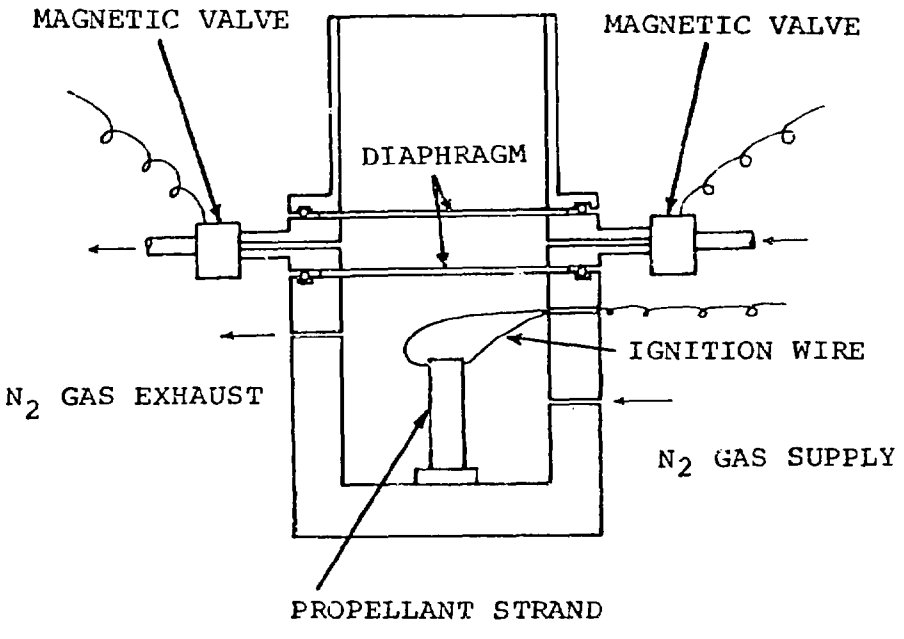

Fig. C-12. Schematic drawing of the strand burner for extinction of propellant burning by rapid depressurization.

APPENDIX D

PROCESSING PROCEDURE OF PNC/TMETN PROPELLANTS INCLUDING CHEMICAL PROPERTIES AND SOURCES OF INGREDIENTS

1. Processing Procedure

The castable double base propellants used in this study were processed by remote control in a Vertical Mixer with no submerged bearings. The ingredients were prepared, weighed and then mixed in heptane to insure thorough distribution. The solvent was removed with heat and vacuum prior to the addition of the gelling agent (TEGDN). After the mixing cycle was completed the propellant was pour cast slowly into a mold for curing.

The steps for processing castable double base propellants are shown schematically in Fig. D-1 and are described in detail as follows.*

I. EQUIPMENT
Atlantic Research Vertical Mixer, 1200 g capacity

Note: Insure proper indexing of mixer blades (see ARC vert. mixer operating procedures)

II. SAFETY PRECAUTIONS**

1. Wear safety equipment: conductive shoes; flame proof coat, buttoned at neck; and full sized face shield.

2. Insure proper grounding of equipment and use stainless steel tools (non-sparking). DO NOT USE hard rubber spatulas.

3. Use stainless steel or conductive plastic beakers.

4. Wipe up spilled material and place all contaminated wastes into disposal container to be burned.

---

*A. T. Camp and C. E. Johnson of the Naval Propellant Plant at Indian Head, Maryland, assisted in setting up these procedures.

**PNC propellants modified with A.P. and No stabilizers may become sensitive with age in storage.

III. BASIC FORMULATION*

PNC (dried)	40%
TMETN (MTN)	50%
Gellation Mix (50% MTN+50% TEGDN)	10%

IV. PNC PREPARATION

1. Place wet nitrocellulose in drying pan - maximum layer thickness - 1/4".

2. Dry in vacuum oven at 50 C and 0.5 cm/Hg vacuum for 24 hours. Note: Install liquid N_2 vapor traps in vacuum line.

3. Weigh pan tare and PNC each successive 2 hours for 8 hours - record weight loss to 0.10 Gr. If stable for 2 weight recordings, heptane has been removed.

4. Screen dried PNC through #25 and #50 sieve before using (remote operation). Dry screened PNC in oven for 48 hours prior to using. Note: Store in conductive plastic bags inside air tight container. Static electricity is a particular hazard when working with dried PNC.

V. ADDITIVE PREPARATION (fine grind salts)

1. Equipment

Fisher Mini Mill
Minimill glass jar (8 oz.)
Steel balls 1/4" 20; 3/8" 25

2. Procedure

A. Weigh out approx. 2 times amount required and place into vacuum oven to dry for 24 hours at 80 C and 0.5 mm/Hg vacuum.

B. After drying weigh out required amount and place into Ball Mill Jar (record tares).

C. Add steel balls and 100 grams heptane. Place on to the mini mill and ball mill for 48 hours.

---

*DO NOT mix heavy metal (e.g., lead and copper) or heavy metal compounds with propellants containing AP.

D. Remove balls and wash in 10 grams heptane. Add total contents to mix. (Salts must be agitated 2 hours on ball mill prior to use.)

Caution: Lead and copper salt dust is hazardous. Wear mask and plastic gloves. Wash hands.

VI. MIXING PROCEDURE

1. Record all tare weights and contaminated tare.
2. Weigh out dried PNC and place into mixer.
3. Weigh out heptane (solvent) (equivalent to 50% of PNC weight) and add to mix to wet PNC.
4. Weigh out additives and add to mix.
5. Weigh out MTN and add to mix.
6. Mix without vacuum for 2 min. at 150 rpm (3.5 dial setting) at 50 C.
7. Apply maximum vacuum (0.5 cm/Hg) and mix for 30 min. (RPM and temperature as per Step 6). Use liquid N_2 vapor trap to remove heptane from vacuum system.
8. Stop mixer and check for full removal of solvent. If smell is present continue mixing for 15 min. as per Step 7 until solvent is removed.
9. Reduce mix temperature to 20 C , mix for 15 min., stop mixer, scrape down sides of mixer cautiously. (see Note 1)
10. Weigh out TEGDN plus stabilizer, and predissolve (warm to 40 C for 10 min.). Add to mix. Note: TEGDN may be mixed with equal amount of MTN to decrease plastisizer effect.
11. Vacuum mix at 0.5"/Hg at 150 rpm and 20 C for 15 min. (Note 2)
12. Remove propellant from mix and pour cast into molds.

Note 1 - CAUTION: Use non-sparking tools only, such as stainless steel - DO NOT use hard rubber spatulas. DO NOT use Berylium copper tools with AP additives.

Note 2 - For low viscosity mixes, to pregel mix, increase mix temperature to 50 C for Step 11. Check mix viscosity

at 10 min. Total mix time at 50 C is 20 min. Monitor mixer load ammeter for indications of excessive thickening.

VII. CURING

1. Place propellant into water bath or sealed vacuum oven for 72 hours at 135 F ± 5 to cure.

2. Chemical Structure of Propellant Ingredients

(a) Material Source

PNC: Plastisol Nitrocellulose (NC)
Nitrogen in Nitrocellulose, 12.56%
mean particle size, 10.0μ
Wet with at least 30% Heptane
Manufactured at Naval Ordnance Station, Indian Head

TMETN: Trimethylolethane Trinitrate
(Metriol Trinitrate, MTN)
Appearance; clear water-white liquid
Manufactured at Trojan Powder Co.

TEGDN: Triethylene Glycol Dinitrate
Appearance; pale yellow liquid
Manufactured at Trojan Powder Co.

EC: Ethyl Centralite
(N, N' - Diethylcarbanilide)
Manufactured at Eastman Organic Chemicals

C: Carbon Powder
(Neo Spectra TA)
mean particle size, 0.01μ
Manufactured at Columbian Carbon Co.

PbSa: Lead Salicylate
(Normal Lead Salicylate, Normasal)
mean particle size,* 10μ
Appearance; fine white to light cream-colored powder
Lead in PbSa 43.5%
Manufactured at National Lead Co.

CuSa: Copper Salicylate
(Monobasic Cupric Salicylate)
mean particle size,* 10μ
Copper in CuSa 29.1%
Manufactured at National Lead Co.

Pb2-EH: Lead 2-Ethylhexoate
$Pb[OOCHC(C_2H_5)(CH_2)_3CH_3]_2$
mean particle size, 6.0μ
Lead in Pb2-EH 41.2%
Manufactured at National Lead Co.

---

*As received particle size. In some formulation, particle is reduced in size by grinding.

PbO: Lead Oxide
mean particle size, 5.0 μ
Manufactured at Allied Chemical Corp.

Pb: Lead Powder
mean particle size, 6.0 μ
Manufactured at Alcan Metal Powders

Cu: Copper Powder
mean particle size, 5.4 μ
Manufactured at Alcan Metal Powders

Sa: Salicylic Acid
(O-Hydroxybenzonic Acid)
HOC_6H_4COOH
Manufactured at Fisher Chemical Co.

(b) Chemical Structure of Materials

(1) NC (12.6% N)

Composition:

	%
C	26.46
H	2.78
N	12.60
O	58.16

X=ONO_2 or OH

C/H Ratio 0.23

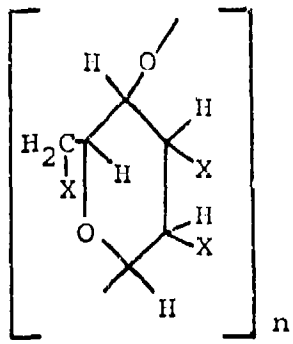

Molecular Weight: $(272,39)_n$

Oxygen Balance:

CO_2 %	-35
CO %	0.6

Density: gm/cc ∿ 1.66

(2) NG

Composition:

	%
C	15.9
H	2 2
N	18.5
O	63.4

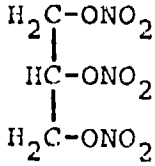

C/H Ratio 0.109

Molecular Weight: 227
$(C_3H_5N_3O_9)$

Oxygen Balance:

CO_2 %	3.5
CO %	24.5

Density: gm/cc, Liquid 1.591

(3) TMETN

Composition:

	%
C	23.5
H	3.5
N	16.6
O	56.4

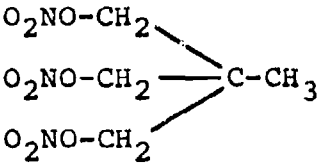

Molecular Weight: 255
$(C_5H_9N_3O_9)$

Oxygen Balance:

CO_2 %	-35
CO^2%	- 3

Density: gm/cc Liquid 1.47

C/H Ratio 0.150

(4) TEGDN

Composition:

	%
C	29.9
H	5.4
N	11.7
O	53.0

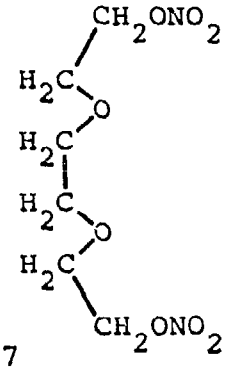

Molecular Weight: 240
$(C_6H_{12}N_2O_8)$

Oxygen Balance:

CO_2 %	-89
CO^2%	-27

Density: gm/cc 1.32

C/H Ratio 0.177

(5) PbSa

Composition:

	%
Pb	43.04

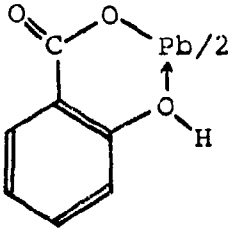

(6) Pb2-EH

Composition:

	%
Pb	41.98

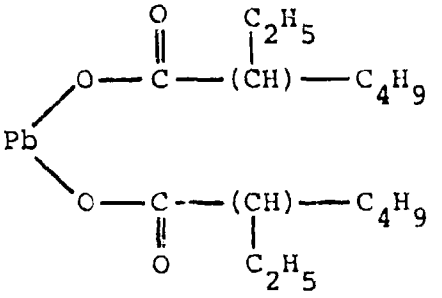

(7) Sa

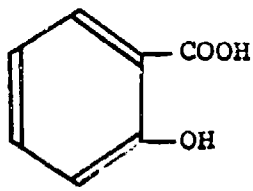

(8) CuSa

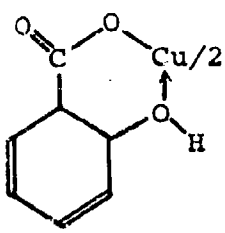

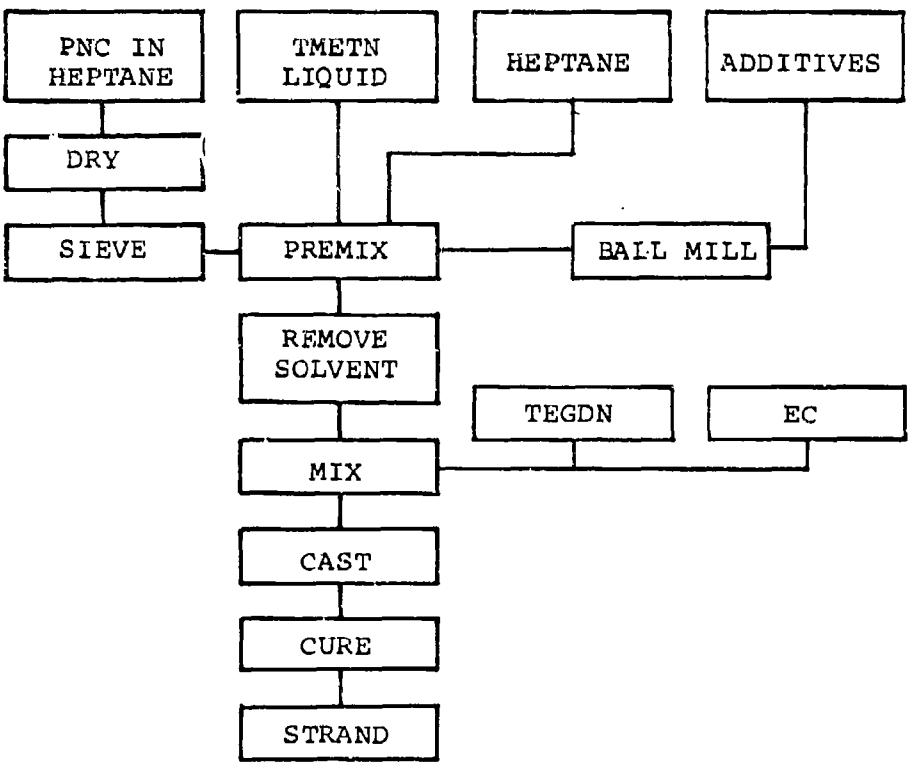

Fig. D-1. Processing of plastisol nitrocellulose propellant.

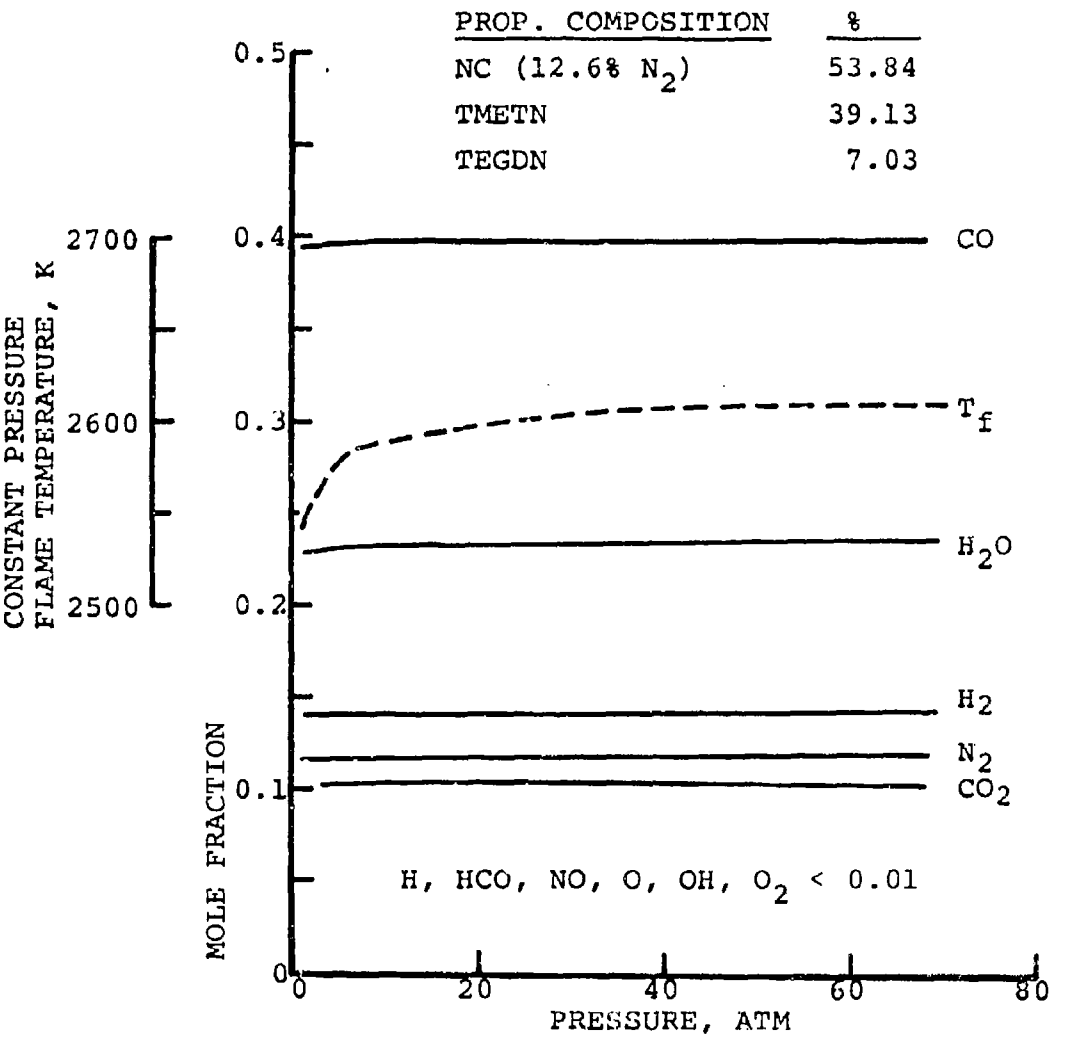

Fig. D-2. Theoretical equilibrium composition products as a function of pressure.

Note: Below approximately 10 atm the actual processes (in strand burning experiments) do not progress fully into the flame zone reactions. Accordingly, below approximately 10 atm the flame temperature and compositions may depart greatly from the above theoretical predictions.